

NASA Technical Memorandum 103825

NASA-TM-103825

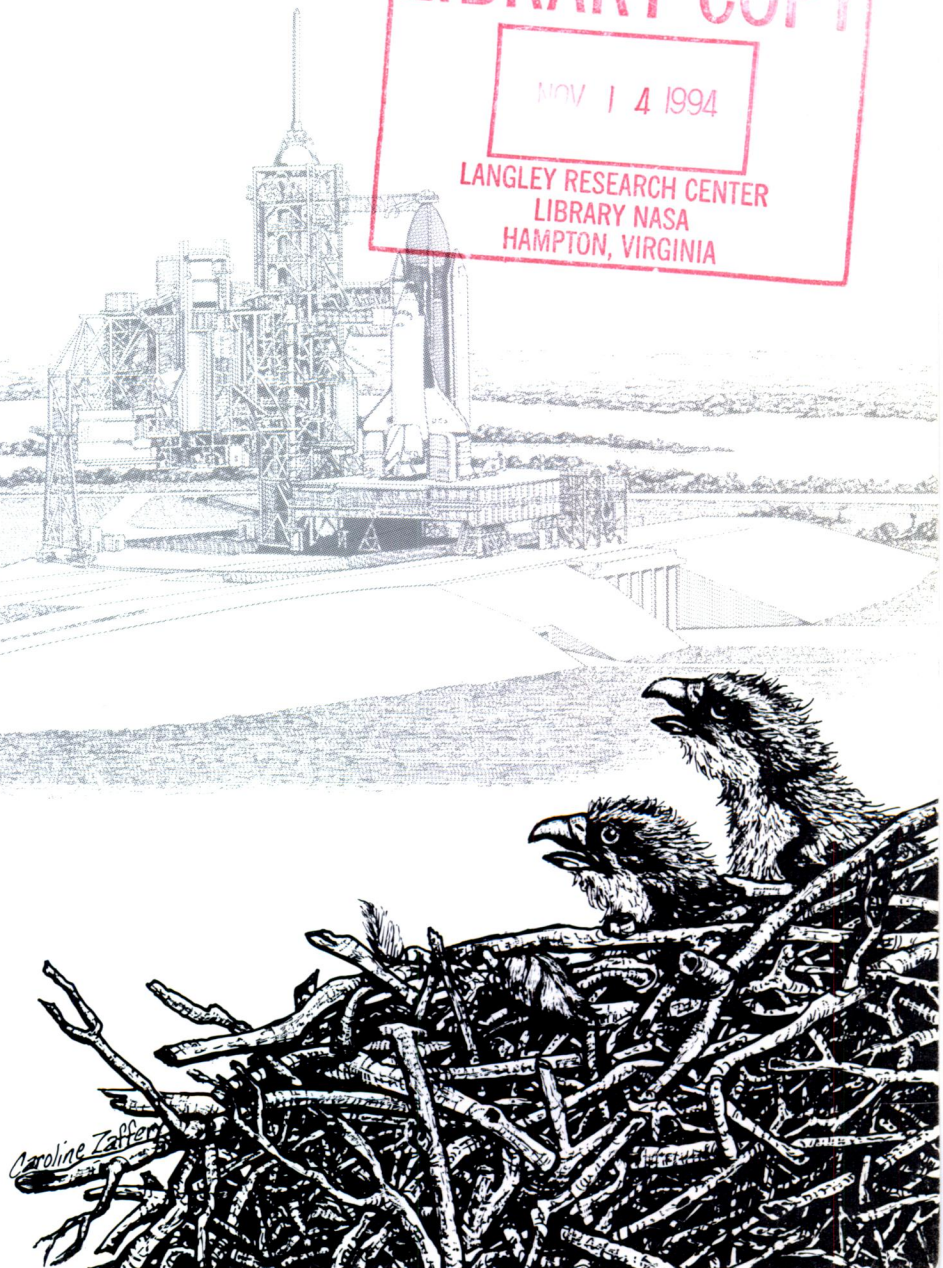
Research and Technology 1991 Annual Report

John F. Kennedy Space Center

NASA-TM-103825 19920009816



LIBRARY COPY
NOV 14 1994
LANGLEY RESEARCH CENTER
LIBRARY NASA
HAMPTON, VIRGINIA



About the Cover

The John F. Kennedy Space Center (KSC) is the Launch Pad of America; however, few realize it is also the site of the Merritt Island National Wildlife Refuge. The refuge lays claim to a larger variety of endangered and threatened species than any other single national wildlife refuge center in the continental United States. KSC is situated on 140,000 acres of land and water that support 22 wildlife species identified on either the Federal or State of Florida list as endangered or threatened.

*This year's cover is the first in a series depicting the coexistence between nature and high technology at KSC. The osprey (*Pandion haliaetus*) is a large, fish-eating bird of prey. The Merritt Island National Wildlife Refuge is home to the largest number of this protected species in Florida.*

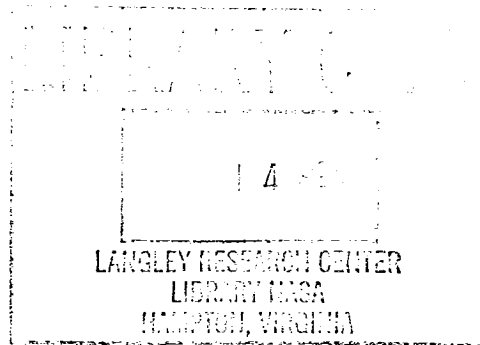
The cover art, a pen and ink rendering by Caroline Zaffery, Boeing Aerospace Operations, Inc., depicts the parent osprey returning to the nest with its prey.

NASA Technical Library



3 1176 01412 7121

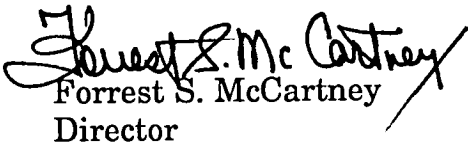
Research and Technology 1991 Annual Report of the John F. Kennedy Space Center



FOREWORD

As the NASA Center responsible for assembly, checkout, servicing, launch, recovery, and operational support of Space Transportation System elements and payloads, the John F. Kennedy Space Center is placing increasing emphasis on its research and technology program. In addition to strengthening those areas of engineering and operations technology that contribute to safer, more efficient, and more economical execution of our current mission, we are developing the technological tools needed to execute the Center's mission relative to future programs. The Engineering Development Directorate encompasses most of the laboratories and other Center resources that are key elements of the research and technology program, and is responsible for implementation of the majority of the projects in this Kennedy Space Center 1991 Annual Report.

Thomas M. Hammond, Technology Utilization Officer, PT-PMO-A, (407) 867-3017, is responsible for publication of this report and should be contacted for any desired information regarding the Centerwide research and technology program.


Forrest S. McCartney
Director

AVAILABILITY INFORMATION

For additional information on any individual report, contact the person identified following the article. Commercial telephone users can dial the listed extension preceded by area code 407. Telephone users with access to the Federal Telecommunications System can dial the extension preceded by 823.

CONTENTS

HAZARDOUS EMISSIONS AND CONTAMINATION MONITORING	1
Evaluation of Hypergolic Oxidizer Vapor Detectors	3
<i>The evaluation of six commercially available portable nitrogen dioxide sensors for personnel safety monitoring resulted in the identification of Draeger Model 190 as the best instrument to meet NASA's needs.</i>	
Evaluation of GMD Systems, Inc., MK-2 Portable Fuel Vapor Detector for MMH, N ₂ H ₄ , and UDMH	4
<i>The initial test results of a portable fuel vapor detector, developed for the detection of hydrazines at 10-ppb concentration levels.</i>	
Hydrogen Umbilical Mass Spectrometer (HUMS)	7
<i>An interim Hydrogen Umbilical Mass Spectrometer will be designed and fielded. This system will measure gas leakage at the hydrogen umbilicals of the Space Shuttle.</i>	
Improved Oxygen Monitors for the Space Station Processing Facility	8
<i>Evaluation of the performance of oxygen monitors based on different technologies for fast response, low maintenance, and proper operation in the presence of solvent vapors and other potential interferences.</i>	
Reliable, Cost-Effective Particle Counter Calibration System	10
<i>Design and testing of a calibration system for optical particle counters that is more flexible and easier to use than commercially available equipment.</i>	
AC Motor Valve Hypergol Leak Detector	12
<i>Summary of a study of Interscan detectors ability to detect monomethylhydrazine and nitrogen dioxide leaks in the Shuttle Reaction Control System / Orbital Maneuvering System alternating current motor valves.</i>	
Selection of Ammonia Analyzers for Use in Space Station Ammonia Loading Operations	16
<i>Testing of ammonia analyzers is based on various technologies for use in the Space Station Processing Facility at Kennedy Space Center.</i>	

CONTENTS (Cont)

Evaluation of FTIR Methods for the Second-Generation Hypergolic Vapor Detection System (HVDS II)	18
<i>Results from a laboratory evaluation of Fourier Transform Infrared (FTIR) technology for possible application in HVDS II to monitor hypergolic propellant vapors at part-per-million levels during Space Shuttle ground operations at KSC.</i>	
Ultrasonic Leak Detection	24
<i>An ultrasonic leak detector/locator system was developed for use in the leak testing of Columbia (STS-35) and was successfully deployed.</i>	
Methods for Using Water in Lieu of Chlorofluorocarbon 113 for Determining NVR Level on Precision-Cleaned Hardware	26
<i>Due to the contribution of chlorofluorocarbon (CFC) solvents to depletion of the ozone layer, it is evident that alternative methods must be developed to replace CFC's. The use of water in lieu of CFC solvents to verify the cleanliness of hardware has been evaluated.</i>	
Development of a Hydrogen Chloride Dosimeter	29
<i>The need for a low-range passive dosimeter for hydrogen chloride has resulted in a general-purpose length-of-stain dosimeter tube. The new geometry improves accuracy and sensitivity and could be applied to sensing other gases.</i>	
Remote Hydrogen Detection	33
<i>A study was performed to examine leak detection technology for use at the STS 17-inch disconnect area. Two technologies were recommended for further research.</i>	
Certification of Coulometric Detection Method for Hydrazine and Monomethylhydrazine	34
<i>Tests were performed for obtaining Nation Institute of Occupational Safety and Health (NIOSH) certification for the coulometric method of detecting hydrazine and monomethylhydrazine vapors.</i>	
Multispectral Imaging of Hydrogen Flames	35
<i>An infrared zoom lens has been demonstrated on a multispectral hydrogen-fire-imaging camera. This camera will be field tested in 1992.</i>	

CONTENTS (Cont)

Feasibility Study - A New Method for Detecting Hydrazine Fuels Using Chemiluminescence	36
<i>An investigation was made of a new analytical hydrazine vapor detection method involving derivatization, concentration, and gas chromatography coupled with chemiluminescence detection.</i>	
Hydrogen and Helium Visualization	40
<i>Several schlieren systems were built and tested. Visualization of hydrogen or helium leaks down to 10 standard cubic centimeters per minute was demonstrated.</i>	
Development of an Interim Active Vanillin Sampler Used to Detect 10 Parts Per Billion of Hydrazine and Monomethylhydrazine in Air	41
<i>Test results of the Interim Active Vanillin Sampler, developed to detect 10-ppb concentrations of MMH and hydrazine.</i>	
COMMUNICATIONS AND CONTROL	44
Direct Fiber to Operational Television Camera System	46
<i>The Fiber Optics, Communications, and Networks Laboratory is participating in the development of a television camera system that will be the prototype for the next generation of an operational television (OTV) system camera for use on the launch pad.</i>	
MECHANICS, STRUCTURES, AND CRYOGENICS	50
Determination of the Effects of Wind-Induced Vibration on Cylindrical Beams	52
<i>This study determined the critical length-to-diameter ratio of hollow cylindrical beams with various loading and end support conditions, subjected to high-velocity steady-state winds causing induced oscillation in the beam.</i>	
Vibration Response Analysis of Launch Pad Structures Subjected to Random Acoustic Excitation	55
<i>For the design of launch pad structures, two approaches (probabilistic and deterministic) are being developed to predict structural response to launch acoustics.</i>	

CONTENTS (Cont)

Design of Vacuum-Jacketed Flexhose Assemblies	57
<i>A design and fabrication approach for the production of precision vacuum-jacketed flexhose assemblies has been developed.</i>	
O-Ring Groove Inspector	58
<i>An inspection device for the solid rocket motor (SRM) O-ring groove was designed and built. It is currently used to inspect all SRM field joints at KSC. Inspection time was reduced from eight hours to one hour.</i>	
Predictive Maintenance Programs at KSC	59
<i>Ground support and facility systems used to support Shuttle and payload processing at KSC are being monitored for vibration, wear particle, and thermal signatures for failure prediction and to avoid unscheduled and costly maintenance activities.</i>	
AUTONOMOUS SYSTEMS	62
Knowledge-Based Autonomous Test Engineer (KATE)	64
<i>Development continues on a model-based reasoning (MBR) approach toward autonomous control and diagnosis of ground support equipment.</i>	
Launch Decision Support System (LDSS)	69
<i>Software tools are being developed to support decisionmaking by the launch team during Shuttle launch countdowns in the areas of time management and anomaly management.</i>	
Robotic Tile Processing System Development	70
<i>Development of a mobile robotic system to inspect and rewaterproof Orbiter bottomside tiles has been initiated.</i>	

CONTENTS (Cont)

INSTRUMENTATION AND DATA ACQUISITION	72
Solid-State Voltage Reference Study	74
<i>A research study evaluates stability characteristics of Solid-State Voltage References (SSVR) at the 10-volt level in a laboratory environment. This study also includes SSVR recovery after battery drain down and compliance/noncompliance with published stability specifications.</i>	
An Inexpensive Remote Data Display System	80
<i>An inexpensive hardware and software system allows multiple users at remote sites to display and print out expendable launch vehicle and/or payload telemetry data.</i>	
MSBLS Flight Inspection System Pilot's Display	81
<i>The Microwave Scanning Beam Landing System (MSBLS) Flight Inspection System Pilot's Display was developed for the pilot of test aircraft to set up and fly a given test flight path determined by the flight inspection test engineers and to aid the aircraft pilot when hazy or cloud-cover conditions exist that limit the pilot's visibility of the Shuttle runway during the flight inspection.</i>	
Low-Flow Vortex-Shedding Flowmeter for Hypergols	86
<i>A flowmeter has been developed that has no moving parts; it measures flows from 1 to 180 gallons per minute.</i>	
BIOSCIENCES	88
Vegetation Studies and Biospherics Research	90
<i>Vegetation studies related to fire effects on wetlands and oak scrub plant communities along with projects related to understanding fire history, launch effects, and potential changes due to elevated carbon dioxide continue.</i>	
Plant Space Biology Program	91
<i>Research into supply plants with water and nutrients and their physiological response to altered gravity continues.</i>	

CONTENTS (Cont)

CELSS: The Interaction of Humans and Plants	93
<i>Experiments were initiated for the quantification of mass and gas exchange between plants and humans in a closed life support system.</i>	
Habitat Assessment Group	95
<i>Maps of scrub jay population centers have been prepared and a habitat suitability model was developed to assist in biological assessments of KSC operations. Other species, such as Indigo snakes, gopher tortoises, and wading birds, are continually monitored to evaluate impacts.</i>	
Orbiter Environmental Simulator	97
<i>The Orbiter Environmental Simulator simulates the Orbiter flight environment.</i>	
Controlled Ecology Life Support System (CELSS) Biomass Production Chamber	98
<i>Crop tests in the CELSS Biomass Production Chamber continued during the past year, including tests with soybean, lettuce, and potato.</i>	
Biomass Production Research	100
<i>The influence of carbon dioxide concentration and spectral quality of electric lighting systems on potato growth and development is being studied for Controlled Ecological Life Support Systems.</i>	
Remote Sensing and Geographic Information Systems	101
<i>The Remote Sensing and Geographic Information System Laboratory has been upgraded with two SUN SPARC2 workstations. Cooperative efforts have been established with KSC Master Planning to share information pertinent to environmental monitoring.</i>	
EPCOT Project	101
<i>The plant nutrient delivery system in the NASA/EPCOT project is now automated for the generation of plant growth data.</i>	
Air Quality Monitoring	102
<i>Air-monitoring instruments and a new trailer have been established at the PAMS site.</i>	

CONTENTS (Cont)

Heat Stress Evaluation of Rescuemen's Protective Suit	104
<i>KSC tests show that the use of a cool vest can retard core temperature buildup during rescue scenarios.</i>	
Biomass Processing Research	105
<i>Development continues on the conversion processes for transforming biomass production chamber crop harvest residues into edible products.</i>	
Porous Tube Plant Nutrient Delivery System	106
<i>Work continues on optimizing the nutrient delivery system design being developed for growing plants in microgravity.</i>	
Aquaculture Research	107
<i>Initial tests using the closed aquaculture system measured the carbon flow through the fish and microbial communities.</i>	
Human Physiology Research Projects: Blood Pressure Control	108
<i>Two research projects were undertaken to determine the effects of acute changes in blood volume and long-term restriction from normal upright posture on the blood pressure control system in man.</i>	
METEOROLOGY	111
Research Studies Using Simulated Lightning	113
<i>The lightning simulator generates simulated lightning in support of lightning atmospheric chemistry research to produce electromagnetic fields and to simulate lightning strikes for structural lightning protection testing.</i>	
Lightning Detection Algorithm	115
<i>A new algorithm for detecting lightning field changes has been designed by Kennedy Space Center and is being integrated into the Electric Field Mill Network.</i>	

CONTENTS (Cont)

Time-of-Arrival Lightning Location System Using Five-Station Wideband Electric Field Measurements	117
<i>A wideband electric-field-measuring network locates sources of lightning-generated electromagnetic radiation up to 50 kilometers from the Shuttle Landing Facility.</i>	
TECHNOLOGY UTILIZATION	120
Automatic Tree Counting System	121
<i>A cooperative project to find a standalone system that rapidly counts trees digitized from a photograph.</i>	
Heat Pipes and Phase Change Materials for Residential Thermal Energy Storage	122
<i>The objective of this effort is to develop a low-cost, compact Thermal Energy Storage module to augment residential space heating for utility load management.</i>	
Thermal Storage Module	124
<i>The objective is to develop a Thermal Energy Storage (TES) system for utility load management utilizing heat pipe technology. This unit stores heat in a solid-to-solid phase change material for discharge during peak load periods.</i>	
Magnetic Resonance Imaging Technology	125
<i>NASA satellite imaging computer technology is being applied to Magnetic Resonance Imaging (MRI) to improve detection and treatment of cancerous tumors.</i>	
Development of a Solid Polymer Electrolyte (SPE) Oxygen Concentrator	126
<i>A solid polymer electrolyte oxygen concentrator is being developed for the production of medical-grade oxygen from air. The device utilizes a solid polymer anion exchange membrane for the cathodic reduction of air to oxygen.</i>	

CONTENTS (Cont)

MATERIALS SCIENCE	128
Protective Coating Systems for Repaired Carbon Steel Surfaces	130
<i>New metal coating products are undergoing laboratory and field evaluation tests to determine their ability to protect repaired carbon steel from the Kennedy Space Center marine and launch environment even if surface preparations are less than perfect.</i>	
Environmentally Compliant Coating Systems for the Shuttle Launch Sites	131
<i>Environmentally compliant, inorganic, zinc coating systems for protection of launch site structures and equipment are undergoing evaluation for use in the Kennedy Space Center environment.</i>	
Protective Top Coating Systems for the Space Transportation System Launch Environment	132
<i>Top coatings, for the protection of zinc-rich primers (applied to launch site structures and equipment) from the acidic residues produced by solid rocket boosters, are undergoing a 5-year, harsh-environment exposure program.</i>	
Corrosion-Protective Coatings From Electrically Conducting Polymers	133
<i>The objective of the research effort is to develop organic corrosion control coatings, which are easily applied and repaired, resistant to the acid launch environment.</i>	
Accelerated Testing of Inorganic, Zinc-Rich Primers	137
<i>Electrochemical techniques are being investigated as an accelerated method for testing the corrosion resistance of inorganic, zinc-rich primer systems for use on Kennedy Space Center launch structures and equipment.</i>	
Stress Testing of Engineering Materials	138
<i>Testing is being conducted on 50 common metallic alloys to determine their susceptibility to stress corrosion cracking in the Shuttle launch environment.</i>	
Development of New Flooring Materials for Clean Rooms and Launch Site Facilities	138
<i>Formulations of PVC and high-density polyethylene for floor tiles, suitable for class-100 clean room applications, were developed.</i>	

CONTENTS (Cont)

Development of a New Chemical-Resistant Fabric for Protective Clothing	139
<i>A program to identify a fabric resistant to toxic propellants used at Kennedy Space Center has been initiated and will eventually result in the next generation of completely encapsulating protective suits.</i>	
Compatibility of Corrosion-Resistant Alloys With Aerospace Fluids	140
<i>A study of alloys resistant to the Kennedy Space Center environment has been initiated to determine their susceptibility to hydrogen embrittlement and stress-corrosion cracking in typically used aerospace fluids.</i>	

Hazardous Emissions and Contamination Monitoring

Kennedy Space Center stores and pumps huge quantities of cryogenics as well as lesser amounts of exotic fluids. The extreme toxicity and volatility of these fluids mandate a comprehensive safety program. Four development laboratories are responsible for implementing the specialized instrumentation hardware and systems that satisfy stringent safety requirements.

Hazardous Gas Detection Laboratory

The Hazardous Gas Detection Laboratory has the continuing task of implementing systems that are capable of measuring (in complex mixtures) gaseous components both qualitatively (specifically hydrogen, helium, nitrogen, oxygen, and argon) and quantitatively (parts-per-billion range). A typical hazardous gas detection system comprises a mass spectrometer, a sample and calibration gas delivery subsystem, and a data acquisition and control system. The laboratory projects receiving the most attention are: (1) applying artificial intelligence/expert systems to aid in real-time diagnostics and troubleshooting, (2) operations monitoring and data interpretation, (3) developing a military specification, and (4) flight-qualified miniature detection systems for advanced launch systems.

Optical Instrumentation Laboratory

The Optical Instrumentation Laboratory develops and tests imaging systems for viewing phenomena that are undetectable to the unaided eye or by normal viewing techniques (for example, hydrogen fires and other thermal emitters and hydrogen and other gas clouds). A laboratory achievement is the design and demonstration of a multispectral television camera that is capable of unambiguously imaging and color coding fuel fires in the infrared and ultraviolet spectral emission ranges. The laboratory is equipped with an optical spectrometer for measuring the emission spectra of an extensive variety of radiating sources.

Toxic Vapor Detection Laboratory

The Toxic Vapor Detection Laboratory (TVDL) is developing two new series of toxic vapor detectors because the commercially available instrumentation does not meet the current Government standards for measuring trace amounts of hypergolic fuels and concentrated ammonia vapors in an ambient background. The TVDL was established to perform research on detection techniques; to design, build, and test prototype and/or modified commercial detectors; and to evaluate new commercial instruments. All research and tests are performed utilizing the TVDL's unique capability to provide a wide range of toxic vapor concentrations at controlled flow rate, temperature, and relative humidity conditions. All tests are computer controlled to provide comprehensive qualitative and quantitative performance evaluations of every instrument tested.

Contamination Monitoring Laboratory

The Contamination Monitoring Laboratory was established to perform contamination monitoring research and development; to develop contamination measuring systems; to evaluate commercially available particle counters, hydrocarbon and nonvolatile residue monitors, and other instrumentation; and to advance the technology in the areas of real-time nonvolatile residue (NVR), real-time particle fallout monitoring, and contamination monitor calibration methodology. The laboratory is equipped with particle counter systems, personal-computer-based data acquisition and control systems, a pulse height analyzer, a research-grade Fourier transform infrared (FTIR) spectrophotometer, nondispersive infrared analyzers, an aerosol standards generation system, an optical microscope, and a normal complement of test and measurement instrumentation.



Hazardous Gas Detection Laboratory



Toxic Vapor Detection Laboratory

Evaluation of Hypergolic Oxidizer Vapor Detectors

Objective

To test and evaluate commercially available portable instruments for nitrogen dioxide detection at and below the new short-term exposure levels.

Background

Recently, the short-term exposure limit (STEL) for nitrogen dioxide was reduced to 1 part-per-million (ppm) in a 15-minute time period. Nitrogen dioxide monitors with data-logging capabilities are required to ensure that exposures do not exceed the STEL. A market survey of commercially available detectors was conducted. According to the claims of four different manufacturers, four instruments were reported to meet NASA's performance requirements. A test plan was designed to evaluate these instruments for performance characteristics required by NASA in a controlled laboratory environment.

Approach

Six detectors representing four manufacturers were chosen for this study. These detectors included two Draeger Model 190 detectors, two Compur Monitox detectors, a Transducer Research, Inc., Odyssey 2001 Gas Analysis System, and an Interscan Model 5150BX. The Transducer Research, Inc., model uses an active sampling system that pumps air to the detection cell, while the other models use diffusive sampling.

Tests were conducted to determine the characteristics of each instrument over a broad variety of conditions. The instruments were tested side by side in a test chamber designed specifically for this program. The nitrogen dioxide in air was prepared by dilution of calibrated gas standards and was verified indepen-

dently by a chemiluminescence detector.

Results and Conclusions

The Draeger Model 190 is the detector best suited to meet the needs outlined by NASA. This instrument is small and lightweight, and it performed well in all of the tests. Some of its strongest points include: a quick response time of 40 seconds to a 90-percent signal at 1 ppm, a recovery time of 50 seconds to 10 percent of a 1-ppm signal, no interferences from the vapors tested, a signal-to-noise ratio of 40 at a 1-ppm signal, and good data collection and transfer capabilities. The Draeger Model 190 is small and light enough to be worn as a personal monitor by a user without discomfort.

The Compur Monitox detector also performed well over the course of the test. It had a signal-to-noise ratio of 100 at a 1-ppm signal, but a slower response time of 90 seconds to a 90-percent signal, and a recovery time of 77 seconds to 10 percent of a 1-ppm signal. This model is also small and light enough to be used as a personal monitor. It had a positive response to hydrazine, awkward data collection, and transfer capabilities. The data collection capability problems could be circumvented by using a better data logger.

The Interscan instrument also performed well as a nitrogen dioxide detector. It had response and recovery times of 55 and 43 seconds at a 1-ppm exposure. There was a minor interference caused by hydrazine. The instrument is too large and heavy for use as a personal monitor and had no local readout to provide information to the user. The data-handling hardware abilities of the instrument were good but the software was often confusing.

The Transducer Research, Inc., Odyssey 2001 was the only active sampling instrument included in the test program. It is somewhat larger than the other monitors. It had response and recovery times of 20 and 60 seconds at a 1-ppm exposure. This instrument has a number of

sampling options that offer a great deal of flexibility such as a programmable autozero. The alarm levels were easily changed. In addition, the data-handling capabilities of this instrument include data transfer from the instrument to a personal computer via a serial link, direct access to an analog signal, and good software.

Contact:

R. C. Young, 867-4438, DL-ESS-24

Participating Organizations:

Naval Research Laboratory (S. L. Rose-Pehrsson)

GEO Centers, Inc. (T. L. Cecil)

NASA Headquarters Sponsor:

Office of Space Flight

**Evaluation of GMD Systems, Inc.,
MK-2 Portable Fuel Vapor Detector
for MMH, N₂H₄, and UDMH**

Objective

To perform an initial evaluation of the conceptual portable fuel vapor detector for 10-part-per-billion (PFVD-10) MK-2 developed by GMD Systems, Inc., intended to accurately monitor the presence of hydrazine (N₂H₄), monomethylhydrazine (MMH), and unsymmetrical dimethylhydrazine (UDMH) to levels of 10 parts per billion (ppb).

Background

Recently the American Conference of Governmental Industrial Hygienists (ACGIH) proposed to reduce present threshold values for N₂H₄, MMH, and UDMH (100, 200, and 500 ppb, respectively) to 10 ppb for all hydrazines. To meet the new proposed requirement and to ensure personnel safety, NASA at Kennedy Space Center (KSC) initiated development of a portable fuel vapor detector capable of quantifying 10 ppb in near-real time. Contracts were let

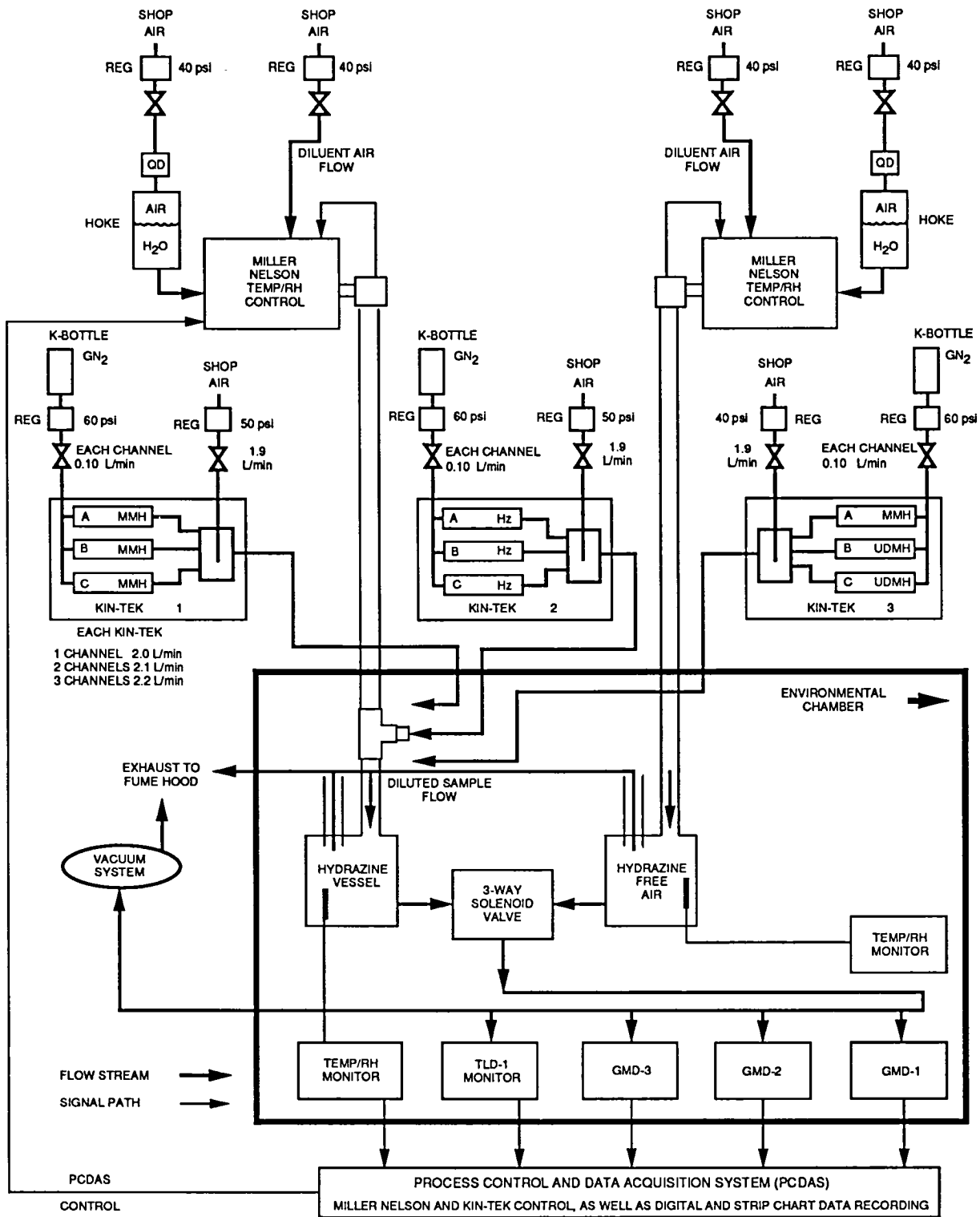
for development of conceptual units to two manufacturers while GMD opted to proceed with a company-sponsored development effort. NASA bought three of the GMD conceptual units for evaluation and qualification testing at the NASA/KSC Toxic Vapor Detection Laboratory (TVDL). In order to test the GMD units now, and the other two conceptual units when they are delivered to NASA/KSC, TVDL designed and assembled a vapor generation system capable of reliably providing a range of 1 to 400 ppb of N₂H₄, MMH, and UDMH vapors over a range of temperatures and relative humidities (RH's). This report covers the tests done on the GMD units to date.

The conceptual GMD instruments detect the presence of the hydrazines by utilizing two colorimetric chemistries: 3-methoxy-4-hydroxybenzaldehyde (vanillin) for MMH and N₂H₄, and 2,4-dinitrobenzaldehyde for UDMH. A paper tape impregnated with the respective organic compound changes to a yellow color when exposed to fuel vapors. The intensity of the color is used to measure the vapor cumulative concentration. In operation, the instrument pumps 200 milliliters per minute of sample through the tape, causing a development of yellow stain in the vanillin-treated paper if one of the hydrazine vapors is present. The GMD MK-2 is a microprocessor-controlled instrument with a liquid crystal display readout and full data storage logging capabilities.

Approach

For this project, a vapor generation system was designed to deliver known concentrations of N₂H₄, MMH, and UDMH at controlled conditions of temperature and relative humidity. The system consists of six components: (1) toxic vapor generator, (2) flow/temperature/relative humidity (F/T/RH) controller, (3) sample vessels (hydrazine vessel and hydrazine-free vessel), (4) temperature/relative humidity monitor, (5) reference vapor concentration monitor, and (6) the GMD MK-2. The test was conducted inside an environmental chamber. The test

Hazardous Emissions and Contamination Monitoring



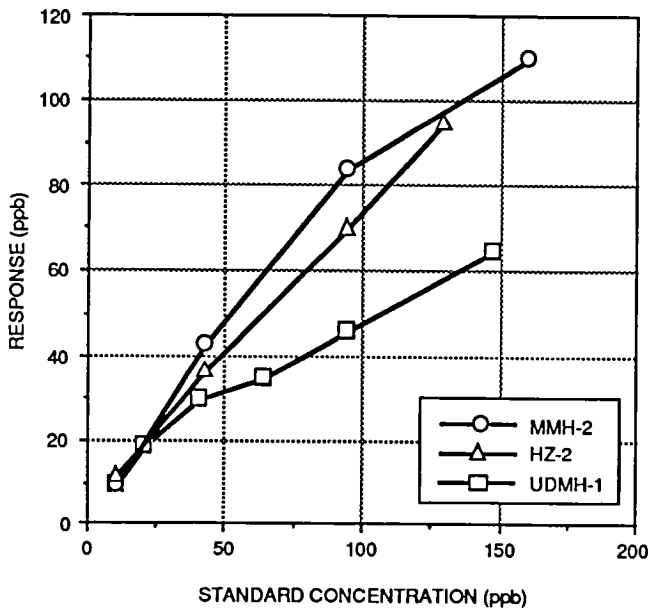
NOTE:
 THE INSTRUMENTS WERE PUT THROUGH TESTS TO MEASURE THE TIME RESPONSE, LINEARITY, AND RELATIVE HUMIDITY. TESTS FOR THE PRECISION, ZERO-AND-SPAN DRIFT, TEMPERATURE DEPENDENCIES, AND INTERFERENCE WILL BE CONDUCTED LATER.

PFVD-10 Apparatus Setup

setup is shown in the figure "PFVD-10 Apparatus Setup."

Results

Linearity. The linearity of the instruments was tested over the range from 10 to 400 ppb. The first round of tests indicated that the linear range for MMH and UDMH was about 0 to 150 ppb. The linear range for N_2H_4 was about 0 to 125 ppb. The MMH and UDMH instrument response to the respective 10-ppb vapors was 10 ± 1 ppb; whereas, the N_2H_4 instrument response



Linearity at 45-Percent Relative Humidity and 25 Degrees Celsius for MMH, N_2H_4 and UDMH

was 14 ppb. Results of the linearity tests for all three of the hydrazines are shown in the figure "Linearity at 45-Percent Relative Humidity and 25 Degrees Celsius for MMH, N_2H_4 , and UDMH."

Response Time. The MMH and N_2H_4 instrument required about 20 minutes to stabilize in response to 10 ppb, and 4 minutes for 20 ppb. As the concentrations increased to 90 ppb, the response time decreased to 2 minutes. The response time for the UDMH instruments was 4

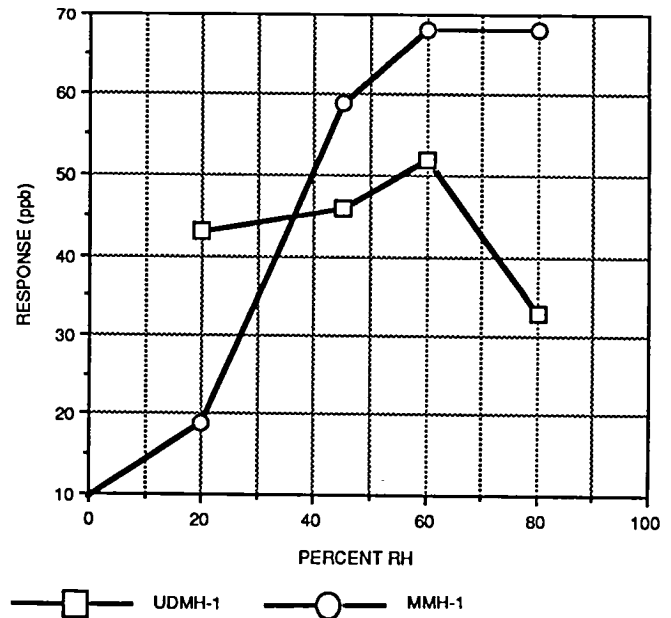
minutes for concentrations of 10 and 20 ppb. The response time improved to 2 minutes at concentrations of 40 to 90 ppb.

Relative Humidity. The instruments were tested with 90-ppb MMH vapor from 10 to 80 percent RH at 25 degrees Celsius. The instrument response to the MMH vapor increased as the RH increased. At 10-percent RH, the instrument showed no response. The instrument read 20 ppb at 20-percent RH. When the RH was increased to 60 percent, the instrument read 68 ppb.

Unlike MMH, the UDMH measurement showed a decreased sensitivity at both low and high RH's. The responses versus percent RH plot for both MMH and UDMH instruments are shown in the figure "Response to 90-ppb MMH and UDMH Versus RH at 25 Degrees Celsius."

Conclusion

These preliminary tests showed that the GMD MK-2 is capable of 10-ppb MMH, N_2H_4 , and UDMH vapor detection under conditions



Response to 90-ppb MMH and UDMH Versus RH at 25 Degrees Celsius

that would normally be encountered in work areas requiring monitoring for 10 ppb of hydrazines (e.g., closed, air-conditioned rooms/laboratories). However, faster response times, reduced RH dependency, and an increased linear dynamic range are required in order to meet the full PFVD-10 specifications. GMD is continuing to work to improve these units with the assistance of testing by the NASA TVDL. A more extensive test is planned to determine whether the GMD MK-2 detectors are suitable for use by NASA and United States Air Force safety personnel.

Contact:

R. C. Young, 867-4438, DL-ESS-24

Participating Organization:

Boeing Aerospace Operations, Engineering Support Contract (N. A. Leavitt)

NASA Headquarters Sponsor:

Office of Space Flight

Hydrogen Umbilical Mass Spectrometer (HUMS)

Objective

To develop a hazardous gas detection system that features high reliability, high accuracy, ease of maintenance, and self-validation and permits operation with minimal human intervention.

Background

A mass spectrometer-based system is required to serve as a temporary backup to the primary hydrogen (H₂) remote sensing system and to provide concentration information beyond the primary system's capabilities. The system measures gas concentrations in and around the Shuttle Orbiter/external tank disconnect hydrogen umbilical and the Orbiter mid-body umbilical unit (OMBUU). In addition, the system includes a capability to support flight readiness firing and to take other measurements. This

system shall be designated the Hydrogen Umbilical Mass Spectrometer (HUMS) and will remain in place until a permanent HUMS II is installed.

Approach

A survey had been conducted to identify process mass spectrometers that were manufactured under strict quality requirements, whose design was sufficiently mature, and had been produced in quantities. Comparing HUMS requirements to the survey findings resulted in the selection of the Perkin Elmer MGA-1200 mass spectrometer. The basic MGA-1200 was ordered with a turbomolecular pump and other features necessary to satisfy HUMS requirements. Earlier vibration testing of turbopumps for the Advanced Hazardous Gas Detection System (AHGDS) program had established that several of these pumps could withstand the vibration environments typical of Shuttle launches. The remaining elements of the system, such as the sampling subsystem, the command and data subsystem, and the associated support equipment, are being defined and produced. There will be a special effort for the development of using knowledge-based techniques to ease the operator interface and decisionmaking process.

Results

The HUMS sample delivery subsystem will be almost identical to a sample delivery subsystem developed for an upgrade of the Backup Hazardous Gas Detection System (BU HGDS). This system has a capacity to handle eight sample lines. An additional portable 14-line sample delivery subsystem is a part of HUMS. This portable addition will enable HUMS to handle up to 21 sample lines in support of flight readiness firing.

A new control and data subsystem featuring ruggedized ROM-based OS9 operating system and control code written in "C" will be supported by a remote control station based on a Silicon Graphics workstation running UNIX/X-Windows-

based display and control features by mouse and keyboard.

Future Plans

Long-term operational testing is being conducted on the pumps that successfully passed the initial vibration tests. The proposed subsystems and components that will comprise the HUMS will be designed, acquired, and tested. This will lead to the integration, assembly, test, and demonstration of an operational HUMS prior to September 1992.

Contacts:

W. R. Helms, 867-4438, DL-ESS-2

J. D. Collins, 867-4449, DL-ESS-24

F. W. Adams, 867-4449, DL-ESS-24

Participating Organizations:

Boeing Aerospace Operations, Engineering Support Contract (C. M. Lampkin and F. Lorenzo-Luaces)

Naval Research Laboratory (Dr. J. R. Wyatt and Dr. M. Ross)

NASA Headquarters Sponsor:

Office of Space Flight

Improved Oxygen Monitors for the Space Station Processing Facility

Background

Large quantities of gaseous nitrogen and helium will be used in processing Space Station Freedom elements in the Space Station Processing Facility at Kennedy Space Center (KSC). These gases will be supplied through a distribution system located in service tunnels. NASA regulations require monitoring for oxygen deficiency in enclosed volumes such as the atmosphere in the service tunnels; therefore, an oxygen-deficiency monitoring system will be installed. Since the oxygen monitors will be used in a safety-related system, fast response time and very reliable service are essential.

Approach

An initial market survey identified instruments based on a wide variety of technologies such as electrochemical, zirconium crystal, and several types of paramagnetic sensors. A number of instruments were procured, and an initial screening of these instruments was then performed during which nonfunctional units were returned to the vendor for repair. Instrument packaging was then assessed for ruggedness and accessibility of components for servicing.

Testing of the instrumentation began with a response time test and included linearity, accuracy, precision, zero drift (100-percent-nitrogen sample) and span drift (breathing-air sample), and long-term testing. In addition to operational characteristics, these instruments were also tested for sensitivity to typical chemical compounds that might be found in the areas they will monitor.

Several different instruments were then selected as candidates for a competitive procurement, and performance specifications were written. Factors used in instrument selection were: (1) 90 percent response time of less than ten seconds, (2) accurate response for samples containing nitrogen and/or helium, and (3) long operational life with infrequent calibration required.

Results

The table "Summary of Oxygen Analyzers Tested" shows the instruments evaluated, their principles of operation, and observations concerning the unit.

One surprising result is that certain oxygen analyzers gave erroneous readings when exposed to an oxygen-deficient sample consisting of a mixture of breathing air and helium. These instruments responded incorrectly to both stable mixtures and changes in the concentration. The detector utilized in the monitors that had

Hazardous Emissions and Contamination Monitoring

Summary of Oxygen Analyzers Tested

Model	Detection Method	Comments
Servomex 570A	Magnetodynamic dumbbell	Unit performed well; too heavy for practical use as a portable
Servomex 1175	Magnetodynamic dumbbell	"B" model faster and more stable than "A"; responded well
Servomex 540A	Magnetodynamic dumbbell	Responded well; analog concentration display and flow indicator may stick on older units
City Cell	Electrochemical cell	"Pressure-sensitive" cell responded improperly in the presence of helium; "nonpressure sensitive" model performed well
Draeger Polytron	Electrochemical cell	Some cells responded in less than 10 seconds, but manufacturer did not guarantee fast response
Delta F Series 500	Nondepleting coulometric	Instrument periodically malfunctioned and alarmed, showing 10 percent oxygen concentration
Neotronics	Electrochemical cell	Responded to methyl alcohol and cleaners; gave false oxygen readings in the presence of helium
Ceramatec Cerion	Zirconium crystal	Requires reference air supply; units plagued with electrical problems and contamination of crystals
Panametrics	Paramagnetic wind	Three models tested; none met all response time and stability requirements; not packaged as complete instrument
Japan Storage Battery	Electrochemical cell	Very stable; long life; inexpensive; did not meet response time requirements
Hartman-Braun Magnos 6G	Magnetodynamic dumbbell	Very stable; did well in testing; no internal pump

problems in helium was an electrochemical cell.

Conclusion

Many of the oxygen analyzers studied suffered from problems related to poor packaging. Certain technologies, (e.g., zirconia crystal), suffered from inherent limitations (such as excessive warmup times and the need for a reference air supply). The requirement for a response time less than ten seconds eliminated many instruments. Some were eliminated from consideration due to a need for frequent calibration. Others were unsuitable because of high maintenance requirements.

The most suitable technology evaluated thus far is based on the paramagnetic properties of oxygen. These instruments do not require frequent calibration or maintenance and do not use expendables such as electrochemical cells.

Contact:

P. A. Mogan, 867-4438, DL-ESS-24

Participating Organization:

*McDonnell Douglas Space Systems Company
(V. V. Bukauskas and L. H. Allen)*

NASA Headquarters Sponsor:

Office of Space Flight

Reliable, Cost-Effective Particle Counter Calibration System

Background

Optical particle counters (OPC's) constitute the primary method for validating acceptable levels of particulate contamination in aerospace clean-room processing facilities. In 1987, an evaluation program conducted at Kennedy Space Center (KSC) revealed a large variation in the readings taken with "calibrated" OPC's from different manufacturers. This variability was found to exist not only when sampling ambient aerosols but also when monitoring a stream of

reference calibration microspheres.

A prime factor contributing to variations in OPC performance was traced to variances in instrument calibration methodology. In 1989, a joint research project with the University of Arkansas at Little Rock was initiated with the expressed goal of improving calibration procedures. A two-step approach was adopted. The first step was to determine the optimal way to generate stable, repeatable concentrations of aerosol particles of known size in the 0.5 to 5.0 micrometer size range. This part of the project was described previously in the Research and Technology 1989 Annual Report, and further details related to this first objective are presented here. The second step will be to develop methods of quantitatively verifying the actual number of particles per cubic foot of sample, thus addressing for the first time the issue of accuracy in optical particle counters.

Approach and Research Plan

All OPC manufacturers now call for the use of reference polystyrene latex microspheres for calibrating their instruments for size discrimination. Since compressed air nebulization is now the method of choice for aerosolizing reference latex particles in the 0.1- to 2.0-micrometer size range, the initial objective is to identify an inexpensive nebulizer with adequate stability and dynamic size range (up to a 5.0-micrometer latex particle). (The vibrating orifice aerosol generator was evaluated and found unsuitable for operation with a particulate suspension.) Once the nebulizer is selected, the preferred suspension medium (e.g., water, isopropanol, etc.) for low-background particle production should then be determined.

An optimal generation system in which to incorporate the nebulizer is then designed, assembled, tested, and characterized. Means for adequately drying and diluting the nebulizer output must be included. The possible influence of varying temperature and humidity in the test aerosol generator (TAG) mixing plenum should

be investigated. Finally, the conditions and modifications necessary for producing and maintaining a stable concentration of aerosol particles must be sought. The various factors that contribute to instabilities in particle concentration should be identified, characterized, and modeled.

Results

A variety of nebulizers were tested: Devilbiss Model 646 (Devilbiss Co., Somerset, PA), the Lovelace Nebulizer (Intox Products, Albuquerque, NM), the Collison Nebulizer (BGI Inc., Waltham, MA), Airlife Solo-Sphere Nebulizer (American Hospital Supply Corp., Montclair, CA) and several medical-grade nebulizers, including the Dart Respiratory Jet Nebulizer (Professional Medical Products, Greenwood, SC). This latter device, the Dart nebulizer, proved the best performer in aerosol output stability and dynamic size range capability. In addition, these units cost only a few dollars each. Tests showed: (1) the Dart is an adequate aerosol product throughout the full 0.5- to 5.0-micrometer size range and (2) the Dart operates better (less background contamination) with latex suspension in reagent grade water compared with isopropanol.

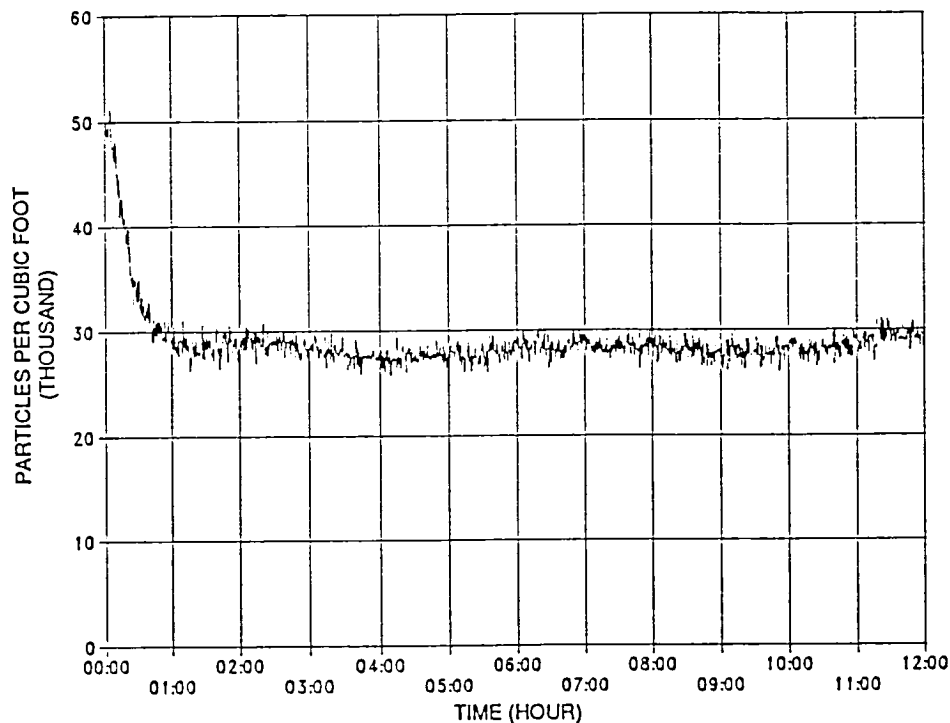
The complete aerosol generator includes an air purification system with separate dryer and filter, a chamber for mixing the aerosol output with dry dilution air, a sampling/drying plenum from which OPC's may continuously sample, and an exhaust route with a high-efficiency particulate air (HEPA) filter for excess aerosol particulates.

Initial and subsequent studies have shown a persistent logarithmic or, in some

cases, linear decrease in particle concentration. By empirically modifying various components of the TAG, it is now recognized that the key to the variability rests with the nebulizer itself. A temperature/humidity probe mounted in the drying/sampling plenum has shown that there is no correlation in output variability with these two environmental parameters. The operating conditions of the nebulizer are the primary factors in controlling TAG output. Factors that minimize the suspension concentration change in time (e.g., operating pressure) are being optimized for producing a stable aerosol concentration (see the figure "Test Aerosol Generator Concentration Versus Time"). Aerosol concentrations can be produced that vary less than five percent per hour over a four-hour period of operation.

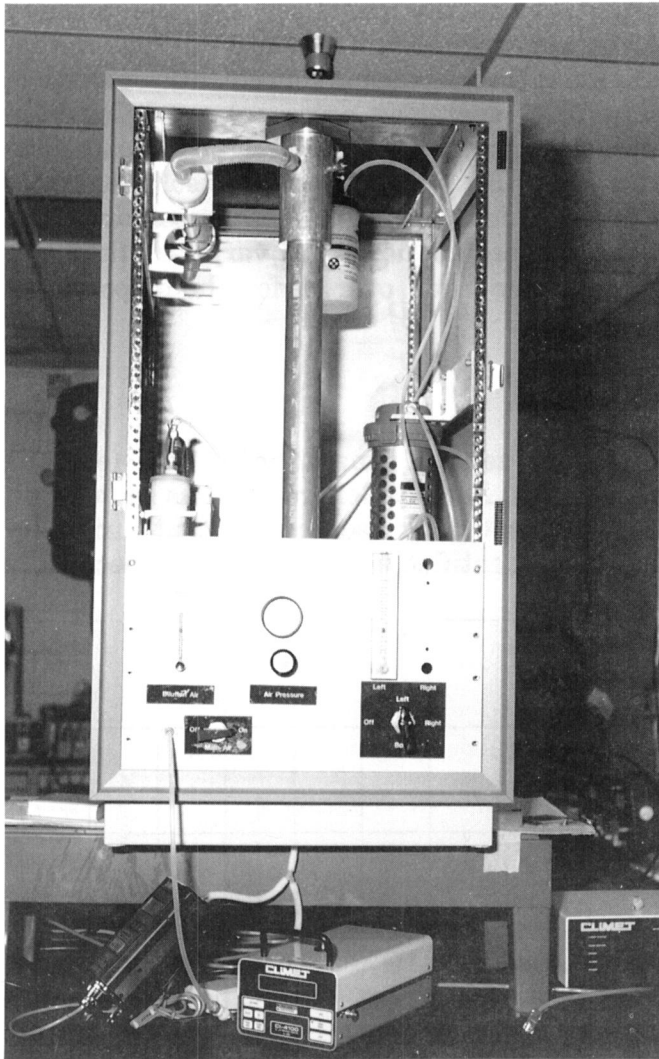
Conclusion

A test aerosol generation system (see the figure "Test Aerosol Generator") has been developed and tested. The source of output variability has been identified as the nebulizer, specifically



Test Aerosol Generator Concentration Versus Time

the reduction in particle suspension concentration within the reservoir. Altering operating conditions to minimize the change in suspension concentration has greatly improved the TAG stability. Although further study is needed to develop a better understanding of factors influencing stability of particle concentrations gener-



Test Aerosol Generator

ated by the system, the current system can be fielded in calibration laboratories at KSC and will provide an inexpensive and reliable method to generate particles for the calibration of OPC's.

Contact:

P. A. Mogan, 867-4438, DL-ESS-24

Participating Organizations:

University of Arkansas at Little Rock (A. Adams)

*McDonnell Douglas Space Systems Company
(V. V. Bukauskas and A. Duong)*

NASA Headquarters Sponsor:

Office of Space Flight

AC Motor Valve Hypergol Leak Detector

Objective

To evaluate the Interscan's capability to detect and quantify monomethylhydrazine (MMH) and nitrogen dioxide (NO₂) leaks in the Reaction Control System/Orbital Maneuvering System (RCS/OMS) alternating current (ac) motor valve housings. Two questions were posed: (1) does the use of different lengths (4 to 11 feet) of the small diameter [1/8-inch inside diameter (ID)] Teflon sample tubes cause discrepancies in the detection and quantification of the MMH/NO₂ and (2) does the limited volume (approximately 27 cubic centimeters) of the sample contained in the valve body prevent detection and accurate quantification of the hypergols present?

Background

Lockheed Space Operations Company (LSOC), under the direction of NASA Vehicle Engineering (TV-FSD-22), performs the postmission processing of the Orbiter. As part of this processing, LSOC tests the ac motor valves that control the flow of hypergols in the RCS/OMS to determine whether the valves are leaking or have leaked. LSOC uses Interscan electrochemical detectors (model 4180 for MMH and model 4152 for NO₂) to detect the presence of MMH and/or NO₂ in the valve bodies. Concern was raised as to whether the Interscans were responsive and sensitive enough when sampling a relatively small sample through a long slender (1/8-inch ID) tube to even be capable of perform-

ing the basic mission. NASA Toxic Vapor Detection Laboratory (TVDL) was requested to perform a complete evaluation to investigate the Interscan MMH and NO₂ detector's ability to accomplish its mission.

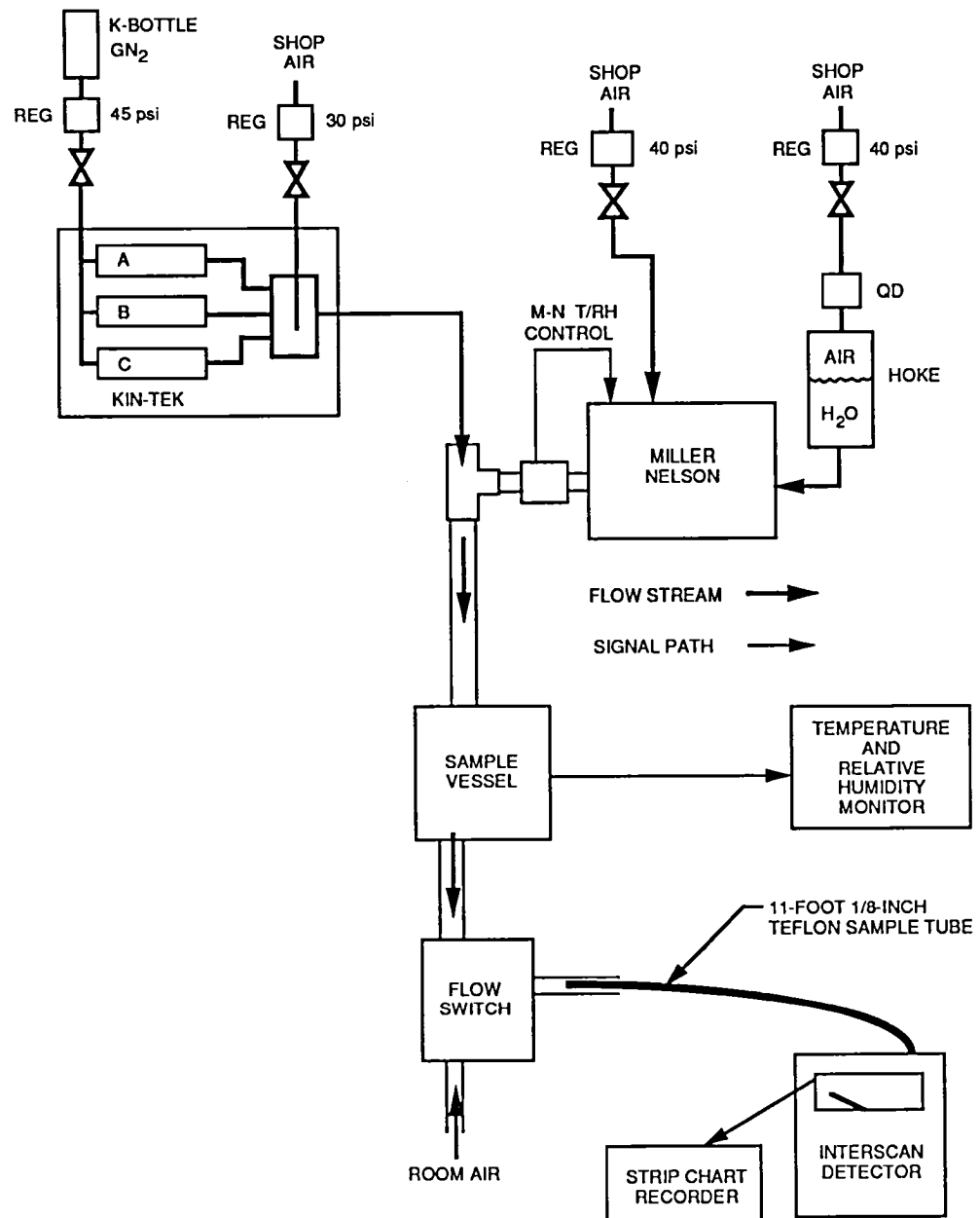
Approach

Dynamic and static tests were devised for the Interscan MMH and NO₂ units. The dynamic test was performed to verify the Interscan's ability to accurately detect and quantify the presence of hypergolic vapors in a constant concentration gas stream. The static test was performed to evaluate the ability of the Interscan to detect known concentrations of hypergols under conditions that simulated actual operational conditions (where the total amount of sample is very limited).

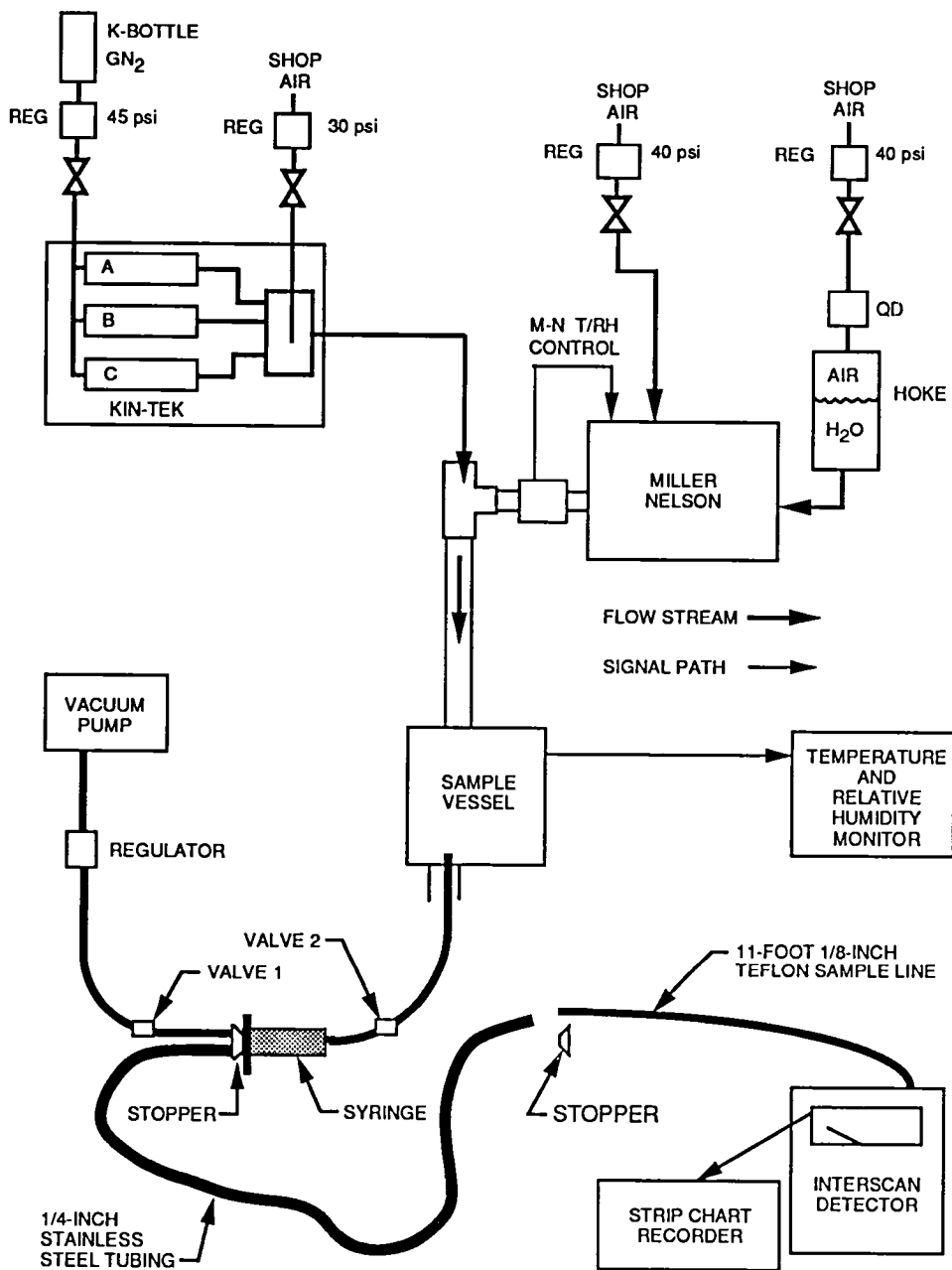
The dynamic test used a test setup (see the figure "Dynamic Test Setup" with a continuous flow of test gas at four different concentrations. MMH concentrations were 1.2, 2.4, 8.4, and 29.5 parts per million (ppm) and NO₂ concentrations were 2.4, 3.5, 12.5, and 33.8 ppm. The samples were taken through two different lengths (4 and 11 feet) of 1.8-inch ID Teflon tubing. A valve (flow switch) was connected to

the end of the sample tube to provide the ability to switch between the zero air (room air) and the calibrated test gas. Data output from the Interscan was visually monitored on the instrument meter and recorded on a strip-chart recorder.

The static test setup (see the figure "Static Test Setup") used a 50-milliliter (mL) syringe to



Dynamic Test Setup



Static Test Setup

simulate the Orbiter's ac motor valve and a 10-foot-long piece of 1/4-inch ID stainless steel tube to simulate the guide tube between the valve and the check port. The same concentrations were used for the static and dynamic tests. Test gas was drawn from the sample vessel through the syringe until the concentration in the syringe reached equilibrium. The syringe was then sealed off by the valve at each end, trapping a

known concentration sample in the syringe to simulate the amount of MMH/NO₂ that would be trapped in the valve body. The contents of the syringe were then sampled by inserting the Teflon sample tube through the stainless steel guide tube. Only the 11-foot sample tube was used for this test, because it was expected to be the most restrictive case.

Results

Interscan MMH Detector

Results of this study are summarized in the table "MMH Results." The slow reaction time, low sensitivity, and lack of reproducibility made the Interscan MMH detector a poor choice for MMH detection under these operational conditions. The long thin sample tube prevented the Interscan MMH detector from measuring the correct concentration. Using different lengths of sample tube required that the unit be calibrated for each length to ensure reasonable accuracy.

The unit failed to detect MMH concentrations as high as 32 ppm when sampling only 6 inches from the simulated motor valve. It only marginally detected the presence of MMH when the sample tube was inserted into the valve body and could not with any degree of confidence quantify the amount present. Thus, the detector would likely record a zero reading even when there was considerable MMH present from a

leaking ac motor valve.

Interscan NO₂ Detector

Results of this study are summarized in the table "NO₂ Results." The Interscan NO₂ unit responded relatively quickly and repeatably to fairly low concentrations of oxidizer. The long thin sample tube did not prevent the unit from functioning adequately. However, tests revealed the ineffectiveness of sampling from 6 inches away from a suspected leaky ac motor valve assembly. Vastly improved results and much higher confidence will be obtained if procedures were changed to require samples to be taken at the edge of valve assemblies.

Conclusions

The MMH detector is not capable of performing the task required and the NO₂ detector is

marginally able to perform its task. These conclusions resulted in three recommendations.

1. Change Operational Procedures. Every effort must be made to draw the sample from as close to the valve body as possible. Test results strongly suggested current procedures would probably fail to detect leaky valves even if there was significant vapor present and the sample was taken from as little as 6 inches away from the valve.
2. Develop New MMH Detector. The current MMH detector is deficient, even if the sample tube can be inserted into the valve body itself. A new detection system, based on the vanillin paper tape technology (applied to the Interim Active Vanillin Sampler for detection of 10 parts per billion of MMH) will be investigated for applicability in the ac motor valve test. Preliminary exploration of alternate

MMH Results

Standard (ppm)	Dynamic Sample*				Static Sample*	
	4-Foot Tube		11-Foot Tube		ppm (6 inches away)	ppm (at valve edge)
	Duration	ppm	Duration	ppm		
0.0	6 s 20 s 1 min	0.0 0.0 0.0	6 s 20 s 1 min	0.0 0.0 0.0	0	0.1
1.2	No data taken		6 s 20 s 1 min	0.0 0.1 0.6	No data taken	No data taken
2.4	6 s 20 s 1 min	0.0 1.6 2.6	6 s 20 s 1 min	0.0 0.1 0.4	0	0.2
8.4	6 s 20 s 1 min	1.2 3.0 10.0	6 s 20 s 1 min	0.1 3.0 5.8	0	1.5
29.5	No data taken		No data taken		0	5.0

*All measurements are the average of three samples.

NO₂ Results

Standard (ppm)	Dynamic Sample*				Static Sample*	
	4-Foot Tube		11-Foot Tube		ppm (6 inches away)	ppm (at valve edge)
	Duration	ppm	Duration	ppm		
0.0	6 s 20 s 1 min	0.0 0.0 0.0	6 s 20 s 1 min	0.0 0.0 0.0	0.0	0.0
2.4	6 s 20 s 1 min	2.80 2.85 2.85	6 s 20 s 1 min	2.30 2.30 2.35	0.0	0.4
3.5	No data taken		No data taken		0.0	0.6
12.5	No data taken		No data taken		0.2	3.5
33.8	No data taken		No data taken		0.8	>10.0

*All measurements are the average of three samples.

procedures/samples to perform this job has generated a potential new system design that could provide more accurate, reliable, and sensitive detection of MMH, while at the same time expedite the postmission processing of the Orbiter.

3. Develop New NO₂ Detector. The current Interscan NO₂ detector appeared able to perform the checkout of the ac motor valves under optimum conditions; i.e., sampling from the edge of the valve body. However, the inability to actually get the sample tube to the valve body may well preclude the Interscan NO₂ detector from actually accomplishing this task reliably. Therefore, the final recommendation is to proceed with the development of a new NO₂ detector of the same type previously proposed. Paper tape technology is currently being developed for NO₂ detection.

Contact:

R. C. Young, 867-4438, DL-ESS-24

Participating Organization:

*Boeing Aerospace Operations, Engineering Support
Contract (M. D. Springer and C. F. McBrearty)*

NASA Headquarters Sponsor:

Office of Space Flight

Selection of Ammonia Analyzers for Use in Space Station Ammonia Loading Operations

Background

The requirement for monitoring ammonia vapor concentrations in the Space Station Processing Facility at the Kennedy Space Center arises from the planned use of ammonia as a refrigerant in Space Station Freedom. Under the current space station design, two separate payload packages will contain tanks that are to be loaded with ammonia prior to a launch.

Because of the toxic and flammable properties of ammonia vapors, monitoring is required both

Hazardous Emissions and Contamination Monitoring

at the Permissible Exposure Limit (25 parts per million) for personnel safety and in the Lower Flammable Limit (16 percent by volume) for facility safety. Sampling locations for ammonia detectors include both the regions near the payload element being serviced and remote locations.

Approach

After gathering all the requirements, an implementation plan was written and approved. A market survey was then conducted to identify promising technologies for ammonia detection above safe concentration ranges for both personnel and facilities. Studies were conducted to identify chemicals (solvents, etc.) that will be used in flight hardware processing areas and may interfere with proper operation of the detector. Instrumentation suitable for evaluation was then procured (see the table "Ammonia Monitors List").

The capability for generation and analysis of

concentrations of ammonia in the air in both ranges was developed. The generation system was then configured so these samples could be produced with controlled variations of temperature, humidity, and flow rate. Provision was made to mix other chemical vapors into the ammonia stream so their effects on the instrument could be observed. The effects of interest included the instrument response to the compound as well as the effect of the presence of the compound on the instrumental response to ammonia (increasing or decreasing its sensitivity).

After a test plan was prepared and the instruments were received, the instruments were inspected, functionally checked, and then screened for their response to the potential interference compounds identified previously. Instruments that passed interference testing were subjected to further testing; however, most instruments responded poorly to interference compounds.

Ammonia Monitors List

Manufacturer	Model	Sensor Technology
Drager	Polytron SE monitor with polytron parts-per-million ammonia sensor	Chemical
EIT	Enterra Series 6200 lower explosive limit (model 88), 2 channel	Chemical
EIT	Enterra Series 6200 parts per million (model 85), 2 channel	Chemical
IST (international)	IST model AG2002/lower explosive limit, lower explosive limit sensor, 2 channel	Catalytic Beads*
IST (international)	IST model AG2002/parts per million, parts-per-million sensor, 2 channel	Catalytic Beads*
MSA	MSA Lira 3200 lower explosive limit ammonia sensor	Infrared
Scott (LEL)	Scott lower explosive limit sensor, 2 channel	Chemical
Sensidyne	Sensidyne ammonia parts-per-million sensor	Chemical

*Operating at a temperature below catalytic mode.

Results

Instrumentation based on electrochemical cells, catalytic combustion, infrared, and other technologies was procured and evaluated. The packaging of several of the instruments was found to be deficient. After initial functional testing, interference compounds were considered; the compounds identified included methyl ethyl ketone, isopropynol, methanol, Freon 113, toluene, acetone, and detergent (FSN 7930-00-926-5280). Some of the instruments exhibited a larger response to interference compounds than to ammonia.

The sensitivity of some of the electrochemical cells (those exhibiting the best response to low concentrations of ammonia) changed dramatically after approximately one month of operation.

Because of the shortcomings of other technologies, Fourier transform infrared (FTIR) detection technology has been selected for use in the Space Station Processing Facility.

Contact:

P. A. Mogan, 867-4438, DL-ESS-24

Participating Organization:

*McDonnell Douglas Space Systems Company
(L. H. Allen and V. V. Bukauskas)*

NASA Headquarters Sponsor:

Office of Space Flight

Evaluation of FTIR Methods for the Second-Generation Hypergolic Vapor Detection System (HVDS II)

Objective

The work presented in this article is a continuation of the ongoing effort to identify the best technology for a second-generation Hypergolic Vapor Detection System (HVDS II) by the NASA Toxic Vapor Detection Laboratory (TVDL). The objective of the HVDS II Phase 2 project is (1) to

refine the most promising existing technologies identified in Phase 1 and (2) to reevaluate these modified technologies against the project goals of long life, reliability, and ability to detect monomethylhydrazine (MMH) and hydrazine (N_2H_4) from 0.5 to 50 parts per million (ppm) with little or no interference from ambient levels of non-hazardous vapors. Four technologies (single-wavelength infrared, photoacoustic infrared, photoionization, and electrochemical) were selected in Phase 1 (see the Research and Technology 1989 Annual Report) for further testing in Phase 2 during 1990 (see the Research and Technology 1990 Annual Report). A fifth technology, Fourier Transform Infrared (FTIR) spectrometry, was identified and tested in 1991 as a part of HVDS II Phase 2. This article presents the results of the FTIR evaluation.

Background

The Space Shuttle utilizes hypergolic propellants for orbital maneuvering and control. Hypergols are highly flammable and corrosive and a leak could cause severe damage if not detected and stopped. These propellants are loaded onto the Shuttle at the launch pad, where NASA uses a Hypergolic Vapor Detection System (HVDS) to sample and measure vapors in the air near sources of the hypergolic fuel or oxidizer. The current HVDS sensors have experienced early failure of the electrochemical cells, drift of the zero reading, and loss of sensitivity over time. These problems have resulted in high operations and maintenance costs due to frequent calibration and replacement. In order to lower the overall system life cycle cost, HVDS II was initiated.

During the evaluation of single wavelength infrared instruments for monitoring low-level MMH, N_2H_4 , or nitrogen dioxide (NO_2) vapors, it was found that no regions in the infrared spectrum are free of interferences. During a hypergol fueling operation, there should be few interfering vapors around the valve skids since the launch pad is cleared of nonessential personnel and all other activity is stopped. In spite

of that, interferences that might be present include water (H_2O), ammonia vapors, and hydrocarbon vapors from the swamp. The most serious interference is ambient H_2O vapor, which in the Florida environment can be as high as 4 percent mole fraction. The same sensors are used to monitor the purge vents during hypergol loading, the two to six weeks until the Rotating Service Structure is rolled back for launch, and system pressurization for flight. The purge vent sample could experience many interferences from other steps in Shuttle processing and any mixture of dry nitrogen or ambient air, changing within a few seconds depending on wind shifts. The instrument used must be insensitive to large changes in H_2O vapor and must not alarm to other nontoxic vapors. In the event of a leak, the sample may contain fuel or oxidizer as vapors or liquid.

Approach

The FTIR platform used for the evaluation is representative of FTIR units available for industrial process control. It is a flex-pivot-type interferometer with a maximum resolution of 1-cm^{-1} , and barium fluoride (BaF_2) windows with a useful transmission of 4,500 to 750-cm^{-1} . The detector was a room temperature triglycine sulphate (TGS) type. The 10-meter path gas cell had aluminum mirrors and BaF_2 windows for resistance to the corrosive effects of MMH and NO_2 . The 6-meter path gas cell had gold-coated glass mirrors. Two different gas cells were evaluated in order to determine the separate effects of the gas cell and the FTIR on the total system performance.

Known concentrations of ammonia (NH_3), NO_2 , and MMH vapors were produced in actively controlled sample streams with a variety of temperature and humidity conditions using the TVDL vapor generation system. Other interference vapors were produced by syringe injection with recirculation into the closed gas cell. This was followed by syringe injection of H_2O to provide calibration spectra of the mixture. For

real-time tests, the TVDL data acquisition and control computer ran a sequence of MMH concentrations under controlled conditions of sample temperature and relative humidity (RH). For the linearity and precision tests, single-beam spectra were taken. Evaluate response time was accomplished using automated analysis software. The long-term stability of the FTIR and the resistance of the gas cell to contamination was tested by repeating the same linearity tests over a four-month period.

Several spectroscopic analytic methods were developed to measure MMH and NO_2 . These mathematical methods were tested against MMH vapor and interference vapors for accuracy and resistance to interferences. The specified interference vapors are NH_3 , isopropyl alcohol (IPA), methyl alcohol (MeOH), fluorocarbons 113 (F113) and 12 (F12), hydrogen sulphide (H_2S), and H_2O vapor. The single-beam spectra collected from the tests were converted to absorbance units [$\text{AU} = -\log_{10}(\text{sample/reference})$] and quantitatively analyzed using several choices of spectral regions. Quantitative analysis was performed using commercially available partial least squares software and analytical methods developed as part of this work.

Several basic analytical methods (not using interferences) were developed. These basic methods were used to measure hardware performance while analytical methods to separate interferences were evaluated separately. Spectra were initially taken at 4-cm^{-1} resolution as a compromise between resolution and speed. After evaluation of the basic methods for linearity, response time, noise, and response to interferences, more elaborate methods were developed to include more components and more refined spectra into the training set. One method used 80 of the available spectra and two regions of various widths. This method (method A) used two components, MMH and NO_2 referenced to dry air. The following parameters are used in a typical two-component method.

Parameters for quantitative analysis method A (spectra: 80, components: 2, regions: 2, and points 176):

Region Number	Left Edge	Right Edge	Points	Comments
1	1004.30	842.239	85	MMH several bands
2	2948.43	2774.85	91	C-H stretch + NO ₂

Another basic method (method B) used three components: H₂O, MMH, and NO₂ referenced to both wet and dry air in 10 training spectra. Typical parameters used in the three component methods are as follows:

Parameters for quantitative analysis method B (spectra: 10, components: 3, regions: 4, and points 230)

Region Number	Left Edge	Right Edge	Points	Comments
1	3000.51	2759.42	126	C-H stretch
2	2929.15	2869.36	32	NO ₂ secondary peaks
3	1442.12	1382.33	32	H ₂ O smaller peaks
4	925.828	850.008	40	MMH several bands

The spectra of MMH and NO₂ with the regions used in method B are shown graphically in the figure "Spectral Regions for a Typical Basic Analytical Method."

Results

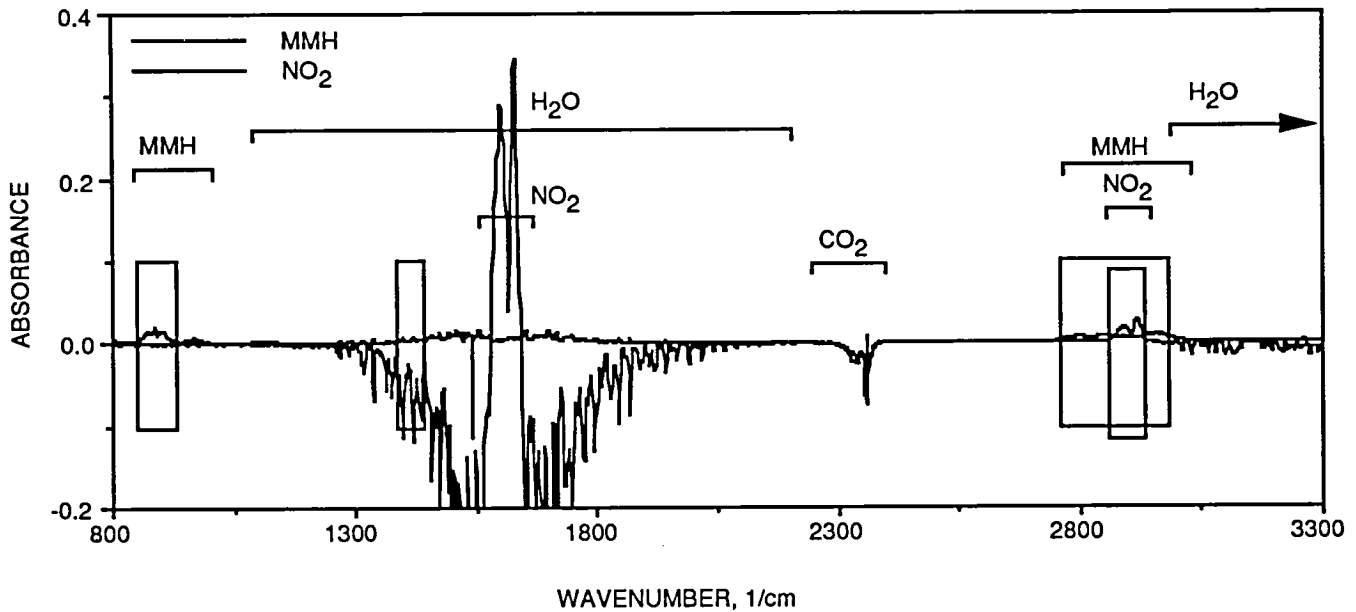
Processing speed was evaluated for two gas cells and two choices of resolution. The speed of the interferometer scan is limited by the TGS detector frequency response. The FTIR model tested required about 2 seconds to acquire a 4-cm⁻¹ spectrum and about 12 seconds to acquire a 1-cm⁻¹ spectrum. This meant that in the 15 seconds available to acquire, analyze, and report the concentrations, four interferograms at 4-cm⁻¹

could be averaged and only one interferogram could be collected at 1-cm⁻¹.

The volume of the gas cell determines the flow rate necessary to provide complete change-out of the sample. The response times of the 10-meter cell with a volume of about 2.5 liters and the 6-meter cell with a volume of about 0.75 liter are shown in the figure "Response Time of the 10-Meter and 6-Meter Gas Cells." The response time of the 10-meter cell is nearly 2 minutes, while the response time of the 6-meter cell is less than 1 minute. The sample flow is 10 liters per minute. The sampling interval is 15 seconds and the quantitative analysis was performed using method B.

The gas cell is the part of the FTIR system that largely determines the sensitivity and speed of a real-time vapor-monitoring application. Neither gas cell performed well enough with the FTIR model tested to meet all the HVDS II performance requirements. The primary factors that determine suitability of the gas cell for this application are compared in the following paragraphs.

The coupling of the FTIR modulated beam into the gas cell uses transfer optics that focus the input beam to the correct point in space. Light loss can occur if the f-number (focal length/diameter) of the coupling optics is not properly matched to the f-number of the gas cell. This was apparently the case with the 6-meter gas cell. Even though the number of reflections and the absorbance path was less than the 10-meter cell, the total throughput was less. In order to produce the same signal voltage after changing from the 10-meter to the 6-meter cell, the detector gain had to be increased to its maximum sensitivity. This resulted in an increase in measurement noise that proved to be unacceptable. The increase in noise relative to the same analytic method can be seen in the scatter of data points in the linearity plots (see the figure "Linearity of Two Analytic Methods in the 10-Meter and the 6-Meter Gas Cells"). Typical linearity results are shown in this figure

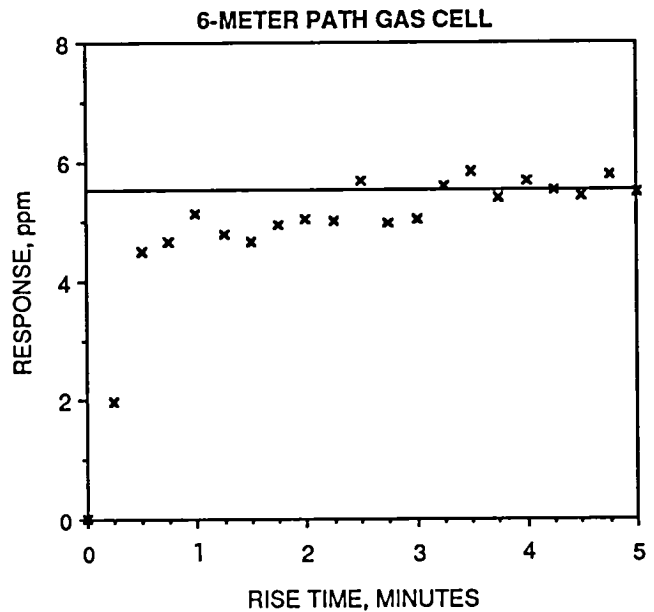
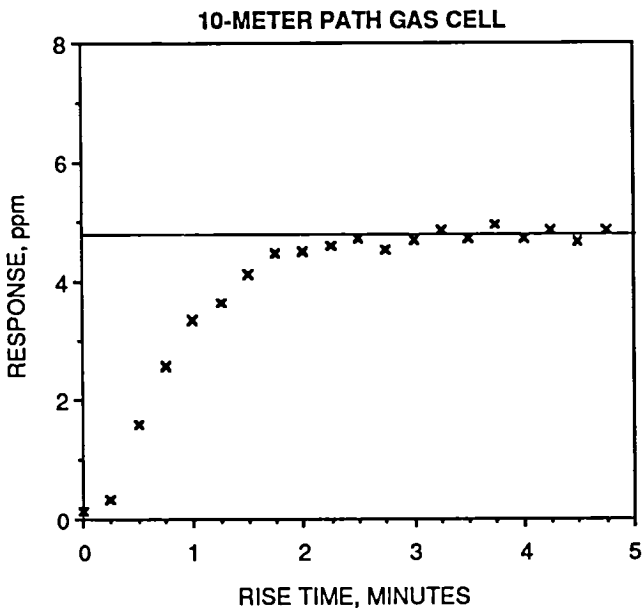


NOTE:
 THE SPECTRA OF MMH AND NO₂ ARE SHOWN FROM 800 TO 3300-cm⁻¹
 RESIDUAL WATER IN EACH THAT WAS NOT EXACTLY REMOVED BY THE REFERENCE
 SPECTRUM. THE ANALYTICAL REGIONS FOR METHOD B ARE SHOWN AS BOXES.

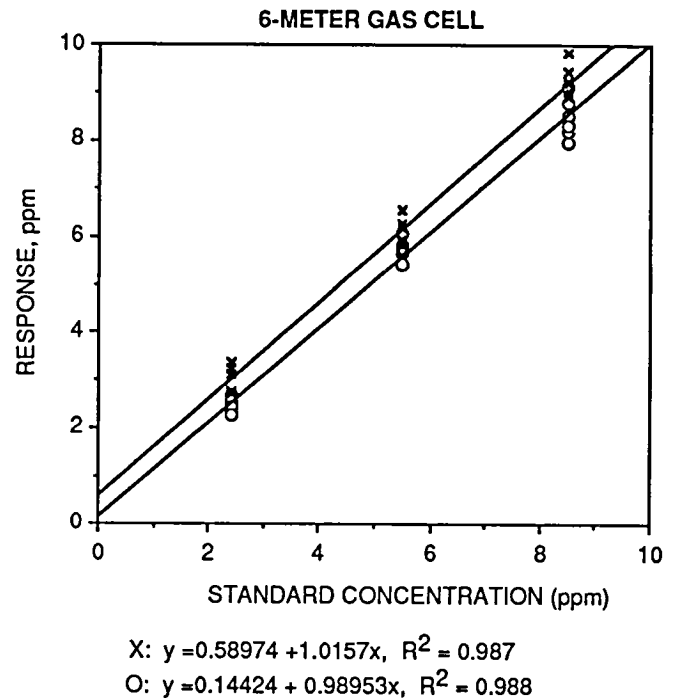
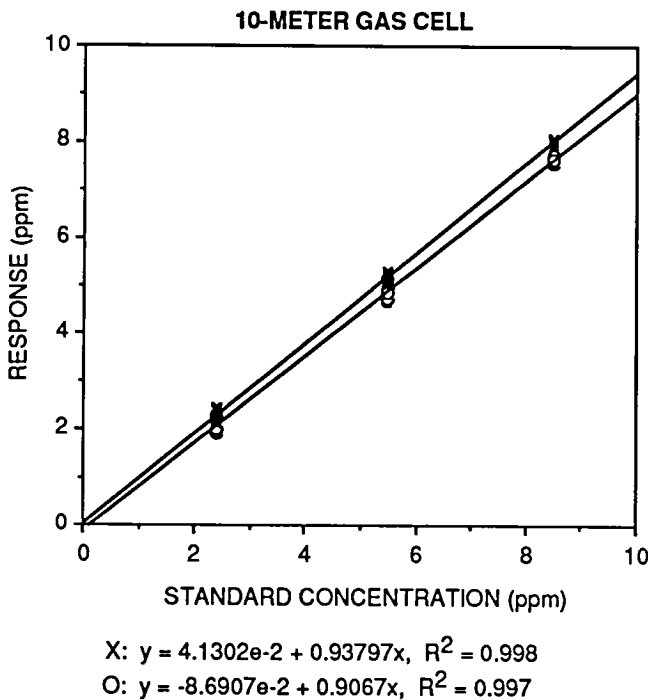
Spectral Regions for a Typical Basic Analytical Method

for two of the basic analytic methods in the 10-meter path gas cell.

In addition to linearity for MMH response, the noise in the NO₂ signal was recorded. The



Response Time of the 10-Meter and 6-Meter Gas Cells



Linearity of Two Analytic Methods in the 10-Meter and the 6-Meter Gas Cells

response of the 6-meter cell has been corrected by a factor of 1/0.59 to compensate for the shorter path length. The X plot symbol is the two component method and the O plot symbol is the three component method. The only significant difference in performance between the two methods was the noise in the NO₂ analysis. The three component method had ±0.5 ppm noise while the two component method had ±5 ppm noise. Both of the basic methods showed severe interference from alcohols and the NH₃ in both the MMH and NO₂ responses. It was concluded that the stronger NO₂ line at 1587-cm⁻¹ would be more than useful in spite of the strong H₂O absorption in the same region. In order to reduce the interference due to H₂O, it was necessary to increase the resolution to 1-cm⁻¹. The advantage of using higher resolution is seen in the figure "FTIR Spectra of the Region From 1450- to 1750-cm⁻¹," which shows the region from 1450- to 1750-cm⁻¹ at 4- and 1-cm⁻¹ resolution. The water absorbance is nearly zero in a region where the NO₂ absorbance has a peak. The small amount of negative water residual in

the NO₂ spectrum is typical of the expected interference due to changes in RH between reference and sample spectrum. It should be noted that the effect on the NO₂ baseline at 4-cm⁻¹ is over half the peak height and that the baseline is near zero in the H₂O spectrum at 1585-cm⁻¹ and 1-cm⁻¹ resolution, which reduces the water interference to acceptable limits.

Water vapor is the single-most important interference with FTIR analysis of hypergol vapors in the Florida environment. Water vapor presents strong absorption bands around the same region of the spectrum as NO₂ and is present at very high concentrations, making condensation on the gas cell mirrors a concern. To further complicate the problem, H₂O concentrations can change up or down after acquisition of a reference spectrum. As a result of this, negative H₂O content is perfectly valid and to be expected in the absorbance spectrum to be analyzed. The overlaid spectra of the vapors to be measured with the vapors to be rejected (see the figures "FTIR Spectra of the Region From

1450- to 1750- cm^{-1} " and "FTIR Spectra of the Region From 850- to 1050- cm^{-1} ") do not present any simple regions where only one spectrum at a time has an absorbance greater than zero. At 4- cm^{-1} resolution, neither the NH_3 or H_2O of the peak regions is resolved sufficiently to have a baseline of zero. At 1- cm^{-1} resolution, only NH_3 peaks are resolved with a zero baseline between, while H_2O is very nearly zero in the region of 1587- cm^{-1} .

In order to separate the overlapping components, a type of method was devised that samples the peaks and zeros of the most rapidly modulated component and over-samples all the other components (similar to the way electrical signals are sampled). It should be noted that the peaks and zeros of NH_3 are sampled and that there are enough samples overall to ensure the bands of other substances are "oversampled." The intent of building the method in this way was to allow the rapid evaluation of new training samples as they are added to the set. Each new method added another component to the training set. The largest method contains MMH, NO_2 , H_2O , MeOH, IPA, and NH_3 spectra in the training set in neat and mixture forms.

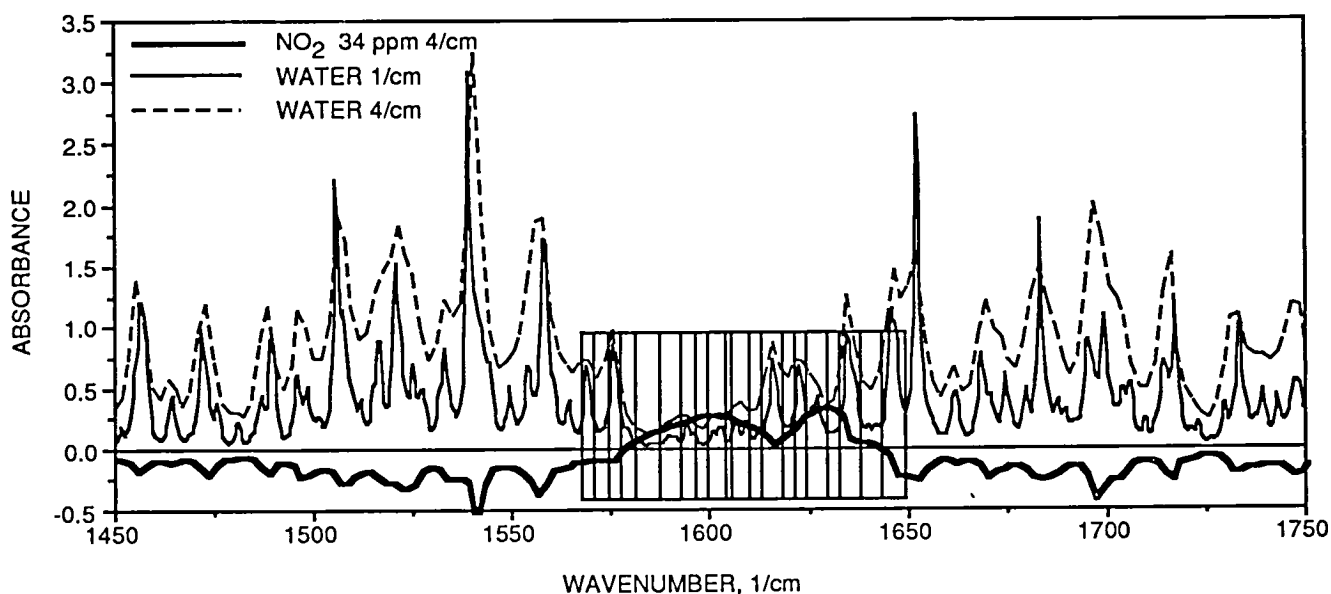
In increasing the resolution to 1- cm^{-1} , the

quantitative analysis problem was simplified because of baseline separation of NH_3 peaks and near baseline separation of H_2O peaks. Another simplification applied was to limit the analysis to the region from 800 to 2000- cm^{-1} . This made it possible to reduce the effect of baseline changes that occur in the IR source emission spectrum (blackbody) with temperature fluctuations.

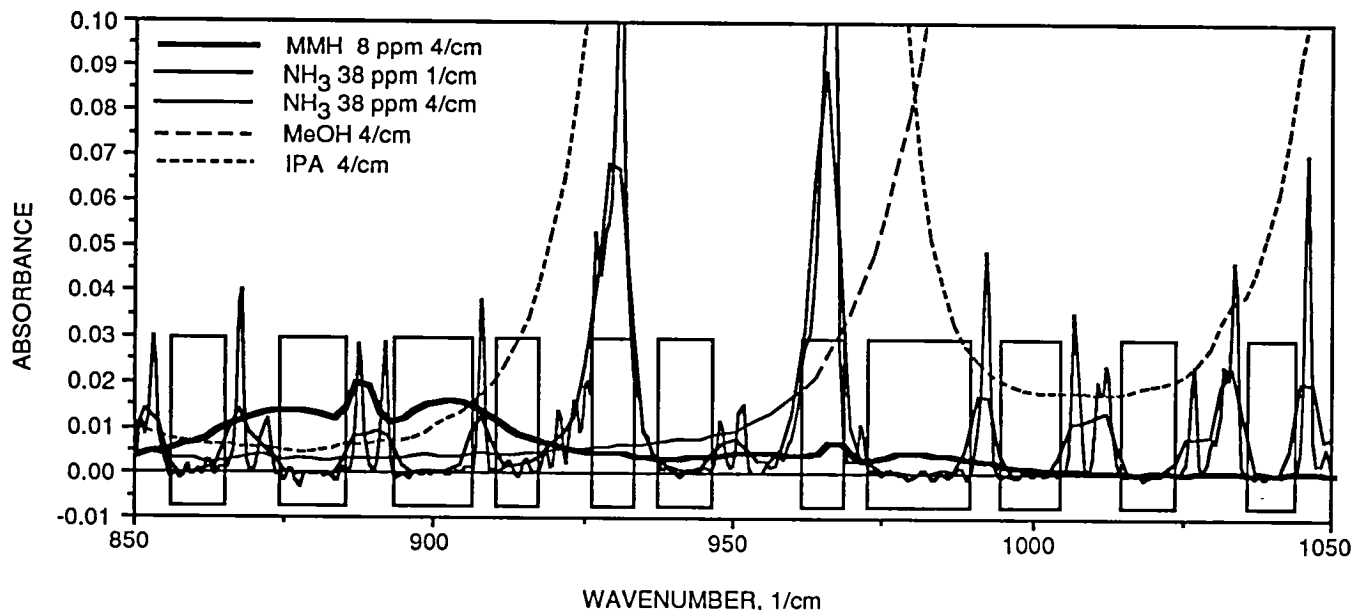
The analytical methods operating at 1- cm^{-1} produced good linearity and rejection of the specified interference vapors and appears to be the minimum resolution required for HVDS II. The oversampling of other vapors in these regions makes the 1- cm^{-1} methods quickly adaptable to the addition of new spectra, as in the 4- cm^{-1} methods. The performance of the FTIR system was limited at 1- cm^{-1} resolution by the time required to acquire spectra. The FTIR model tested took about 12 seconds to acquire one 1- cm^{-1} spectrum, so that averaging was not possible in the 15 seconds needed to give a system response time under 1 minute.

Conclusions

The durability and sampling speed of the gas cell can be made to meet the requirements of HVDS II. The gas cell should have a volume of



FTIR Spectra of the Region From 1450- to 1750- cm^{-1}



FTIR Spectra of the Region From 850- to 1050-cm⁻¹

about 1 liter and a path length of 10 meters. The focal length should be about 0.25 meter so that the number of reflections is not excessive; that is, the cell is not overly sensitive to mirror degradation. The transfer optics should be matched to the gas cell to provide the best throughput possible, and the mirror coatings and windows should not be degraded by moisture or the chemicals to which they will be exposed.

The experience gained while developing several analytical methods suggests that the quality of the training spectra and the order in which they are included in the training set are critical factors in producing a successful calibration for any number of components. In general, the known components in large concentrations should be first in the set and be carefully selected mixtures of lower concentrations following in random order. This would allow the software to most accurately identify the real components in the mixtures.

The most important conclusion of this work is that FTIR, with a suitable gas cell, will provide sufficient sensitivity and response time to meet the performance requirements of HVDS II. While the system tested did not meet all the

requirements in any one configuration, it is clear that an FTIR system that is optimized for HVDS II application will be able to meet all the requirements. Based on the work reported here, NASA is preparing a procurement for four prototype FTIR instruments, optimized for the HVDS II application, from different suppliers for evaluation as components of the final system configuration.

Contact:

R. C. Young, 867-4438, DM-ESS-24

Participating Organization:

Boeing Aerospace Operations, Engineering Support Contract (C. B. Mattson)

NASA Headquarters Sponsor:

Office of Space Flight

Ultrasonic Leak Detection

Objective

To rapidly develop and fabricate an ultrasonic leak detection system for use in the Space Shuttle aft section during leak testing.

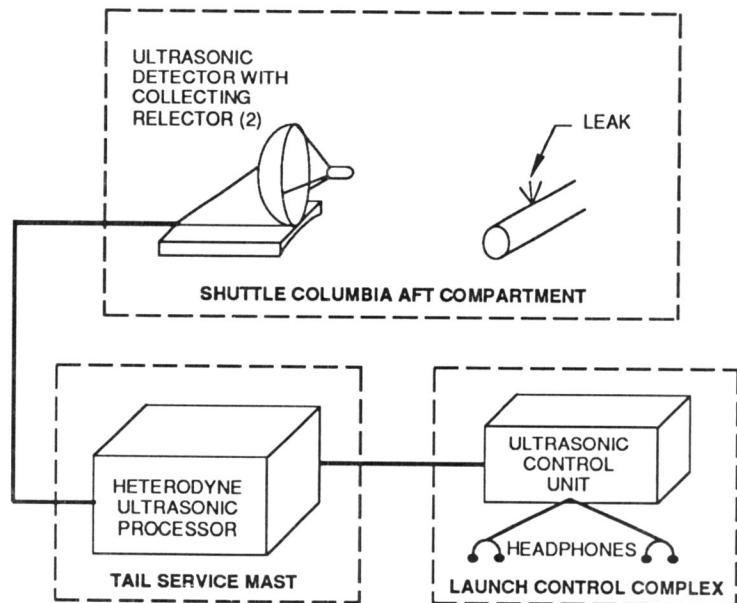
Background

During the summer of 1990, the Shuttle fleet was grounded due to hydrogen leak problems. As a result of this, various research efforts were started in a variety of fields to aid in locating these leaks and in returning the Shuttles to flight. In the early fall, the decision was made to perform a leak test on Columbia's aft section. Based on demonstrations given by Engineering Development and Engineering Support Contract (ESC) engineers, operations personnel requested that an ultrasonic leak detection system be developed and fabricated in time for this test.

Approach

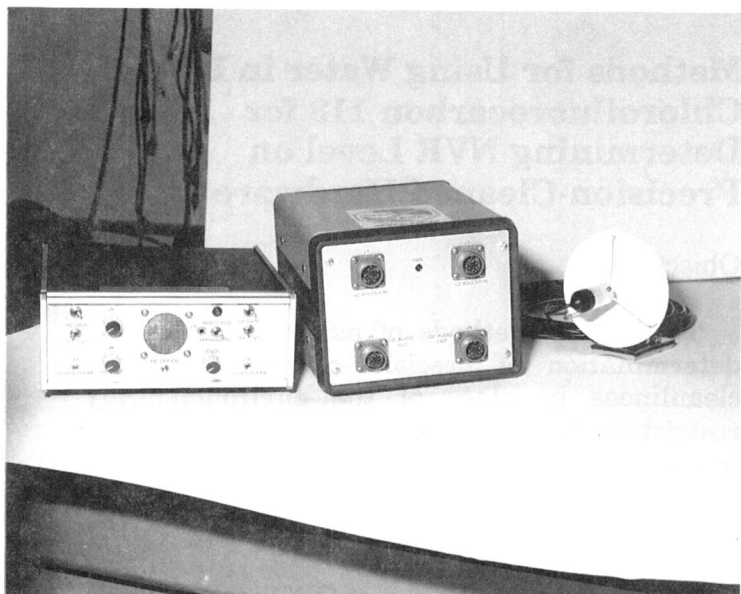
Ultrasonic leak detection is a well-known technology and off-the-shelf hardware exists to locate and measure the sound emission given off by a jet-type leak. The difficulty with the present application was that a unit needed to be designed and built rapidly that would be compatible with both Shuttle safety and the needs of operations. The safety issue was met by placing only a passive ultrasonic transducer with a bleed-off resistor in the Shuttle aft compartment. No power was sent to the transducer, thus minimizing the possibility of sparking within a potentially hydrogen-rich environment.

Each transducer was mounted into a receiving horn that was attached to a bracket so it could be clamped to a pan-and-tilt camera. This arrangement gave each transducer a limited field of view, which roughly matched that of the camera to which it was mounted, allowing a remote operator to hear the ultrasonic emission from the flight hardware component under observation. The signals from two transducers were sent over approximately 100 feet of cable to the Tail Service Mast (see the figure "Ultrasonic Leak Detection System Used for Columbia's Aft Test"). At this



Ultrasonic Leak Detection System Used for Columbia's Aft Test

location, the ultrasonic signals were mixed down to the audio region, filtered, amplified, and prepared for transmission to the Launch Control Center (LCC). At the LCC, a control unit was used to allow the system operator to listen in on a selected ultrasonic signal. The gain, heterodyne frequency, and transducer could be selected from this remote location.



Ultrasonic Leak Detection System

Results

Two complete systems (one served as a back-up) were designed, fabricated, and tested in time for Columbia's aft fueling test (see the photograph "Ultrasonic Leak Detection System"). During the test, two ESC operators manned the control console in the LCC and monitored the ultrasonic signals searching for leaks. No unexpected leaks were found, but the system proved itself by locating a leak emerging from a bagged flange. This leak was substantiated by other monitoring equipment and demonstrated the usefulness of the system. Operations personnel have subsequently explored the use of ultrasonic leak detectors for use around the launch pad to monitor Freon and nitrogen leaks.

Contacts:

*J. D. Collins, 867-4449, DL-ESS-24
F. W. Adams, 867-4449, DL-ESS-24
R. Mizell, 861-2964, TV-ETD-23*

Participating Organization:

Boeing Aerospace Operations, Engineering Support Contract (R. B. Cox, Jr., A. P. Schwalb, R. C. Youngquist, S. M. Gleman, and S. Simmons)

NASA Headquarters Sponsor:

Office of Space Flight

Methods for Using Water in Lieu of Chlorofluorocarbon 113 for Determining NVR Level on Precision-Cleaned Hardware

Objective

To develop methods of using water for the determination of precision-cleaned hardware cleanliness in place of the environmentally restricted chlorofluorocarbons (CFC's) presently in use.

Background

Due to the contribution of CFC's to the ozone depletion problem, the Materials Science Labora-

tory at Kennedy Space Center was tasked in 1990 to develop an alternative cleaning fluid for CFC 113. Three fluids were considered: a substitute CFC-type solvent, isopropyl alcohol, and water. Water is perhaps the most desirable chemical to use for this purpose from the standpoint of safety and cost. It is nontoxic, nonflammable, inexpensive, environmentally friendly, recyclable, does not need to be qualified from a materials compatibility standpoint, and presents a large savings potential in material costs. For these reasons, the CFC replacement chemical working group decided to pursue the use of water as the replacement chemical for CFC's in the cleaning validation process.

Approach

The challenges of using water for determining nonvolatile residue (NVR) materials are two fold: (1) the limited solubility of these materials in water and (2) the difficulty of analytically determining these organic materials in a water matrix. It was believed that enough material could be removed to be chemically detected and that the amount removed would probably be reproducible, even if not complete.

To solve the first problem, how to remove trace quantities of NVR materials from hardware [i.e., more than 1 milligram per square foot (mg/sq ft)], two techniques were evaluated: water ultrasonication and low-pressure hot-water impingement. These two techniques would be necessary to process the wide diversity of hardware shapes and sizes.

Over 20 typical NVR materials found at KSC (see the table "NVR Materials") were tested to determine the practicality of removing them from hardware with demineralized water. Quick-look feasibility tests using either low-pressure (gravity flow) 70-degree-Celsius (°C) water impingement or 80-kilohertz ultrasonication in 52 °C water were effective in removing at least a partial quantity of each NVR material applied to the parts.

NVR Materials

Ultrasonic Testing

<u>Hydrocarbon Greases</u>	<u>Silicone Greases</u>
Amoco Rykon 2 Mobil Mobilux 2 Titan Lube Chevron SRI MIL-G-3545C MIL-G-23549C	DC-55M DC-44 DC-33 Drilube 822
<u>Silicone Fluids</u>	<u>Fluorocarbons</u>
DC-200 DC-FS-1265	Krytox 240AC Halovac 100SB Braycote 640AC
<u>Hydraulic Fluids</u>	<u>Hydrocarbon Fluids</u>
MIL-H-5606 Houghton Safe 1055 Mobil Jet II Shell Tellus 32 MIL-H-83282	Mineral Oil Castrol Motor Oil MIL-G-8188C

The second problem, analyzing the material removed, was approached by analyzing the water samples from the ultrasonic and impingement NVR removal tests. The water from the NVR removal tests was analyzed using the following methods:

- a. Total Organic Carbon (TOC)
- b. Surface Tension (ST)
- c. Turbidity
- d. Infrared Attenuated Total Reflectance (IR-ATR)
- e. Ultraviolet (UV) Scattering/Fluorescence (UV-EXCITATION-280 nm)

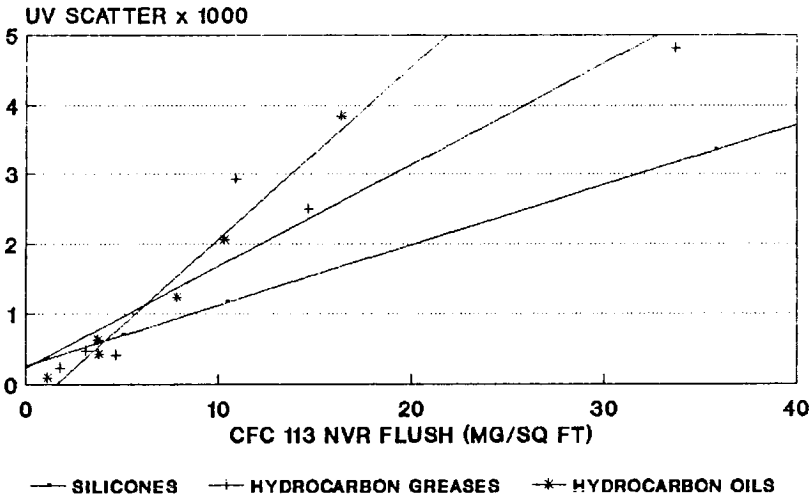
All the methods evaluated were capable of detecting most of the NVR materials of interest. The quantitative nature and sensitivity of the methods varied widely, however.

This testing was conducted to determine the ability of water in conjunction with the previously described analytical chemistry methods to determine the "NVR cleanliness level" of small batches of stainless steel fittings. The batches consisted of mixtures of about 30 AN stainless steel tube fittings including plugs and B-nuts totaling about 0.7 square foot, which were contaminated by dipping in various mixtures of oils, greases, hydraulic fluids, and silicones suspended/dissolved in CFC 113. After drying overnight at 104 °C, the parts were ultrasonicated at 52 °C in water for 10 minutes. The water was then tested for NVR contaminants by the methods previously described. At this point, a CFC 113 NVR determination was run on the parts.

Ultraviolet scattering and fluorescence were demonstrated to be suitable for measuring the amount of NVR material removed from hardware during ultrasonication for any specific material class. Because of a fairly uniform response across the various NVR material classes, UV scattering appears to be a stronger candidate for additional evaluation (see the figure "Summary of UV Water Data, UV Scatter"). The fluorescence measurement (see the figure "Summary of UV Water Data, UV Fluorescence") is probably not suitable for general use because of the widely varying response to different NVR materials.

The TOC method of analysis was the most applicable for analyzing the NVR removed by ultrasonication of parts. TOC gave a linear response to all the NVR classes and could detect surface contamination in the 3- to 5-milligram-per-square-foot range for all liquid-oxygen-sensitive materials. The figure "Summary of TOC Water Data" shows a composite of TOC relationships with CFC 113 flush data for each NVR class.

Although capable of analytically responding to



Summary of UV Water Data, UV Scatter

different concentrations of NVR materials, turbidity has a potential problem when used with ultrasonication. This problem is due to the generation of minute particulate from new parts during ultrasonication, which is indistinguishable from the NVR emulsion.

IR-ATR and surface tension, although showing some response to the different NVR levels, did not correlate well with CFC 113 surface contamination measurements.

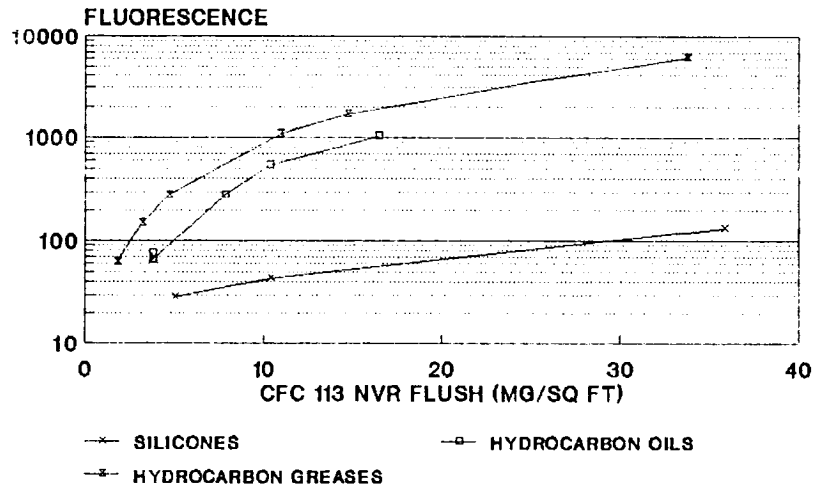
Impingement Test Results

It is anticipated that water impingement rinsing will be utilized in the precision-cleaning verification of large items that are impractical to test in an ultrasonic cleaner. The rinse water will be collected and tested for contaminants using the same analytical methods developed for small parts in the ultrasonic tests.

Several tests were conducted to evaluate the variables that affect the rinsing process. Preliminary tests evaluated nozzle type, water temperature, and pressure. Additional tests were performed using 1-square-foot stainless steel plates to evaluate rinse volume and NVR detection. The sample plates

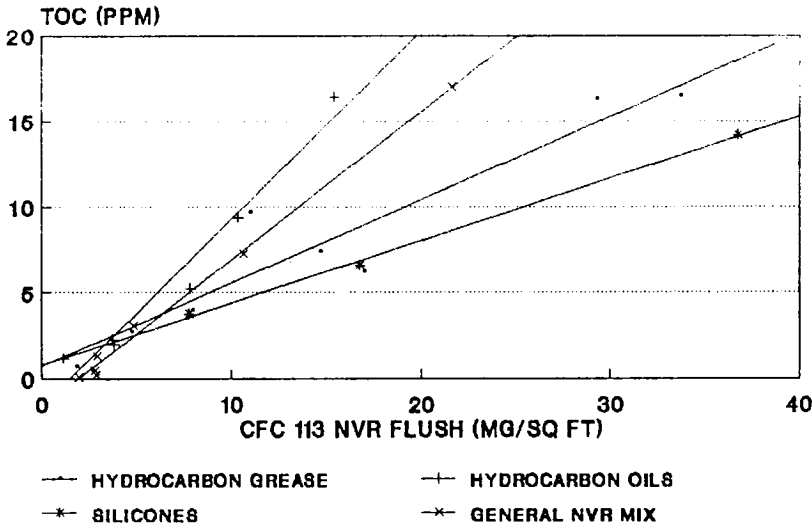
were contaminated with approximately 7 milligrams of the general NVR mixture. After drying overnight, the test plates were rinsed with 100, 200, 300, and 500 milliliters of water. The rinse water was then ultrasonicated for ten minutes and analyzed for TOC content. It was clearly evident from this test that the smaller volume of rinse water produces the most concentrated sample.

With 100 milliliters selected as the rinse volume, additional tests were conducted with various contaminant amounts on the 1-square-foot area sample plates. The same general mix of contaminants was used with controlled test conditions of 70 °C and 20 pounds per square inch gage using a 1/8-inch diameter nozzle. The results in the figure "Water Data Versus CFC 113 Flush Data, General NVR Mixture" show a direct correlation of the TOC analysis with the NVR residue as determined by a CFC 113 rinse.



Summary of UV Water Data, UV Fluorescence

Using TOC to determine NVR levels, test data indicates that water impingement is a viable candidate for determining the cleanliness of stainless steel surfaces and will be further evaluated.



Summary of TOC Water Data

Participating Organizations:

*KSC Materials Science Laboratory,
DM-MSL (G. J. Allen, C. W. Bassett,
M. D. Buckley, W. L. Dearing,
J. F. Jones, M. J. Lonergan,
P. J. Welch, and M. K. Williams)*

*University of Central Florida
(J. Batten and C. Clausen)*

*University of South Carolina
(S. B. Skinner)*

NASA Headquarters Sponsor:
Office of Space Flight

Summary

The use of water as a verification fluid for precision cleaning looks promising. Ultrasonication and impingement together with TOC and UV scattering will be further evaluated with larger quantities of parts and with additional types of materials such as aluminum and non-metallics.

Contact:

C. W. Hoppesch, 867-7051, DM-MSL

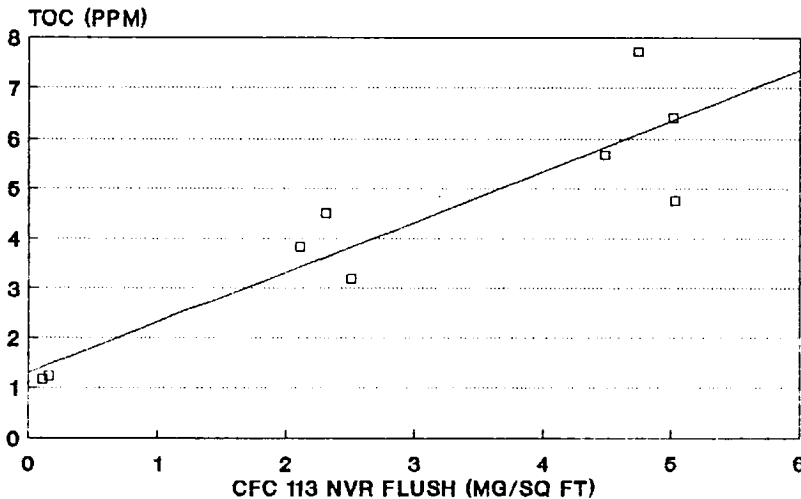
Development of a Hydrogen Chloride Dosimeter

Objective

To map the hydrogen chloride (HCl) vapor dose produced within a 1.5-mile radius during a Space Shuttle launch.

Background

Payload customers for the Space Shuttle have recently expressed concerns about the possibility of payloads being contaminated, while they await launch on the inactive pad, by plume effluents from a Shuttle launch at the adjacent active launch pad. As part of this overall study, a ring of inexpensive dosimeters was to be deployed around the active pad in the distance between Pads A and B. Coupled with active measurements of the HCl intrusion through the air-handling system on the active pad, it was possible to model the expected HCl concentrations at the inactive pad inside the Payload Changeout Room should the plume pass directly over an inactive pad during a future launch.



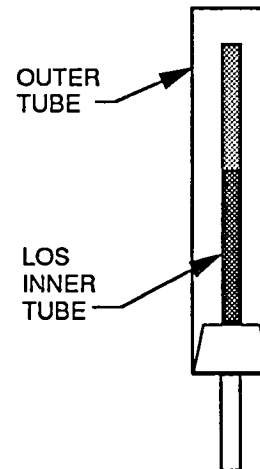
*Water Data Versus CFC 113 Flush Data,
General NVR Mixture*

Initial studies of paper badge dosimeters based on a modification of the hydrazine-vanillin chemistry and bromophenol blue (BPB) dye revealed that rapid fading of the color developed by these systems would make their use difficult since several hours would elapse between exposure and readout of the doses received. With the date for deployment rapidly approaching, the factors that would affect fading on these two different dosimeter chemistries were evaluated.

Approach

The effects of different substrates, solvent systems, and the possible volatilization of HCl from the badges were studied. Interaction of the substrate with the dye formulation could be most quickly seen by dropping 100 microliters (μL) of the dye test solution onto a horizontally suspended substrate and watching for color changes at the edge of the spreading drop. Many papers were found to be basic or acidic by using acid or base forms of the BPB dye. Even Chromo I and silica gel thin-layer chromatography plates, while pH neutral, exhibited rapid fading of any developed color unless heavy acid exposures were used. Only when Teflon filter disks or glass substrates were used could light exposure colors be retained, although these substrates appeared to be saturated in areas of light dye concentration. This observation led to suspicion that the porous hydrophilic substrates allowed the transport of unreacted bases from the interior parts of the substrate, causing the surface color developed during light exposures to be converted from the acid form back to the base form. The use of very thin substrates reduced the fading rate, but the dynamic range was lost.

These effects led to exploration of a length-of-stain (LOS) type of device. Because of the sensitive and permanent color changes observed on glass plates, the inside wall of a 100- μL Drummond capillary glass pipet was coated. Producing a consistent thin film of BPB on the inner surface proved difficult. Mixing the dye in a binder (such as nail polish) produced a thick coating with the same fade problems. Coating of



Length-of-Stain Tube

the outside surface proved much easier and resulted in the geometry shown in the figure "Length-of-Stain Tube."

The device consists of an inner tube or rod, with a smooth, nonporous surface (glass is used in the present model). This inner tube is coated with dye, often over a binding layer to promote adhesion of the dye. The inner tube or rod is then inserted into an outer inert tube, which serves as the diffusion barrier and weather shield for the inner tube.

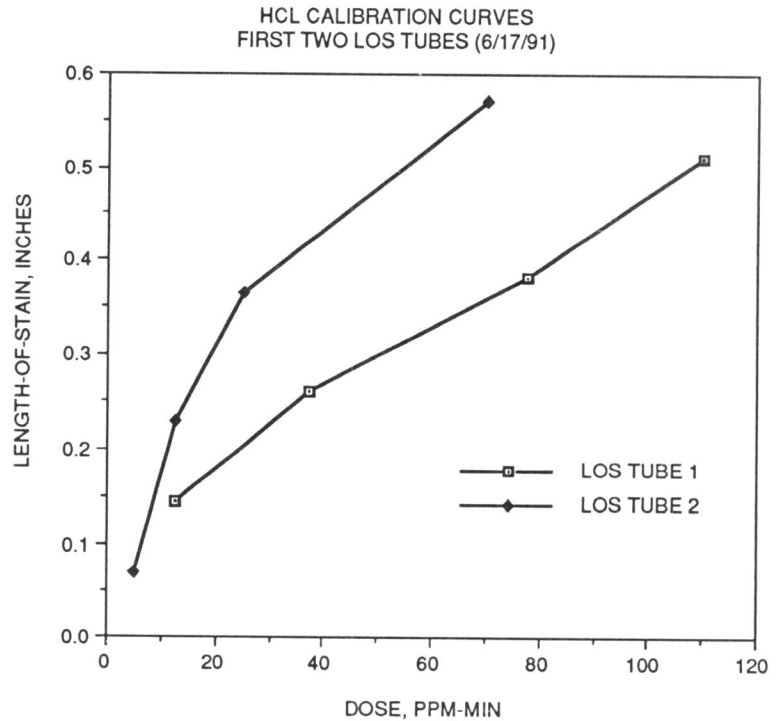
The ratio of the inner tube outside diameter (OD) to the outer tube inside diameter (ID) allows the user to modify the dynamic range and sensitivity of the device. That is, by using a large outer tube and a small inner tube, the device becomes more sensitive, responding to dose levels below 2 parts per million (ppm)-minutes. Conversely, a device where the outer tube is a close fit over the inner tube will have little diffusion area with a large dye-covered area and will, therefore, be insensitive. These geometric variations are shown in the figure "Variable Range Geometries."

The use of a smooth continuous substrate for the LOS stain support yields a fine-grained stain interface yielding a high-resolution device capable of distinguishing small changes in total dose.

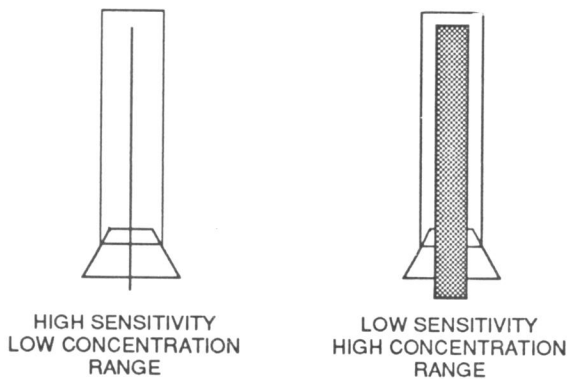
Existing LOS tubes use a dye carrier (such as silica gel) that is packed into a glass tube. This arrangement yields a relatively high-range device with a coarse-grained interface. The typical range of a commercial LOS tube for HCl, used in a passive diffusion sampling mode, is 2 to 20 ppm for 8 hours of exposure. This is a total dose of 1,000 to 10,000 ppm-minutes. Since expected exposure times are only 5 minutes, then the concentration would have to be at least 200 ppm to be detectable by these devices.

Results

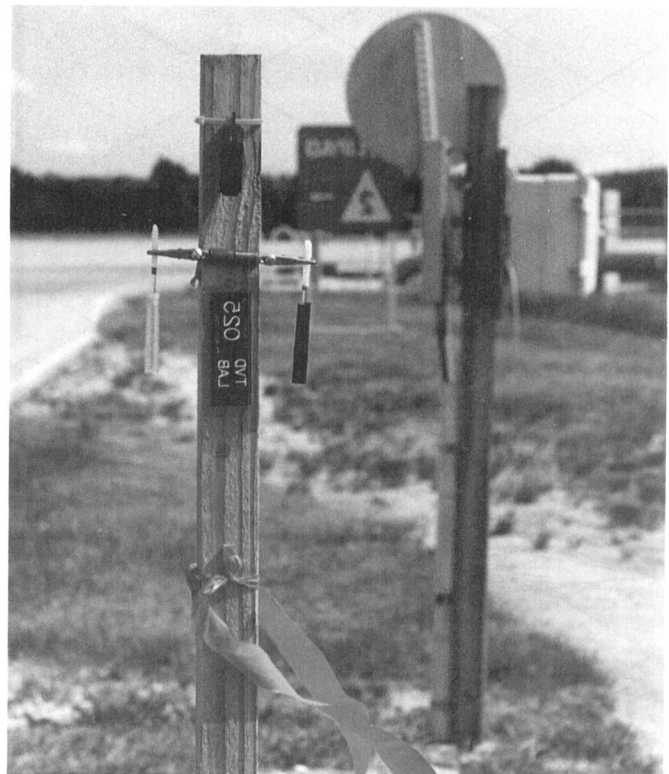
The first devices produced showed very good sensitivity, although the first two samples lacked reproducibility. The calibration curve for these early devices is shown in the figure "Early Response Curves, HCl LOS Tubes." Contrast these results with the curves obtained for the latest deployment that included over 300 LOS tubes. The figure "Early Field Study of Dosimeter Tubes" (a typical field installation) shows a clear outer tube and the same device with black electrical tape on the outer tube to prevent sunlight bleaching of the dye. A paper-badge-type dosimeter is also shown at the top of the stake. The information in the figure "Response Curves for LOS Tubes, STS-48" represents the data from ten tubes, two each from five different batches.



Early Response Curves, HCl LOS Tubes



Variable Range Geometries



Early Field Study of Dosimeter Tubes

tion around the Shuttle launch pad, ensuring that clean-room air is free of measurable quantities of HCl vapor.

Further work will be done to deploy a more sensitive version similar in construction to the version shown in the figure "Variable Range Geometries" for the next launch. In the future, an effort will be made to expand this concept to the quantitation of other air contaminants. The concept disclosed in this report is thought to have many applications in the field of passive dosimetry and has been submitted as an idea disclosure at NASA Kennedy Space Center. Licensing may be available for commercial use of the concept.

Contact:

D. Lueck, 867-4438, DL-ESS-24

Participating Organization:

Boeing Aerospace Operations, Engineering Support Contract (Z. G. Laney and D. J. Curran)

NASA Headquarters Sponsor:

Office of Space Flight

Remote Hydrogen Detection

Objective

From a remote observation location, to locate suitable technologies that could be used to measure hydrogen leak rates at the 17-inch hydrogen disconnect of the Shuttle.

Background

During the summer of 1990, the Shuttle fleet was grounded due to hydrogen leak problems. As a result of this, various research efforts were started in a variety of fields to aid in locating these leaks and in returning the Shuttles to flight. It was decided to establish a working group, based jointly out of Johnson Space Center (JSC) and Kennedy Space Center (KSC), to locate suitable technologies that could be used to

remotely measure hydrogen leak rates from the 17-inch hydrogen disconnect.

Approach

The effort began in September 1990 with the generation of a detailed requirements document. The document stated that nonintrusive instrumentation was desired which would allow real-time monitoring of hydrogen leak rates at the 17-inch disconnect from locations either on the Mobile Launcher Platform (MLP) or the Fixed Service Structure (FSS). Specifications were given detailing the leak problems, the environment, the operation of a leak detection instrument, possible locations for the use of leak detectors, and other limitations that would be placed on the instrument. The requirements document was circulated to multiple NASA centers, several industrial and research locations, and other interested parties. It was requested that potential technologies be documented and returned to Kennedy Space Center for consideration by an evaluation team that would meet in February 1991.

While awaiting a response to the specification document, a literature search was made of the public domain for appropriate technologies. The search was done over a four-month period and generated over 100 articles of interest. The most appropriate were selected, summarized, and placed into a data base for future reference.

In October, a potential candidate technology, Raman scattering, was tested at JSC. Five KSC representatives participated in this test, both as observers and active participants, operating the mass spectrometer reference system, helping to devise the testing, and documenting the results. In January, the results of this test were distributed to the evaluation team. It was determined that Raman scattering was a potentially useful approach, but the testing carried out at JSC did not adequately demonstrate the limitations of this technology.

During the months of October through Febru-

ary, 27 different responses to the requirements document were received at KSC. In February, the evaluation team (made up of representatives from KSC, JSC, Lewis Research Center, Langley Research Center, Jet Propulsion Laboratory, Stennis Space Center, and Marshall Space Flight Center as well as three engineers from Rockwell International Corporation) met at KSC to review the responses. The first day of the meeting covered background talks, and a tour was made of the launch pad. The second and third days were spent reviewing the 27 responses with the intent of making recommendations to the Shuttle Program Office at JSC as to which technology should be developed and installed at KSC.

Results

The evaluation team decided the best approach for solving the hydrogen leakage problem consisted of a Raman system that monitors the 17-inch area for hydrogen concentration levels and an image processing system that uses water plume dynamics evaluation to determine leak rates. This decision was documented as a formal presentation to be made to the Shuttle Program Office; but, due to its implementation costs and high risk, was turned down for current funding.

The project generated exposure of the hydrogen leak problem and produced documentation detailing the requirements useful instrumentation must be able to meet for use at the launch pad to solve leakage problems.

Contacts:

*W. R. Helms, 867-4438, DL-ESS-2
J. D. Collins, 867-4449, DL-ESS-24
F. W. Adams, 867-4449, DL-ESS-24*

Participating Organization:

Boeing Aerospace Operations, Engineering Support Contract (R. C. Youngquist, S. M. Gleman, C. B. Mattson, and W. E. Rutherford)

***NASA Headquarters Sponsor:
Office of Space Flight***

Certification of Coulometric Detection Method for Hydrazine and Monomethylhydrazine

Objective

To obtain National Institute of Occupational Safety and Health (NIOSH) certification of the coulometric method developed for the detection of hydrazine and monomethylhydrazine (MMH).

Background

Hydrazine and MMH are used by NASA at Kennedy Space Center (KSC) as hypergolic fuels for the Space Shuttle. The health risk associated with exposure to these chemicals has led the American Conference of Governmental Industrial Hygienists to propose a reduction in the threshold limit values of compounds to 10 parts per billion (ppb) in an eight-hour workday. A coulometric method to detect and quantify hydrazines at the proposed level was developed at the Naval Research Laboratory (NRL) under NASA sponsorship. The coulometric method has become an integral part of the research efforts at NASA KSC and NRL by providing a quantitative measure of the hydrazine or MMH in test gas streams. The certification of this method by NIOSH is desired to allow its use as a standard method.

Approach

A test plan was prepared to evaluate the coulometric detection method and ensure that it met the NIOSH standard requirements. The test plan included accuracy, precision, and interference studies.

Results

The limits of detection and the limits of quantification for the coulometric method were determined to be 1.5 and 4.5 ppb of MMH, respectively, for a 10-liter gas sample. In-

ing the sample size would decrease these limits. For the purposes of this study, the limit of detection was defined as three times the standard deviation and the limit of quantification was ten times the standard deviation of blanks. The accuracy of the coulometric technique was determined relative to two NIOSH colorimetric standard methods: para-dimethylaminobenzaldehyde and phosphomolybdic acid. From the comparison data, the coulometric method was found to be accurate from 100 ppb to 1,500 ppb in 10 liters of air. Lower concentrations could not be compared directly because the NIOSH methods were not capable of quantification at those levels.

Liquids standards were used to show that the coulometric detection technique was linear from less than 1 to 500 ppb. A determination of the upper limit of the technique was not identified but was shown to be at least 1,500 ppb in the accuracy tests in which the sample was diluted.

The determination of the precision of the coulometric technique produced a pooled standard deviation of 4 percent, which is significantly better than the 8 percent required by NIOSH. The pooled standard deviation was calculated over the range of 1 to 500 ppb and included 50 data points.

The interferences that were tested included those expected at NASA KSC and included ammonia, 2-propanol, and chlorofluorocarbons 12, 113, and 114. None of these compounds was found to cause any appreciable interference. However, the coulometric technique is a nonspecific one and, therefore, could be susceptible to interferences. Verification of hydrazine or MMH could be accomplished with dosimeter badges developed previously by NRL under NASA sponsorship.

A paper describing the coulometric method for detection of hydrazine and MMH and the results as outlined here has been submitted to the Journal of the American Industrial Hygiene Association.

Contact:

R. C. Young, 867-4438, DL-ESS-24

Participating Organizations:

Naval Research Laboratory (J. R. Wyatt and S. L. Rose-Pehrsson)

GEO Centers, Inc. (T. L. Cecil and K. P. Crossman)

NASA Headquarters Sponsor:

Office of Space Flight

Multispectral Imaging of Hydrogen Flames

Objective

To develop a room-temperature imaging system using multispectral television (MTV) techniques that can detect and display hydrogen flames, discriminate them from other infrared sources, and interlace compatibly with the existing Launch Complex 39 Operational Television System (OTV).

Background

A better instrument that can reliably detect and display the presence of a hydrogen fire has been on the Shuttle program's "want list" for some time. When the Shuttle's STS-14 launch aborted with a cutoff after main engine start, the existing hydrogen fire detectors went into alarm. This condition signals a hydrogen fire on the launch pad. With the current detectors, the exact location and intensity of the fire was indeterminable. The launch team had insufficient information to react adequately to the problem and quickly ensure the safety of the crew, associated flight systems, and ground support equipment. As a result of this event, efforts were initiated to develop a solution that would provide information about not only the presence but also the location and intensity of a hydrogen fire. MTV is one of these efforts.

Approach

A multispectral imaging technique was proposed to allow discrimination of hydrogen fires from other infrared sources. Early on, it was suggested that the MTV camera utilize three spectral bands, one in the ultraviolet, one in the visible, and one in the infrared. However, early experimentation showed that the amount of useful information in the ultraviolet band was minimal. Therefore, the ultraviolet band was not used in the early prototype design and, instead, effort was concentrated on using the visible and infrared bands.

After studying the infrared emission spectra of hydrogen flames, it was shown that a hydrogen fire could be easily discriminated against most infrared emitters by comparing the intensity in just two infrared bands. An appropriate infrared detector was chosen to form the basic element of the camera, and the electronics and optical development was begun.

Results

At this date, a laboratory prototype of the MTV camera has been demonstrated within the laboratory. The MTV camera uses a high-quality visible camera to generate the timing information for the infrared portion of the system. The infrared camera uses silicon and germanium optics to focus an infrared image onto a pair of detector arrays. One of the arrays produces the signals from which the infrared image is created, while the other determines whether the image is a hydrogen fire or some other infrared emitter.

The information from the detector arrays is sent to a multiplexing board, where serial data streams are generated, and then to a digitizing board where the infrared information is converted to digital form and stored in dual-ported memory. The infrared data is then read out of memory at standard video rates (clocking information is supplied by the visible camera and special electronics) and converted into a video television signal. If the infrared signal is small,

just the visible image is displayed on a monitor. If the infrared signal is greater than a selected value, the visible image is replaced by the infrared image. The infrared image is color-coded red if the emitter is a hydrogen flame and green if it is any other infrared emitter.

The operations personnel have requested that the MTV camera have a zoom lens capability for both the visible as well as the infrared portions of the spectrum. For the visible, this was a straightforward requirement because the necessary components are off-the-shelf items; but, in the infrared, this problem required significant development. At this date, a prototype infrared zoom lens has been demonstrated that can be operated remotely from a computer. It will soon be tied into the visible zoom lens so the two track each other.

Future Plans

The next few months will be devoted to finalizing the prototype system so it can be handed over to operations personnel for testing in the field. If the performance of the unit is satisfactory, a final version for field use will be fabricated and delivered to operations.

Contacts:

J. D. Collins, 867-4449, DL-ESS-24

F. W. Adams, 867-4449, DL-ESS-24

Participating Organization:

Boeing Aerospace Operations, Engineering Support Contract (R. C. Youngquist, S. M. Gleman, C. B. Mattson, and W. E. Rutherford)

NASA Headquarters Sponsor:

Office of Space Flight

Feasibility Study - A New Method for Detecting Hydrazine Fuels Using Chemiluminescence

Objective

To investigate the potential of a new analytical technique for the detection of hydrazine

vapors. The new method proposed that vapors of hydrazine, monomethylhydrazine (MMH), and unsymmetrical dimethylhydrazine (UDMH) could be sampled, derivatized, concentrated, and subsequently analyzed by gas chromatography coupled with chemiluminescence detection.

Background

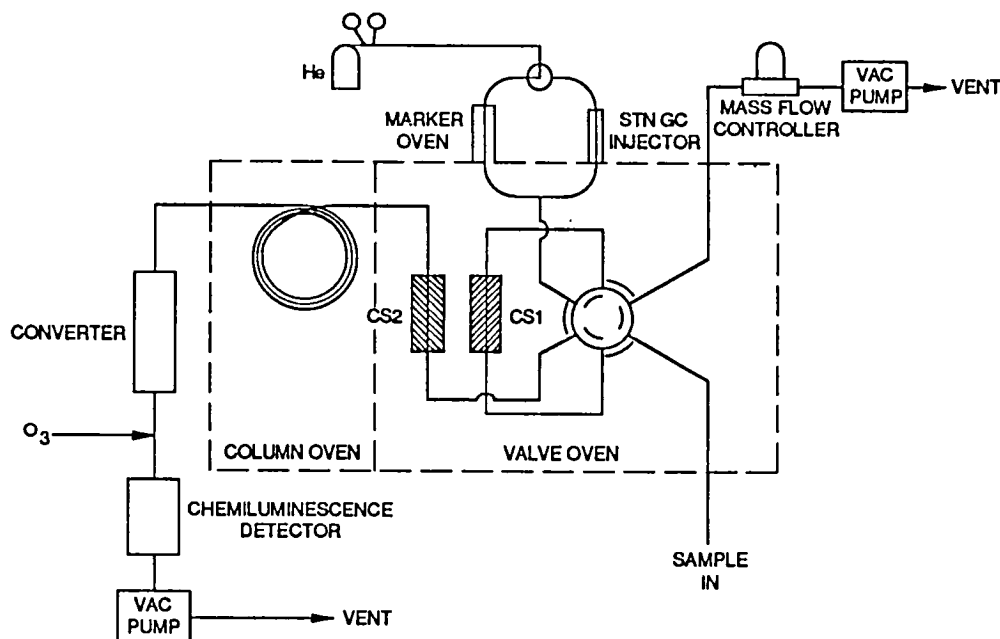
Hydrazines are used in large quantities by NASA and the Department of Defense as hypergolic fuels. These compounds, although highly useful, are also corrosive and suspected human carcinogens when present in air at low levels. At high levels, they pose fire and explosion hazards and are potent toxins. Recently, the American Conference of Governmental Industrial Hygienists proposed that the threshold limit values of the hydrazines be dropped to 10 parts per billion (ppb). No technology currently exists that can measure hydrazine vapors at both the high and low levels of interest. The goal of this investigation was to determine the potential of detecting hydrazine vapors when present in the concentration range of 0.010 to 20 parts per million (ppm) by gas chromatography coupled with chemiluminescence.

Approach

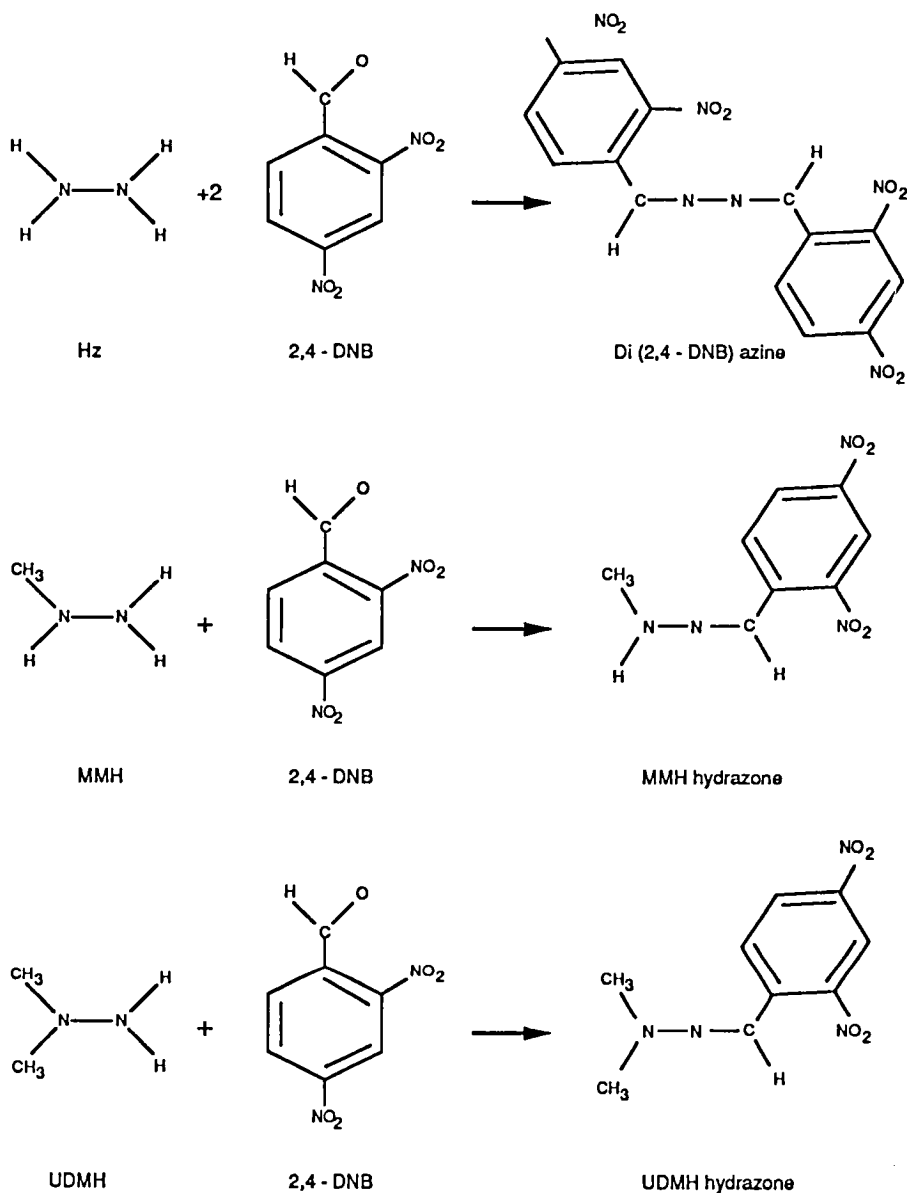
The analysis consisted of two major steps. First, vapors were sampled and derivatized. Second, the derivatives were analyzed by gas chromatography coupled with chemiluminescence detection. A breadboard instrument was constructed to perform the entire analysis automatically (see the figure "Breadboard Hydrazine Monitor").

Sampled hydrazine vapors were derivatized 2,4-dinitrobenzaldehyde (DNB) to form their hydrazones (see the figure "Reaction of Hydrazines With 2,4-Dinitrobenzaldehyde"). The derivatization was accomplished on a cold spot (CS1). The cold spot also served to concentrate the sample. Analyzing the hydrazines in their derivatized form facilitates concentration of the sample, thus reducing the detection limit of the method. The derivatization step also improves selectivity because only those sample constituents that react with the DNB will be concentrated for analysis.

Chemiluminescence detection with gas chromatography was chosen for the analysis of the hydrazine derivatives because the technology has shown great success in drug and explosives detection at low detection limits. The hydrazones are desorbed from CS1 and are captured on a second cold spot (CS2) for injection into the gas chromatography column. Gas chromatography provided a means of separating the derivatives prior to detection to further improve selectivity. Newly developed high-speed gas chromatography techniques were employed to reduce the separation time to less than 10 seconds. The hydra-



Breadboard Hydrazine Monitor



Reaction of Hydrazines With 2,4-Dinitrobenzaldehyde

zones are heated to 800 degrees Celsius over nickel oxide in the converter. The pyrolysis products are nitric oxide and combustion products. The nitric oxide is detected using the chemiluminescent reaction of nitric oxide with ozone, where the amount of light released is proportional to the amount of nitric oxide present. Chemiluminescence analysis is very sensitive and selective. Using a test vapor gas generation system to provide hydrazine vapors at known concentrations in air at controlled rela-

not 100 percent. The breadboard was not as sensitive as expected. To achieve detection at low concentrations, the sample time needed to be increased. The detection of the entire concentration range may be possible with one instrument if the sample time is varied. The incomplete reaction of the hydrazines with DNB would not be a problem if it were consistent. Unfortunately, it was not consistent in the breadboard as configured for this test. Increases in relative humidity improved the reaction efficiency and

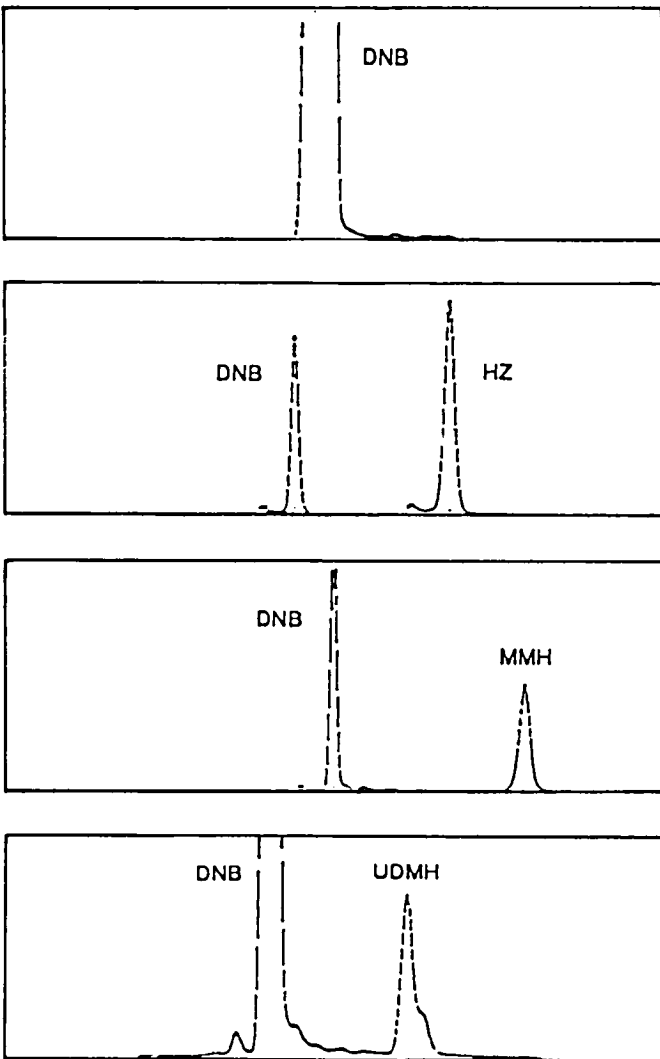
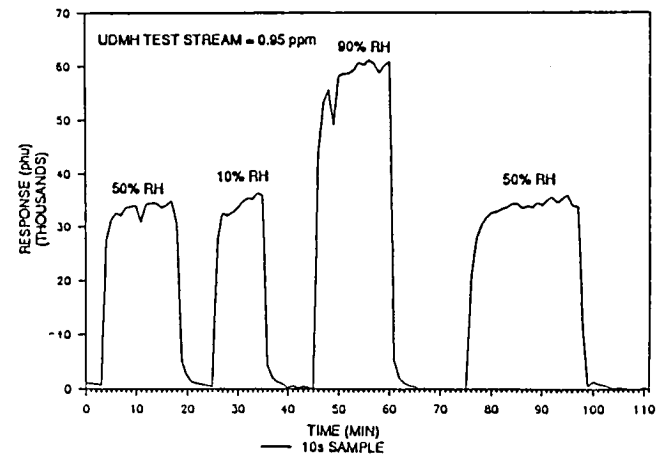
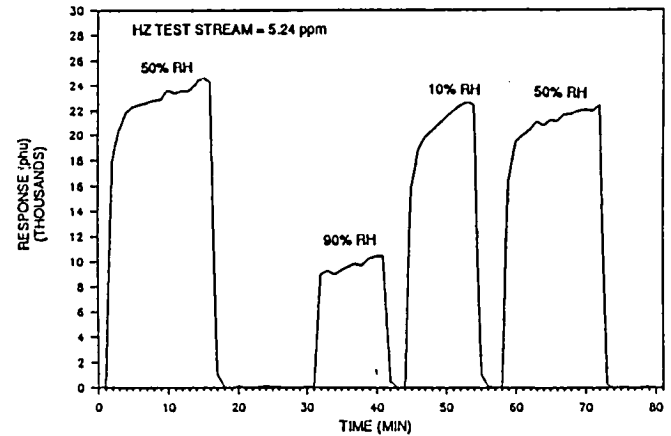
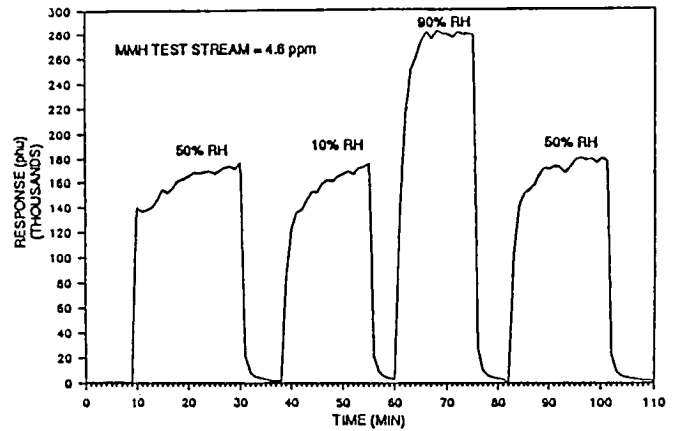
tive humidity, the breadboard monitor was tested for sensitivity, linearity, relative humidity effects, and stability.

Results

The breadboard did detect hydrazine, MMH, and UDMH as shown in the figure "In Situ Derivatization of Hydrazine Vapors Introduced by Automatic Sampling." Columns were found that could separate the hydrazine, MMH, and UDMH derivatives, although the hydrazine derivatives presented a problem. The reaction with hydrazine can form a hydrazone with only one DNB molecule or an azine with two DNB molecules if it goes to completion. The azine compound is almost twice the size of the other hydrazones and is difficult to move through the column that separates the hydrazines. A less polar column provided the detection of the vapors, but did not separate MMH and UDMH. The response of the breadboard was not linear over the range of 0.10 to 20 ppm (see the figure "Instrument Response Versus Concentration"). This suggests that the reaction with DNB is

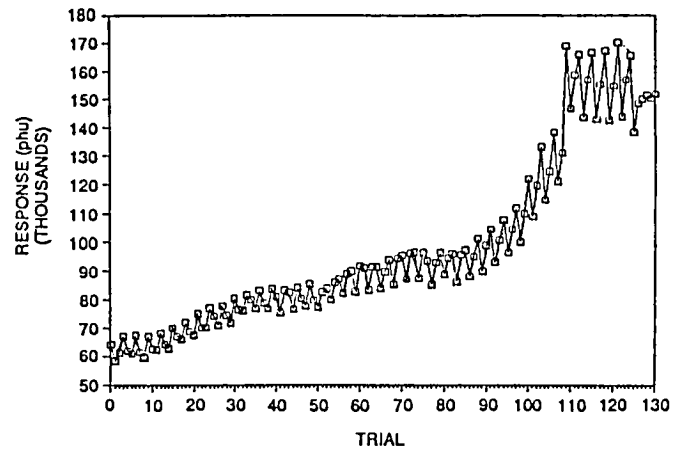
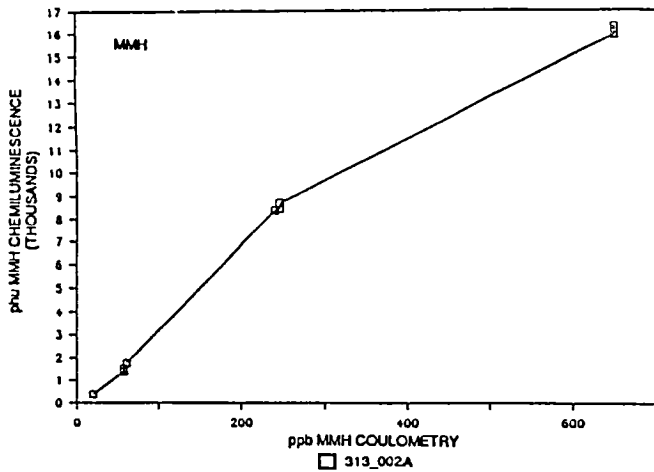
increased the response of MMH and UDMH (see the figure "Response Versus Relative Humidity"). The signal for hydrazine goes down because more azine is formed and the instrument, as configured for that test, detected the hydrazine rather than the azine. The calibration stability was poor over three days (see the figure "Calibration Drift, MMH Test Stream 5 ppm").

Although not fully successful as tested, the program did demonstrate the feasibility of the gas chromatographic/chemiluminescence technology. The technology does detect hydrazine, MMH, and UDMH. The system is capable of

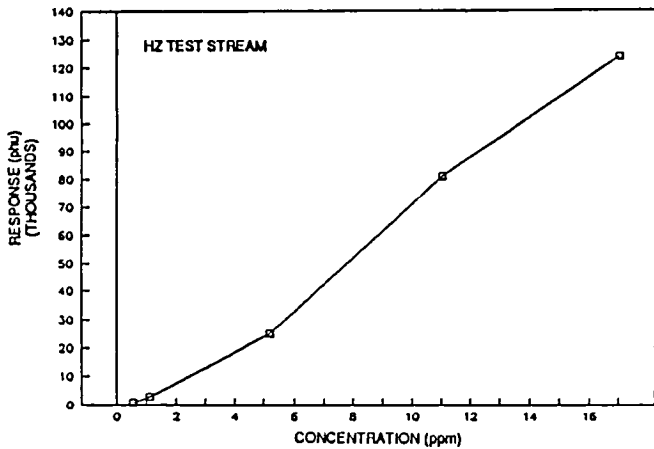


In Situ Derivatization of Hydrazine Vapors Introduced by Automatic Sampling

Response Versus Relative Humidity



Calibration Drift, MMH Test Stream 5 ppm



measuring a wide dynamic range through sample manipulation such as changing the concentration time on the first cold spot. A better derivatizing agent might overcome the problems in reaction efficiency. A humidified carrier gas could eliminate the relative humidity effects.

Contact:

R. C. Young, 867-4438, DL-ESS-24

Participating Organizations:

Naval Research Laboratory (J. R. Wyatt and S. L. Rose-Pehrsson)

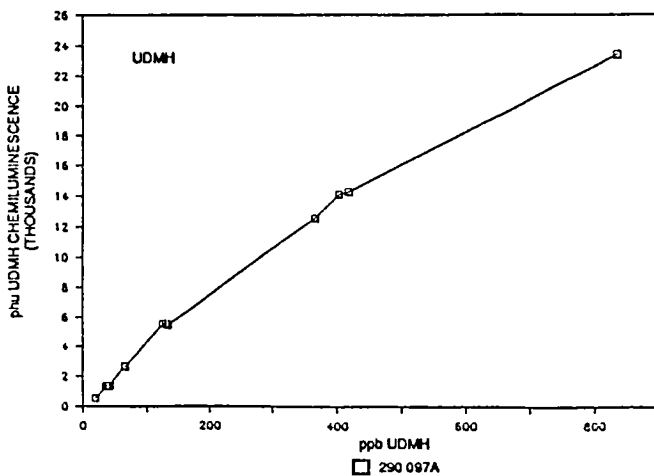
Thermedics, Inc. (S. MacDonald and D. Rounbehler)

Aerospace Corporation (H. Takimoto and G. Loper)

U. S. Air Force /Space Division (K. Held)

NASA Headquarters Sponsor:

Office of Space Flight



Instrument Response Versus Concentration

Hydrogen and Helium Visualization

Objective

To find and demonstrate technologies that permit hydrogen and helium leaks to be visualized or imaged.

Background

In May 1990 hydrogen leaks were detected on STS-35. These leaks and another hydrogen leak on STS-38 grounded the Space Shuttle fleet for over six months. Once detected, it became imperative to locate the hydrogen leaks. Several technologies were investigated that showed promise. One of these was a schlieren method.

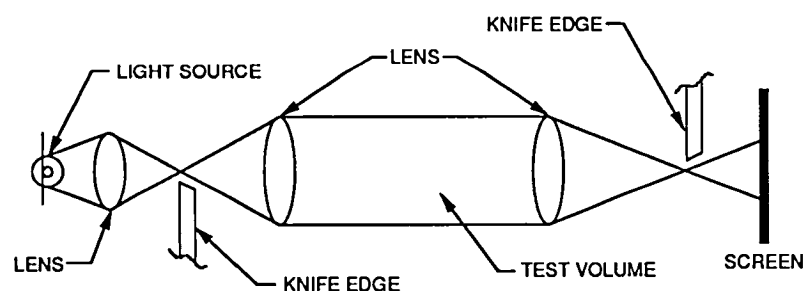
Approach

After an extensive literature search, several potential technologies were identified. One method, the schlieren method, was based on the 130-year-old Foucault knife-edge test used for measuring mirror figures or striae in optical glass. This method uses an optical system that is set up to vary the intensity of the pattern in the image plane with a change in the refractive index inside the test volume. A schematic of a simple schlieren system is shown in the figure "Schlieren System."

This method and several variations thereof were built and tested. Some of these methods were: a double-ended schlieren system using a knife edge, a large (16 by 72 inches) test volume Ronchi ruling/mirror system, a small hand-held system for field testing, and a double grid system.

Results

Visualization of both hydrogen and helium leaks was demonstrated down to about 10 standard cubic centimeters per minute. The



Schlieren System

large test volume system was used to precisely locate hydrogen jets for analysis and frequency correlation with a mass spectrometer. Preliminary investigations of a single-ended schlieren system based on an electronic speckle pattern are complete. Future work in this area is planned.

Contact:

J. D. Collins, 867-4438, DL-ESS-24

Participating Organization:

Boeing Aerospace Operations, Engineering Support Contract (S. M. Gleman and R. C. Youngquist)

NASA Headquarters Sponsor:

Office of Space Flight

Development of an Interim Active Vanillin Sampler Used to Detect 10 Parts Per Billion of Hydrazine and Monomethylhydrazine in Air

Objective

The objective of this project was to develop a sampler capable of detecting 10-part-per-billion (ppb) concentrations of monomethylhydrazine (MMH) and hydrazine that would be available prior to the introduction of the portable fuel vapor detector for 10 ppb (PFVD-10) in the 1994 timeframe. This sampler was to be based on a vanillin-coated paper tape colorimetric technology that was already in use at Kennedy Space Center (KSC) for passive detection of MMH. The sampler would use a personal portable pump to actively draw air through the paper to quickly concentrate a sample, yielding quantitative analyses of concentrations as low as 10 ppb in less than 5 minutes.

Background

Hydrazine and MMH are used widely in the military, private industry sectors, and the Space Shuttle program.

Recently, there has been a proposal by the American Conference of Governmental Industrial Hygienists (ACGIH) to lower the hydrazine-based vapor exposure limits to 10 ppb. NASA management instructions require meeting this standard to ensure worker safety. Because no manufactured instrument is available for dynamic 10-ppb detection, industrial hygienists with the Space Shuttle program have no real-time method to comply with these new regulations. To prepare for these expected low limits, the PFVD-10 project was initiated to develop suitable detection instruments over the next few years. In the meantime, the NASA KSC Instrumentation Section, Toxic Vapor Detection Laboratory, developed an interim method to monitor the workers' breathing air.

Approach

Paper sensitive to hydrazine and MMH was purchased commercially from GMD Systems, Inc. GMD uses Chroma 1 chromatography paper treated with a 2 percent w/v vanillin (4-hydroxy-3-methoxy-benzaldehyde) in 0.5 percent v/v phosphoric acid-isopropyl alcohol solution. Quantitative color detection was performed with a Minolta Chroma Meter model CR-200 using the luminosity chroma hue angle (LCH°) coordinate system. A semiquantitative color evaluation was made with a color comparator wheel that is available from GMD Systems Inc. Two different intrinsically safe personal air sample pumps were tested: the MSA Flow-Lite Pro and the Ametek (DuPont) Alpha 1.

The interim active vanillin sampler (IAVS) prototype design consists of an intrinsically safe personal air sample pump that draws ambient air through the vanillin-coated filter paper contained in a specially designed filter holder. Data was gathered on various spot diameters, flow rates, and sample times over a range of MMH vapor concentrations for a wide range of temperatures and relative humidities. The best combination of spot diameter, flow rate, and sample times was used to create the two prototype units.

Results

The vanillin-treated paper is colorless until it is exposed to air containing hydrazine or MMH. After as little as 3 minutes of sampling 10 ppb of hydrazine or MMH, the paper turns yellow. Optimally, these vapor concentrations may be determined in the workplace by drawing a 2-liter-per minute air sample for 5 minutes, then either matching an existing vanillin color comparator wheel or reading with a commercially available color analyzer. When using the LCH° reference system, the luminosity (L) and hue angle (H) remain fairly constant, while the chroma (C) is proportional to the logarithm of the vapor concentration between 3 ppb and 3 parts per million (ppm). The IAVS demonstrated very little dependency on relative humidity and temperature (at temperatures above 5 degrees Celsius), which will permit direct use of yellow color intensity for detection of hydrazine or MMH vapors in the air without correction for relative humidity or temperature.

Conclusion

The two prototype IAVS units were field tested at KSC between February and May of 1991 by industrial hygienists from EG&G and by safety personnel from Lockheed Space Operations Company (LSOC). Both organizations were given each type of unit and asked to provide their opinions about desirable and undesirable features of the units.

Personnel from EG&G made several recommendations and comments.

1. A pump with an elapsed timer that would automatically stop the pump after 5 minutes, obviating the need to have an accurate timer at the job site, was recommended.
2. The tape roll dispenser was favored because it was convenient in the field; however, design changes were recommended for improvement in both the ease of operation and the airtightness. The latter would prevent degrada-

tion of the paper tape from long-term exposure to humidity or ambient low levels of hypergolic fuel vapors.

3. Both pumps performed well; however, the MSA pump utilized a visible rotometer and a simple on/off switch, which was superior during Self-Contained Atmospheric Protective Ensemble (SCAPE) suit operations.
4. A modification to fit the paper tape as near the exterior as possible would aid the GMD color wheel assessments while the paper was still in the holder.

The LSOC Safety group indicated they were uncomfortable with the slowness of the IAVS and would have preferred an immediate indication of the presence of hydrazine and MMH vapors (comparable to a Gieger-Muller radiation survey instrument). They also indicated they would like an automatic timer shutoff and preferred a paper roll dispenser over the single-

disk-type screw cap holder.

In summary, the first-generation prototype of the IAVS system quickly quantifies the vapors of hydrazine and MMH in concentrations between 3 ppb and 3 ppm at normal, above-freezing air temperatures and over a wide range of relative humidities. The IAVS is uncomplicated, utilizes a nontoxic detector paper, and is intrinsically safe for most Class I, II, and III hazardous areas. This interim active vanillin sampler has been tried in actual work conditions and meets the current guidelines for the speed of sampling and analysis.

Contact:

R. C. Young, 867-4438, DL-ESS-24

Participating Organization:

*Boeing Aerospace Operations, Engineering Support
Contract (D. M. Blaies and N. A. Leavitt)*

NASA Headquarters Sponsor:

Office of Space Flight

Communications and Control

Fiber Optics, Communications, and Networks Laboratory

The Fiber Optics, Communications, and Networks Laboratory provides engineering support for Kennedy Space Center (KSC) copper and optical fiber cable plants. The major share of its human and material resources is assigned to the evaluation and application of state-of-the-art fiber optics communications technology. This includes fibers, connectors, splicing techniques, electro-optic receivers and transmitters, and multiplexing. Three other laboratory tasks are: (1) maximizing the utilization of the existing fiber optic and copper cable plants, (2) providing the technical expertise and hardware for the video and photo-optical systems used in support of KSC technical operations, and (3) defining and furnishing test equipment necessary for the maintenance of communications, video, and photo-optical systems.

The Networks section of the laboratory is dedicated to a wide range of computer-network-related activities. This area serves as the primary operations hub and network control center of the KSC data network. The majority of all network monitoring, troubleshooting, and support is performed from this location. This laboratory is also responsible for the evaluation and application of advanced network systems technologies.

Fiber Optics and Communications Section

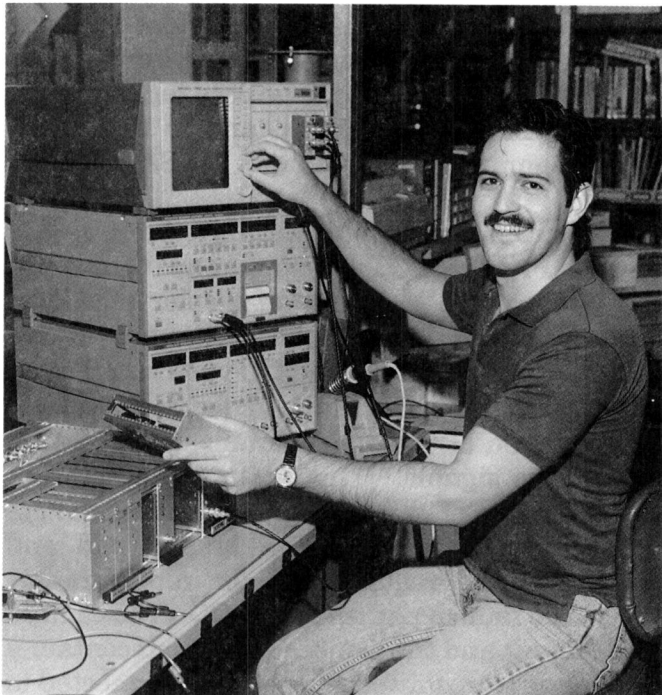
The Fiber Optics and Communications section of the laboratory is dedicated to exploring and developing new communications techniques for the copper and optical fiber communications systems at KSC. One of the major ongoing development efforts is in the area of Wave Division Multiplexing (WDM). WDM allows two wavelengths of light [1,300 nanometers (nm) and 1,550 nm] to travel down a single optical fiber. WDM techniques allow for unidirectional and bidirectional communications. Utilization of this technology will permit KSC to make more efficient use of its existing fiber optic cable plant.

WDM technology also plays a major role in another laboratory project, the development of a television camera system that will be the prototype next-generation operational television system for use on the launch pad. This project, termed Fiber Direct Operational Television, uses a single optical fiber to connect the camera to the control panel. The camera control unit and the camera head each contain a fiber optic transmitter and receiver connected to the optical fiber via a WDM device. Signals for synchronization and control of the pan-and-tilt head are transmitted from the camera control unit to the camera head on one optical wavelength (1,300 nm) while the camera's video output and status information are returned on the same fiber at a different wavelength (1,550 nm).

Also ongoing is the development of a Remote Monitor and Alarm System. The laboratory staff is designing a Remote Terminal Unit (RTU) that will be placed at various remote locations and will communicate the status of KSC's fiber optic communications equipment. The system will be anchored by a central monitor that will receive the status information from all RTU's, interpret the data, and report on the physical health of the fiber optic equipment. The central monitor will utilize state-of-the-art graphics and computing technology to make the system extremely flexible and user friendly.

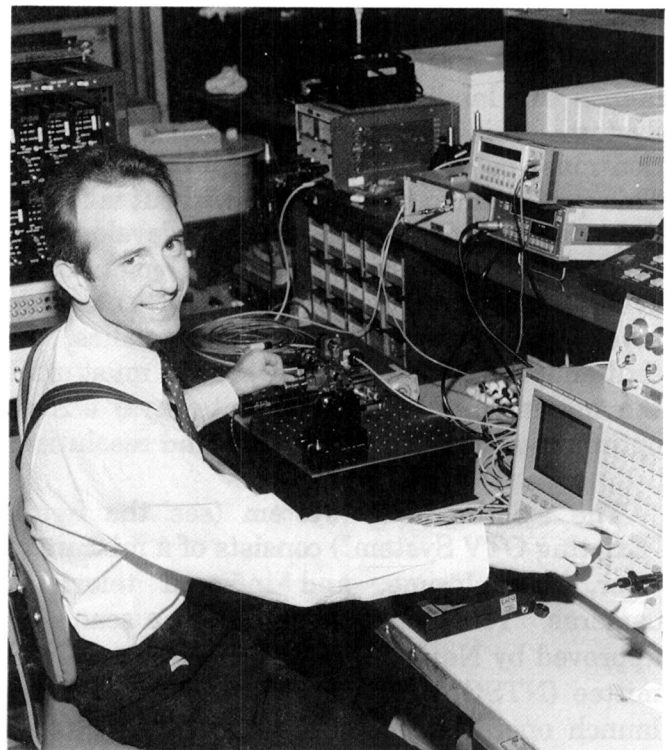
Networks Section

The Networks area of the Fiber Optics, Communications, and Networks Laboratory is dedicated to a wide range of computer-network-related activities. This area of the laboratory is currently the location of several prototype systems under development and a primary test site for a variety of field test systems. These prototypes include Premises wiring distribution systems, wide area network routing configurations, and a CAD-based networks documentation and cable tracking system. This networks documentation system is using the Engineering Development Laboratory facility as a pilot program and will include in the future all facili-



High Data Rate Prototype

ties at KSC. Another area of special interest is the evaluation and development of high-speed networking, including the emerging FDDI



*Wave Division Multiplexing
Development*

Another high-speed networking project is the FDDI Transmission System prototype design and evaluation. This prototype will provide the groundwork for the implementation of a high-speed data network backbone to interconnect all KSC facilities. Several other testbeds are scheduled to be implemented in the laboratory in the near future, including a Network Operating System testbed and an Open Systems Interconnection (OSI) protocol evaluation testbed.



Fiber Optics Connector Study

Direct Fiber to Operational Television Camera System

The Fiber Optics, Communications, and Networks Laboratory is participating in the development of a television camera system that will be the prototype for the next generation of an operational television (OTV) system camera for use on the launch pad. The OTV system at Kennedy Space Center (KSC) provides real-time and recorded visual information necessary to conduct and document hazardous and nonhazardous activities during daylight and nighttime operations involving buildup, integration, launch, and landing of the Space Transportation System. This engineering and safety information must be of the highest achievable quality. This quality must be sustained without material degradation and during duplication, development of training aids and materials, engineering evaluation, and analysis for the detection, investigation, and correction of anomalies. To that end, each element of the system must meet the maximum performance criteria to ensure optimum overall picture quality and resolution.

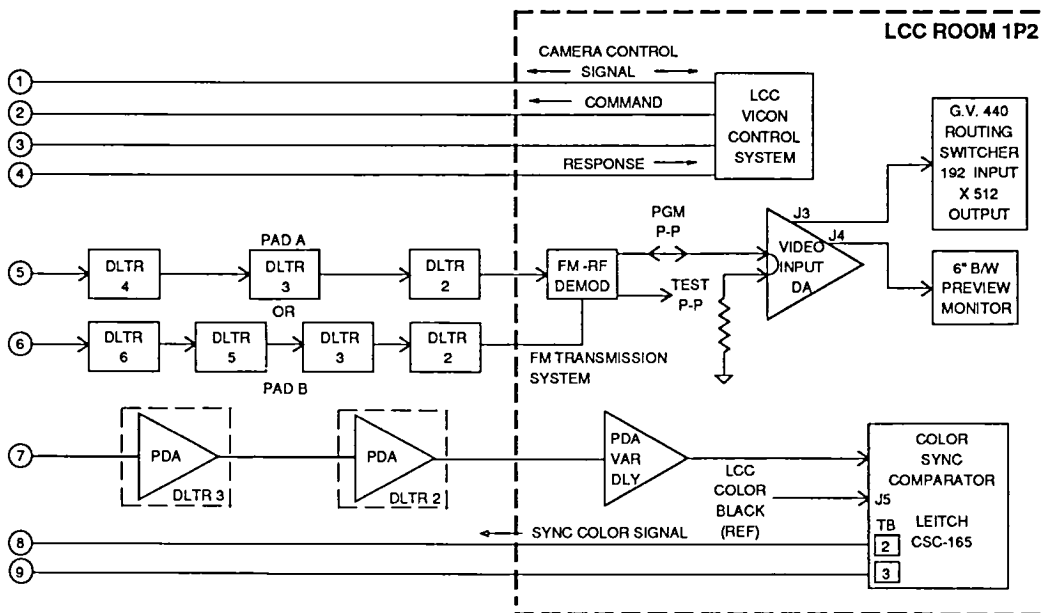
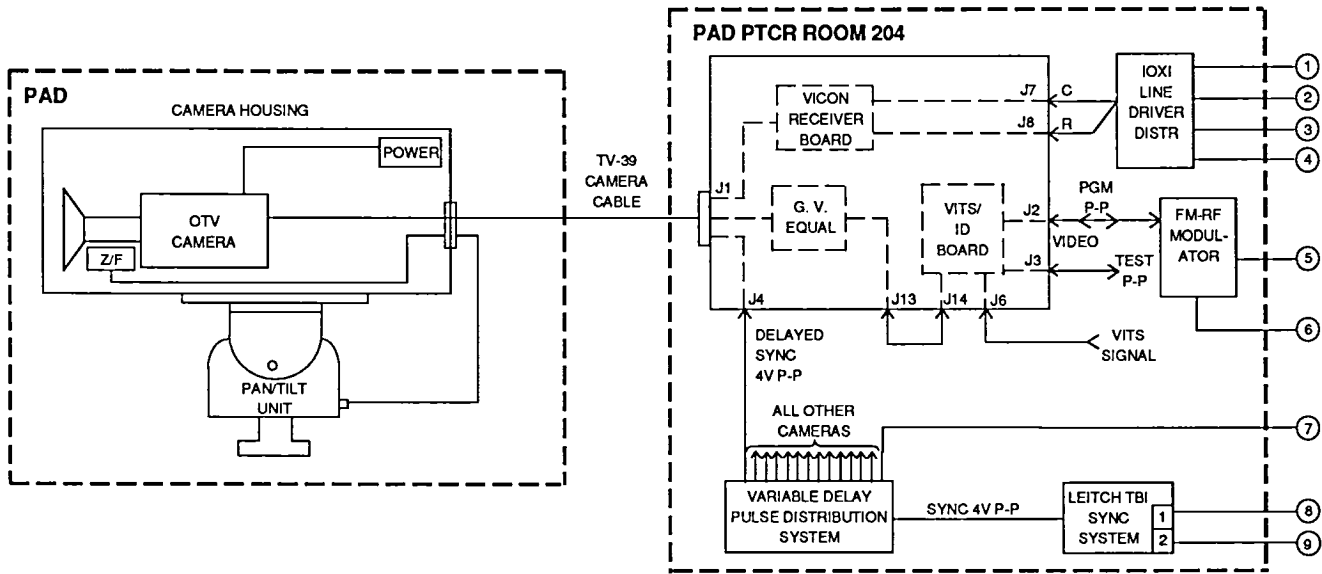
The existing OTV system (see the figure "Existing OTV System") consists of a mixture of color, monochrome, and infrared television cameras. Television cameras with a scan rate approved by National Television Systems Committee (NTSC) are presently used to monitor launch operations. At the launch pad, these cameras are connected to camera control units in the Pad Terminal Connection Room (PTCR) via TV-39 multicore camera cable. The camera control units contain built-in video equalizers to compensate for loss in transmission on this cable. The video output from the camera control units is connected to a frequency modulation radio frequency (FM-RF) modulator; the radio frequency outputs of these modulators are combined onto coaxial trunk cables. The trunk cables proceed through numerous repeater stations to the Launch Control Center (LCC). In the LCC, the radio frequency signal from these trunks passes through a splitter to individual

demodulators. The demodulated video signal is then fed to a video routing switcher for distribution to the end users, to recorders for documentation of launch operations, and to the NASA Select Channel for use at other NASA centers.

The prototype OTV camera system (see the figures "Prototype OTV System" and "Camera at the Launch Pad") consists of a color television camera at the launch pad connected to the camera control unit in the LCC via a single fiber optic cable, which is utilized for bidirectional transmission of video, synchronization, control, and status signals. This prototype eliminates the necessity of equipment for camera control and synchronization at the launch pad and eliminates the requirement for repeaters between the launch pad and the LCC. The camera control unit and the camera head each contain a fiber optic transmitter and receiver connected to the optical fiber via a wavelength division multiplexer. Signals for synchronization and control of the camera and control of the pan-and-tilt head are transmitted from the camera control unit to the camera head on one optical wavelength (1,330 nanometers), while the camera's video output and status information are returned on the same fiber utilizing a different wavelength (1,550 nanometers).

The prototype system has been used continuously to transmit and study analog transmission of composite video from the camera. The camera has been successfully operated during STS-48 and STS-44 launches. The prototype system is being used to study analog transmission of composite video from the camera.

A series of tests of the existing and prototype television transmission systems were conducted to evaluate the potential benefits of fiber optic transmission for OTV signals used in monitoring and documenting launch processing operations at KSC. These tests supplied both subjective and objective data on the benefits of improvements in this transmission media to the monitoring of launch processing operations. Some of the measured improvements attributed to fiber optic

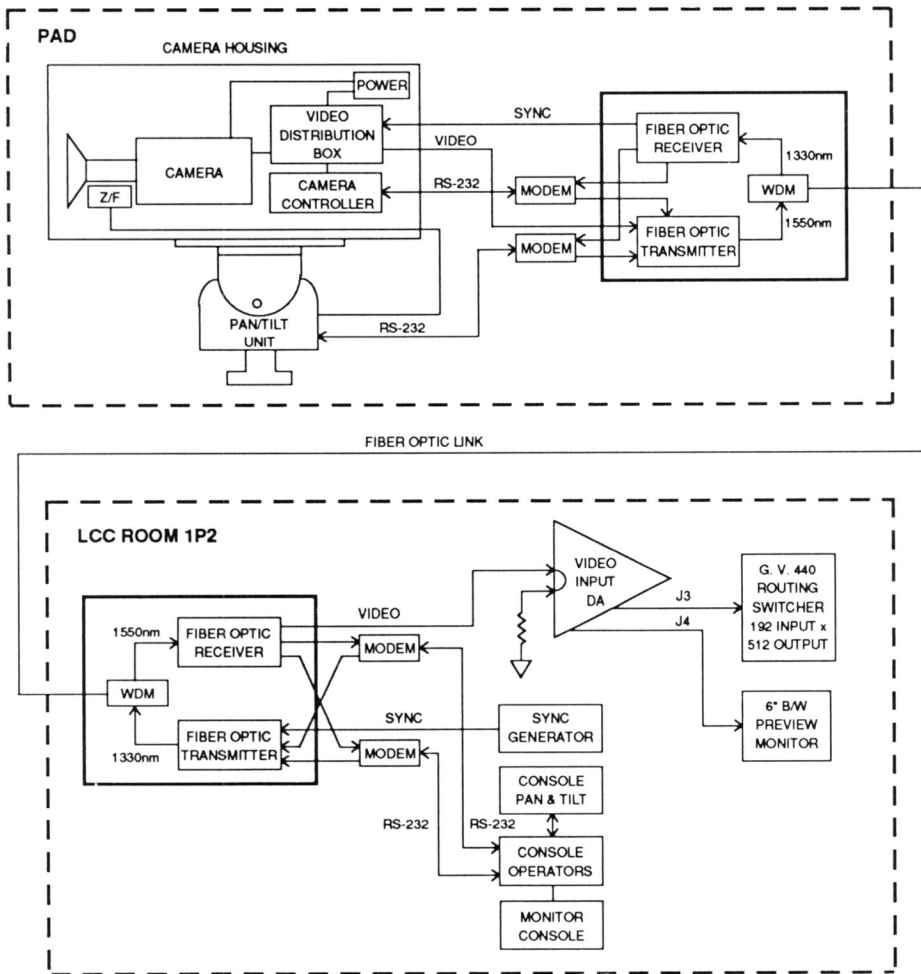


Existing OTV System

transmission include: (1) an increase in the resolution of the camera signals from approximately 356 lines to 672 lines, (2) a decrease of distortion attributable to a differential phase from 2 degrees to 0.91 degree, (3) a differential gain from 3 percent to 0.84 percent, and (4) an improvement in the signal-to-noise ratio from 56 decibels to 66 decibels.

A second prototype camera station and trans-

mission system is being developed. This prototype camera station is intended to be field deployed on the Fixed Service Structure at the pad. Its purpose is to allow the further definition of system specifications in the area of modular control system designs, multiple camera control over a local area network (LAN), improved operator interface, automatic monitoring and fault reporting, and definition of other requirements unique to the actual launch envi-



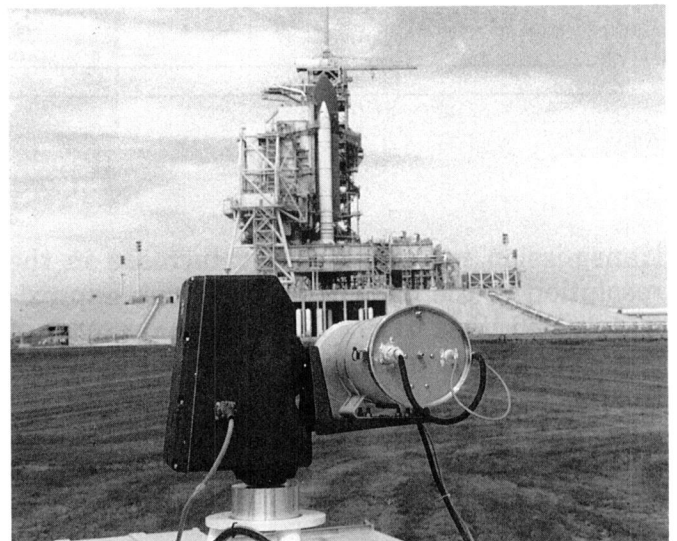
Prototype OTV System

ronment related to its new system design. The system operation will be evaluated in the severe launch environment (i.e., vibration, temperature, shock, and humidity conditions).

While microprocessor-based systems for camera control are used in the existing OTV system, the camera interfaces are primarily hardware based. This situation results in system limitations on the type, number, and compatibility of control functions that can be interfaced. The first prototype control system uses serial data communication with a microprocessor-based camera to maximize the ability to address and control camera functions. The prototype system software has been written in C language. The software provides the user access

to and status reporting of the camera system functions, including control of the camera, lens, pan-and-tilt mechanism, and lighting system.

A second prototype control system is under development (see the figure "Typical Camera Control System for Multiple Cameras"). This system addresses multiple camera systems of differing functions by use of modular software driver packages for each type of system to be controlled. In addition, the software design is object oriented to permit ease of operator reconfiguration as additions, deletions, and changes are made to the system. The second prototype uses a LAN to permit multiple users access to all camera systems on the network as shared resources. Individual permission tables could permit restrictions to be imposed on the functions



Camera at the Launch Pad

Mechanics, Structures, and Cryogenics

The sheer magnitude of the mechanical systems and attendant structures at Kennedy Space Center (KSC) requires unique facilities and equipment to solve design and operations problems or to advance the state of the art in mechanical and civil engineering. Four major areas that support the mechanics, structures, and cryogenic design and research effort are: (1) the Launch Equipment Test Facility, which is the primary testbed for full-scale, proof-of-concept testing of the umbilicals, service arms, holddown posts, and other ground-to-vehicle electrical and fluid connections used at the launch sites; (2) the computer-aided design and computer-aided engineering facilities, where modeling is accomplished through an extensive design software library; (3) the Prototype Laboratory, which provides the services and tools to rapidly convert the engineering designs to hardware; and (4) the academic community in which conceptual design and theoretical analyses are performed.

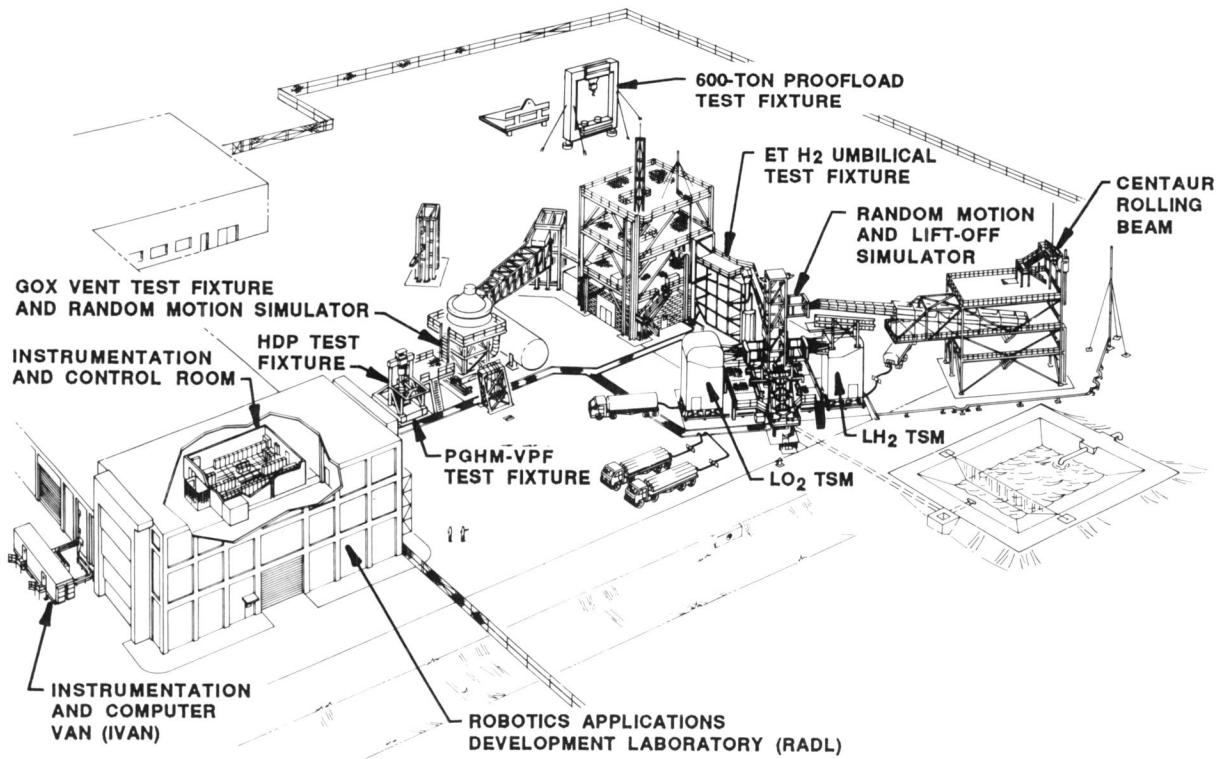
Launch Equipment Test Facility

The Launch Equipment Test Facility is a unique engineering complex dedicated to the development and qualification testing of virtually all the NASA launch equipment mechanisms. The facility's test fixtures and supporting

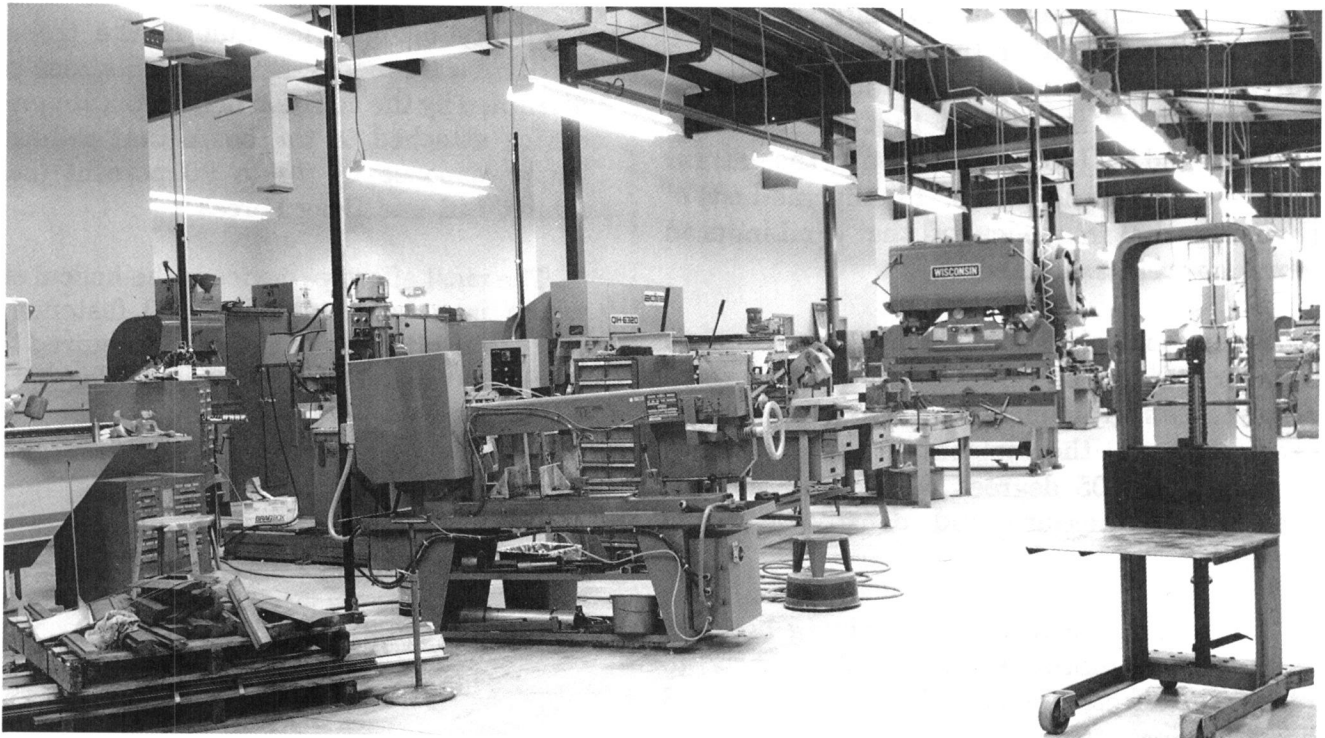
electrical/electronic systems have the capability to simulate launch-site conditions such as cryogenic loading and flow, pyrotechnic operation, random motion, abort motion, liftoff motion, and other phenomena associated with launch operations. An extensive measurement system is available to obtain, record, display, and analyze data associated with the testing. The facility also supports development and qualification testing of fluid system valves and other components, free-fall restraints, load-bearing fixtures and lifting slings, and robotic applications development.

Prototype Laboratory

The Prototype Laboratory provides KSC with a civil-service-staffed facility that has the capability to develop, fabricate, modify, model, breadboard, and/or test all manner of electrical and mechanical passive or active components, subsystems, and systems on a nonproduction or limited-production basis. The technical staff has the versatility to work from rough sketches as well as from formal engineering drawings. The laboratory is composed of a mechanical department (including metal working, sheet metal forming, welding, and a high-pressure fluid test cell), a woodworking and model-making department, an electrical/electronic department, and an instrumentation department.



Launch Equipment Test Facility



Prototype Laboratory

Determination of the Effects of Wind-Induced Vibration on Cylindrical Beams

Many of the launch facilities at Kennedy Space Center (KSC), such as the Rotating Service Structure and the Fixed Service Structure at the launch pads and the Launch Equipment Test Facility (LETF), are constructed of cylindrical beams. A method was needed for determining which beams would be affected by wind-induced vibration; the study is described in detail in KSC-DM-3538.

The objective of this study was to determine a critical length-to-diameter ratio (L/D_0) of a hollow cylindrical beam subjected to wind-induced vibration. The sizes of beams ranged from 4 to 24 inches, inclusive of all standard thicknesses, and were composed of American Society for Testing and Materials (ASTM) A53 grade A and grade B [4- to 12-inch nominal pipe size (NPS)] and American Petroleum Institute (API) grade X42 (4- to 12-inch NPS). Calculations used a maximum steady-state wind speed of 130 miles per hour (mph) associated with hurricane conditions possible at KSC. Also examined were the effects that different end supports and load conditions have on the natural frequency (f_n) of the beams. Finally, methods of changing the frequency of the wind-induced vibration were examined.

Other constraints limited: (1) the Reynold's number (R) to less than 10^6 , where the wake remains nonturbulent and vortex formation is predictable; (2) the ambient temperature to a maximum of 105 degrees Fahrenheit; and (3) atmospheric pressure and density to being standard.

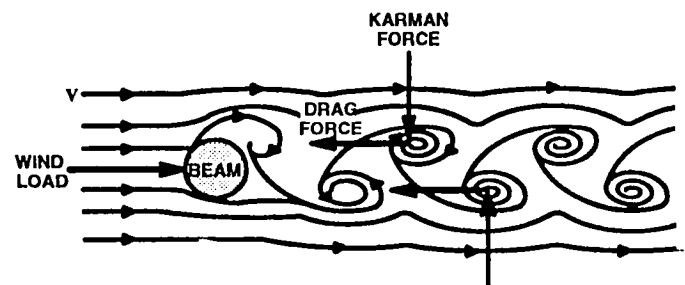
The research involved determining how the wind causes vibration in cylinders, how to reduce the effects of wind-induced vibration, and how the beam oscillation changes with increased wind velocity.

Computations using a spreadsheet program were first performed to determine each cylinder's R for wind velocities ranging from 0 to 200 mph in 5-mph increments. The frequencies of the wind-induced vibration for each cylinder were also computed at these wind velocities.

The natural frequencies of the cylindrical beams were computed for each loading and end support condition for each L/D_0 from 1 to 25. Once the natural frequencies were known, the cutoff resonance frequency ranges were computed and the corresponding L/D_0 determined. From this data, trends in the L/D_0 were analyzed for each beam size, load type, and end support condition. The combined load analysis, performed using finite element analysis, simulated the effects of multiple loads in all possible combinations of bending, axial, and torsional forces and moments.

Research showed that the beam vibrations were caused by the formation of Karman vortices in the cylinder wake producing lift and drag forces on the cylinder resulting in transverse and inline oscillations, with the inline vibration frequency being twice that of the transverse oscillation frequency. These oscillations can be disrupted by the addition of a vortex suppression device attached to the beam that reduces the beam response by 70 to 90 percent (see the figure "Lift and Drag Forces").

The most effective device is the helical strake, which is a band (usually flat) fastened at a particular pitch (length of beam required for the strake to encircle 360 degrees). The optimum



Lift and Drag Forces

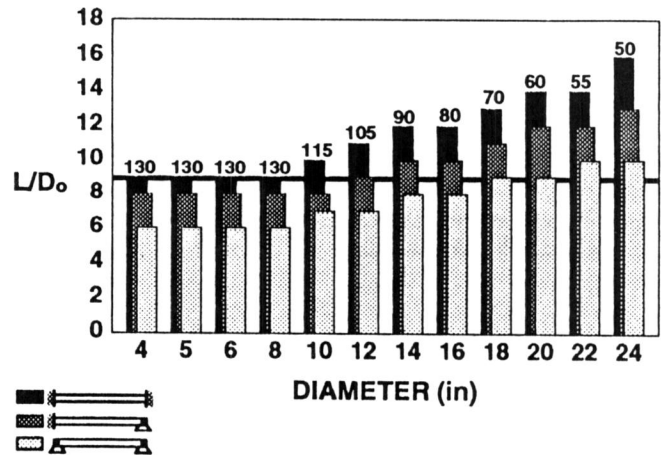
configuration is to place three sharp-edged strakes, $0.1D_0$ high, at 120-degree intervals around the cylinder with each strake at 60-degree angles to the beam. These devices are simple and economical solutions since the strakes are positioned independently of the wind direction, do not increase the dimensions of the beam excessively, and can be maintained easily against corrosion. (See the figure "Helical Strake.")

Computations of R for each beam showed that R was more than 10^6 for diameters greater than 8 inches at wind velocities faster than 130 mph. These beams were limited in this analysis to maximum wind velocities associated with R equal to 10^6 . The figure "Transverse Vibration, No Loads" shows the L/D_0 associated with the cutoff frequency versus beam diameter for the transverse vibration in unloaded beams. The black bars represent the welded support condition, the lightest gray is the pinned supports, and the medium gray is the combination weld-pin connections. The horizontal line represents the L/D_0 associated with the natural frequency at 130 mph for each size beam with welded end connections, independent of R. The number above each group of bars is the maximum steady-state velocity for which that beam size is valid for this study with regard to R. The trends showed that at a particular wind velocity, 130 mph in this case, every size beam exhibited the



3 PARALLEL STRAKES
120° APART
 $3.6 D_0 < \text{PITCH} < 5 D_0$
HEIGHT = $0.1 D_0$

Helical Strake

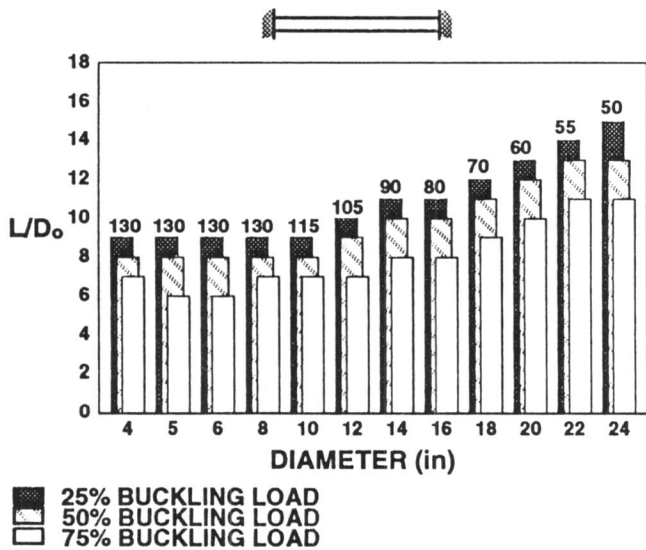


Transverse Vibration, No Loads

same L/D_0 corresponding to its particular cutoff frequency for each loading condition. But, because of the limitations with R, the larger beams' data showed higher L/D_0 .

The chart also shows that the greatest L/D_0 avoiding the wind-induced vibration frequency range was produced in the welded end support condition for every size beam. In other words, the more rigid the support connection, the longer and more slender the beam can be before the effects of wind-induced vibration become a factor. This was evident for every type of applied load.

Focusing on the rigid, welded support condition, the figure "Transverse Vibration, Uniform Axial Loads" shows the effects of applied uniform axial loads on transverse vibration frequency in terms of L/D_0 and beam diameter. The numbers above the bars indicate maximum steady-state wind velocities valid for each size beam; and the dark, striped, and white vertical bars are the results from the application of 25, 50, and 75 percent buckling loads, respectively. The chart indicates that as the compressive axial load increases, the natural frequency of the beam decreases along with the corresponding L/D_0 . Conversely, if uniform tensile loads are applied to the beam, the natural frequency would increase in the beam resulting in a greater cutoff L/D_0 . The 25 percent buckling load



Transverse Vibration, Uniform Axial Loads

situation produces almost no difference in the results compared to the transverse vibration in unloaded beams. Therefore, the lower the compressive loading, the greater the L/D_0 can be for a beam before it is affected by wind-induced vibration.

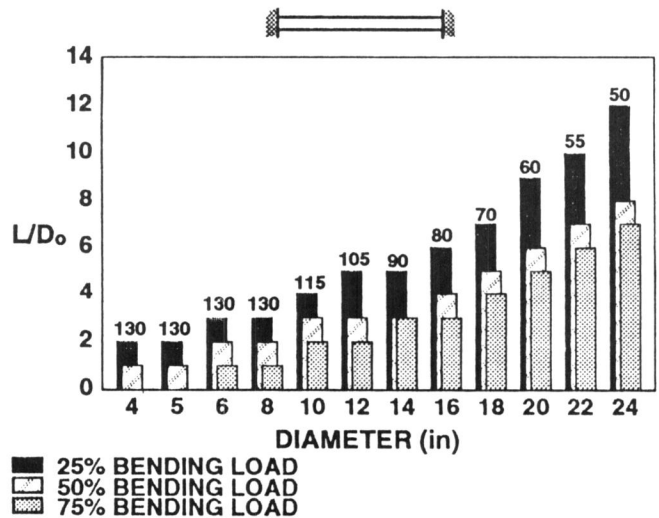
Similarly, the L/D_0 decreases as increasing bending loads are applied to the beam. This is shown in the figure "Transverse Vibration, Bending Loads" with 25, 50, and 75 percent of the maximum bending loads applied to the beams. Again, the numbers above the bars are the maximum valid steady-state wind velocities for each beam in the analysis. The bending loads drastically reduce the natural frequency of the beams to the point where, whenever any of these loads are applied, wind-induced vibration should be considered.

Natural frequencies were computed for longitudinal, shear, and torsional applied loads. These loads produce higher frequency vibration in planes of motion other than transverse, like wind-induced vibration, and are not a factor when considered individually. When they were applied in any combination with each other or applied to axial and bending moments and forces, they reduced the transverse natural frequency by 19 to 93 percent of that of the

unloaded beam. This resulted in beams with lower L/D_0 values being affected by the wind-induced vibration.

It was concluded from this study that the regularly forming vortices in the cylinder wake exert lift (Karman) and drag forces on the cylinder causing it to oscillate in line and transverse to the flow. The effects of the wind-induced vibration can be minimized by decreasing the L/D_0 (increasing the outside diameter or decreasing the length of the beam) or by adding a vortex suppression device, like helical strakes, which can reduce the response of the beam by as much as 90 percent of the plain beam.

The conditions that resulted in the largest L/D_0 that did not interfere with the resonance frequency range were produced in the unloaded beam with welded end support conditions. The results for the welded beam were greatest for all loading conditions compared to the pinned beam's results. The highest L/D_0 values were also obtained for beams that carried less than 50 percent of the maximum applied axial and bending loads. The vibration from other applied loads (shear, longitudinal, and torsional) create motion in planes other than transverse and do not contribute to the wind-induced response if each is the sole load applied to the beam. But, all loads must be considered when they are



Transverse Vibration, Bending Loads

applied in any combination because, together, they can produce natural frequencies 19 to 93 percent less than those of unloaded beams.

Several recommendations were made based on these conclusions. First, only rigidly bolted or welded connections should be used to support the beams. Second, the L/D_0 should be decreased, whenever possible, preventing the beam's induced response from lying within the resonance frequency range. This can be done by decreasing the overall length of the beam, adding rigid supports along the beam length, and increasing the beam diameter. Finally, helical strakes should be added to the beam to reduce the induced response in the beam when it must be designed with an unacceptable L/D_0 .

Contact:

E. A. Artusa, 867-7584, DM-MED-33

NASA Headquarters Sponsor:

Office of Space Flight

Vibration Response Analysis of Launch Pad Structures Subjected to Random Acoustic Excitation

Background

During a Shuttle launch, structures in the proximity of the launch pad are subjected to intense acoustic pressures generated by rocket exhausts. The design of some structures, particularly those having a large area-to-mass ratio, is governed by the launch-generated acoustic environment, a relatively short but very intense random pressure transient. The factors influencing the acoustic excitation process and the resulting structural response are numerous and cannot be predicted precisely. The objectives of this on-going research program at Kennedy Space Center (KSC) are twofold:

1. To accurately characterize the launch-induced near-field acoustic environment using previous launch measurements

2. To develop a reliable method for predicting the response of structures subjected to the launch pad acoustic environment

Acoustic Field Characterization

The acoustic environment generated by the launch of the Space Shuttle is random transient and requires special data processing programs to account for the nonstationary character of the measured pressures. Because this acoustic pressure field is extremely complex, it does not lend itself to a simple analytical description and/or field idealization. Almost all of the commercially available data processing software involve stationary data assumptions and, therefore, are unsuitable for the present application.

Traditionally, the power spectral density (PSD) and an alternate form, the 1/3-octave band sound pressure level (1/3-OBSPL), are often used to describe the acoustic environment. For structural response analysis, besides spectral density of the pressure field at any location, cross-spectral density at any two locations on the surface of the structure must also be known.

On-going research at KSC attempts to use available measurements from past launches to gain physical insight to accurately define launch-induced acoustics. A considerable effort has been expended to develop a comprehensive "acoustic data base" comprising special functions. This data base is statistical and derived from a multiple sensor/multiple launch combination covering a time span beginning with STS-1 (4/12/81) and ending with STS-30R (5/4/89). Five types of functions that characterize launch-induced acoustic fields and have an application in the response analysis are:

1. Pressure PSD
2. Normalized cross-power spectral densities (NCPSD's)
3. Amplitude probability densities (PD's)
4. Response spectra (RS)
5. Pressure correlation lengths (PCL's)

Response Analysis Methods

The purpose of taking acoustic measurements is their application to vibration response analysis and environmental testing. The choice of a reliable analysis method is subject to observations drawn primarily from processed launch measurements. Research indicated that the existing finite element method (FEM) programs do not have the capability for an "exact type solution." Moreover, the unavailability of proper functions (cross-power spectra) and limited understanding of the generated acoustic field near exhausts compounded the development of an exact solution. Lack of a unique method of response analysis has also necessitated emergence of two different approaches, based on experience and observations of launch acoustic measurements.

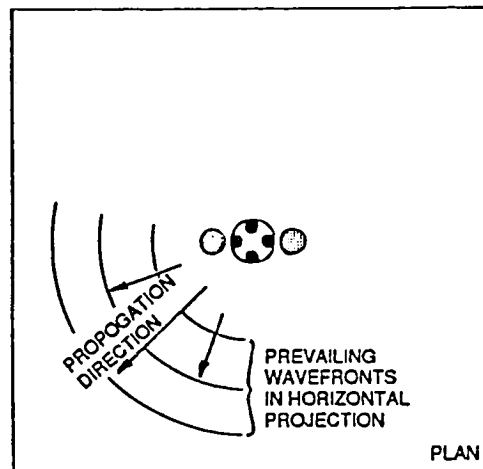
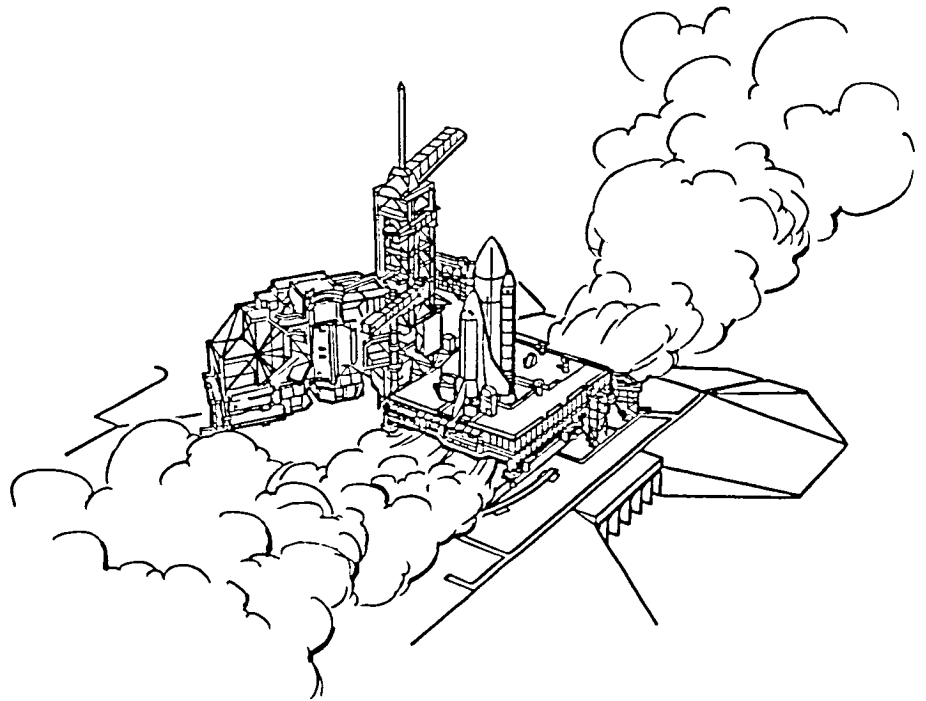
Probabilistic Method

The first method, called probabilistic, is based on the classical solution of random vibration theory. The solution is a stationary input/response relation and requires definition of the acoustic field in terms of auto- and cross-power spectra. In most instances, only auto-power spectra were used in applications, while cross-power spectra were substituted by assumed models of acoustic field. One such model, so called "white noise decay," was incorporated into a widely used FEM program for response analysis. Research at KSC indicates that the white noise decay model does not reflect launch-induced acoustics. Moreover, the probabilistic method yields

mean square response and not peak response required for design applications. The peak response is estimated by this method by assuming a probabilistic distribution of amplitudes, which substantially affects the predicted response.

Deterministic Method

The second approach, termed deterministic, evolved when prompted by a deficiency of the probabilistic method to predict response in the



Typical Near-Field Acoustics

low-frequency range of the launch transient, where most pad structure resonances are observed. This approach uses measured pressure time histories (no assumptions involved) as a dynamic load on the system. The response solution is obtained by integrating an uncoupled (by means of modal analysis) system of equations of motion, resulting in a peak response of each normal mode. This solution also has its inherent drawbacks. Of significance is the peak generalized modal load which, in multispan structures and higher than fundamental modes, requires correct load placement to ensure an absolute peak.

Results

A critique of the above-mentioned response analysis methods indicated that, while neither is without limitations, they both have a rightful place in the analysis. More importantly, they both rely on and require measurements. The comparison between the two approaches (probabilistic and deterministic) has led to a newly developed function processed from limited launch data (NCPDS). This function most suitably characterizes the launch-induced acoustic field and is required by both response analysis methods. The transformed analytical solution formulas of the two approaches contain NCPDS's, either directly or as other functions of NCPDS's. A substantial difference between the methods is in the number of NCPDS's required by each. Whereas the probabilistic method requires thousands of NCPDS's, only a few NCPDS's are needed in the deterministic method.

Presently, commercially available FEM codes do not provide capability to perform either of the response analysis methods. Continuing research will focus on this limitation and attempt to expand the acoustic data base composed of the above functions to other launch pad locations. In light of the limited user options embedded in the commercial FEM codes, there exists a strong justification to develop an advanced response analysis method, requiring input of an accurate-

ly characterized acoustic field such as the NCPDS.

Contact:

R. E. Caimi, 867-4181, DE-MED-11

Participating Organization:

Boeing Aerospace Operations, Engineering Support Contract (R. N. Margasahayam and V. Sepcenko)

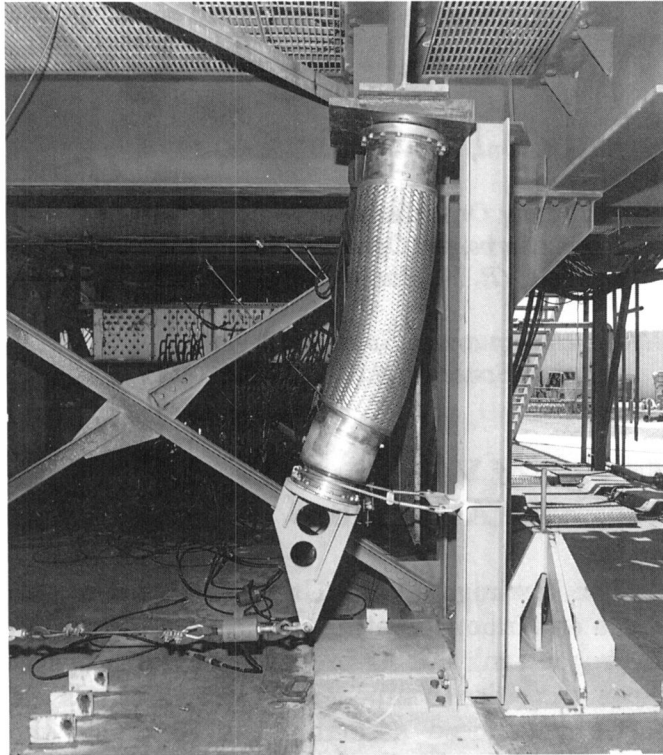
NASA Headquarters Sponsor:

Office of Space Flight

Design of Vacuum-Jacketed Flexhose Assemblies

The Hydrogen Vent Umbilical System provides continuous venting of the Space Shuttle's hydrogen tank during propellant loading operations. A critical component in this system is the forward flexhose assembly that connects the external tank with the umbilical hardline. This flexhose is unique in that it must function as both a compliant connection (for vehicle tracking) and a structural member (for T-0 disconnect). The flexhose is a vacuum-jacketed assembly composed of concentric pairs of bellows and braids (10-inch outer diameter) welded to forward and aft hardline segments. The figure "Restrained Bending Test Setup" shows an existing flexhose undergoing a flexure test that simulates the disconnect motion.

A new design for the forward flexhose has been developed based on mechanical test data, spring rate analysis, and system performance information. This optimum design allows the production of a flexhose of precise overall length, bellows spring-constant, and braid stiffness. The detailed fabrication steps were developed so that these design criteria would be met with the annulus evacuated. Because this flexhose is highly subject to pitting corrosion in the launch environment, the alloy Hastelloy C-22 was specified for the outer bellows material. A similar material, Hastelloy C-276, was used for the outer braid.



Restrained Bending Test Setup

One flexhose has been fabricated in accordance with the new assembly drawing. Following successful mechanical testing of this prototype flexhose assembly, the design will be used to replace the existing forward flexhoses for the hydrogen vent system. The fabrication procedures and testing methods developed through this project can also be extended to the production of any vacuum-jacketed flexhose assembly. The design approach is especially useful where precise dimensions or predictable mechanical characteristics are required.

Contact:

J. E. Fesmire, 867-3313, DM-MED-41

Participating Organizations:

Boeing Aerospace Operations, Engineering Support Contract

Microflex, Inc.

NASA Headquarters Sponsor:

Office of Space Flight

O-Ring Groove Inspectoscope

Objective

To develop and field an instrument to inspect the O-ring groove of the capture feature of the redesigned Shuttle solid rocket motor (SRM) field joint.

Background

The O-ring groove of the Shuttle SRM is inspected for defects in its surface. This inspection was previously performed using a dental mirror and a flashlight. The inspector would walk around the suspended SRM segment and try to see defects, a process that took approximately eight hours.

Approach

Several technologies were examined, including direct vision by periscope, camera periscopic devices, and modified miniature borescopes. After evaluation, the modified miniature borescope was chosen since it had the best perspective view of the O-ring groove. This technology provided the best operator orientation within the groove.

A special magnetically levitated carrier was designed for the borescope since accurate positioning on the segment was critical. The entire head, including the carrier, the borescope and the fiber optic light source, was designed for use in close proximity to open SRM propellant grain.

The carrier was designed by Morton-Thiokol and the optics and electronics were designed by the NASA Electronic Engineering Directorate (DL) Special Instrumentation Laboratory. The final system consisted of a carrier with its associated instrumentation and a support rack. The carrier head consisted of a conductive plastic trolley into which a borescope and its light source were mounted. It also had an optical encoder for segment position indication. A miniature color TV camera was mounted directly

onto the borescope and was also borne by the carrier head.

The information from the carrier head, in the form of TV signals and position pulses along with all power for the devices, is sent to the support rack. These signals interface with the support rack by a light-weight cable. The support rack contains a camera control unit, video monitor, 3/4-inch studio-quality VCR, computer, genlock keyer, microphone and preamp, and high-intensity light source.

The unit was thoroughly tested to rigorous specifications to validate it for use with the SRM's. The unit was completely documented and field tested.

Results

The O-ring groove inspectoscope is currently used for groove inspection on all SRM field joints at Kennedy Space Center. The groove inspection time has been reduced to less than one hour with a video record of all inspected grooves.

A motor has been added to the original carrier trolley to allow remote operation of the inspection. This allows the inspectors direct control and access to the information while preventing personnel from being underneath a suspended load.

Planned work includes optics optimization to allow one pass inspection and on-the-spot automated defect analysis.

Contacts:

*C. H. Bell, 867-3185, DL-ESS-23
D. R. Stubbs, 867-3036, DE-PMO-5
J. D. Collins, 867-4438, DL-ESS-24
R. P. Mueller, 861-2955, TV-MSD-24
P. W. Schmid, 861-2935, TV-MSD-24
W. R. Helms, 867-4449, DL-ESS-2*

Participating Organization:

Boeing Aerospace Operations, Engineering Support Contract (S. M. Gleman, W. D. Haskell, J. E. Thompson, and G. K. Rowe)

*NASA Headquarters Sponsor:
Office of Space Flight*

Predictive Maintenance Programs at KSC

Vibration analysis, ferrography, and thermography are predictive maintenance programs being used at Kennedy Space Center to monitor health and predict imminent failures of ground support equipment and facility systems that support Shuttle and Payload Processing. Examples of the equipment and systems being monitored include crane gearboxes, crawler transporters, environmental control systems, liquid oxygen pumps, and power systems. Future plans include investigation of other predictive maintenance programs and expansion of existing programs to monitor equipment and systems supporting NASA's industrial operations.

During the past two years, the emphasis of predictive maintenance at KSC has been to: (1) understand the capabilities and limitations of each program, (2) integrate and correlate the data to determine the health of equipment and systems, and (3) implement pilot programs and expand current programs.

Vibration analysis monitors the vibrational amplitude of rotating equipment to locate anomalies that could lead to component/system failure (see the figure "Vibration Analysis Equipment"). Ferrography is a wear particle analysis used to monitor particulate matter in the lubricant contained in systems where there is moving contact between surfaces. Specifically, ferrography monitors particulate matter quantity, type, and wear characteristics to determine accelerated wear before catastrophic component/system failure (see the figure "Ferrographic Analysis Equipment"). Thermography is the process through which surface temperature patterns and variations are measured by converting an object's infrared electromagnetic signature into a visible image. This allows for diagnosis of problems due to adverse temperature gradients

when not visible to the naked eye (see the figure "Thermographic Analysis Equipment").

Currently, the vibration analysis program monitors about 300 systems that support Shuttle flow operations. On numerous occasions, early identification of potentially catastrophic failures and proper corrective maintenance scheduling have provided a significant return on investment for the program. Plans are to expand the vibration analysis program to include approximately 2,200 pieces of rotating equipment supporting Shuttle processing and to investigate its applicability to payload processing equipment. The ferrography program is currently in place to monitor approximately 30 pieces of equipment and facility systems that support payload processing; during the next year, about 90 pieces of equipment and facility systems will be included in the ferrography program. Similarly, the

thermography program is in place to monitor payload processing facility electrical panels, and plans are to expand the program to include electric motors and motor control centers. Pilot programs for ferrography and thermography are underway for equipment and systems supporting Shuttle processing.

Contacts:

*M. Espiritu, M. Miller, J. Giles, and S. Young;
867-7470; CS-GSD-12*

B. G. Graf, 867-3981, RT-ENG-2

Participating Organizations:

*McDonnell Douglas Space Systems Company
(B. Bauerlin, E. Bowman, and K. Jones)*

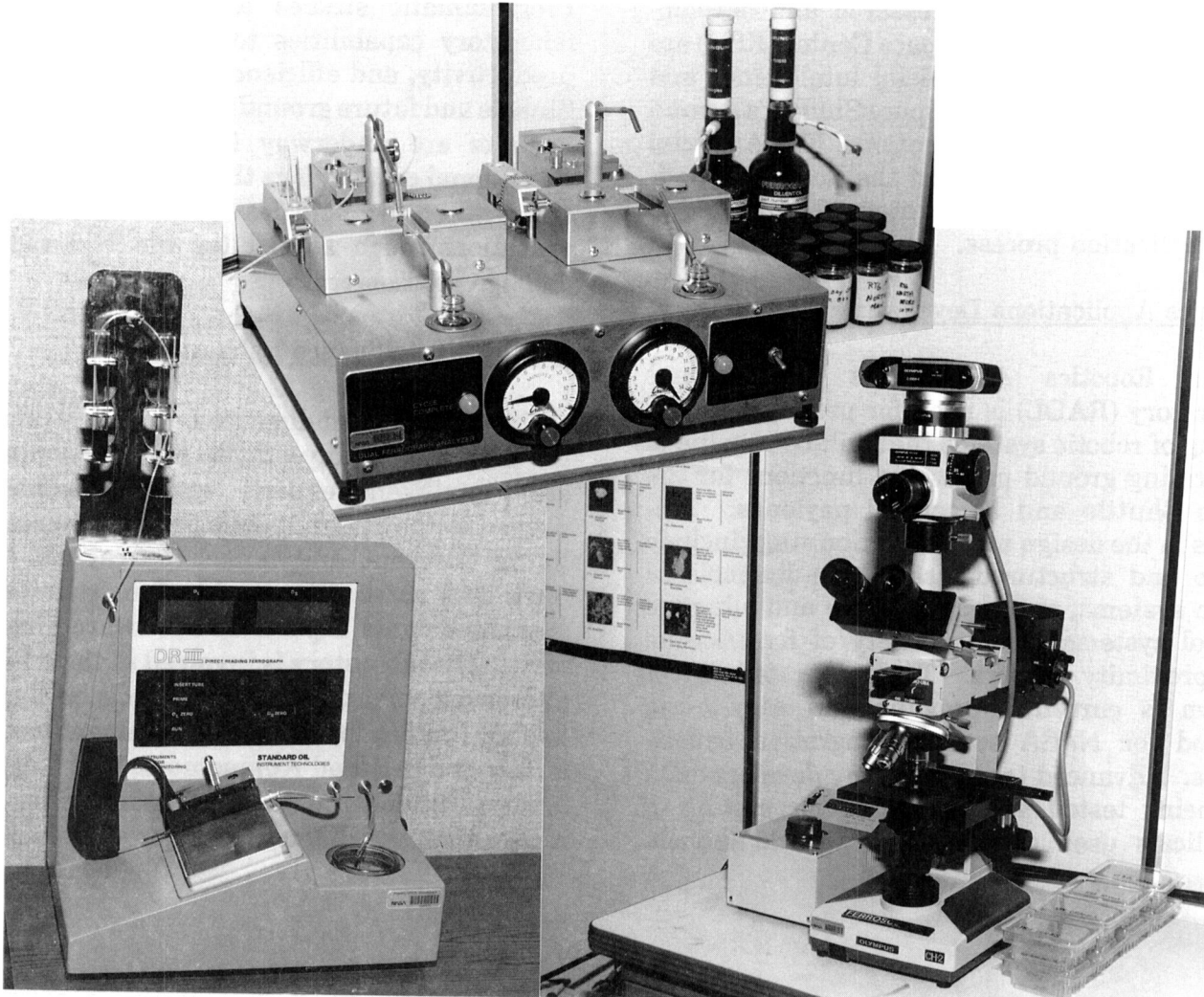
*Lockheed Space Operations Company
(G. McCorquodale and L. Gibson)*

NASA Headquarters Sponsor:

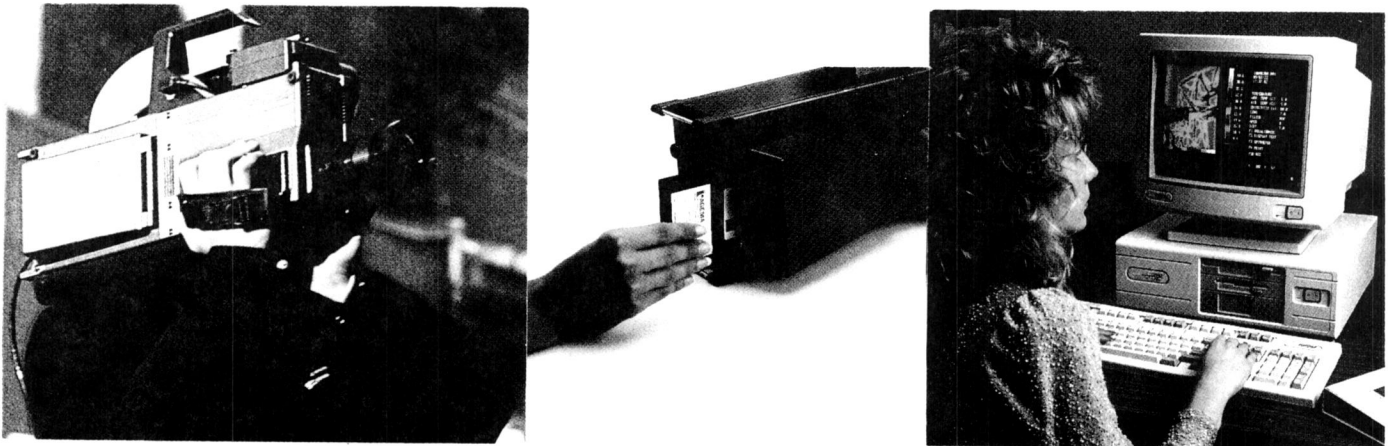
Office of Safety and Mission Quality



Vibration Analysis Equipment



Ferrographic Analysis Equipment



Thermographic Analysis Equipment

Autonomous Systems

Autonomous systems research and development efforts at Kennedy Space Center (KSC) are focusing on applying artificial intelligence and robotics technology to the Space Shuttle's ground processing and launch operations. The Artificial Intelligence Laboratory and the Robotics Applications Development Laboratory are engaged in this application process.

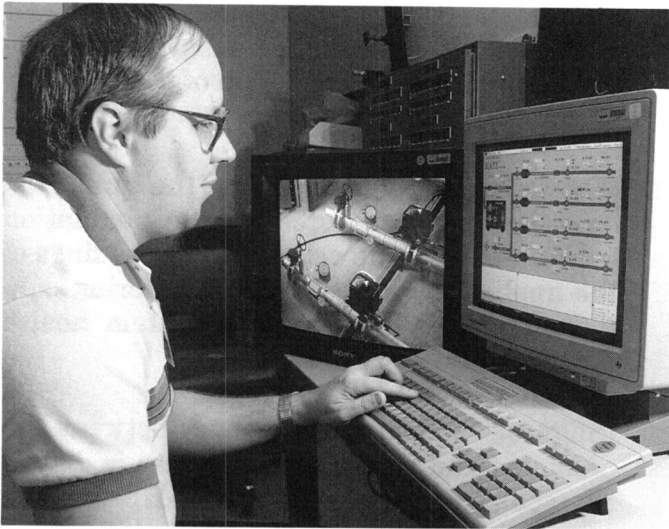
Robotics Applications Development Laboratory

The Robotics Applications Development Laboratory (RADL) is used for prototyping and testing of robotic systems that will be capable of performing ground processing functions for the Space Shuttle and associated payloads. Elements in the design and evaluation stage include stereo and structured laser three-dimensional vision systems, real-time reactive and adaptive control systems, and a variety of force/torque and proximity sensors. The integrated RADL system is currently providing an easy-to-use testbed for NASA sensor integration experiments. Advanced target tracking developments are being tested and evaluated for mating of umbilicals used during space vehicle launch.

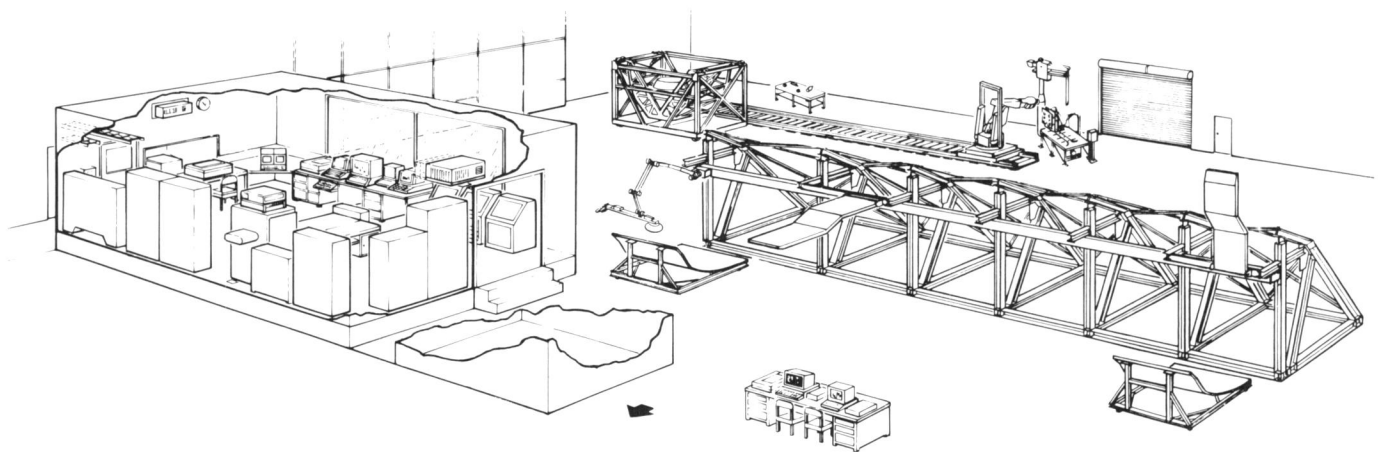
Programmatic studies are underway to use laboratory capabilities to enhance the safety, productivity, and efficiency of KSC facilities for Shuttle and future ground processing operations. Projects are underway that should generate operational cost savings through the integration of advanced technologies for ground processing operations, such as Orbiter tile and radiator damage assessment.

Artificial Intelligence Laboratory

The Artificial Intelligence Laboratory provides the capability to investigate and develop artificial intelligence/expert systems technology needed by the Space Shuttle program for streamlining checkout and launch operations. The laboratory serves as a working environment for systems domain experts and software programmers. The laboratory is involved in the analyses and development of a Launch Decision Support System (launch feasibility management tool) and a Knowledge-Based Autonomous Test Engineer system (autonomous control, monitoring, fault recognition, and diagnostics for troubleshooting).

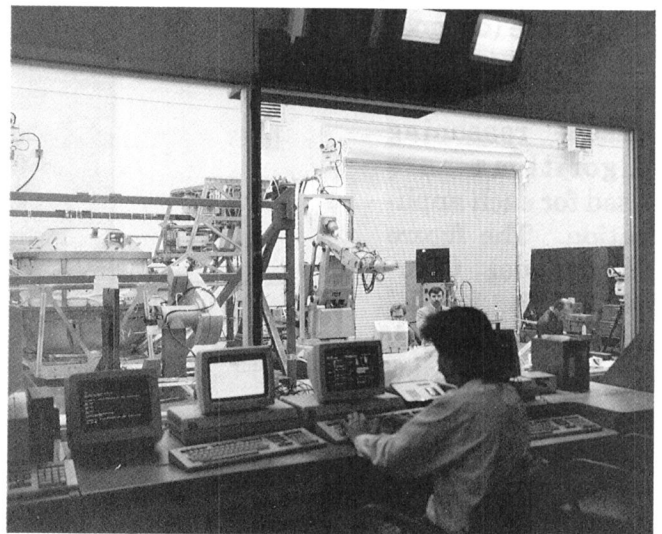


Robotics Applications Development Laboratory



Robotics Applications Development Laboratory

Artificial Intelligence Laboratory



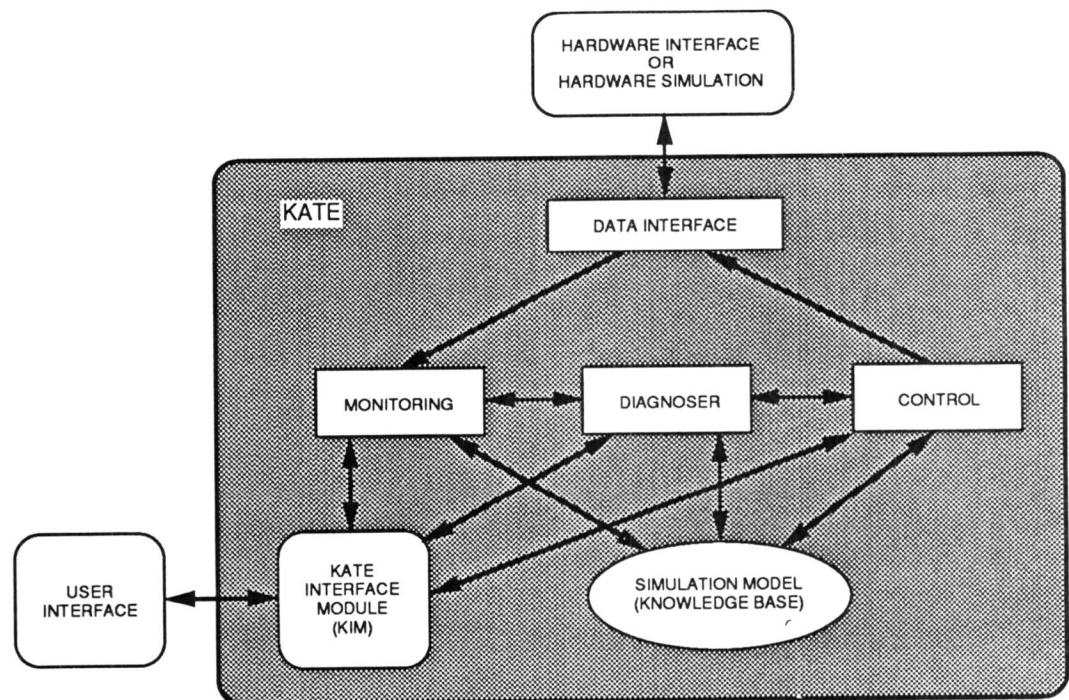
Knowledge-Based Autonomous Test Engineer (KATE)

Model-based reasoning (MBR) systems are being developed for a variety of applications that include system health monitoring, diagnosis, control, training, and design. The common theme in all MBR systems is an explicit representation of the structure and function of the modeled system. Unlike most other reasoning paradigms, MBR models directly represent the components that comprise the physical system. MBR algorithms enable the prediction of system behavior from the behavior of its parts. It is this predictive system behavior, based on the structure and function of the components, that gives MBR its power and usefulness.

For the past several years, the Artificial Intelligence Section, Engineering Development Directorate, at Kennedy Space Center has been developing a real-time model-based reasoning system that can diagnose anomalies and either control or provide control advisories for ground launch operations. The system resulting from these efforts is called KATE.

KATE is a generic software shell for which each application requires only a knowledge base (or model) of the system. The same model-based reasoning algorithms are used for each application. The figure "Functional Overview of KATE" provides a graphical/relational view of the subsystems within KATE. The four main reasoning subsystems are:

1. **Simulation:** Using a component-based model of a system, the simulation subsystem generates a quantitative prediction of the behavior of the application system.
2. **Monitoring:** By comparing the predicted sensor values generated by the simulation subsystem with the actual sensor readings of the application system, the monitoring subsystem is able to provide a system health functionality.
3. **Diagnosis:** When a discrepancy between the predicted and actual sensor values is detected, the diagnosis subsystem exploits the structural and functional relationships of the components in the model to determine the failed component that would explain the discrepancy.
4. **Control:** When a particular component behavior is desired, the control subsystem is able to determine from the model the set of commands required to attain the desired state.



Functional Overview of KATE

Over the past year, several new facilities have been developed that extend KATE's capabilities and prepare it for an operational environment. These include an Explanation facility for diagnosis, a Control Procedure facility, and a Single-Point-of-Failure Analysis facility.

Explanation (EP) Facility

The EP facility enables the KATE user to follow the reasoning that the diagnoser employed during any diagnosis. The EP facility can be invoked after a diagnosis is complete and recreates the diagnosis in an explanation environment. The facility runs independently and without affecting anything else KATE might be doing at the time. The major features of the EP facility are:

1. **Trace:** The Trace feature allows the user to show a trace of each step in the diagnosis. The trace displays a description of the values tried for each component and a brief reason why or why not the component was considered a suspect.
2. **Why/Why Not Queries:** The Why/Why Not Queries feature allows the user to ask why a particular component was or was not a suspect. The EP facility responds with a detailed account of that component's involvement in the diagnosis.
3. **Discrepant Measurement (DM) Selection:** Using the DM selection feature, the user may select a subset of DM's and then re-do the diagnosis in an Explanation mode. The feature is useful when a failure has occurred and KATE is unable to diagnose it because it included DM's unrelated to the failure.

Control Procedure Facility

A high-level Control Procedure facility was developed to enable KATE to perform system control. In the past, KATE only performed component-level control, and it was left to the KATE user to ensure the system as a whole was operating correctly. The Control Procedure facility provides a mechanism for KATE to read and execute control procedures just as the Launch Processing System executes procedures from Operations and Maintenance Instructions.

Each Control Procedure facility is defined with a high-level language and can be nested within other procedures. A Control Procedure facility is to be defined with a *name*, a set of *preconditions* that specify what conditions must be satisfied before the procedure can be activated, a set of *actions* that is a series of operations to be taken when the procedure is activated, and a *safing* procedure that specifies an action to be taken upon encountering a nonrecoverable failure. (See the figure "Example of a KATE Control Procedure.")

The table "Control Procedure" describes the set of allowable operations in a Control Procedure. An example line of a Control Procedure

```
(defprocedure SUCTION-LINE-CHILDDOWN
:pretty-name "Suction Line Chilldown"
:comment "Performs chilldown of the pump suction line."
:preconditions
((V ST-UP (8 ± 4 psig) "Storage tank ullage press"))
:actions
((C PV20 OPEN "Open LOX engine pogo valves")
(H ST-UP (8 ± 4 psig) "Maintain storage tank ullage pressure")
(V/D A9 CLOSED "Verify/close ST vent valve")
(V A98 CLOSED "Verify pump A127 suction valve closed")
(C A86461 OPEN "Open transfer line fill valve")
(WC (V A86454 (< 4.0 psig)) (1800 sec)
"Wait until skid inlet press falls below 4.0 psig")
(WT (10 sec) "Wait 10 sec")
(CAM A86462 "Focus camera on TSM drain valve")
(VV A86462 CLOSED "Visually verify TSM drain valve closed")
(C A86461 CLOSED "Close transfer line fill valve")
(WT (200 sec) "Wait 200 sec")
(V A196 OPEN "Verify bypass valve open"))
:safe
((PROC EMERGENCY-HALT)))
```

Example of a KATE Control Procedure

Control Procedure

Character	Operation	Explanation
PROC	Procedure	Execute a control procedure
V	Verify	Verify the status of a component
V/D	Verify/do	Verify status or control component
VV	Visually verify	Visually verify with camera
VV/D	Visually verify/do	Visually verify or control component
VM	Verify measurement	Verify a sensor reading
C	Control	Control component to desired state
M	Maintain	Control/maintain component
WT	Wait time	Wait a time interval before proceeding
WC	Wait condition	Wait for condition before proceeding
S	Select condition	Select condition before proceeding
CAM	Camera	Command camera to focus on component

translates as follows:

Action: (V ST_UP (8 ± 4 psig) "Storage tank ullage press")

Meaning: Verify the storage tank ullage pressure is 4 to 12 psig before proceeding.

By combining KATE's component control capability with this Control Procedure facility, a robust control system has evolved. However, it is still desirable to run KATE in a monitor-only mode. The Control Procedure facility was designed with this in mind and can operate either as the primary or advisory control system. The advisory control mode differs from control mode only in the fact that the commands (e.g., open valve or turn pump on), instead of being sent to the hardware, are sent to the user. If failures do occur and corrective actions need to be taken, the control advisory system reports the actions as if it were the control agent.

Single-Point-of-Failure Analysis (SPFA) Facility

Physical systems are oftentimes dependent upon a number of critical (nonredundant) components. For instance, if the distributor or fuel pump in a car fails, the car will not run. Adding redundant components in performance-critical areas can make a car more fault tolerant. Consequently, a truly fault-tolerant physical system must be designed to limit the number of nonredundant components.

In general, the intent of the SPFA facility within KATE is to give insight into which objects are critical for system performance. The SPFA facility simulates component failures and lists the components whose failure would cause loss of system control. With this understanding of a system's "weakest links," a control engineer can focus attention on potential trouble areas that would require prompt attention in the event of a failure.

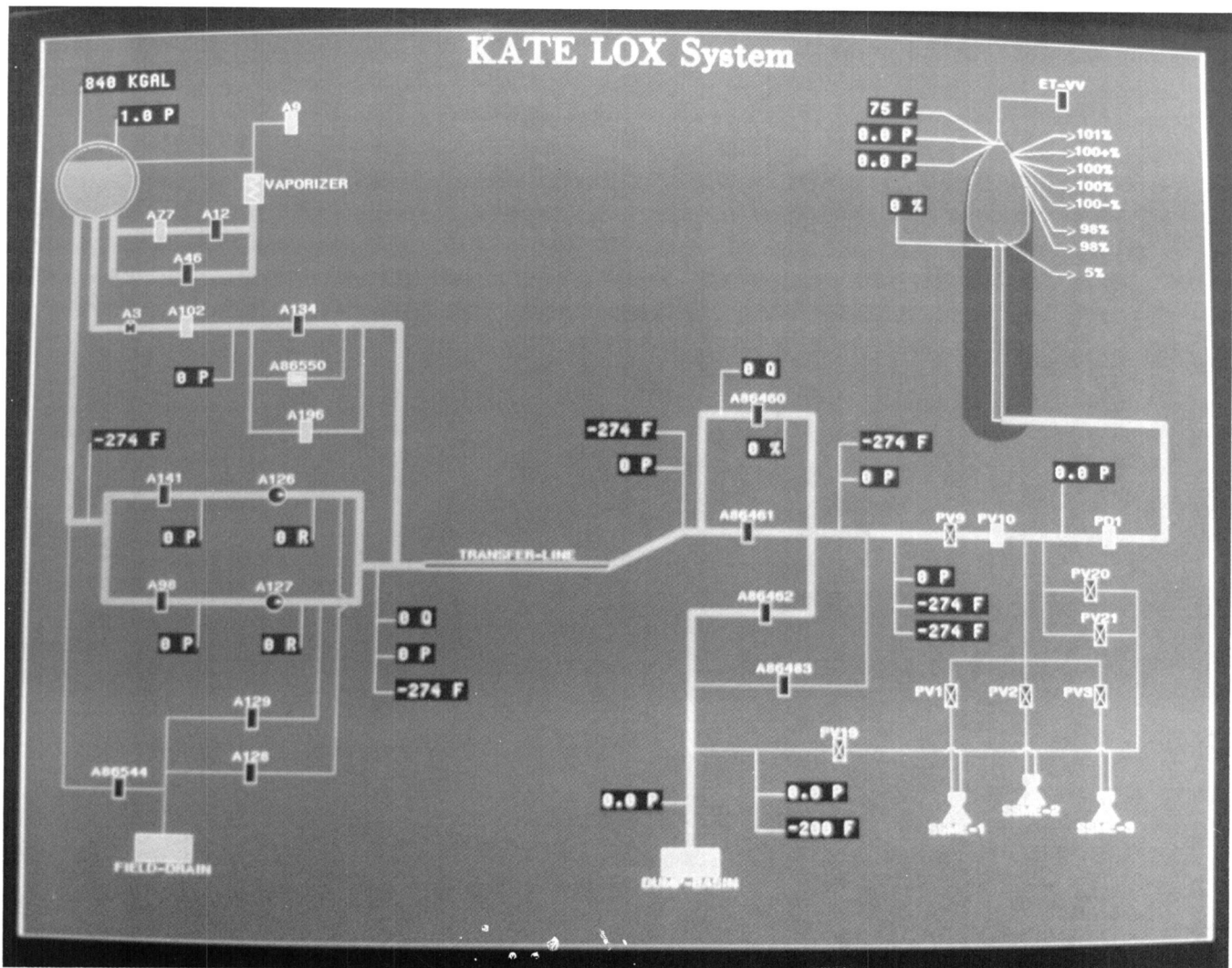
The SPFA facility is not only an aid for designing fault-tolerant systems but can also provide a mechanism to dynamically detect the weakest links in a system following a component failure. In other words, the SPFA facility can evaluate the system's ability to function with failed components and can identify which components are critical for nominal performance.

Applications

Work continues in the development of two KATE applications: the liquid oxygen (LOX) tanking system and the autonomous launch

operations (ALO) projects.

1. LOX: The KATE-LOX project (see the figure "KATE Liquid Oxygen Overview") has been quite successful over the last year. The KATE-LOX system monitored live LOX tanking data for each Shuttle launch attempt this year. During the LOX tanking of STS-43, KATE correctly diagnosed a failed replenish flowmeter 15 minutes before system engineers were notified of the discrepancy by the Launch Processing System. In addition to actual launches, KATE was tested several times against the Shuttle Ground Operations



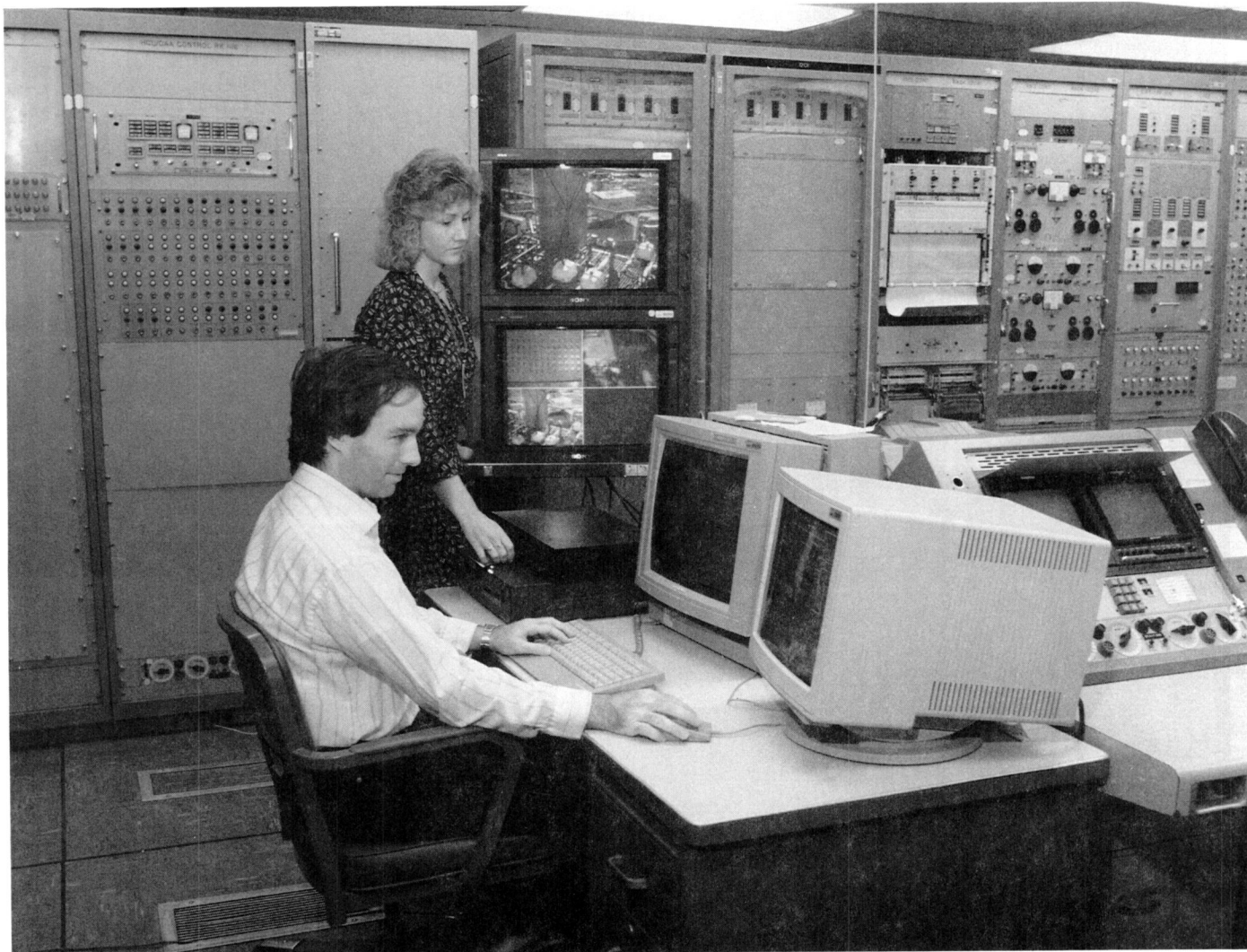
KATE Liquid Oxygen Overview

Simulator (SGOS). The knowledge base has grown to include over 1,700 objects and is approximately 80 percent complete. There are currently 13 data sets, each containing 10 to 12 hours of actual tanking data. The data is used for both testing knowledge bases by playing the data back through KATE and building knowledge bases by analyzing the data.

As a result of the successes and the interest from the LOX engineers, a KATE-LOX users group has been established. The group is tasked with identifying user requirements

and merging those requirements with the current KATE development plans. The knowledge base is scheduled to be completed in December 1991 and a demonstration of KATE-LOX in Firing Room 2 is planned.

2. ALO: During fiscal year 1991, the KATE-ALO project (see the figure "KATE-ALO Control Room Setup") successfully achieved many milestones. Demonstrations against a water (H₂O) tanking system have been presented to various NASA and contractor personnel from all over the country. Some of the capabilities demonstrated by the KATE-ALO



KATE-ALO Control Room Setup

application are single-point-of-failure analysis, system control advisories, component redundancy management, and real-time simultaneous plotting of multiple system measurements. The KATE-ALO system also demonstrates autonomous system control, the first model-based reasoning software system to do so. This is done by reading system operation instructions from computer files and translating them into an internal representation that KATE can understand.

Current plans are to integrate the previously prototyped Environmental Control System (ECS) and the ALO-H₂O tanking system applications, with the goal of demonstrating the capability to simultaneously monitor/diagnose/control multiple physical systems. Also in the planning stage is an integration with Martin Marietta Aerospace Group, Denver, Colorado, which is developing a supervisory software system that will interact with multiple KATE systems. The demonstration plan is to manage a launch scenario just as a launch director currently does, with a high-level scheduler querying/interacting with many KATE systems. Each KATE system will represent one of many critical launch subsystems.

Ongoing Development Work

Because there remain some fundamental MBR problems to be resolved, the development of KATE is ongoing. One of the most challenging research questions is how to improve the way KATE reasons with time. Other areas of ongoing research include combining qualitative with quantitative reasoning to help solve some problems inherent in quantitative simulation and how to verify and validate a model-based reasoning system.

KATE development efforts in 1992 will also include building a Knowledge-Base Building Tool, rewriting the User-Interface into a MOTIF X Window environment, rewriting the KATE kernel into C++ in UNIX on a 486 platform, and

analyzing the current capabilities of KATE with the goal of developing well-understood solutions to current limitations.

Contacts:

B. L. Brown, J. E. Galliher, P. A. Mullenix, T. O'Brien, and C. L. Parrish; 867-3224; DL-DSD-23

Participating Organization:

Boeing Aerospace Operations, Engineering Support Contract (S. R. Beltz, S. Budzowski, E. P. Dean, R. J. Edwards, C. H. Goodrich, R. J. Merchant, C. O. Pepe, M. J. Schnitzius, H. W. Yu, and C. L. Walker)

NASA Headquarters Sponsor:

Office of Space Flight

Launch Decision Support System (LDSS)

The overall objective of the LDSS project is to develop prototypes of tools for the launch team that support decisionmaking during Shuttle launch countdowns. The specific objectives of the project were determined in a feasibility study to be time management and anomaly management.

Time Management

Time management by the NASA Test Director (NTD) simplistically consists of those decisions required by the extension of the T-9 minute hold or invocation of an unplanned hold at one of the remaining hold points. This requires maintaining mental models of the dynamic state of the countdown and managing the process that determines when to resume the count. Time management integrates information currently available on firing room clocks and hard-copy timelines, correlates the information graphically in real time, and calculates countdown-specific times and intervals.

Time management by the NTD during the terminal count was begun in 1989. The time

management prototyping was completed in 1991. The real-time field prototype has been field tested against Shuttle countdown simulations, terminal countdown demonstration tests, and launch countdowns for the Shuttle flows during 1991. The prototype was composed initially of an integrated display as described in the Research and Technology 1990 Annual Report. A what-if spreadsheet was added in May. The what-if spreadsheet assists in calculating the maximum hold time remaining and equivalently the latest resume time. It can also be used to devise a plan with an intermediate hold point. A situation advisor concept prototype was completed at the end of 1991. The situation advisor monitors the countdown and assists in off-nominal situations.

The time management real-time field prototype with the integrated display and the what-if spreadsheet will be rewritten as production software and transitioned to operations in 1992. The situation advisor will not be further developed in 1992.

Anomaly Management

Anomaly management by the Shuttle Project Engineer during the terminal count was begun in January. The initial objective of anomaly management is to facilitate reaction to violations of launch commit criteria (LCC). The facilitation is accomplished by providing computer-mediated access to the LCC and Background (LCC&B) document, by automating display of the appropriate LCC&B page when an LCC violation occurs, and by providing the capability for the Shuttle Project Engineer to selectively plot the measurements involved in the LCC violation. A concept prototype was completed in February. The specification for a real-time field prototype was completed at the end of 1991.

The real-time field prototype will be implemented and tested in 1992.

Development

The real-time field prototypes have been developed on 486 personal computers with color monitors in Microsoft Quick C 2.5 under DOS.

Other Plans for 1992

The mockup of workstations for the NTD's and Orbiter Test Conductor's (OTC's) is a new initiative for 1992. This will involve adding a computer to the existing NTD and OTC consoles, a human factors layout of the workstations, the porting of application software to the workstations, and the development of a user interface consistent with the Common Operational Research Equipment (CORE) project. The application software will be time management and anomaly management, as previously presented, and operations maintenance instruction management (under development at Ames Research Center).

Contacts:

*A. E. Beller, 867-3224, DL-DSD-23
F. J. Merlino, 867-4735, TP-VPD-1
J. Simon, Jr., 861-3993, TV-PEO-2*

Participating Organization:

Boeing Aerospace Operations, Engineering Support Contract (H. G. Hadaller, M. J. Ricci, and M. B. Richardson)

NASA Headquarters Sponsor:

Office of Space Flight

Robotic Tile Processing System Development

Design and development of a prototype system to robotically process bottomside Orbiter tiles began in January 1991. This is a 3-1/2-year development effort that will conclude with a demonstration of the prototype mobile robotic system in June 1994. This system will integrate state-of-the-art systems in navigation, control, mobility, manipulation, information management, and sensor technologies to inspect and

rewaterproof bottomside Orbiter tiles in the Orbiter Processing Facility at Kennedy Space Center (KSC) and the Dryden Flight Research Facility.

A design team representing a variety of organizations was assembled. Team member responsibilities were broken down as follows.

Project Management:

- NASA KSC

Vision System (anomaly detection and end-effector positioning and registration):

- Langley Research Center and subcontractor SRI International

Rewaterproofing End-Effector:

- Rockwell International, Space System Division, Robotics Group

Mobile Positioner (i.e., robot):

- Base -- Carnegie Mellon University, Field Robotics Center
- Elevator/Fine Positioner -- Carnegie Mellon University, Field Robotics Center

Information Management System/System Engineering Support:

- Boeing Aerospace Operations (NASA KSC's Engineering Support Contractor)

The efforts for 1991 focused on defining all system functional requirements (e.g., process, facility, environmental, and mobile positioner) and initiating the design and development process. Preliminary design reviews were held for the vision system and rewaterproofing end-effectors, the mobile base, and the information

management system (i.e., workcell controller). The mobile base 60-percent design review was also conducted and corresponding long-lead-time parts were ordered. Additionally, the software requirements specification for the information management system was completed and development hardware and software were procured and delivered.

Planned accomplishments for 1992 include the final design, fabrication, and testing of the mobile base. Technology demonstrations will also be made to show the capabilities of the following subsystems.

1. Vision system capabilities: end-effector positioning and tile registration, gross anomaly detection (i.e., chips, gouges, etc.)
2. Mobile base: mobility, navigation, and user interface
3. Rewaterproofing tool capabilities
4. Information system: user interface, two of seven interfaces to existing NASA data bases

Contact:

T. A. Graham, 867-4181, DM-MED-12

Participating Organization:

Boeing Aerospace Operations, Engineering Support Contract (J. R. Bledsoe and R. P. Bennett)

NASA Headquarters Sponsor:

Office of Aeronautics, Exploration and Technology

Instrumentation and Data Acquisition

The measuring systems that monitor every facet of the Shuttle checkout and launch process (including non-Shuttle tests) must be more reliable than the systems they monitor. The instrumentation and data acquisition laboratories have the responsibility to ensure that Kennedy Space Center (KSC) is provided with the latest technology in monitoring hardware and techniques.

Transducer and Sensor Laboratory

The Transducer and Sensor Laboratory is the focal point for Centerwide ground support equipment and institutional utility system's instrumentation research and development. The activities include: (1) developing new families of instrumentation using internal resources and the resources of industry and academia; (2) publishing design and procurement specifications; (3) performing comprehensive evaluation, qualification, and long-term environmental testing for prototype and off-the-shelf hardware; (4) developing and qualifying signal conditioning or hardware interface electronics; and (5) providing common or special instrumentation components for special test programs.

Landing Aids Laboratory

The Landing Aids Laboratory develops the flight test instrumentation used in the checkout and calibration of the Microwave Scanning Beam Landing System (MSBLS) and the Tactical Air Navigation (TACAN) system. Current work is concentrated on applying the Global Positioning System (GPS) navigation signals to the calibration of the landing aids systems. Other supporting work includes developing a pilot display and evaluating an infrared tracking system.

Data Acquisition Development Laboratory

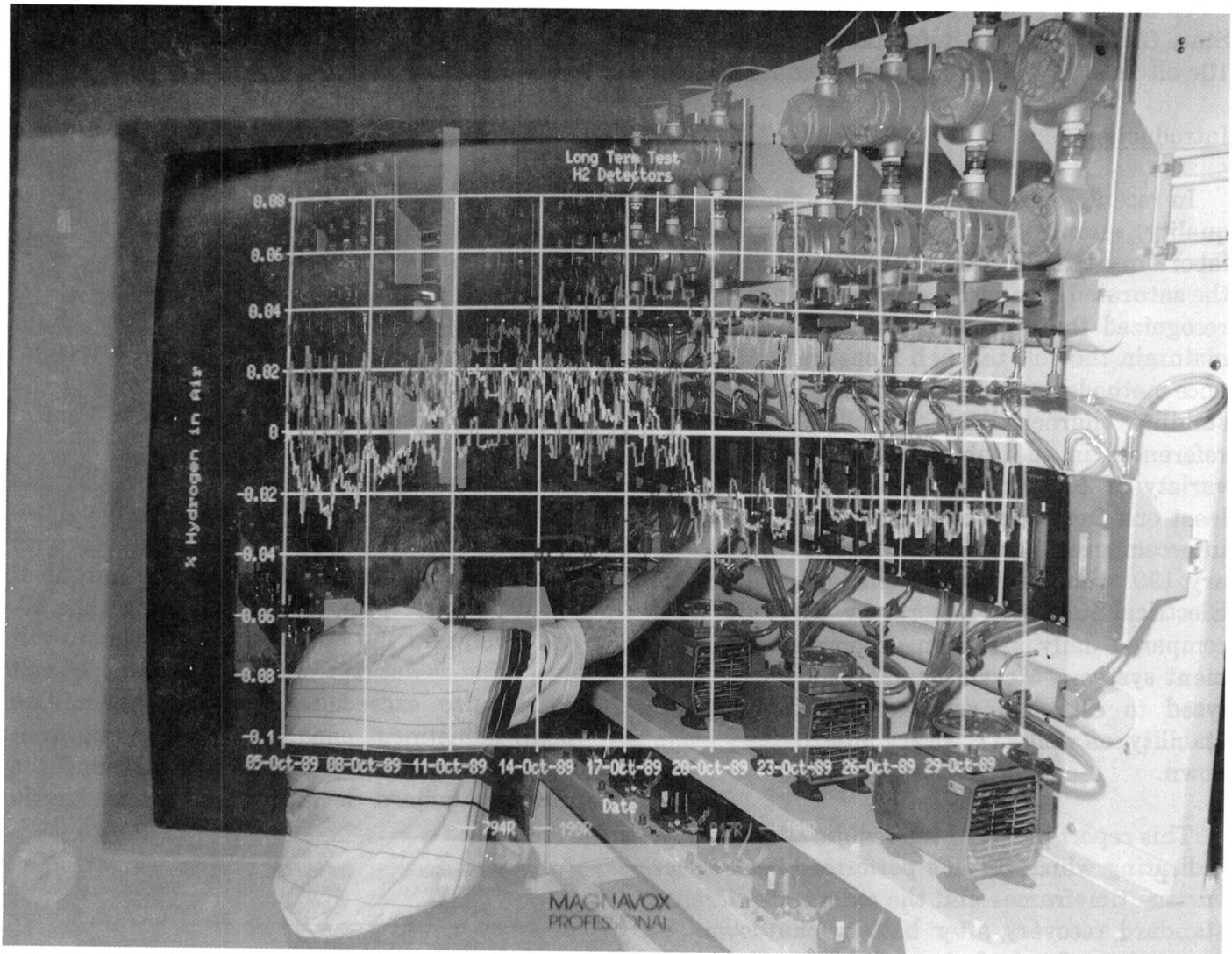
The Data Acquisition Development Labo-

ratory is responsible for applying the latest technology to the data acquisition process. The two data acquisition systems currently supporting the KSC ground instrumentation are: (1) the Launch Complex 39 Permanent Measuring System (PMS), which collects the environmental and special measurements data generated during Shuttle launches and (2) the Launch Equipment Test Facility (LETF) mobile van, which monitors ground support equipment verification tests.

A third system is under development to provide support for short turnaround testing requirements. This Fast Response Instrumentation Van (FRIV) will also be used as a test bed for new data acquisition tools and techniques.

Electronic Security Development Laboratory

The Electronic Security Development Laboratory is used to develop and integrate new security systems for use at KSC. This is done primarily by performing specialized qualifications testing on candidate hardware for use in the unique environment presented by the area. Candidate systems are selected and then tested against vendor specifications and KSC requirements. Formal test reports are issued as sensitive documents and are under controlled release. It should be stressed that only specialized tests for KSC's specific environment are usually run. Other qualification data are taken from other sources such as Sandia Laboratories and the Department of Defense. There may be instances where full testing will be done at KSC. Integration testing will be done to verify system concepts and designs. To do this, hardware similar to that present at existing security sites is used to test new hardware installations and verify adequate operation.



Transducer and Sensor Laboratory

Solid-State Voltage Reference Study

Objective

To evaluate stability characteristics of Solid-State (Zener) Voltage References (SSVR) at the 10-volt level in a laboratory environment.

Introduction

In recent years, SSVR's have attained a high quality, allowing a means for maintaining a laboratory standard of voltage, thus replacing the saturated standard cell (Weston cell). NASA recognized the advantages of using SSVR's to maintain the volt through measurement assurance methods and initiated a study to determine stability characteristics of solid-state voltage references in the laboratory environment. A variety of commercially available SSVR's (at least one from each known manufacturer) was intercompared over the December 1989 to January 1991 timeframe at Kennedy Space Center Electrical Standards Laboratory. The units were compared daily using an automated measurement system. Measurement results were analyzed to establish short-term and long-term stability, as well as recovery after battery drain down.

This report presents the results of this study, indicating which SSVR's performed better over various timeframes and the extent of reference standard recovery after battery shutdown. A comparison of manufacturers' specifications with the actual data is also presented to indicate compliance/noncompliance with published specifications. (See the figure "Ten-Volt Test Arrangement.")

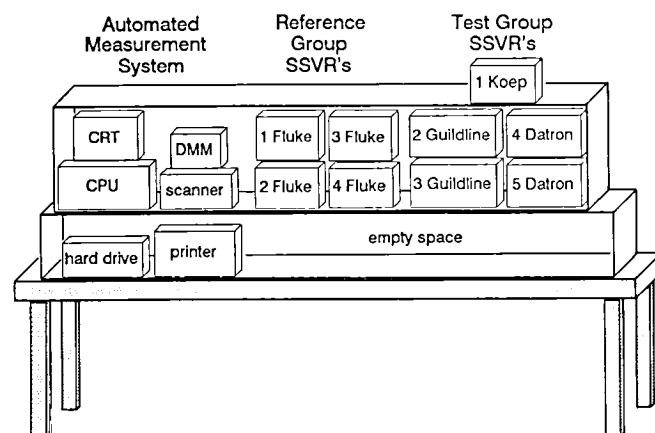
Background Information

A Solid-State Volt Intercomparison System was developed and put on line in December 1989. This system initially consisted of:

- 4 Fluke 732A-Solid State Volt References
- 1 Koep VTS 3012 Ovenized Regular Trancell-III/8C
- 1 Valhalla Scientific 2734A Direct Voltage Reference Standard
- 1 Datron 1271 Selfcal Multimeter
- 1 Data Proof 320A Standard Cell Scanner
- 1 Data Proof VRMP-HP Voltage Reference Maintenance Program
- 1 HP 2225A Printer
- 1 HP 9153C 332 Computer/Controller
- HP-IB Cables

The system operated in an automated mode using the HP Computer System and the Data Proof Volt Maintenance Software to drive the scanner switch and the digital voltmeter. Modifications were made to the Data Proof Maintenance Software program in order to use the Datron 1271 Selfcal Multimeter.

After two weeks of testing, the Valhalla Scientific 2734A Direct Voltage Reference Standard was rejected due to noncompliance with manufacturer's specifications on the output at the 10-volt level, the 30-day stability on the 10-volt level, and the output noise on the 10-volt level. The deviation from nominal of the 10-volt output also exceeded the 5-parts-per-million (ppm) adjustment capability. When this unit was removed from the measurement system, the process standard deviation was reduced by 50



Ten-Volt Test Arrangement

percent. This standard was replaced in October 1990 with a Fluke 732A.

During the next four months, the following additional SSVR's were added to the system:

- 2 Datron 4911 DC Voltage Reference Standards
- 2 Guildline 4400 Portable DC Voltage Standards

All the SSVR's were assigned to a different test group for data collection as follows:

<u>Group</u>	<u>Reference Standard</u>
RG1* (Ref. Group):	4 Fluke 732 A (1 output/box)
Test 1:	1 Koep VTS 3012 (2 outputs/box)
Test 2:	1 Guildline 4400 (4 outputs/box)
Test 3:	1 Guildline 4400 (4 outputs/box)
Test 4:	1 Datron 4911 (4 outputs/box)
Test 5:	1 Datron 4911 (4 outputs/box)

* Note: The four Fluke boxes are sub-grouped as RG1-1, RG1-2, RG1-3, and RG1-4.

Intercomparisons of all the outputs were run daily, using a left-right balanced design. The system operated in automated mode, allowing the intercomparisons to be run at night and reduce the impact on routine laboratory work. The data was saved in files according to group name.

In June, a 24-hour short-term stability test was run. Measurements were taken hourly to determine the stability of each SSVR.

During the September/October 1990 timeframe, a Fluke Reference Standard (RG1-3) was sent to the National Institute of Standards and

Technology (NIST) for intercomparison. The value assigned to this unit by the NIST was used to determine the value of the Reference Group mean and establish its drift rate.

In December, 5-day and 10-day short-term stability tests were run. Measurements were taken daily, simulating a laboratory intercomparison run.

The collection of daily intercomparison data for use in this report was completed on December 22, 1990. It was subsequently decided that a test on battery shutdown and startup recovery of the reference standards be done. During the week of January 13, 1991, selected SSVR's were shut down to simulate battery failure/shutdown during transport or an extended alternating current (ac) power outage in the laboratory.

Analysis and Results

Short-Term Stability

Although short-term stability cannot be used to accurately predict long-term drift, it can give valuable information about the day-to-day variations of the reference standards. Laboratory intercomparisons of SSVR's normally last between five and ten days, with readings usually taken one to two times per day. Round-robins and Measurement Assurance Programs (MAP's) are also scheduled on these timeframes. These test results represent the variation that would likely be observed during an intercomparison. The timeframes selected include a 24-hour, 5-day, and 10-day span. Analysis of the results and comparisons between the different manufacturers for best stability is provided in the following paragraphs.

Twenty-Four-Hour Short-Term Stability

The Solid-State Volt Intercomparison System was programmed to operate in automated mode, taking hourly intercomparison readings over a 24-hour timeframe. The table "Twenty-Four-Hour Stability Results" shows the results of the

Twenty-Four-Hour Stability Results

Group Identification	Number of Outputs	Range (μV)	Standard Deviation (μV)	F-Test Significant (95 Percent)
RG1-1	1	0.330	0.104	No
RG1-2	1	0.350	0.092	No
RG1-3	1	0.420	0.098	No
RG1-4	1	0.570	0.155	--
Test 1	2	0.895	0.267	Yes
Test 2	4	0.900	0.214	No
Test 3	4	0.805	0.240	Yes
Test 4	4	0.623	0.158	No
Test 5	4	0.698	0.179	No

intercomparison. The F-test was run on the variability of the mean of each test group at the 95-percent significance level, using the least stable subgroup of the Reference Group (RG-4) as the basis for comparison. This test determined if the larger variations observed for other units were statistically significant. The larger variations of Test 1 and Test 3 were statistically significant. Although there was no significant difference between the remaining Groups, RG1-2 and RG1-3 had the smallest standard deviations.

Five-Day Short-Term Stability

Intercomparison data between the different groups was taken for five consecutive days. A five-day span was chosen to simulate the variations that can occur during a normal laboratory intercomparison. The results of the intercomparison are shown in the table "Five-Day Stability Results." Once again, the F-test was run on the variability of the mean of each test group at the 95-percent significance level, using the Reference Group (RG-1) as the base for comparison. Test 1 was significantly different from the other Groups and was the least stable. RG1-2

and RG1-4 showed the smallest standard deviations.

Ten-Day Short-Term Stability

Short-term stability characteristics of the different groups were evaluated over a ten-day timeframe. Intercomparison data was taken for ten consecutive days, and the results are shown in the table "Ten-Day Stability Results." The F-test was run on the variability of the means of the groups at the 95-percent significance level and showed that Test 1 and Test 3 differed significantly from the other groups, indicating they were the least stable. Again, RG1-4 was used as the base for the comparison used in the F-test. There was no significant difference among the other groups, although RG1-2 and RG1-3 showed the smallest standard deviation.

Long-Term Stability

The long-term drift/slope and standard deviation of a standard is a measure of its overall stability. The optimum situation is a standard with a flat slope, possessing small short-term

Five-Day Stability Results

Group Identification	Number of Outputs	Range (μV)	Standard Deviation (μV)	F-Test Significant (95 Percent)
RG1-1	1	0.416	0.157	--
RG1-2	1	0.449	0.151	No
RG1-3	1	0.452	0.156	No
RG1-4	1	0.446	0.153	No
Test 1	2	1.416	0.575	Yes
Test 2	4	0.925	0.317	No
Test 3	4	0.865	0.322	No
Test 4	4	0.380	0.164	No
Test 5	4	0.613	0.201	No

and long-term standard deviations. In the real world, these characteristics do not necessarily coexist and tradeoffs must be made. The long-term drift of a standard can be used to accurately predict its future behavior. The more linear

the drift, the smaller the standard deviation and the better the prediction. The drifts of the standards under test were fairly linear. A regression analysis of the data was performed as shown in the table "Long-Term Stability Analy-

Ten-Day Stability Results

Group Identification	Number of Outputs	Range (μV)	Standard Deviation (μV)	F-Test Significant (95 Percent)
RG1-1	1	0.893	0.231	No
RG1-2	1	0.580	0.175	No
RG1-3	1	0.667	0.201	No
RG1-4	1	0.813	0.263	--
Test 1	2	2.064	0.672	Yes
Test 2	4	1.165	0.338	No
Test 3	4	1.612	0.515	Yes
Test 4	4	0.726	0.251	No
Test 5	4	0.839	0.254	No

*Long-Term Stability Analysis
Regression Output for Solid-State Voltage References (Mean)*

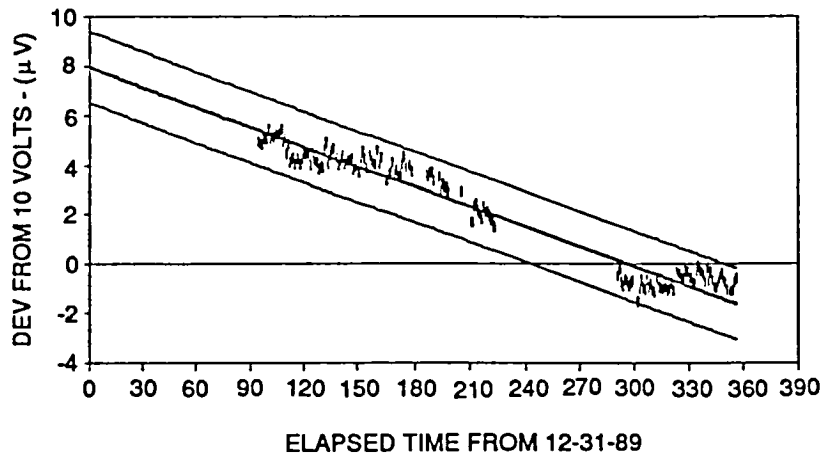
Group Identification	Number of Outputs	Intercept Value (μV)	Slope ($\mu\text{V}/\text{day}$)	Standard Deviation (μV)	Degree of Freedom
RG1-1	1	1.971	0.07913	0.35898	250
RG1-2	1	-0.06	0.07479	0.64023	250
RG1-3	1	1.35249	0.02503	0.31186	250
RG1-4	1	2.31399	0.0726	0.37516	250
Test 1	2	0.59086	-0.03602	1.53	250
Test 2	4	-23.09	-0.10951	2.43	222
Test 3	4	-26.13	-0.09499	2.17	222
Test 4	4	6.79	-0.03335	0.53	165
Test 5	4	7.95	-0.0269	0.48	165

sis Regression Output for Solid-State Voltage References (Mean)." The intercept value, slope, and the standard deviation are displayed to indicate the long-term stability of the different groups. The F-test was run on the variability (standard deviation) of the drift for the groups at the 95-percent significance level, using RG1-2 as the base for the comparison. Test 1, Test 2, and Test 3 differed significantly. RG1-3 and Test 5 showed the best long-term stability (combination of smallest slope and standard deviation). Test 2 and Test 3 were the least stable overall. The figure "Ten-Volt SSVR Study, Mean of Test 5" represents a typical drift plot of a test group, showing the actual data with the predicted slope.

and average outputs at the 10-volt level. Because the objective of this study was to evaluate the overall stability of the group, the average output specifications were used. One manufacturer did not publish a stability specification for the average output for the reference standard

Comparison of Actual Data Versus Manufacturer Specifications

The published specifications for the different reference standards give stability information on the individual



| MEAN — LL
 — FIT — UL

Ten-Volt SSVR Study, Mean of Test 5

(see the table "Actual Data Results Compared to Published Manufacturer Specifications"). The published specification for long-term drift was compared with the actual data taken for each group. All but one of the groups met the manufacturer's specifications.

Battery Shutdown/Recovery

Solid State Standards generally perform at their best when supplied with continuous power and kept at a constant temperature. Power losses may occur to the reference standard because of long shipping times or an extended ac power outage in the laboratory. Ideally, when the reference standard is repowered, the value of the reference voltage should return to its original value and slope.

The actual recovery time and shift of the voltage value for the SSVR's after complete power loss was not known. A battery shutdown/recovery test was performed on four different

reference standards (Test 1, Test 2, Test 4, and one-cell SSVR), each representing one of the four manufacturers of SSVR's. The units were switched to battery power and allowed to run down. After shutdown, the units were resupplied with ac power and intercompared in the Solid-State Volt Intercomparison System. The figure "Ten-Volt SSVR Study, Recovery of Typical One-Cell SSVR" shows the shift in the value of an SSVR under test after the battery shutdown and the length of time for recovery.

Conclusions

The stability characteristics of commercially available SSVR's have been independently determined and hardware configurations and automated test sequences for maintaining a laboratory volt at sub-ppm accuracy levels have been established by this study. The SSVR may have application to Space Station that will require a stable on-orbit voltage reference for scientific work.

*Actual Data Results Compared to
Published Manufacturer Specifications*

Group Identification	Number of Outputs	Slope ($\mu\text{V}/\text{day}$)	Drift ($\mu\text{V}/\text{year}$)	Manufacturer Specification ($\mu\text{V}/\text{year}$)
RG1-1	1	0.07913	28.88245	30
RG1-2	1	0.07479	27.29835	30
RG1-3	1	0.02503	9.13595	30
RG1-4	1	0.0726	26.49900	30
Test 1	2	-0.03602	-13.14730	15
Test 2	4	-0.10951	-39.97115	-30 $\pm 20^*$
Test 3	4	-0.09499	-34.67135	-30 $\pm 20^*$
Test 4	4	-0.03335	-12.17275	10
Test 5	4	-0.0269	-9.81850	10

* Indicates the individual drift of each output as opposed to the average output of the box.

The development of this automated system saved several hundred manhours in manual labor for this effort. Much of the testing was accomplished after work hours, with little or no impact to normal laboratory operations. A similar automated system will be implemented at each NASA Center as funding is made available.

Outlook

The use of an automated system has given NASA the ability to perform an internal Volt Measurement Assurance Program (VMAP). SSVR's used in the study have been distributed to various NASA Centers, ensuring that each Center can participate. Kennedy Space Center has taken a leadership role on this issue and will report on the progress in 1992.

Contacts:

K. J. Berland, 867-1481, SI-PEI-1B

J. P. Riley, 867-4737, SI-PEI-1B

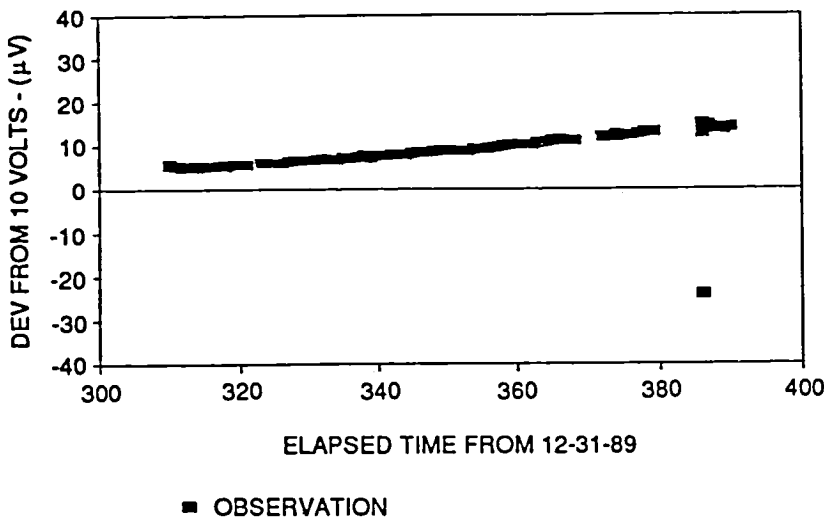
Participating Organization:

EG&G Florida, Inc., Base Operations Contract

(F. R. Manginelli and J. H. Tidwell)

NASA Headquarters Sponsor:

Office of Safety and Mission Quality



Ten-Volt SSVR Study, Recovery of Typical One-Cell SSVR

An Inexpensive Remote Data Display System

For many years, engineers have been sent from other NASA centers and contractor home plants to Hangar AE at Cape Canaveral Air Force Station (CCAFS) to participate in the prelaunch engineering evaluation of the launch readiness of expendable vehicles. This has been an expensive undertaking, with upwards of 100 personnel on temporary duty. An ongoing effort has been made to devise a method to send the entire telemetry data link to remote locations, thereby permitting the engineering staff to participate without traveling. However, the bandwidth required to accomplish this has been a stumbling block.

One of the major sources of the telemetry data is the Computer-Aided Recording and Display System (CARDS), a Commodore Amiga-based computer system located in Hangar AE. It was determined during the original design of this system that the update rate of the cathode-ray tube (CRT) displays is optimized at one update every two seconds. Any faster update makes the data considerably more difficult for the engineers to interpret. The system internal to Hangar AE has successfully operated in this manner for many years.

At Vandenberg Air Force Base (VAFB), it was necessary to get data to the Space Launch Complex 2 (SLC-2) (Delta) blockhouse from the primary station at Building 836. The values of all measurements were already stored in memory in a sequential manner and are updated continuously at full sample rate. These values are sampled every two seconds, and the resulting block of data is transmitted over an available data circuit. The need to update the remote displays at only a once-per-two-second rate provides two seconds over which to transmit the data. This made it possible to

transmit very large numbers of measurements over data lines having only 56 thousand bits of bandwidth. At SLC-2, an existing microwave link served the purpose and worked well. A similar remote system at the Lewis Research Center (LeRC) provided the LeRC engineering staff with both a training opportunity during non-NASA missions and perhaps reduced the travel expense during NASA missions. This installation was completed this summer and is now operational. The data path for the LeRC link is unusual in that the program support communications network (PSCN) system is being used.

The system provides a full set of data, including time, all raw measurements, and calculated measurements, such as orbital parameters and sequence of events. Much of this calculated data must be processed at the central computer and retransmitted in the two-second block, since these measurements require the use of every sample of data rather than just a periodic sampling.

Another advantage of this system is that the software in the remote computer is the same software as that used in the central system, except for the changes required for the communications protocol. The data viewed by engineers at both locations is always the same. When the software and the initialization (coefficients, etc.) are modified, they are sent from the central system to the remote system over the same communications link as the data, using the same software and protocol. Therefore, the software is compatible and the initialization information is completely up to date. All this can be accomplished without operator intervention at the remote end (other than power on and off).

New requirements have now been generated for similar remote systems supported from Hangar AE. One is planned for the Payload Hazardous Support Facility at Kennedy Space Center to support both the Advanced Communications Technology Satellite (ACTS) and Mars Observer Transfer Orbit Stages (TOS). Another

is planned for Hangar AM at CCAFS to support the Shuttle Pallet Satellite (German) (SPAS) Orbiting Retrievable Far and Extreme Ultraviolet Spectrometer (ORFEUS) mission, and one is designated for the Johnson Space Center payload user's area to support the TOS Payload Operational Control Center for ACTS.

Contact:

D. A. Brown, 853-9543, CV-PSD-1

Participating Organization:

McDonnell Douglas Space Systems Company

NASA Headquarters Sponsor:

Office of Space Flight

MSBLS Flight Inspection System Pilot's Display

The Pilot's Display is used in conjunction with flight inspection tests that certify the Microwave Scanning Beam Landing System (MSBLS) used at Space Shuttle landing facilities throughout the world.

The Pilot's Display was developed for the pilot of test aircraft to set up and fly a given test flight path determined by the flight inspection test engineers. This display also aids the aircraft pilot when hazy or cloud-cover conditions exist that limit the pilot's visibility of the Shuttle runway during the flight inspection. The aircraft position is calculated using the Global Positioning System (GPS) and displayed in the cockpit on a graphical display. The runway, desired flight path, and "fly-to" needles are displayed for the pilot, as well as other information used by the flight inspection test engineers. A variation of the software and hardware also aids the pilot to fly inspection flights for Tactical Air Navigation ground stations at the Shuttle landing sites.

Requirement

The Pilot's Display is used to coordinate the

test requirements of the inspection team with the test aircraft pilot. The test requirements consist of radials (wherein the aircraft flies toward the runway at a constant altitude) and glide slopes (which are landing approaches at set angles; see the figure "MSBLS Flight Inspection Flight Profiles"). This display shows the pilot the correct flight path to fly and provides "fly-to" needles so the aircraft can remain on the correct flight path during the different flight inspection test runs.

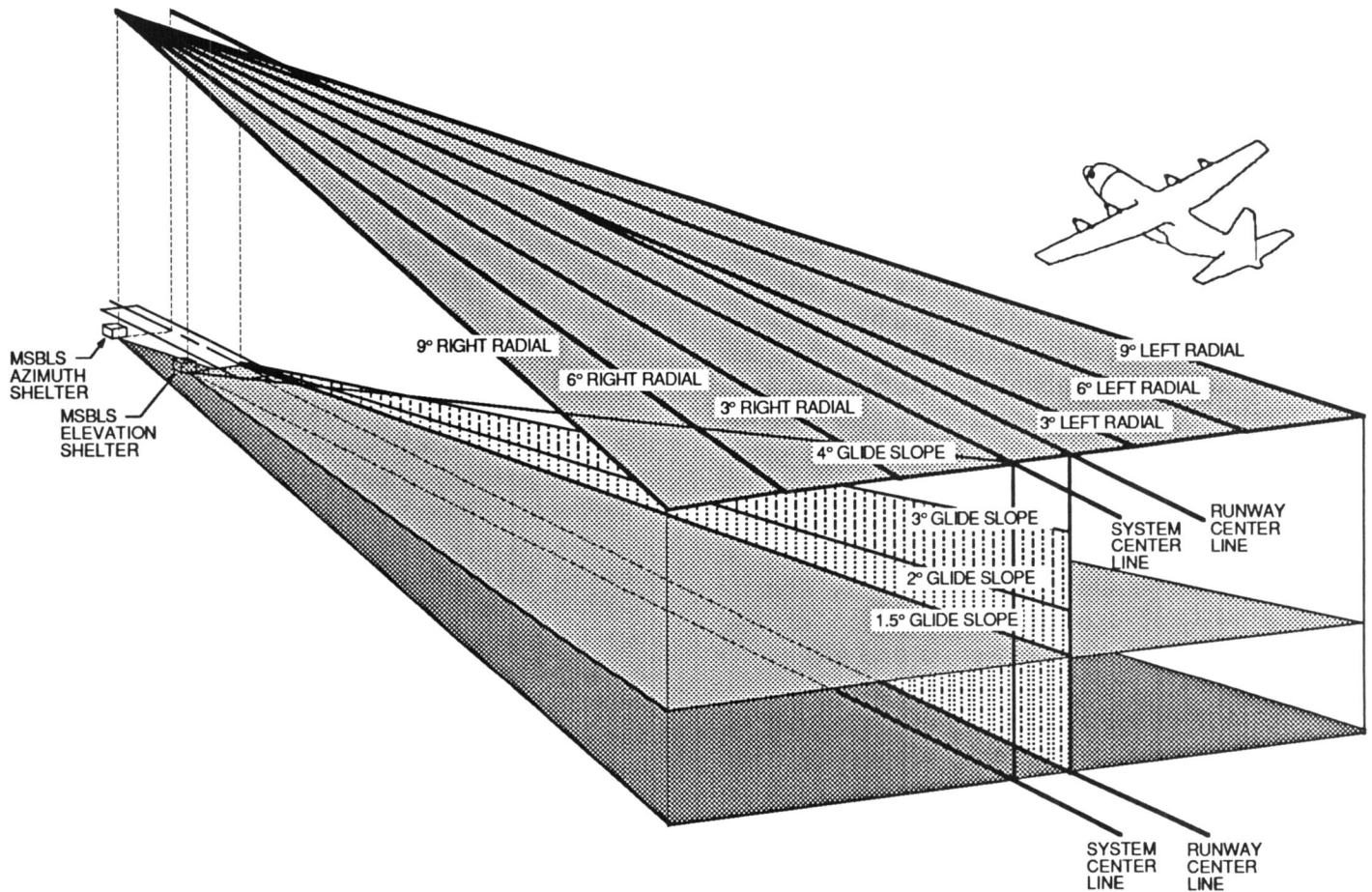
Aircraft Position Determination

The Pilot's Display and the MSBLS Flight Inspection System use the GPS data to determine aircraft position in real time. The GPS operates by the use of 21 satellites, when fully deployed, in 12-hour orbits that continuously

broadcast their identification, position, and time in space. The position of the aircraft is determined by receiving the information transmitted by any four of the satellites and by computing the position using the orbital information the satellites provide and the time the information takes to travel from the satellite to the aircraft.

GPS Errors

The GPS satellites transmit information on two frequencies: 1575.42 megahertz (L1 carrier) and 1227.60 megahertz (L2 carrier). The L1 carrier contains a precision code (P-code) ranging signal and a coarse/acquisition (C/A) code. The L2 carrier contains only the P-code, which is intended solely for military use. The GPS receivers used by the MSBLS Flight Inspection System can receive only the L1 carrier frequency



MSBLS Flight Inspection Flight Profiles

and can process only the C/A code. The use of the two frequencies allows a GPS receiver (which receives both L1 and L2 carriers) to compensate for the effects of the ionospheric and tropospheric delays, and it also greatly improves the accuracy of the computed position. This type of GPS receiver can correct for another source of error called selective availability (SA). The SA is an intentional error placed in the satellite's information, and only receivers that can process the P-code are able to correct for this error in real time.

Differential GPS

The effects of the GPS errors previously described can be reduced for those with only C/A receivers (receives only L1 carrier) by using a technique called differential GPS, which is the technique used by the MSBLS Flight Inspection System. Differential GPS uses two C/A receivers, a receiver located in a user vehicle and a reference receiver at a known fixed location. Since both receivers see the same errors, the reference receiver calculates the errors from the information about its known location and transmits the error information to the user receiver to correct its calculated position. A set of GPS receiver equipment is located at the MSBLS elevation transmitter shelter (see the figure "MSBLS Flight Inspection System") and a set is located in the aircraft with MSBLS receivers and

decoders. This configuration of equipment sets up the GPS data in the differential mode for the MSBLS flight inspections.

System Configuration

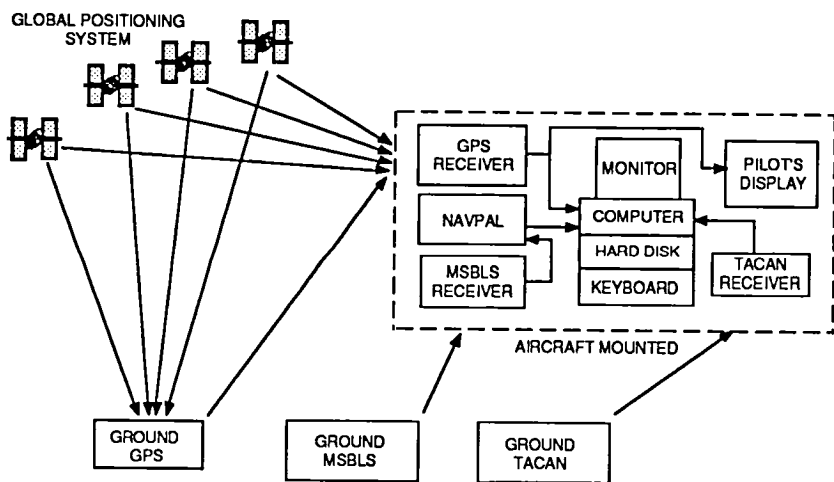
The Pilot's Display (see the figure "Pilot's Display System Block Diagram") receives the GPS position data from the same GPS receiver used by the MSBLS Flight Inspection System. The GPS receiver is initialized by the MSBLS Flight Inspection System computer and is set to receive and compute position data from satellites along with correction data from the reference receiver. The GPS receiver provides coordinate data (corrected X, Y, and Z in differential mode) to the system computer over an RS-232 serial data link at a data rate of 9,600 baud. The ground GPS receiver/modem (reference receiver) is initialized as the origin of the Pilot's Display coordinate system. The ground GPS receiver/modem will transmit position corrections for the coordinate system based on bias and drift errors in the GPS signal.

Display

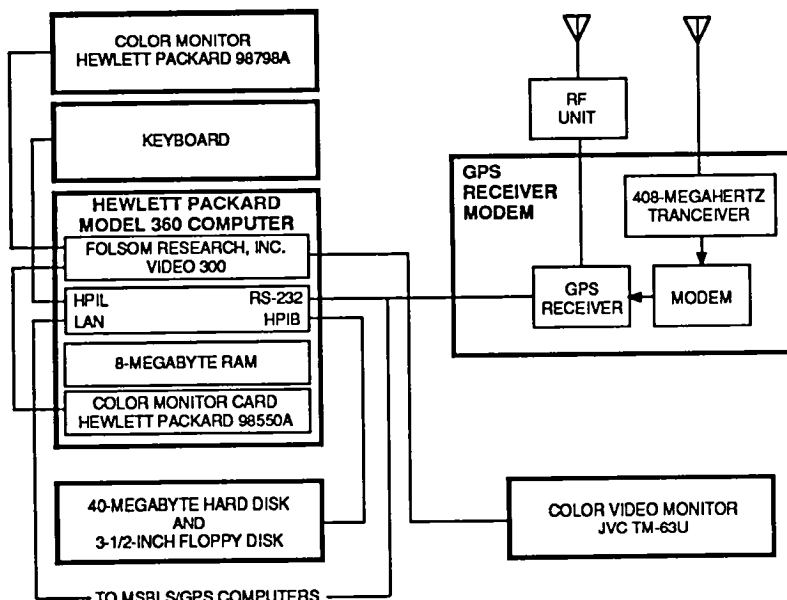
The Pilot's Display computer is programmed to compute and display the aircraft's position in real time on a video monitor. The display shows a pair of "fly-to" needles (see the figure "Pilot's Display"). The distance of each needle from the center of the display represents the aircraft's offset from the desired flight path. These offsets are computed once per second and are the differences of the aircraft's computed position and the chosen flight path. The pilot corrects the course of the aircraft by flying the aircraft so the needles move toward the center of the display as the error in the flight path is reduced.

Pilot's Monitor

The output of the computer color monitor card is sent to a graphics



MSBLS Flight Inspection System



Pilot's Display System Block Diagram

format conversion card (Folsom Research, Inc., Video 300 Card), which converts the computer graphics format to National Television System Committee (NTSC) television signals. The Video 300 Card outputs a standard NTSC video signal that is sent over coax cable to the aircraft flight deck to the pilot's color monitor (5-inch JVC TM-63U).

System Inputs

The Pilot's Display program uses GPS information from a GPS receiver to provide real time updates of the position of the aircraft. To accomplish this, the Pilot's Display program reads the data coming from the GPS receiver via a 9,600-baud serial link between the receiver and the Pilot's Display computer. The nonposition information contained in the data stream is filtered out, and the remaining information is used to determine the aircraft's position. This information appears about once a second in the data stream. The program can also replay GPS information previously recorded to a file. This file can only contain GPS position data and is not filtered in any way. The data will be replayed at about five times its normal rate of once a second.

The Pilot's Display computer is also connected to an analog-to-digital (A/D) converter that is connected to temperature and pressure transducers. The A/D converter is connected to the Pilot's Display computer via a Hewlett Packard Interface Bus (HPIB) link. During real-time data display, it is queried whenever a position update is received on the GPS data stream (once a second) and the information is displayed to the operator and logged to a file, along with the current time (from the GPS data), for later analysis.

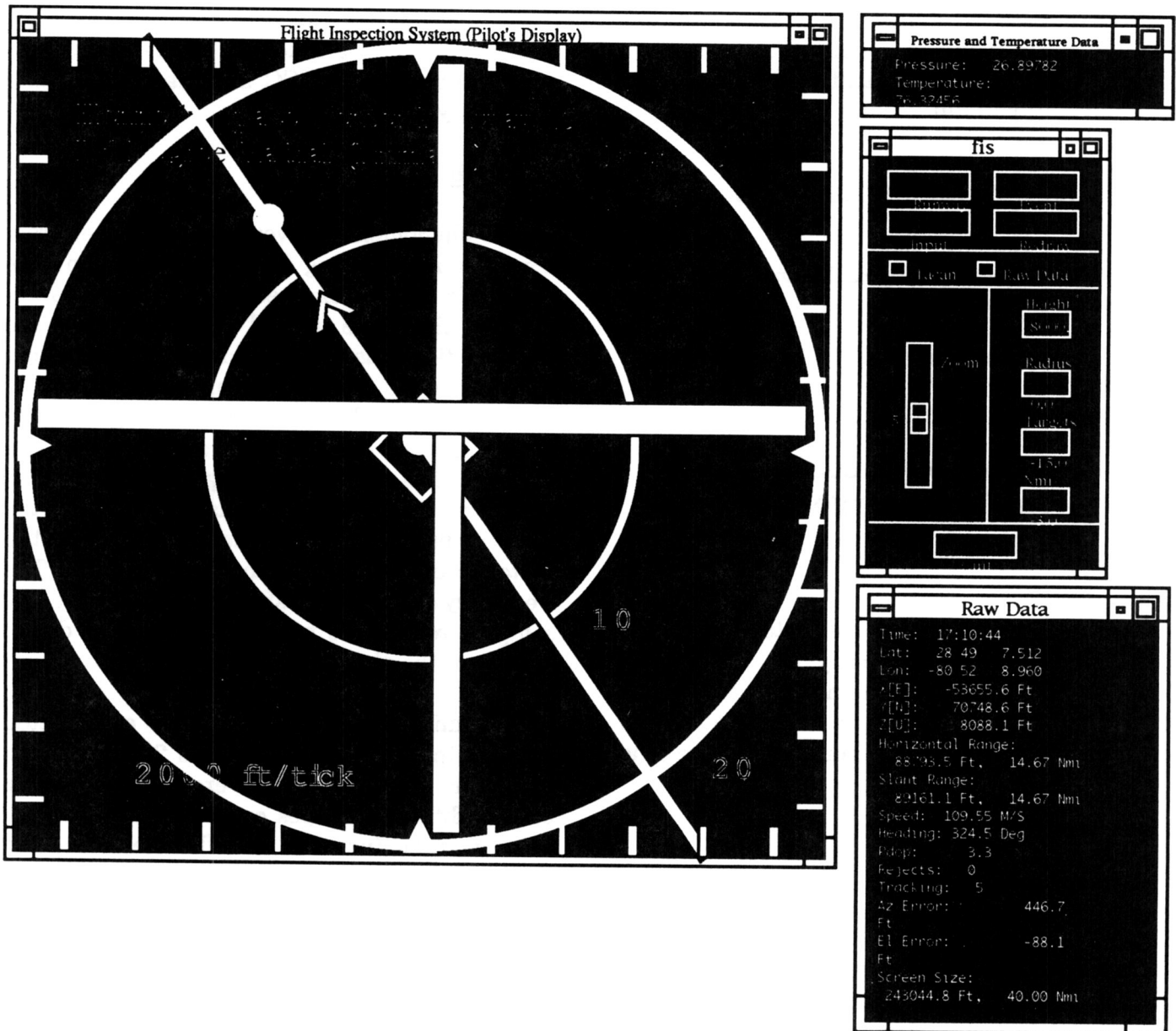
Program Calculations

The program for the Pilot's Display calculates distances and errors by translating the raw GPS data and comparing it to the selected runway and event information. The raw GPS data gives position in longitude and latitude, and this information is converted to local east, north, and up (x,y,z) coordinates.

The program calculates two types of deviation: elevation and azimuth. Both are measured in feet. Elevation deviation is the distance that the aircraft is above or below the flight path. Azimuth deviation is the distance that the aircraft is to the left or right of the flight path.

Elevation deviations are calculated two different ways, each for a different type of flight event. If the event has no glide slope, then the elevation deviation is simply the difference between the desired and actual height. For glide-slope events, the only difference is that the desired elevation has to be calculated based upon the aircraft's distance.

Azimuth deviations are handled in two ways, each for a different type of flight event. If the flight path is radial (i.e., a straight line), the difference between the aircraft's heading and the desired flight path heading is calculated by rotating the aircraft's position about the system



Pilot's Display

origin by an angle equal to the sum of the runway heading and the desired aircraft heading.

If the flight path is circular, azimuth deviations are calculated by determining the distance of the plane from the system origin and subtracting that from the desired distance. The sign of the deviation is determined by calculating the angular difference between the aircraft's heading

and a tangent to the circular flight path.

Conclusions

MSBLS flight inspections have become more efficient with the Pilot's Display. The display coordinates the test engineer's requirements with the pilot of the test aircraft and provides the pilot a direct indication of how well he is maintaining the test flight. This system has

also been used to follow the progress of the aircraft while flying from one Shuttle landing facility to another, demonstrating the use of GPS as a navigational aid.

Contact:

M. M. Scott, Jr., 867-3185, DL-ESS-23

Participating Organization:

Boeing Aerospace Operations, Engineering Support Contract (T. Erdogan)

NASA Headquarters Sponsor:

Office of Space Flight

Low-Flow Vortex-Shedding Flowmeter for Hypergols

Objective

Develop a 1/2-inch flowmeter to replace the turbine flowmeters currently in use in the launch pad hypergolic systems. The flowmeter should have no moving parts and be capable of measuring flows ranging from 1 to 10 gallons per minute.

Background

Hypergolic fuels are used by the Shuttle Orbiter for its reaction control system and orbital maneuvering system engines. To monitor the loading of the propellant, turbine flowmeters are currently used. After each load, the flowmeters must be removed, cleaned, and recalibrated. This operation becomes increasingly expensive as the number of launches increases. Vortex-shedding flowmeters are used in cryogenic systems where the lack of moving parts is a necessity. However, market surveys revealed there were no vortex-shedding flowmeters available for the low flow rates required by the propellants loading system. Investigations were launched to determine if a flowmeter of the desired characteristics could be developed. The initial work was done by Kennedy Space Center

(KSC) and the University of Florida. The work described here is a follow-on development program conducted by KSC and California State University at Sacramento.

Approach

The phenomenon of vortices being shed from a surface in a flowing fluid is not new, and the application of vortex shedding to the measurement of flow rate is well established. For a uniform flow past a circular cylinder, vortices are formed at the two separation points and shed off regularly in an alternating fashion. These vortices move downstream in a regular pattern. The vortex-shedding flowmeter works on the principle that the mass flow rate of the fluid is proportional to the frequency of the vortex shedding behind the shedder bar. The frequency of the vortex shedding is measured by a highly responsive pressure transducer downstream of the shedder bar.

A family of flowmeters was constructed ranging in size from 1/2-inch to 2-inch outside diameter. The flowmeters were built so shedder bars of different shapes could be interchanged. Tests were conducted on each flowmeter size and shedder bar shape to determine which design produced the most desirable results. The tests were conducted using two flow benches. A pressurized flow system was used for flows below 10 gallons per minute, and a variable frequency drive pump was used for flows above 10 gallons per minute. Tests were performed with Freon or water, which closely match the specific gravities of nitrogen tetroxide and hydrazine, respectively.

Results

After testing the various designs, it was determined that the vortex-shedding phenomenon can be adequately measured using a responsive pressure transducer. The pressure pulses for rectangular and trapezoidal shedder bars

were the cleanest and produced the most consistent results. Comparisons of the data acquired from the vortex-shedding flowmeters and existing turbine flowmeters showed a correlation of 99.2 percent. Work will continue this year on a unit suitable for use in hypergols. Once qualification and field testing are complete, the design will be released to industry for manufacture.

Contacts:

*W. E. Larson and R. M. Howard, 867-3185,
DL-ESS-23*

Participating Organization:

*California State University at Sacramento
(Dr. Ngo Dinh Think)*

NASA Headquarters Sponsor:

Office of Space Flight

Biosciences

Biosciences research and development at Kennedy Space Center (KSC) are conducted in several disciplines and by support from the following dedicated facilities and resources:

Environmental Monitoring and Ecological Studies
Plant Space Biology Program
Controlled Ecological Life Support System
Human Physiological Studies
Life Sciences Flight Experiments Program

Environmental Monitoring and Ecological Studies

The Environmental Monitoring Laboratory provides monitoring support for air quality, water quality, and environmental impact analyses. Equipment includes a fully operational chemistry laboratory for sample analyses using an atomic absorption spectrophotometer, a Technicon autoanalyzer, an inductive coupled plasma analyzer, and gas chromatographs. A remote sensing, geographical information system laboratory provides for use of satellite and aerial imagery in support of ecological research and environmental support of KSC operations. Microbiological laboratories provide ancillary support to these activities, as well as for all other flight, research, and clinical microbiological requirements at KSC. They are equipped with automatic microbiological identification systems, automatic plate counters, and a wide range of sampling equipment.

Because of the common occupancy of 144,000 acres of subtropical natural habitat by KSC, the Merritt Island National Wildlife Refuge, and the Cape Canaveral National Seashore, many rare and endangered species of wild life undergo continued surveillance. This is accomplished with on-scene and remote assessment methods and joint agency collaboration.

Plant Space Biology Program

Activities in this program explore the unique requirements and responses of plants grown in space. There are inhouse controlled plant growth units, varying gravity devices (clinostats for the

equivalent of microgravity and centrifuges for hypergravity), directed development of nutrient delivery systems capable of functioning in microgravity, and supporting laboratories. The program also monitors for NASA Headquarters adjunctive research by nearly two dozen outside plant investigators and seeks flight opportunities for methods and hardware systems developed for the space environment.

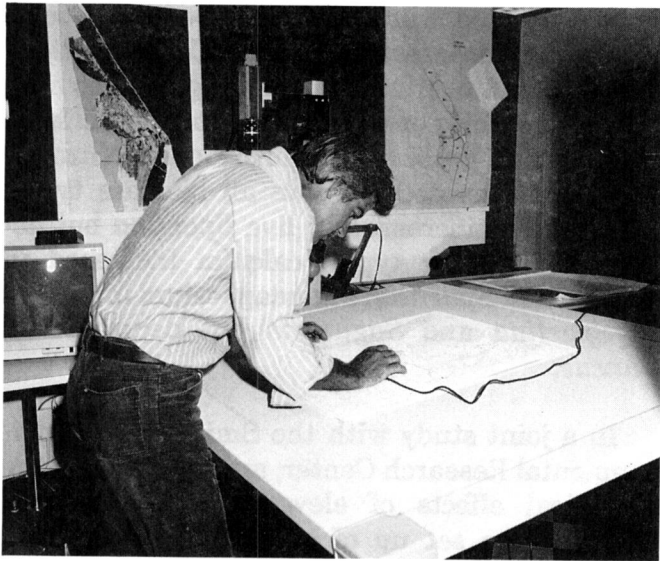
Controlled Ecological Life Support System (CELSS)

The CELSS concept first became a reality in America in 1986 with the construction and operation at KSC of a large closed chamber capable of growing plants under highly controlled conditions. This breadboard project has now produced from seed to harvest several replications of five edible crops under varying nutrient, energy, and environmental conditions. This has amassed great experience for a multidisciplinary team and a vast data base of truly unique plant-growth information.

In support of this CELSS Biomass Production Chamber, there now exist organic and inorganic chemical, gas analytical, and microbiological laboratories; control systems for light, nutrient, and environment; and adjunct capabilities for food preparation, waste resource recovery, and early integration of the human being into the system. The aggregate facilities and capabilities for a CELSS at KSC are recognized as pioneering work in this unusual, but essential subsystem for permanent human habitation off earth.

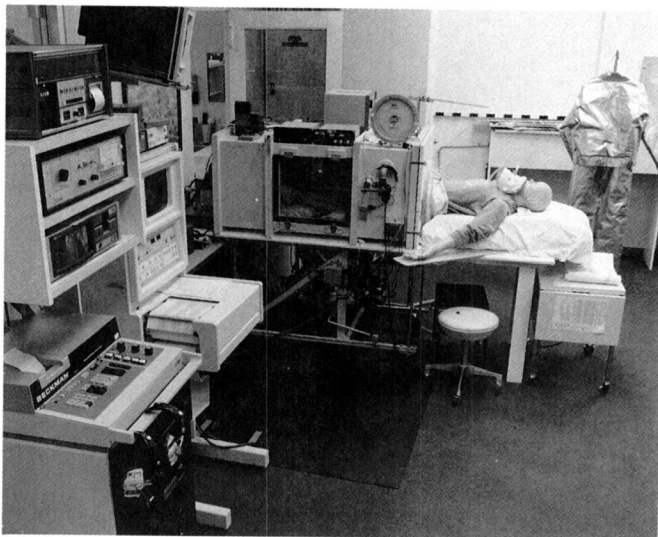
Human Physiological Studies

Two distinct but interrelated thrusts in human studies have been pursued at KSC. These contribute directly to further understanding of and solutions to problems experienced in human space flight. Expertise and facilities have focused on human exercise, locomotion, and orthostatic responses since they are all modified after exposure to microgravity. Research involves both mechanisms contributing to adverse adaptations and methods for either ameliorating or fully



Environmental Monitoring and Microbiological Laboratory

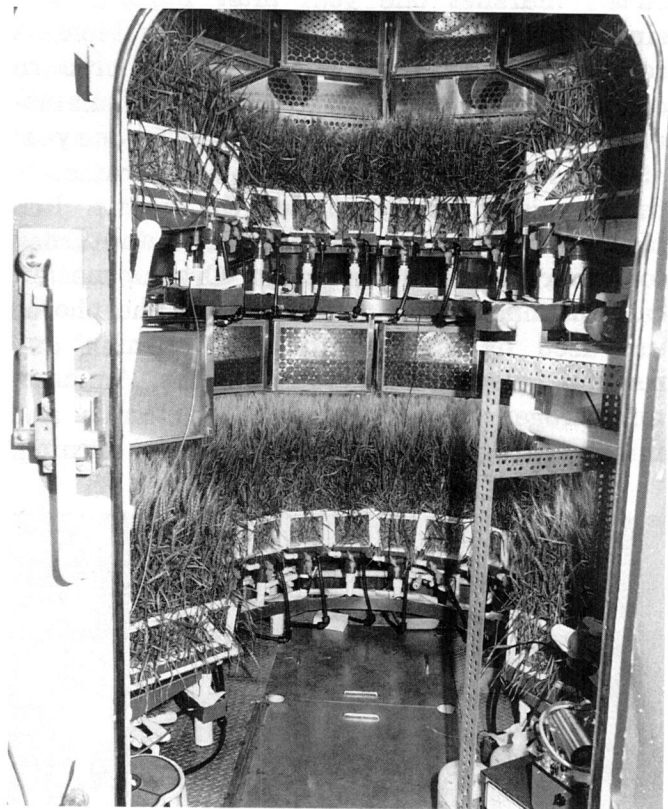
countering these contrary responses. These activities are supported by physiological stress and muscle function laboratories, muscle biopsy and histochemical assay capabilities, muscle imaging, and clinical support to subjects. In addition, development and use of more practical and less costly analogs to simulate microgravity effects upon the locomotor muscle system have been achieved.



Biomedical Research Laboratory

Life Sciences Flight Experiments Program

This program operates several facilities dedicated to the support of life science's principal investigators whose flight experiments must eventually come to KSC. Many investigators also require concurrent ground control phases of their experiments. For this support, the Life Sciences Support Facility, located in Hangar L on the Cape Canaveral Air Force Station, has the latest in animal holding rooms and support laboratories



Life Sciences Support Facility

configurable to the requirements of the investigator. Plants are similarly accommodated.

In the Operations and Checkout Building at KSC, the counterpart for human flight experiments is called the Baseline Data Collection Facility. It has multiple laboratories that may readily be adapted for pre- and postflight experiment needs. KSC personnel with these resources either assist investigators or act as their surrogates.

Vegetation Studies and Biospherics Research

Research on the effects of fire on wetlands at Kennedy Space Center (KSC) as a part of the NASA Biospherics Program continued with the analysis of data from the sites studied in conjunction with Langley Research Center. A paper published on the recovery of marsh vegetation and biomass after fire showed that species composition of *Juncus roemerianus* and *Spartina bakeri* marshes one year after burning was similar to the preburn compositions, but biomass composition was only one-third of preburn composition. A manuscript prepared to summarize changes in marsh soil chemistry for one year after the fire showed changes in soil parameters that persisted for varying lengths of time. Soil pH increased immediately postburn but returned to preburn levels in one month. Organic matter, calcium, magnesium, potassium, and phosphorus increased by one month after burning and remained elevated for 6 to 12 months. Ammonium-nitrogen was elevated at 6 months and nitrate-nitrogen at 12 months after burning,

apparently due to interactions between seasonally varying water levels and fire. Concentrations of some plant nutrients in standing crop biomass of marsh species one year after burning differed from that of preburn concentrations. Nitrogen concentrations decreased in all biomass types; phosphorous increased in live *Spartina* but decreased in other types; calcium increased in *Juncus* and *Spartina*; and magnesium increased in *Spartina* and *Sagittaria* but decreased in *Juncus*.

In a joint study with the Smithsonian Environmental Research Center, an evaluation of the ecological effects of elevated carbon dioxide included the set up of a research trailer and carbon dioxide supply at the study site.

Collection of vegetation and soils data for KSC continued with the completion of chemical analyses of soil samples for many parameters.

Work on the fire ecology of scrub vegetation proceeded with the resampling of permanent transects that burned in 1986 at 48 months after



A Control Burn in KSC Wetlands

the fire. Data analyzed through 36 months after fire showed little change in species occurrence, but dominance patterns changed where saw palmetto (*Serenoa repens*) and scrub oaks (*Quercus* spp.) both occurred because saw palmetto regrew more rapidly after fire than the oaks. Structural features such as vegetation height required longer to recover.

A project to determine the historical patterns of fires on the KSC landscape was initiated. Aerial photography taken over the last 20 years will be used to determine the occurrence, frequency, and aerial extent of past fires. This should help explain vegetation patterns seen on the landscape and, when combined with other data, contribute to understanding habitat quality.

Monitoring of launch effects on vegetation continued with the determination of deposition patterns and vegetation effects for launches STS-35, STS-37, STS-38, STS-39, STS-40, STS-41, STS-43, and STS-48. These effects were summarized in quick-look reports. A GIS data base of predicted and actual deposition patterns from all past launches was established and is being used to evaluate the accuracy of model predictions and cumulative effects of launches.

Contact:

W. M. Knott, Ph.D., 853-5142, MD-RES-L

Participating Organization:

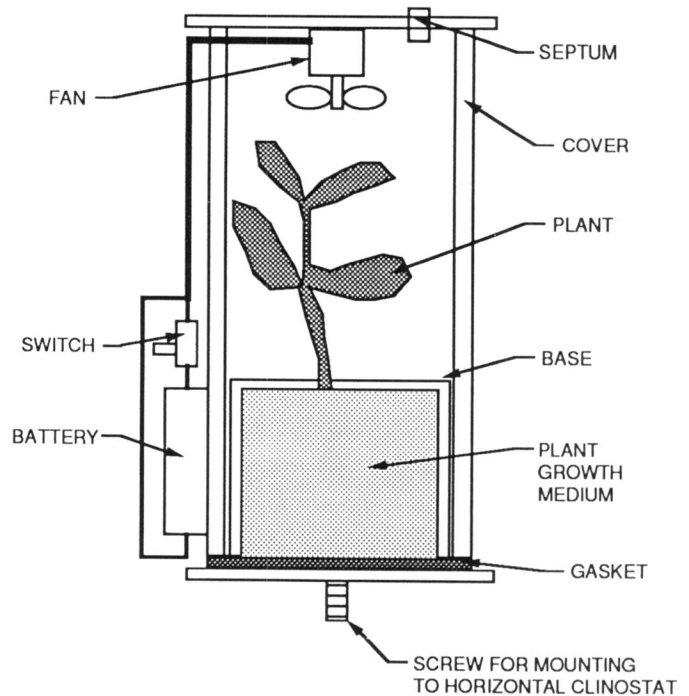
The Bionetics Corporation (P. A. Schmalzer, Ph.D.)

NASA Headquarters Sponsor:

Office of Space Flight

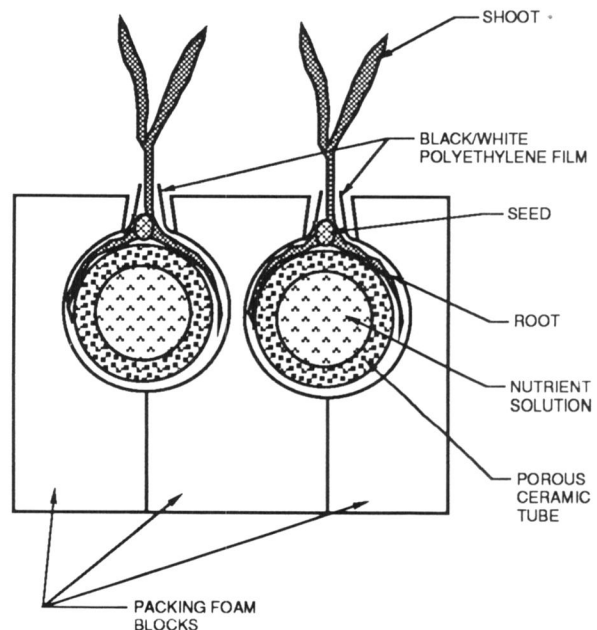
Plant Space Biology Program

In an effort to examine the influence of gravity on higher plant photosynthesis and carbohydrate metabolism, technology development occurred along several fronts. Development of the Tubular Membrane System (TMS) for supplying water and nutrients to plants in

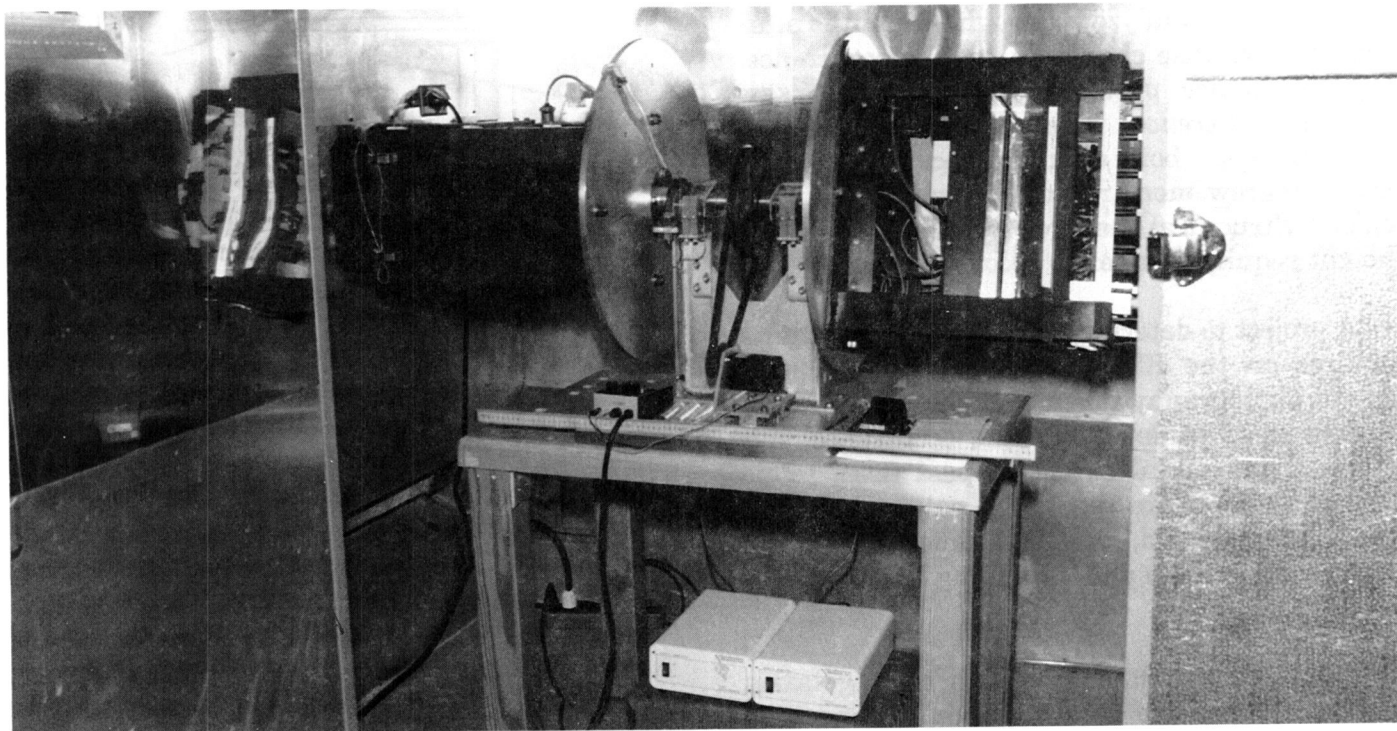


Sealed Chamber for Plant Growth and Gas Exchange Measurements on a Clinostat

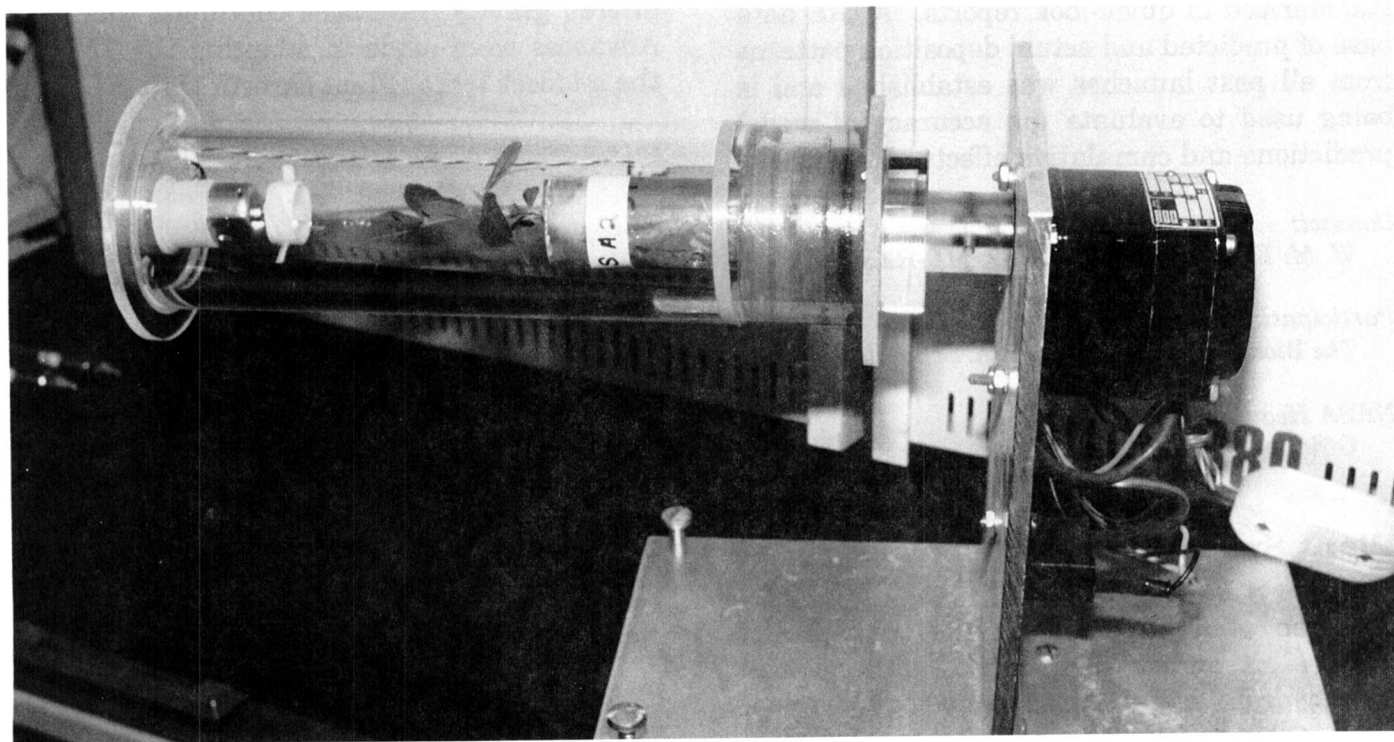
altered gravity conditions continued this year. Advances were made in adapting the TMS for the middeck locker Plant Growth Unit (PGU). A



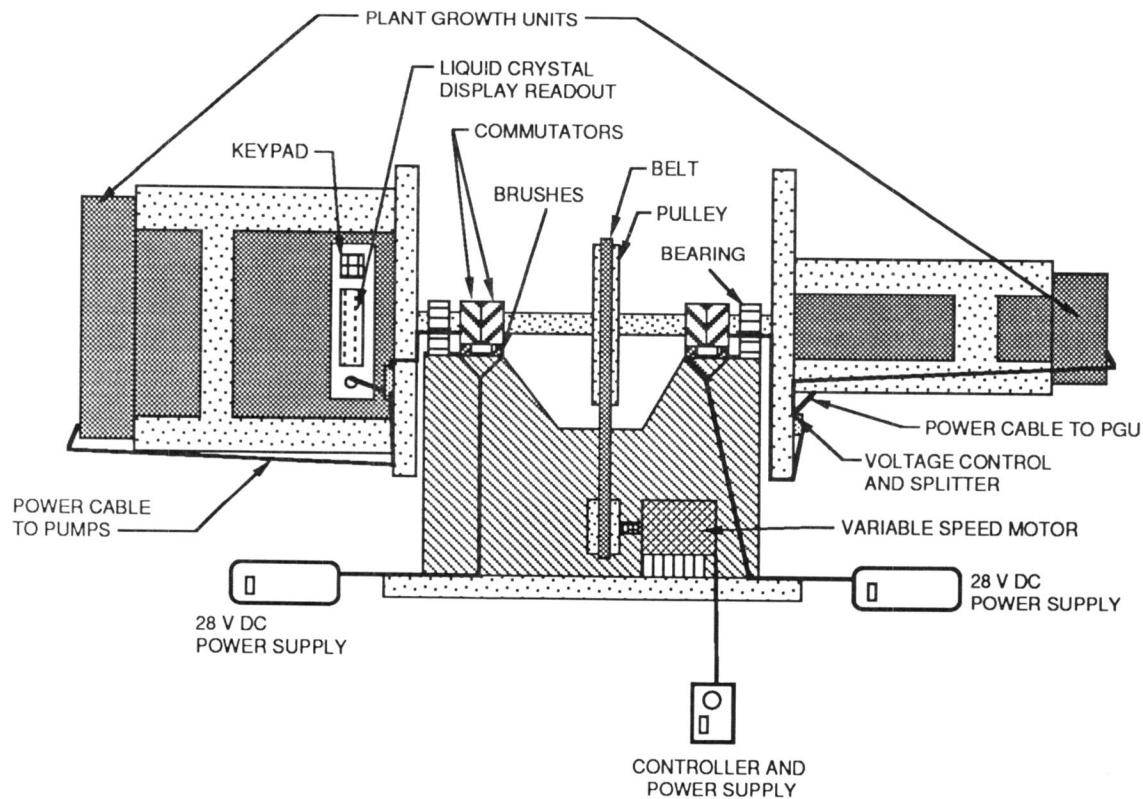
Porous Tube Plant Growth Unit Cross Section



Clinostat for the PGU



*Sealed Atmospheric Gas Exchange Chamber for Plants
in Altered Gravity Treatments*



Clinostat for Rotating the Space Shuttle Middeck Locker Plant Growth Unit

number of miniaturized TMS units of varying pore sizes were designed and fabricated that are integrated into the small Plant Growth Chambers (PGC's) that are integrated into the PGU. Comparative tests between the TMS units and other media have been initiated. Pump and reservoir modules have also been constructed and have been utilized within a mockup of the PGU. A clinostat, which can rotate two of these mockups, has been constructed, and the TMS has supported plant growth for up to two weeks at a time under altered gravity conditions produced by the clinostat.

Improvement and development of a cylindrical chamber that can be atmospherically sealed and mounted on a small clinostat for measuring the effect of altered gravity on plant photosynthesis and respiration continued. Using this chamber, it has been shown that horizontal clinorotation results in an increase in the photo-

synthesis/respiration ratio of pea and maize seedlings.

Contact:

W. M. Knott, Ph.D., 853-5142, MD-RES-L

Participating Organization:

The Bionetics Corporation (C. S. Brown, Ph.D.)

NASA Headquarters Sponsor:

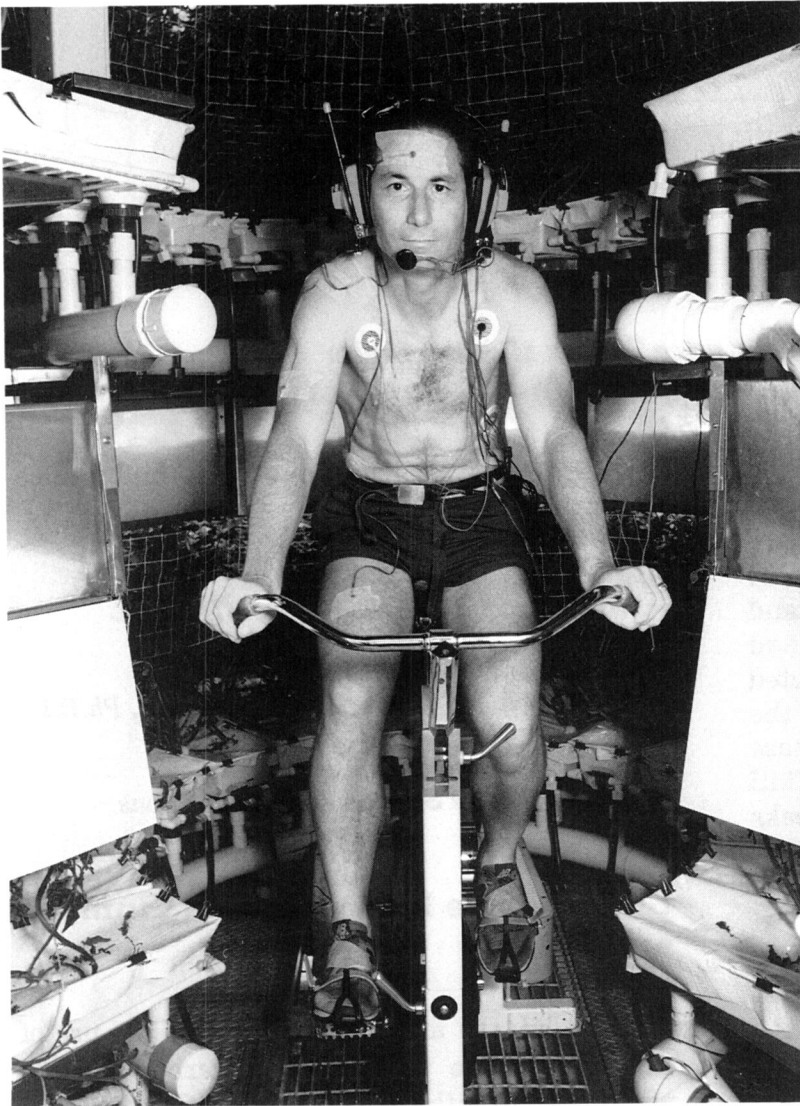
Office of Space Sciences and Applications

CELSS: The Interaction of Humans and Plants

Since human metabolism requires the use of oxygen and the production of carbon dioxide while photosynthesis in plants uses carbon dioxide to produce oxygen, it is clear that the quantification of mass and energy exchange

between plants and humans is critical to the planning and development of effective and efficient life support systems for space travel and exploration.

This relationship becomes even more critical when metabolic demand is increased by physical work requirements. Based on this premise, a series of experiments were conducted as part of NASA Space Life Sciences Training Program (SLSTP) to determine the characteristics of gas and heat exchange between growing plants and working human subjects in a "closed" chamber.



*Subject Performing Exercise in the
CELSS Chamber*

Subjects were asked to exercise for 30 minutes at 25, 50, and 75 percent of their maximal oxygen uptake while placed in the Controlled Ecological Life Support System (CELSS) biomass production chamber with a growing potato crop (see the figure "Subject Performing Exercise in the CELSS Chamber").

Measurements of gas exchange (oxygen uptake and carbon dioxide production), heart rate, sweat rate, and body temperatures were made on subjects before, during, and after exercise while ambient temperatures and gas levels in the chamber were closely monitored. Preliminary results suggest that the carbon dioxide produced by subjects working at 25 percent of their maximal oxygen uptake (similar to walking at a normal pace) provided the carbon dioxide required by the plants at their normal growth conditions.

Additional studies will be conducted during the next year. Further analysis of the data from these experiments will provide important information regarding the impact of man living and working in a closed environment during spaceflight or planetary exploration and the factors that should be considered in order to develop the most effective and efficient life support systems.

Contacts:

*V. A. Convertino, Ph.D., 867-4237,
MD-RES-P*

*J. C. Sager, Ph. D., 853-5142,
MD-RES-L*

*W. M. Knott, Ph.D., 853-5142,
MD-RES-L*

D. F. Doerr, 867-3152, MD-ENG

Participating Organization:

*NASA Space Life Sciences Training Program (I. D. Long, M.D., and
W. R. Munsey)*

NASA Headquarters Sponsor:

Office of Space Sciences and Applications

Habitat Assessment Group

The buffer zones for space operations provided by the lands and waters of Kennedy Space Center (KSC) represent an area with biological diversity that is unsurpassed among most Federal facilities in the continental United States. Fourteen endangered and threatened wildlife species occur at KSC; many other species are under review for listing or are listed as endangered or threatened by the State of Florida.

A review of scientific literature was used to identify species of conservation concern that are



Indigo Snake

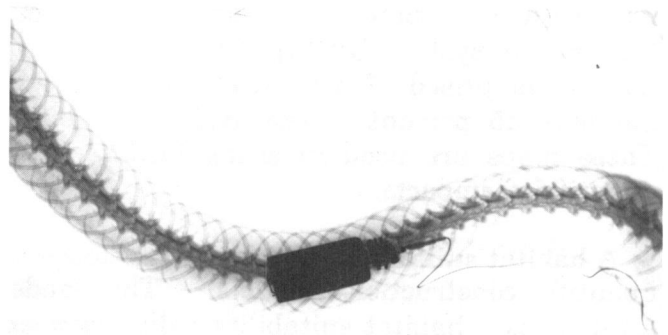
maintaining both United States and Florida populations. This provides a tool to evaluate the effects of proposed operations at KSC on biological diversity.

Nearly 400 Florida scrub jays have been banded in five sites on KSC and the adjacent Cape Canaveral Air Force Station. Two sites near the Titan launch pads are used to evaluate launch effects in a study funded by the U.S. Air Force. Another site is used to evaluate road and facility construction impacts in a study funded



Florida Scrub Jay

not yet listed as threatened or endangered. Approximately 100 wildlife species that are in peril or are otherwise declining occur as residents on KSC or at least use KSC habitats during migration. This demonstrates the coexistence possible among a large assemblage of native wildlife and one of man's greatest technological achievements. A ranking system was formulated based on the species' vulnerability to development in the United States, Florida, and KSC, and based on the relevance of KSC for



Indigo Snake With Transmitter

by the National Park Service. This includes a study before the project, monitoring of construction, and a study after construction to evaluate the impact predictions.

Long-term studies on territory size and composition, reproductive success, and survival are being performed in two areas to distinguish habitat conditions where reproduction exceeds mortality ("sources") from conditions where mortality exceeds reproduction ("sinks"). Studies of colorbanded birds were conducted in 20 territories in 1988, 40 territories in 1989, 50 territories in 1990, and 44 territories in 1991. Focal animal sampling was also used to quantify scrub jay behavior, food acquisition, and habitat use for individual birds.

Florida scrub jay population maps were developed that identified the location of 86 percent of the KSC scrub jay population which comprised 44 percent of the potential habitat. This can be used for land-use planning and habitat management. Primary and secondary habitats within population centers were also mapped using remote sensing and Geographical Information System (GIS) applications. Primary habitat comprised 57 percent of the population but only 15 percent of the available habitat. These maps are used in siting facilities and quantifying impacts.

A habitat suitability model was developed to quantify construction impacts. The model establishes a habitat suitability value between zero and one for a habitat patch. The acreage of the patch multiplied by its suitability is used to determine the number of habitat units associated with the patch. Habitat lost to construction must be offset in accordance with the Endangered Species Act. The total habitat lost to



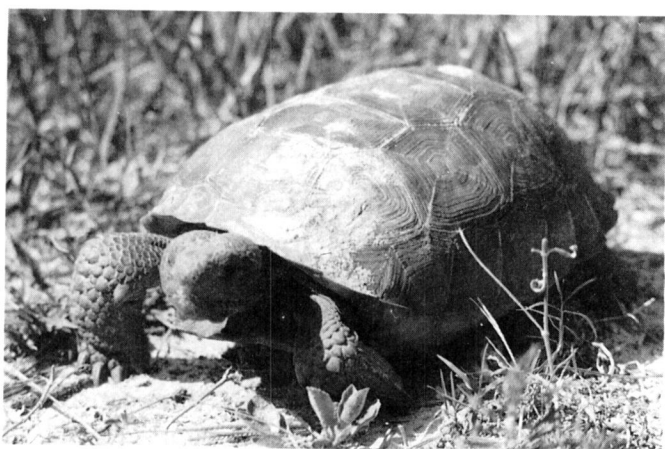
Wood Stork Nest at Bluebill Creek Colony South of Launch Complex 39A

facility development for the next three years was estimated. A plan was developed to compensate the loss by creating scrub on abandoned orange grove sites and restoring scrub that no longer supports the wildlife species that once were its inhabitants. Some of the habitat lost to new facilities is within areas that are difficult to manage. The compensation plan was designed to restore large landscapes into less fragmented habitat that more closely resembles natural conditions. This not only enhances its management potential but enhances its suitability for wildlife.

Radio tracking studies of indigo snakes are revealing habitat use and movements; thirteen have been tracked since the study began four years ago. GIS applications are used to analyze habitat use. These predators require large amounts of habitat. The average home range has been nearly 300 acres for males and 76 acres for females. Home range boundaries have shown little overlap among males; however, female boundaries may overlap home ranges of one or more males. It is unknown whether there is overlap among the home ranges of females.

Indigo snakes use a wide variety of habitat; it is unclear whether they prefer or avoid certain habitat types. Some have shown a preference for well-drained areas and others have shown a preference for disturbed areas. Only large expanses of open water appear to be avoided. Radio-tagged snakes have readily crossed dirt and gravel roads but appear to avoid paved roads.

Aerial surveys of wading birds are performed to quantify the importance of different habitats for feeding and to evaluate seasonal and yearly variations in the number of wading birds using KSC. GIS applications are used to determine the types of habitat surveyed and the proportion



Gopher Tortoise

sampled relative to the total at KSC. Nesting and roosting sites on natural islands and spoil islands, created from dredge material, are identified. The number and species of wading birds using these islands are quantified on a seasonal basis in a cooperative project with the U.S. Fish and Wildlife Service. These data, combined with data collected in feeding habitat, are used to estimate the size of the wading bird population at KSC.

A camera system was developed to formulate and test correction factors that convert gopher tortoise burrow counts to tortoise densities and to investigate burrows used by many other species of conservation concern. Less than 20

percent of active and inactive burrows are actually occupied by gopher tortoises during much of the year. Radio tracking studies showed that individual gopher tortoises often use many burrows. A study funded by the Florida Game and Fresh Water Fish Commission showed that gopher tortoises occupy a wide range of habitat conditions in scrub and pine flatwoods at KSC. They prefer areas with the most food, such as disturbed and recently burned areas, and do not require well-drained areas as once believed. Higher densities also tend to occur in poorly drained scrub and pine flatwoods where there is more food. These studies have shown that gopher tortoises often inhabit flooded burrows during periods when ground water levels are near the surface, even when there are many unoccupied burrows that are not flooded nearby.

Contact:

W. M. Knott, Ph.D., 853-5142, MD-RES-L

Participating Organization:

The Bionetics Corporation (D. Breininger)

NASA Headquarters Sponsor:

Office of Space Flight

Orbiter Environmental Simulator

The Space Shuttle temperature, humidity, and carbon dioxide levels are dynamic and mission specific. These environmental changes may introduce variables into flight experiments that could obscure test results. The Orbiter Environmental Simulator (OES) was developed to resolve this problem by precisely duplicating mission-specific changes in temperature, relative humidity, and carbon dioxide levels in ground control experiments. The OES consists of a plant growth chamber modified to include dynamic control by a microcomputer. Orbiter Calibrated Ancillary System (CAS) data, archived from a particular mission, is loaded into the microcomputer which in turn controls the plant growth chamber to dynamically match



Orbiter Environmental Simulator Control Unit

Orbiter environmental conditions. This system has been successfully employed to support postflight ground control experiments for the Chromosomes and Plant Cell Division in Space Experiment (CHROMEX), the Characterization of Neurospora Circadian Rhythm (CNCR) Experiment, CHROMEX-2, and Spacelab Life Sciences-1 (SLS-1) which were manifested on STS-29, STS-32, STS-41, and STS-40, respectively. The OES will be used to simultaneously support ground control experiments for the International Microgravity Laboratory (IML-1).

Contact:

W. R. Munsey, 867-4551, CP

Participating Organization:

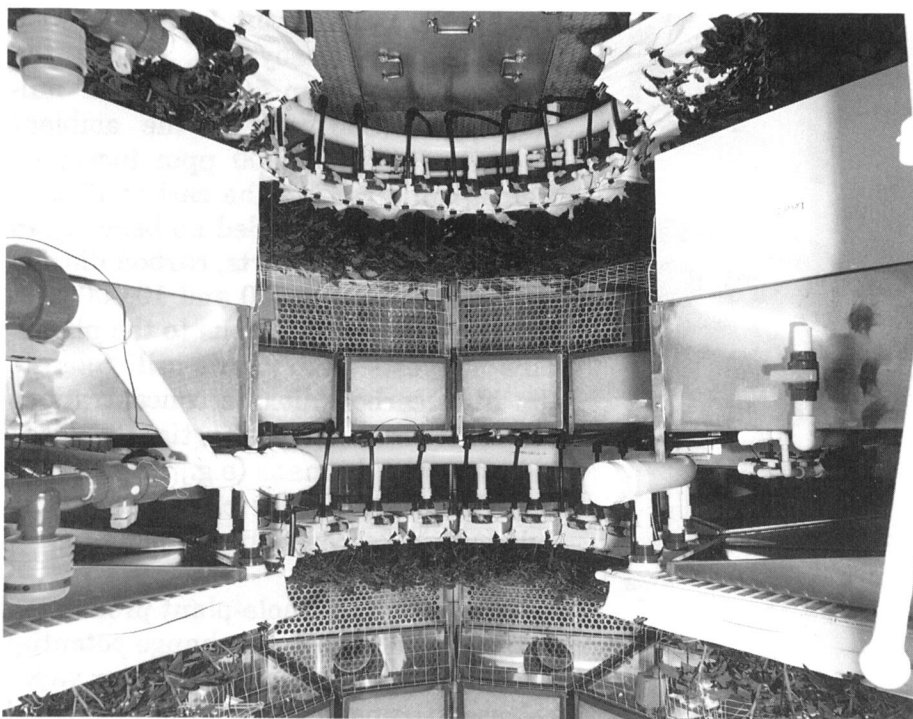
The Bionetics Corporation (C. R. Hargrove)

NASA Headquarters Sponsor:

Office of Space Sciences and Applications

Controlled Ecology Life Support System (CELSS) Biomass Production Chamber

Crop production trials with soybean (*Glycine max*) and lettuce (*Lactuca sativa*) were continued throughout 1991 to complete comparisons of growth under high-pressure sodium and metal halide lamps. In addition, the first test with potatoes (*Solanum tuberosum*) was conducted. Results showed no consistent differences with regard to lamp spectrum, but yields of soybean were strongly influenced by total irradiance provided to the plants. In addition, reducing the photoperiod (daily light interval) from 12 hours to 10 hours promoted proportionately more seed development. The best yields averaged about 600 grams of seed dry weight per square meter for soybean, 3,100 grams fresh weight per square meter for lettuce, and 8,000 grams fresh weight per square meter (1,280 grams dry weight per square meter) for potato tubers. Comparisons with research conducted in plant growth chambers suggest that yields of both soybean and potato can be increased by optimiz-



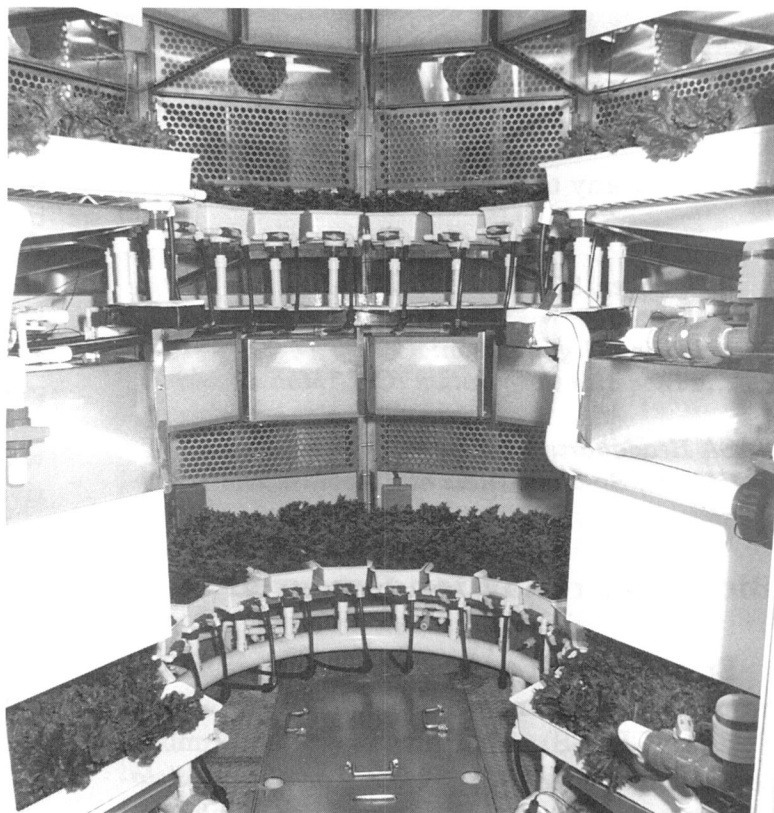
Potatoes Growing in the Biomass Production Chamber

ing environmental conditions in the Biomass Production Chamber.

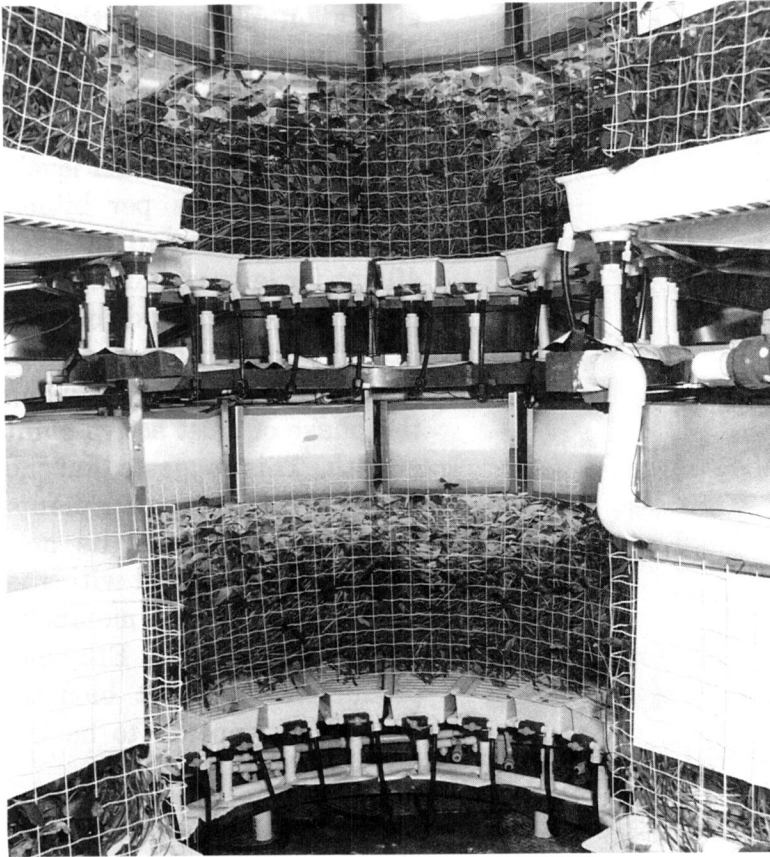
Throughout all these trials, plant carbon dioxide uptake (photosynthesis), dark period carbon dioxide release (respiration), and water vapor release (transpiration) were monitored. Short-term tests showed that photosynthesis was strongly influenced by the amount of photosynthetically active radiation provided to the crop stand and by the concentration of carbon dioxide in the chamber atmosphere. Stand transpiration, on the other hand, was strongly influenced by the leaf-to-air water vapor pressure deficit (VPD), where increasing the VPD increased transpiration.

In addition to carbon dioxide exchange and water vapor release, plants can produce and release hydrocarbons to the atmosphere. One of these hydrocarbons, ethylene, is known to have profound

effects on plant growth and development. Ethylene levels in the chamber were monitored throughout the life cycle of the crops. Maximum levels reached 70 parts per billion (ppb) for soybean and just over 40 ppb for lettuce and potatoes (from a background of less than 5 ppb). In all cases, the peak levels occurred during the phase of most active plant growth. This suggests that the ethylene comes from the plants themselves and that its production is correlated with the amount of plant metabolic activity and growth. Ethylene production per unit biomass for lettuce appears to be the



Lettuce Growing in the Biomass Production Chamber



*Soybeans Growing in the Biomass
Production Chamber*

highest for any of the crops tested so far.

Contact:

J. C. Sager, 853-5142, MD-RES-L

Participating Organization:

The Bionetics Corporation (C. L. Mackowiak)

NASA Headquarters Sponsor:

Office of Space Sciences and Applications

Biomass Production Research

Environmental tests with various candidate crops for the Controlled Ecological Life Support System (CELSS) using plant growth chambers continued during 1991, focusing on potato (*Solanum tuberosum*) growth and yield with different carbon dioxide concentrations and spectral

irradiance from different lamps. As with previous tests of soybean, raising the carbon dioxide from 500 parts per million (ppm) (350 ppm is the ambient concentration) to 1,000 ppm increased yields, while raising the carbon dioxide beyond 1,000 ppm added no benefit. In contrast to some reports, carbon dioxide concentrations of 5,000 and 10,000 ppm were not toxic or injurious to the plants. This suggests that plants will tolerate the high carbon dioxide concentrations commonly encountered in tightly closed habitats with humans (e.g., Space Shuttle, Space Station, etc.) without any substantial decrease in productivity.

In addition to whole-plant production data, rates of leaf gas exchange potential (stomatal conductance) and water vapor release (transpiration) were tracked throughout the growth and development of the potatoes (see the figure "Potatoes Produced Hydroponically for the CELSS"). Similar to previous reports, raising the carbon dioxide from near-ambient levels to 1,000 ppm caused leaf stomata (pores) to partially close, which in turn reduced water loss through transpiration. However, raising the carbon dioxide from 1,000 to 5,000 or 10,000 ppm caused an opposite effect and increased stomatal conductance and transpiration. These findings contrast with long-established beliefs that high carbon dioxide generally causes stomatal closure. Such data may be particularly pertinent to controlling water production rates by crops in bioregenerative life support systems for space.

Similar to previous tests with soybean, potato stems elongate more under high-pressure sodium (HPS) lamps than under metal halide (MH) lamps. This most likely is caused by the lack of sufficient blue light in the HPS spectrum, but further testing is required. In addition, a naturally occurring physiological injury to potato leaves, called oedema or intumescence, is more prevalent under HPS lighting. The injury



Potatoes Produced Hydroponically for the CELSS

develops as small swellings or callus-like tissue on the leaf surface and generally does not adversely affect growth and yield. Our tests suggest that the increased oedema under HPS lamps at low irradiance may be severe enough to affect plant growth. The injury can be prevented by providing the plants with low levels of blue/ultraviolet radiation, which is lacking in the HPS spectrum.

Contact:

R. M. Wheeler, 853-5142, MD-RES-L

Participating Organization:

The Bionetics Corporation (C. L. Mackowiak)

NASA Headquarters Sponsor:

Office of Space Sciences and Applications

Remote Sensing and Geographic Information Systems

The Remote Sensing and Geographic Information System (GIS) Laboratory now has upgraded computer support with the acquisition of two

SUN SPARC 2 workstations. Earth Resources Data Acquisition System, Inc. (ERDAS) image processing, GIS software, and Environmental Systems Research Institute (ESRI) ARC/INFO GIS software are supported on each platform. The two workstations are networked with three personal computers via a network file server and a graphics emulator. This allows for the movement of files from one platform to another and the mounting of entire file systems across the network. Image data files can be exported to either a Calcomp 1044 GT pen plotter or a Tektronix 4696 ink jet printer.

The laboratory is presently working closely with KSC Master

Planning in data sharing and data conversion. Currently ARC/INFO data files can be converted to DXF files that can in turn be read by the Master Planning Intergraphy system. In addition, Master Planning files can be converted to DXF files, which are then converted to ARC/INFO coverages. This mutual sharing of existing data will allow for significant savings in manhours and will eliminate the costly duplication of existing data.

Contact:

W. M. Knott, Ph.D., 853-5142, MD-RES-L

Participating Organization:

The Bionetics Corporation (M. Provanča)

NASA Headquarters Sponsor:

Office of Space Flight

EPCOT Project

The six hydroponic plant growth display racks at Disney's EPCOT Center have operated continuously since 1987. Visitors to The Land pavilion



Hydroponic Plant Growth System at The Land Pavilion at EPCOT

are introduced to the plant growth methods currently being studied at NASA/KSC as part of the Controlled Ecological Life Support System (CELSS) Breadboard Project. The system was enhanced during 1989 with a state-of-the-art computer control system that controls pH, flow, and temperature of the nutrient solution. This control system was the first prototype of a user-friendly, menu-driven system and was incorporated into the CELSS Breadboard Project as soon as it was verified as operationally ready. The interaction with EPCOT has allowed NASA to evaluate this control system under operational conditions using researchers who are unfamiliar with the system to test it, identify problems, and generate growth data on selected crops. Research on plant pathogens in hydroponic systems was continued during the past year by research-

ers at EPCOT. Interaction between these researchers and the NASA staff will transfer some of this expertise to the CELSS Breadboard Project.

Contact:

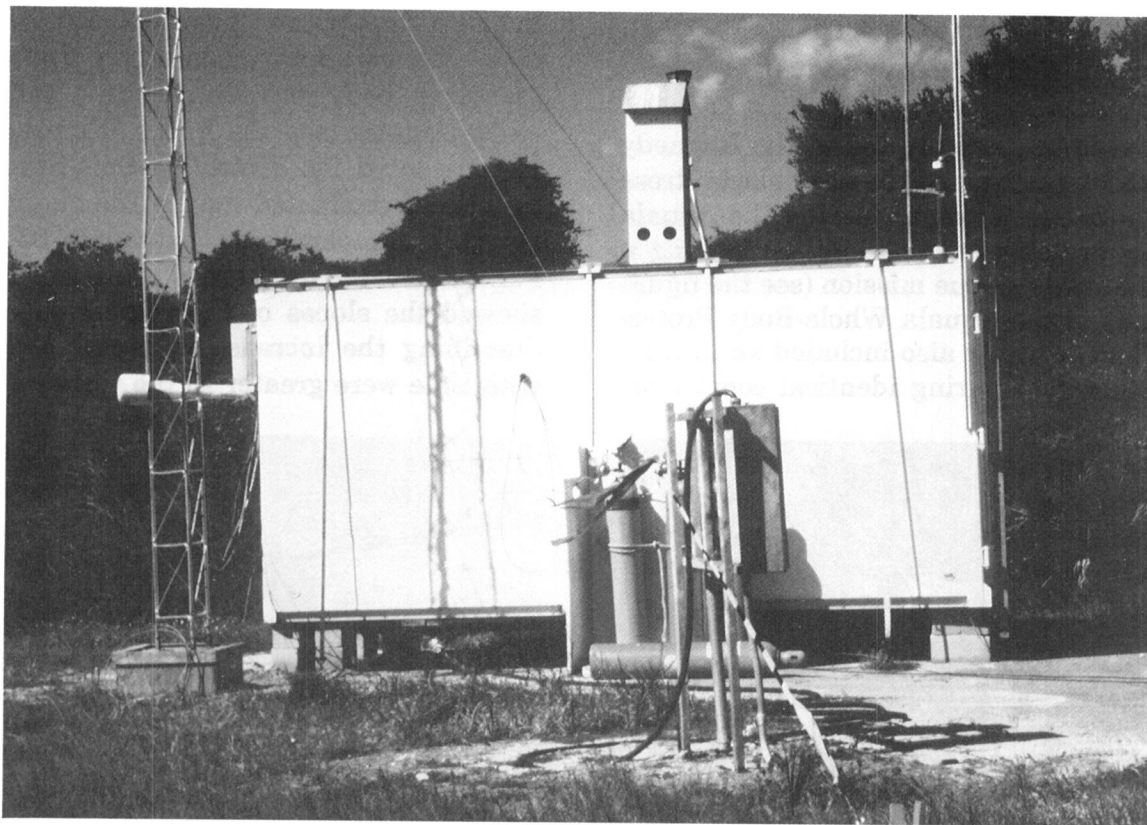
D. W. Chamberland, 853-5142, MD-RES-L

Participating Organization:

The Bionetics Corporation (J. O. Bledsoe)

Air Quality Monitoring

Long-term ambient monitoring of the Environmental Protection Agency (EPA) and the Florida Department of Environmental Regulation (DER) priority pollutants (ozone, sulfur



Permanent Air Monitoring Station

dioxide, carbon monoxide, nitrogen oxides, and particulates), as well as local meteorological conditions, continued at the permanent air monitoring station (PAMS). A new trailer was installed on the site with new microprocessor-controlled instrumentation that will help eliminate older instrumentation problems such as zero and span drift. Instrumentation used for sampling employs different analytical techniques including the following: ozone (ultraviolet absorption), sulfur dioxide (pulsed ultraviolet fluorescence), carbon monoxide (gas filter correlation infrared absorption), and nitrogen oxides (gas chemiluminescence). The data is collected once per minute by a Hewlett Packard (HP) data logger tied via a modem to an HP-9000 mainframe computer. The data is validated using the EPA and DER Quality Assurance guidelines. The historic trend of increasing ozone levels continued during 1990 but has declined during 1991. The three-year theoretical number of expected exceedances stays at 2.0. There were

no other exceedances of Federal or State air quality standards during the year.

A second trailer is being established to begin work on the global climate change/greenhouse gas effects of enhanced (twice ambient) carbon dioxide on native scrub vegetation using open-top chambers. Data on carbon dioxide and other parameters will be collected and sent to the same HP-9000 mainframe as used by PAMS. In addition, some isoprene and other light hydrocarbons will be sampled in these chambers using a portable gas chromatograph.

Contact:

W. M. Knott, Ph.D., 853-5142, MD-RES-L

Participating Organization:

The Bionetics Corporation (J. H. Drese)

NASA Headquarters Sponsor:

Office of Space Flight

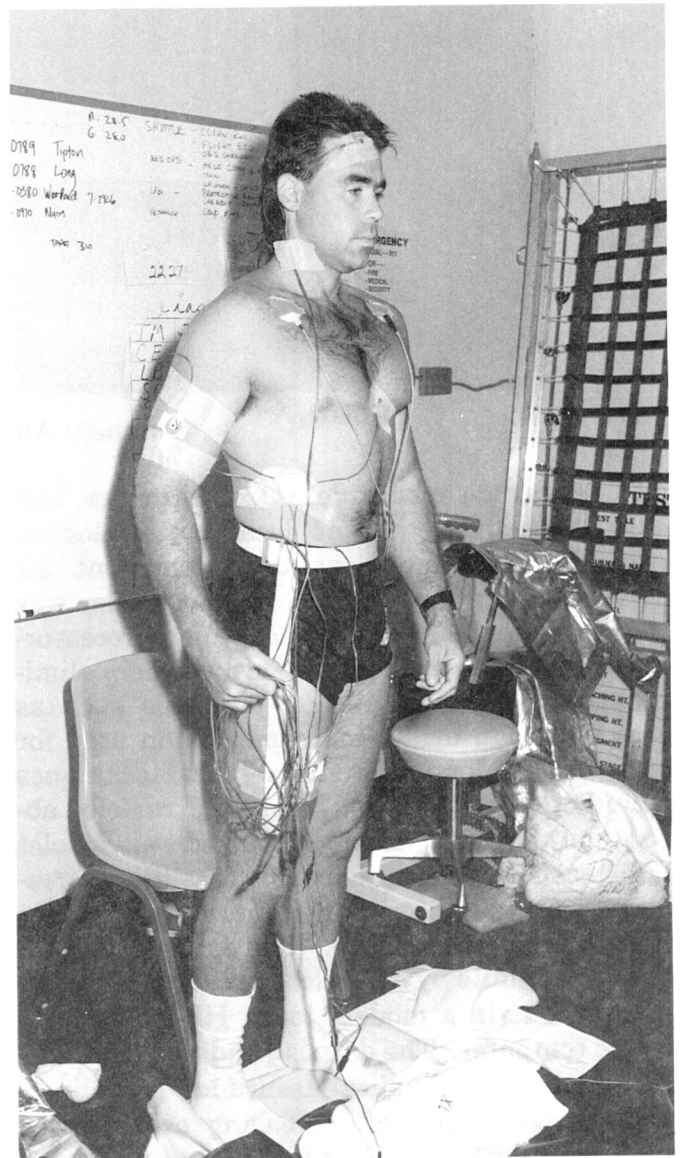
Heat Stress Evaluation of Rescuemen's Protective Suit

A field study was conducted at the Kennedy Space Center to determine the physiologic stress imposed on fire-rescuemen wearing the Aquala whole-body protective suit while performing a simulated Shuttle rescue mission (see the figure "Field Study of the Aquala Whole-Body Protective Suit"). The study also included an evaluation of a cool vest during identical conditions.



Field Study of the Aquala Whole-Body Protective Suit

Subjects for this study were the actual rescue crew who were instrumented for five skin temperatures, body core temperature, and an electrocardiogram (see the figure "Fire-Rescueman Instrumented for Protective Suit Study"). All tests were conducted during the summer when ambient temperatures exceeded 85 degrees Fahrenheit (29.4 degrees Celsius). Results showed the slopes of the regression equations describing the increase in rectal temperature with time were greater in the tests without the



Fire-Rescueman Instrumented for Protective Suit Study

vest and, furthermore, could be used to predict the time that a locally selected maximum core limit temperature would be reached. Skin temperatures, average heart rates, and sweat rates were all significantly less for the tests conducted with the vest. In summary, the candidate cooling countermeasure manufactured by the Steele Company provided some relief from thermal stress despite the addition of 7.5 pounds (3.4 kilograms) of additional weight to the ensemble and some loss of mobility.

Contact:

D. F. Doerr, 867-3152, MD-ENG-A

Participating Organizations:

*NASA Biomedical Engineering Office, MD-ENG-A
(H. E. Reed, G. R. Triandafilis, A. B. Maples,
M. R. Duvoisin, and B. C. Slack)*

*The Bionetics Corporation (K. J. Myers, M.D.;
D. Woodard, M.D.; M. L. Lasley, RN; and
J. L. Polet, RN)*

NASA Headquarters Sponsor:

Office of Space Flight

Biomass Processing Research

The scaleup and integration of the cellulose conversion process into the Controlled Ecological Life Support System (CELSS) Breadboard Project has progressed. These processes had been selected to provide maximal conversion of Biomass Production Chamber (BPC) crop residues into either edible products or recycled crop nutrients. Efforts have continued to provide research bioreactor hardware and control systems for the breadboard-scale operation.

Installation, testing, and operation of the breadboard-scale "leachate" reactor have been completed. This reactor functions to extract water-soluble organic and inorganic compounds from BPC crop residues in preparation for subsequent processes. The leached inorganics will be returned to the crop hydroponic solutions in the BPC to recycle mineral nutrients. The

fate of the soluble organic compounds has not been decided, but alternatives include: (1) mineralization to carbon dioxide by either crop root-inhabiting microbes or aerobic and anaerobic digestion reactors or (2) use for production of microbial biomass (such as vegetative mycelia of the edible oyster mushroom, *Pleurotus ostreatus*, or a mixture of microorganisms suitable for feeding to fish).

Research on utilization of inedible crop residues continued with the primary emphasis on enzymatic conversion of residue cellulose into glucose. The focus this year was on the scaleup of bioreactors to handle the crop residue output from the BPC. Several successful BPC-scale runs (using a 10-liter fermentor) of cellulase enzyme production by *Trichoderma reesei* and supplemental beta-glucosidase enzyme production by *Aspergillus phoenicis* were completed. Both enzymes were produced from leached BPC wheat residues and took about 10 days. At harvest of the runs, enzyme levels and activities were equal to those obtained in previous laboratory studies, which were done on a much smaller scale. The fermentor enzyme products were successfully used in breadboard-scale cellulose conversion bioreactor studies to produce glucose from leached BPC wheat residue.

As with other processes, a breadboard-scale bioreactor was designed for enzymatic hydrolysis of crop residue cellulose. This year saw procurement, installation, testing, and preliminary operational tests of a 19-liter stirred tank reactor with a 50-degree-Celsius temperature control. This reactor was run twice to test the ability of cellulase and beta-glucosidase enzymes, produced in 10-liter breadboard-scale fermentor runs, to convert leached BPC wheat residue cellulose into glucose. Maximal glucose levels of 6 grams per liter were obtained after only 48 to 72 hours of reactor operation. Although only amounting to 25 percent theoretical conversion of residue cellulose, these glucose levels were equal to concentrations obtained previously in laboratory scale studies of enzyme hydrolysis of similar BPC residues. A doubling of this conver-

sion efficiency can be expected when the residues are pretreated with a strong base to remove the lignin and hemicellulose residue components, which prevent the remaining cellulose from being enzymatically hydrolyzed to glucose. However, a source of this strong base has yet to be identified in an operational CELSS.

During the next year, the focus of biomass processing will be on the completion of a five-replicate study of integrated enzyme production and enzymatic hydrolysis of leached BPC wheat residues in order to conclude this portion of our breadboard-scale analyses of these processes.

At the conclusion of this study, the focus will shift to resource recovery through aerobic and anaerobic microbial digestion of crop residues. Other resource recovery research to be initiated this next year is the production of microbial biomass suitable for fish diets and the integration of mineral recovery from leachates and from crop residue combustion with crop production (replenishment of hydroponic nutrients).

Contact:

W. M. Knott, Ph.D., 853-5142, MD-RES-L

Participating Organization:

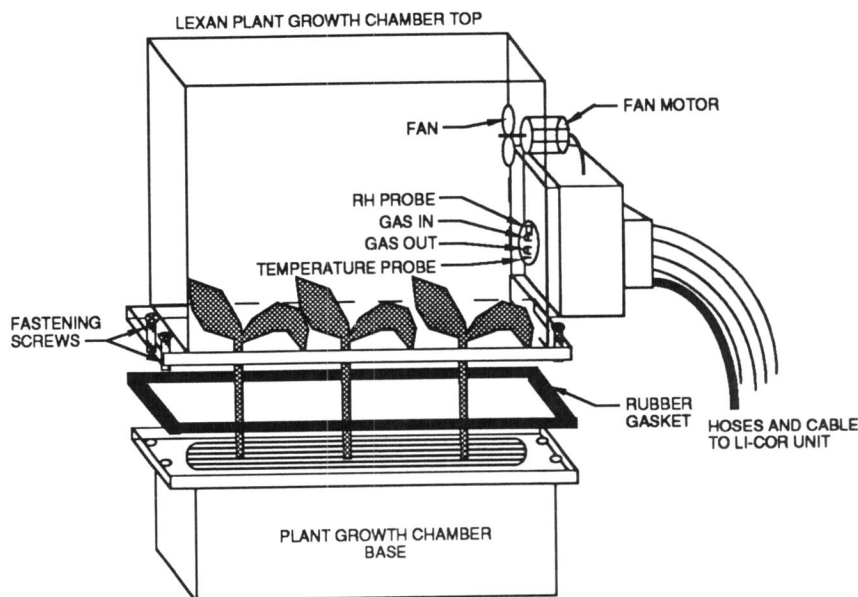
The Bionetics Corporation (D. Strayer, Ph.D.)

NASA Headquarters Sponsor:

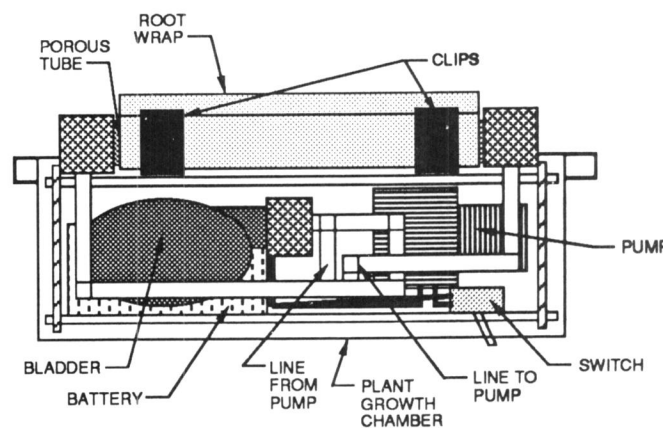
Office of Space Sciences and Applications

Porous Tube Plant Nutrient Delivery System

The Porous Tube Plant Nutrient Delivery System (PTPNDS) (formerly the Tubular Membrane System) is a plant nutrient delivery system being developed for growing plants in



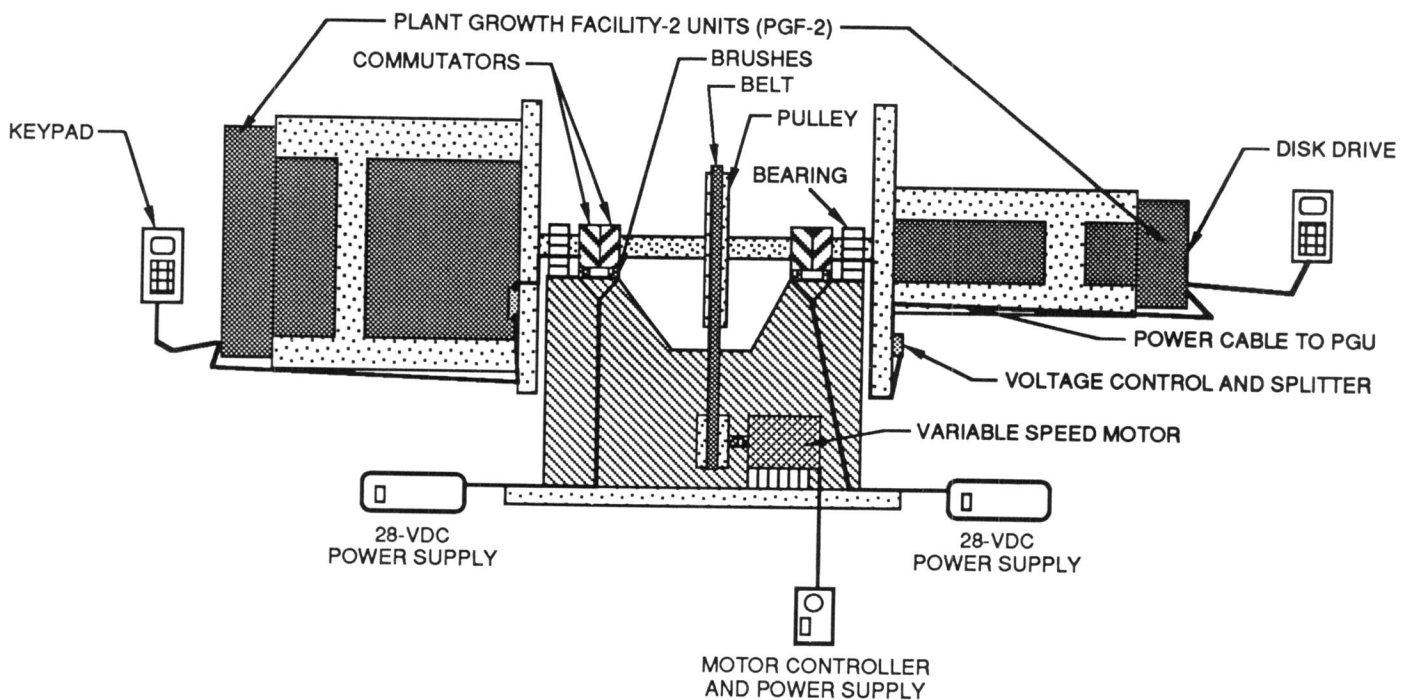
Plant Growth Chamber Cover for Gas Exchange Measurements



Porous Tube Plant Nutrient Delivery System for the Plant Growth Chamber

microgravity. Research has continued with the successful growth of several crops of radishes. Radishes have been grown both with a conventional hydroponic plant nutrient solution and with an aqueous solution of inedible plant material ash (from combustion) made slightly acidic (pH equals 6.0) with nitric acid.

Miniaturization of the PTPNDS has continued with the construction of prototypes that could be completely contained in the small Plant Growth



*Clinostat for Rotating the Space Shuttle Middeck Locker
Plant Growth Facility-2*

Chambers that fit in the middeck locker Plant Growth Unit. These prototypes have been used to grow cucumber plants in both vertically and horizontally rotating conditions. This was done to determine the effects of altering gravity on the system operation and on plant growth.

Contact:

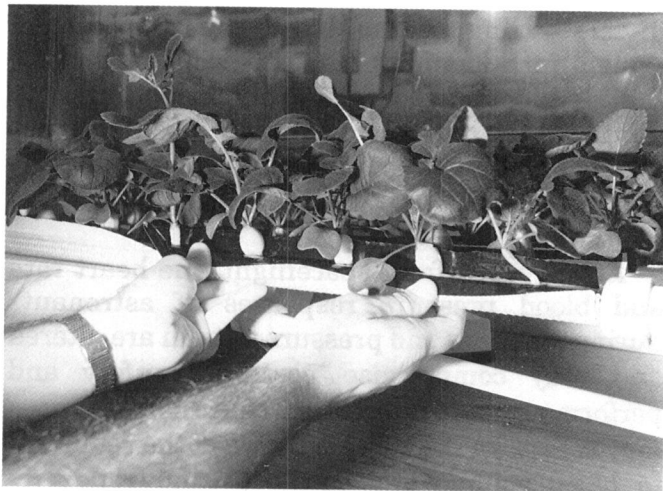
W. M. Knott, Ph.D., 853-5142, MD-RES-L

Participating Organization:

The Bionetics Corporation (T. W. Dreschel)

NASA Headquarters Sponsor:

Office of Space Sciences and Applications



*Radishes Growing on the Porous Tube Plant
Nutrient Delivery System*

Aquaculture Research

The development of aquaculture as an integral part of the Controlled Ecological Life Support System (CELSS) biomass production and resource recovery efforts was continued. Initial collection of critical mass flow data through the computer-controlled, atmospherically closed aquaculture system was completed. Respiration values for the total system, fish, and associated microbial community have been calculated. System instabilities have been identified and corrective modifications are ongoing. Continued collection and monitoring will allow for complete

in astronauts, Kennedy Space Center (KSC) investigators measured cardiovascular reflexes before and after blood volume was decreased (by diuretics) and increased (by drinking fluids). Changes in reflex responses similar to those reported in astronauts were observed. Further analysis of the data from these experiments will provide important information regarding which reflex adaptations can be reversed by employing fluid replacement techniques similar to those currently used and which adaptations require other types of countermeasure treatments such as exercise.

KSC physiologists have reported long-term absence of exposure to routine 1-G upright posture (i.e., spaceflight, bedrest, or wheelchair

confinement) attenuated the response of the carotid-cardiac baroreflex, and this dysfunction was associated with orthostatic hypotension. They also reported that the baroreflex response could be enhanced following an acute bout of intense exercise. Based on these previous findings, a collaborative study was undertaken with the Spinal Injury Center at Humana Hospital-Lucerne in Orlando, Florida, in an attempt to determine if a single bout of maximal exercise performed by paraplegics could eliminate orthostatic hypotension. Ten paraplegics, who had been confined to a wheelchair for at least three years, were asked to perform an acute bout of exercise with their arms until they reached volitional exhaustion (see the figure "Paraplegic Subject Performing Exercise").

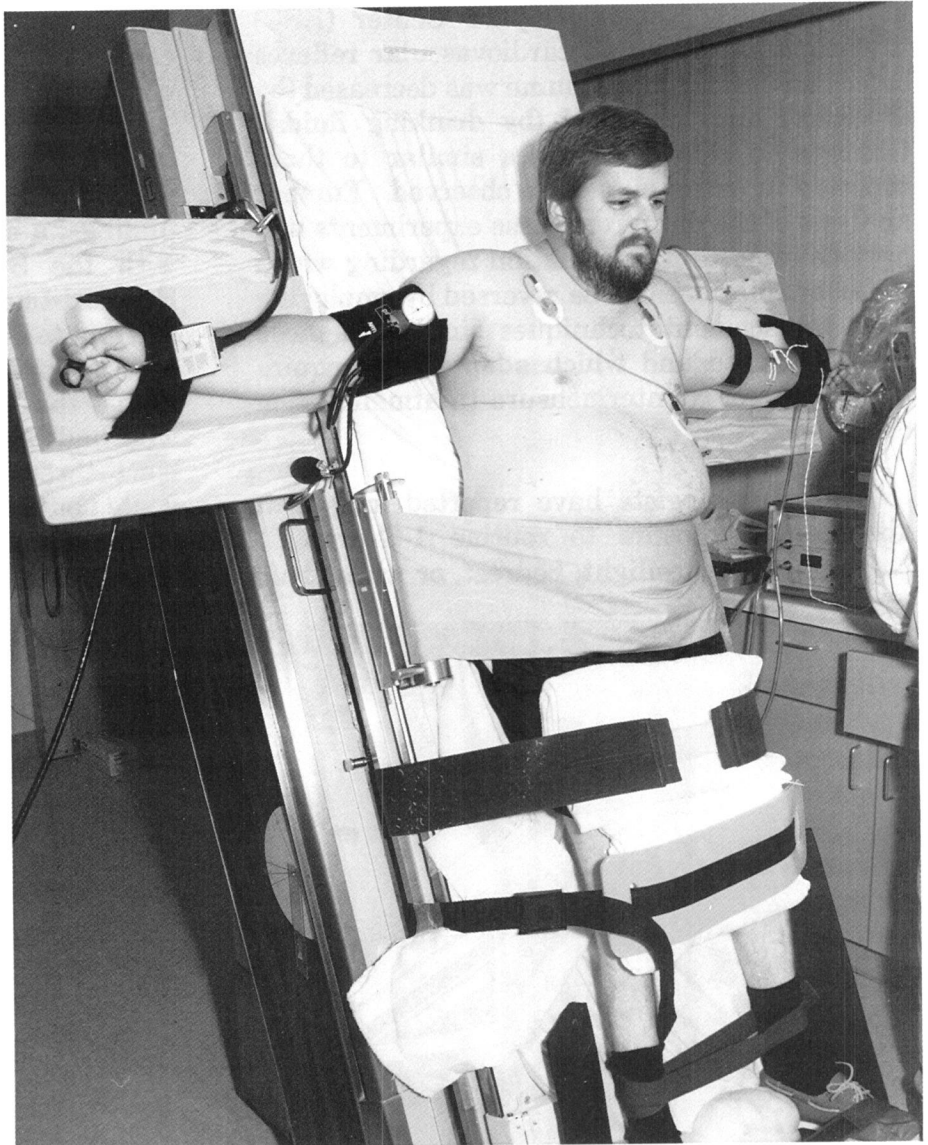


Paraplegic Subject Performing Exercise

Twenty-four hours after the exercise, reflex responses associated with increasing heart rate and vasoconstriction were measured and the volunteers underwent an upright posture test on a tilt table (see the figure "Paraplegic Subject During Tilt Table Test") to determine their orthostatic hypotension response. Exercise increased baroreflex responses and eliminated orthostatic hypotension compared to a control test with no exercise. Besides their clinical implications, these results may provide an important basis for the use of acute intense exercise within 24 hours prior to reentry as a possible countermeasure against the development of postflight orthostatic hypotension in astronauts.

In addition to the ground-based research program, KSC investigators have been involved in collaborative activities with scientists at the Johnson Space Center to support the measurement of baroreflex responses in astronauts following the landings of STS-39 and STS-43 at KSC. These flight experiments are critical to the development of a data base that will provide descriptive information about physiological adaptation to spaceflight and allow for the verification of ground-based models.

Additional bedrest and exercise studies will be conducted during the next year. The results from present and future experiments should provide critical information about the human cardiovascular adaptations to long-term spaceflight and needed development of countermea-



Paraplegic Subject During Tilt Table Test

asures against adverse effects.

Contacts:

*V. A. Convertino, Ph.D., 867-4237, MD-RES-P
D. F. Doerr, 867-3152, MD-ENG*

Participating Organizations:

*Humana Hospital-Lucerne (J. D. Shea, M.D.)
University of Florida (K. A. Engelke)*

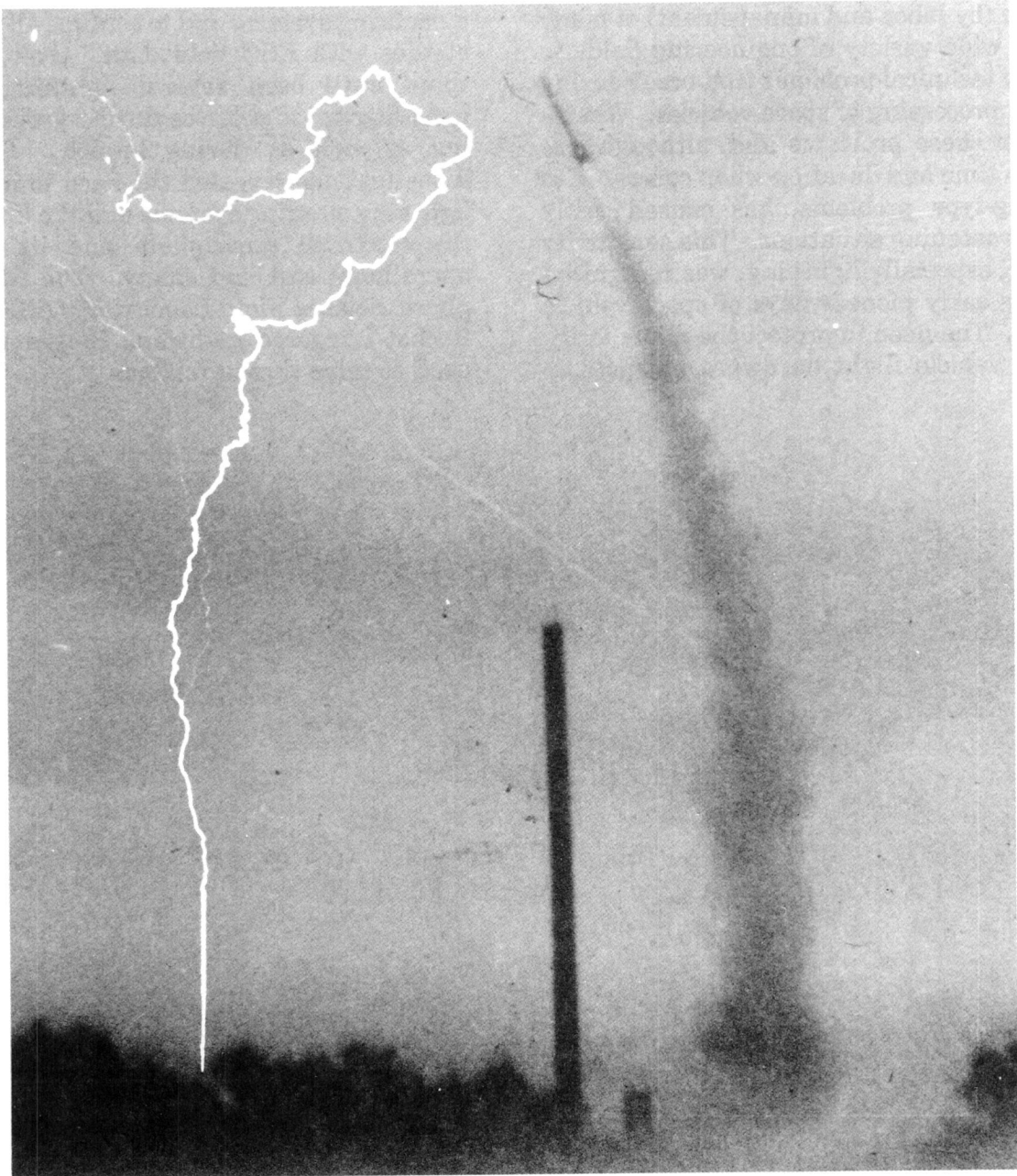
NASA Headquarters Sponsor:

Office of Space Sciences and Applications

Meteorology

Kennedy Space Center (KSC) and the USAF 45th Space Wing (formerly the Eastern Space and Missile Center) cover an area of 40 by 25 kilometers and are frequently called America's Spaceport. This title is earned through the integration (by labor and management) of many skills in a wide variety of engineering fields to solve many technical problems that occur during the launch processing of space vehicles. Weather is one of these problems and, although less frequent in time and duration when compared to engineering-type problems, has caused costly and life-threatening situations. This sensitivity to weather, especially lightning, was recognized in the very early pioneer days of space vehicle operations. The need to protect the many facilities, space vehicle flight hardware, and person-

nel from electrified clouds capable of producing lightning was a critical element in improving launch operations. A KSC-wide lightning committee was formed. The committee was directed to improve lightning protection, detection, and measuring systems and to confirm all theoretical studies with KSC field data. Over the years, there have been several lightning incidents involving space vehicles during ground processing as well as during launch. Subsequent investigations revealed the need to improve the lightning warning systems and the knowledge of the electrical atmosphere and its effects on operational cost and safety. The KSC Atmospheric Science Field Laboratory (ASFL) and the Rocket-Triggered Lightning Program are being used to solve these problems.

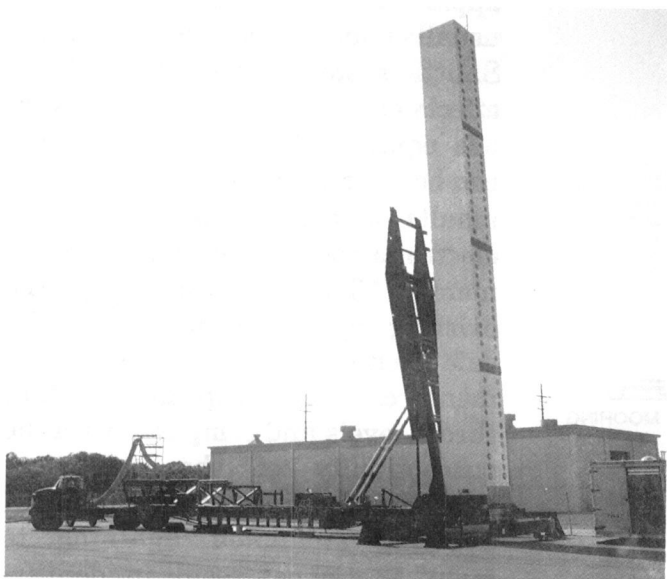


Rocket-Triggered Lightning

Research Studies Using Simulated Lightning

The lightning simulator, using two 6-million-volt Marx generators, was recently acquired by the Kennedy Space Center on loan from Wright-Patterson Air Force Base for use in lightning simulation studies and is now operational (see the figure "Six-Million-Volt Lightning Simulator"). These studies are performed jointly by the 45th Space Wing (formerly the Eastern Space and Missile Center) and KSC. The lightning simulator is 9 feet wide, 84 feet long, and 19 feet high in the horizontal retracted position. In operation, it is raised to a vertical position and is about 65 feet tall. The simulator weighs approximately 110,000 pounds. Plans for the addition of hydraulic stabilizing outriggers to the simulator's trailer will allow for increased mobility to testing sights. To reduce series inductance, the simulator uses two 6-million-volt generators operating in parallel to give a short-circuit current of 60,000 amperes at 6 million volts. The total energy produced is about 150,000 joules.

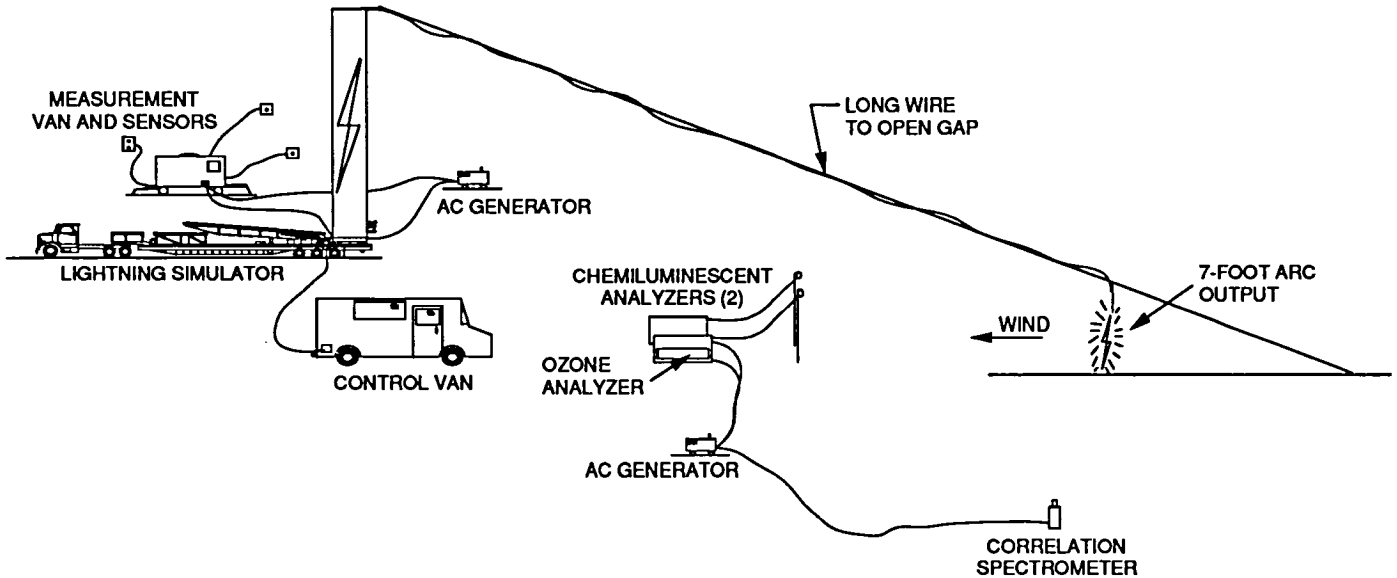
The lightning simulator was utilized in support of testing by Argonne National Labora-



Six-Million-Volt Lightning Simulator

tories, Chicago, Illinois. Argonne National Laboratories, interested in the chemical products formed in the air during triggered lightning discharges (specifically the nitrogen oxides), was aided by the lightning simulator's production of 7-foot arcs of simulated lightning. Quantifying the nitrogen dioxide (NO_2) production following the simulated lightning's chemical reaction with air was achieved by a correlation spectrometer sighting downwind of the arc. Furthermore, direct measurements of ozone, nitric oxide (NO), and NO_2 present were made by an ozone analyzer and two chemiluminescent analyzers. When placed downwind of the arc, these instruments are capable of capturing the ozone and NO_x plumes formed from the discharge (see the figure "System Configuration for Argonne National Laboratories"). Because of the ability to reproduce simulated lightning discharges with repeated similar waveforms, the lightning simulator was ideal for conducting controlled lightning tests. Combined with its ability to reproduce simulated lightning discharges in one location at a greater rate than the occurrence of triggered lightning, Argonne was able to reduce the level of uncertainty in their calculated creation of nitrogen products by lightning. Through the acquired data, Argonne hopes to understand global production rates of nitrogen oxides by lightning and their effects on global climate changes.

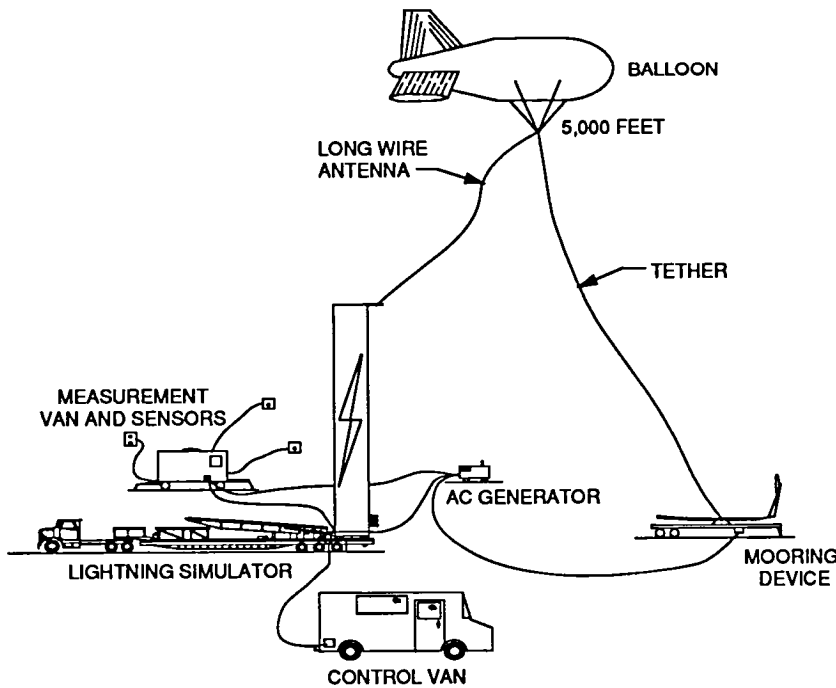
Further applications for the lightning simulator include producing high voltages and currents in a balloon-supported antenna [see the figure "System Configuration for Generating Electromagnetic Fields (Balloon)"] that radiates electromagnetic fields with essential characteristics similar to those of lightning. The output of the lightning simulator in this configuration results in the formation of a decaying rectangular current waveform with a high rate of rise of current over 60,000 amperes per microsecond, with a 6,000-ampere peak, and a period of about 20 microseconds for a balloon height of 5,000 feet. A helicopter may be used to suspend the output antenna to about 10,000 feet [see the figure "System Configuration for Generating



System Configuration for Argonne National Laboratories

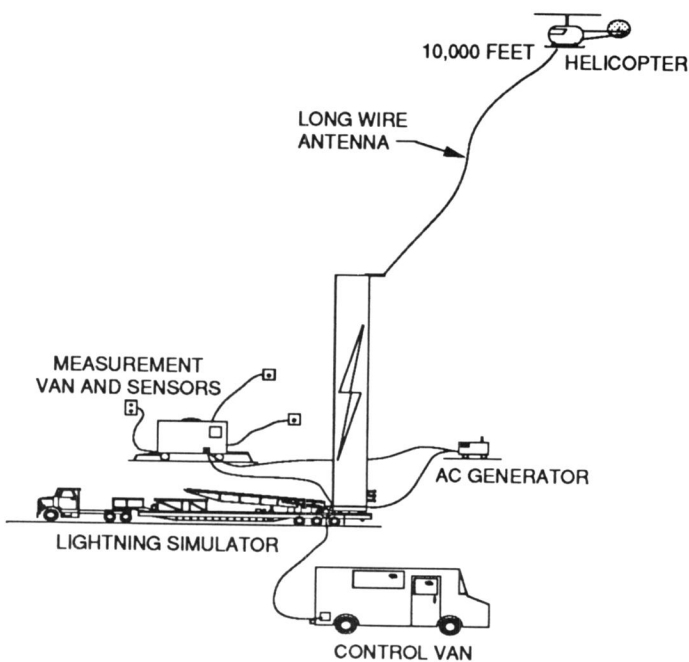
Electromagnetic Fields (Helicopter)"]. The electromagnetic radiation will be produced at known locations in order to help calibrate lightning location systems.

Additionally, using the lightning simulator to



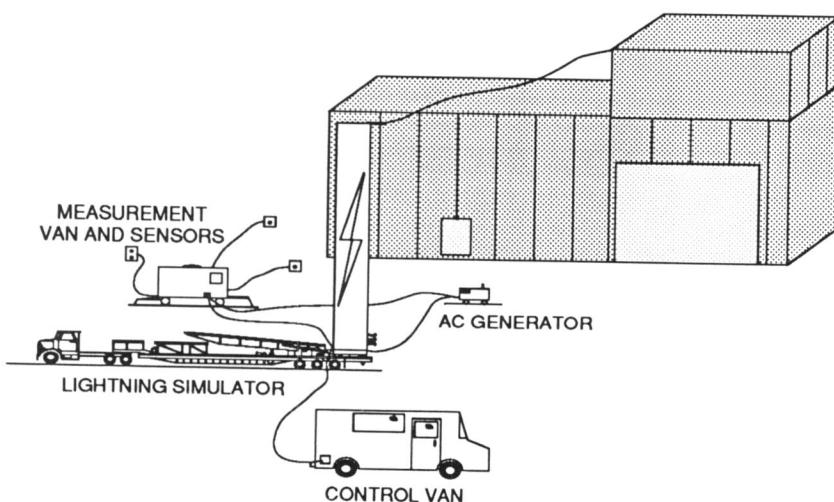
System Configuration for Generating Electromagnetic Fields (Balloon)

inject known currents at typical lightning attach points on a building determines the vulnerability of the facility to lightning (see the figure "System Configuration for Facility Lightning Protection Tests"). It is planned to install improved protection on selected buildings in stages to determine the effectiveness of these measures in providing a safe environment for both equipment and personnel. This knowledge can be applied to other facilities (facilities usually housing operations critical to Shuttle systems) where the induced effects of lightning could cause serious equipment damage. Currents can be injected at low levels with the results monitored using sensitive electromagnetic measuring instruments. This monitoring keeps the existing equipment in the facility safe from damage. These measurements can be extrapolated to full-threat levels and compared with the susceptibility of the equipment housed in those facilities. Similarly, applying simulated lightning to guard shacks can result in identifying and correcting personnel haz-



System Configuration for Generating Electromagnetic Fields (Helicopter)

ards. These evaluations would then lead directly to modifications to correct the problems identified, resulting in the elimination of equipment damage and hazards to personnel and the possible relaxation of work restrictions during lightning warning periods.



System Configuration for Facility Lightning Protection Tests

Contact:

W. Jafferis, 867-3404, DL-ESS-22

Participating Organization:

Boeing Aerospace Operations, Engineering Support Contract (J.R. Stahmann and A. J. Eckhoff)

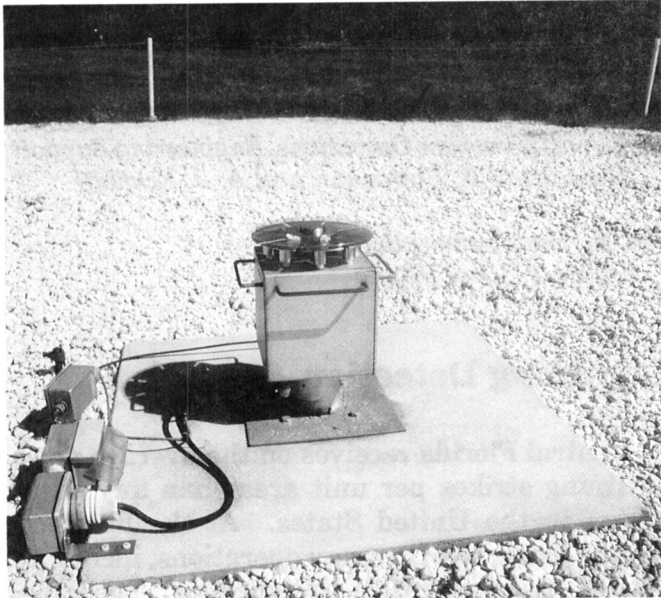
NASA Headquarters Sponsor:

Office of Space Flight

Lightning Detection Algorithm

Central Florida receives on the average more lightning strikes per unit area than any other region in the United States. At the Kennedy Space Center (KSC), many operations, including launch, are susceptible to lightning. The Electric Field Mill Network is one of the tools used for both forecasting and detecting lightning occurrence. The Electric Field Mill Network consists of 31 sensors (see the figure "Electric Field Mill Located on KSC"), separated by 2 to 4 kilometers, over both the KSC and Cape Canaveral Air Force Station areas.

This report focuses on using the electric field sensors as lightning detectors. This technique may also be used with a different time scale to simplify the identification of stormy versus fair weather. The electric field due to cloud electrification is slowly varying; but, the effect of a lightning flash on the electric field is abrupt. Lightning creates a discontinuity in the electric field. This discontinuity is on the average about 0.5 second and the magnitude of the discontinuity is related to the distance from the lightning, the type of lightning, and the magnitude of the lightning charge transfer. The electric field sensors detect all types of lightning occurring within the network. Lightning that occurs off the network is detected only if it is sufficiently large and close. Since noise can also cause abrupt discontinuities



Electric Field Mill Located on KSC

similar to lightning, the algorithm must test several criteria (described below) before lightning is confirmed.

The discontinuity is detected by advancing a four-sample window (0.3 second) and calculating the variance of those four points about a line. When the variance exceeds a threshold, about 1,000 volts squared per meters squared, the beginning of a discontinuity is identified. The end of the discontinuity is similarly identified by advancing a four-sample window until the variance drops below the threshold. If the interval for a given mill exceeds the allowable limits (about 2 seconds), that mill is eliminated from consideration. The discontinuity interval for each mill is then mapped to a time line. The first mill that detects the discontinuity is used to set the start time and the mill that detects the last sample of the discontinuity is used to set the stop time.

The electric field change is then calculated for each mill by taking the difference of the electric field before and after the discontinuity and compensating for the slowly varying portion of the electric field (i.e., the electric field due to other charge transfer mechanisms, such as

advection). If two or more mills detect a sufficiently large field change, the discontinuity is then identified as a flash.

The previous algorithm used to detect lightning was far more complex and not sensitive. The sensitivity of the new algorithm is limited by the accuracy of the instrument and the inherent noise in the electric field and the ability of the user to invalidate bad sensors.

Contact:

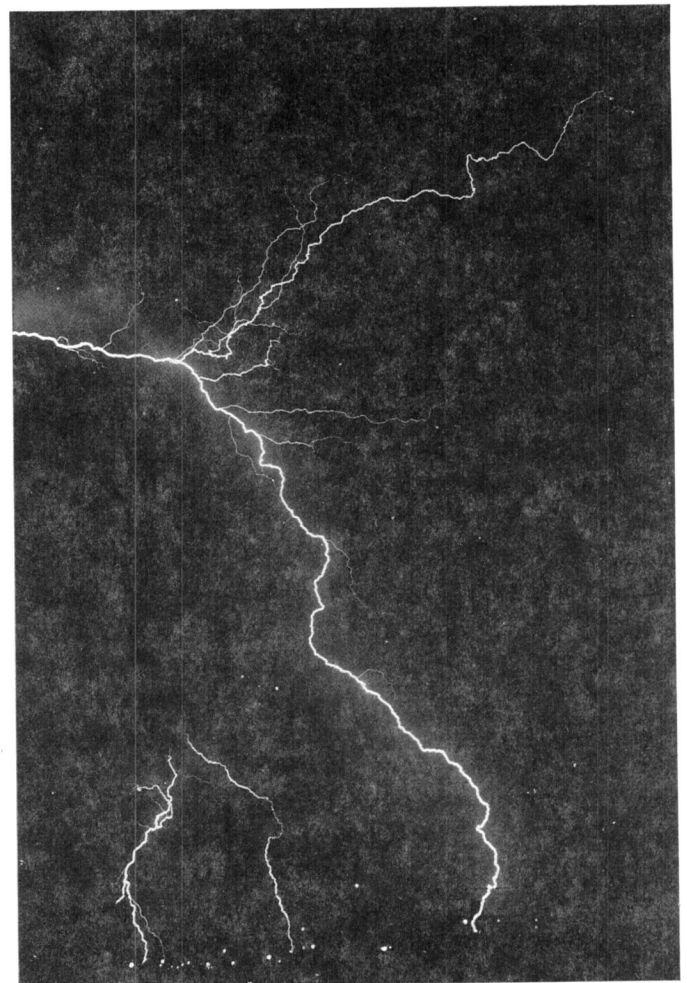
L. M. Maier, 867-4409, TE-CID-3

Participating Organization:

NYMA (S. J. Schaefer and P. M. Mulligan)

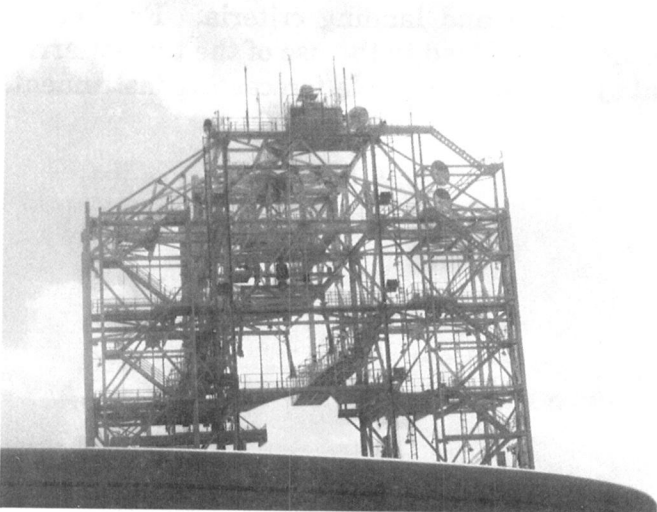
NASA Headquarters Sponsor:

Office of Space Flight



Time-of-Arrival Lightning Location System Using Five-Station Wideband Electric Field Measurements

A wideband electric-field-measuring network, which can locate the sources of lightning-generated electromagnetic radiation, has been developed and installed at Kennedy Space Center. Five stations, each consisting of electric-field receivers with a 3-decibel bandwidth of 600 hertz to 3.5 megahertz are used for the measurements. Four remote stations, separated from the central station by 8 to 11 kilometers, are connected to the central station by analog fiber optics or by a combination of microwave and fiber optics. After the electric-field pulses received at the four remote stations are transmitted to the central station (see the figure "Microwave Antenna Site at the Mate/Demate Device"), they, along with the central station data, are: (1) continuously recorded using frequency modulation (FM) channels on an analog magnetic tape with a 500-kilohertz bandwidth and (2) digitized at a 20 megasamples per second rate and subsequently stored on optical disks. The digitizing system is based on a five-channel LeCrox TR-8818 digitizer and is capable of storing up to 27 200-microsecond duration records per lightning flash.



Microwave Antenna Site at the Mate/Demate Device

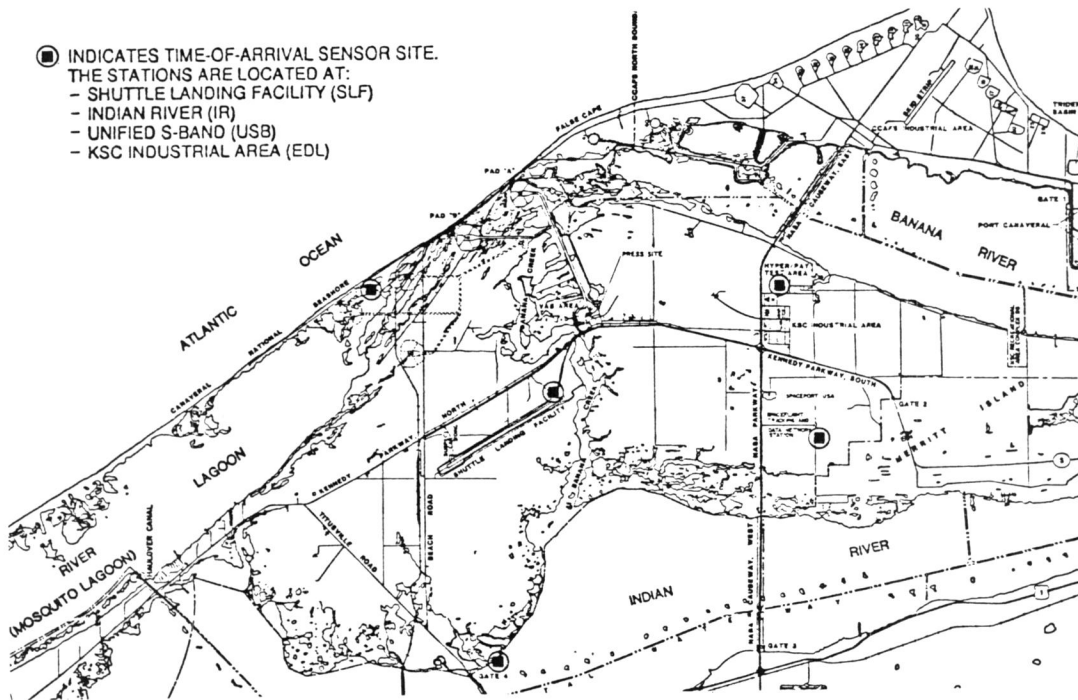
The locations of the five receiving stations are shown in the figure "Wideband Electric-Field-Measuring Network." A typical microwave antenna is shown in the figure "Microwave Antenna at UC9." Two different flat-plate antennas are used at each station, as shown in the figure "Receiving Flat-Plate Antennas."

The operation of the remote stations is fully controlled from the central station. Receivers and antennas can be changed to obtain different sensitivities, thus allowing the measuring of signals generated from thunderstorms located from exactly overhead and up to a distance of about 50 kilometers. Calibration and test timing signals are also remotely controlled.

Source locations of the electric-field pulses are determined by measuring the differences in the times of arrival of these pulses at the five different locations. Although four stations are usually sufficient to determine the location of a source using time-of-arrival techniques, five stations are used to provide redundant measurements and to allow for checking the accuracy of the locations. Three-dimensional locations are obtained for the sources of electric-field waveshapes generated by both intracloud and cloud-to-ground natural and triggered lightning. The accuracy of the locations within the network is within a few tens of meters.

The time-of-arrival system will be further tested using rocket-triggered lightning. Since the point of contact with the ground is known, a comparison with the locations provided by the time-of-arrival system will allow for a better assessment of its location accuracy. Additionally, currents measured at the base of the lightning channel generated by rocket-triggered lightning, in conjunction with wideband electric fields measured at the five stations, will be used to test the different return stroke models discussed in the scientific literature.

The system became operational in August 1991. As of this writing, over 35,000 electric-field pulses from intracloud and cloud-to-ground

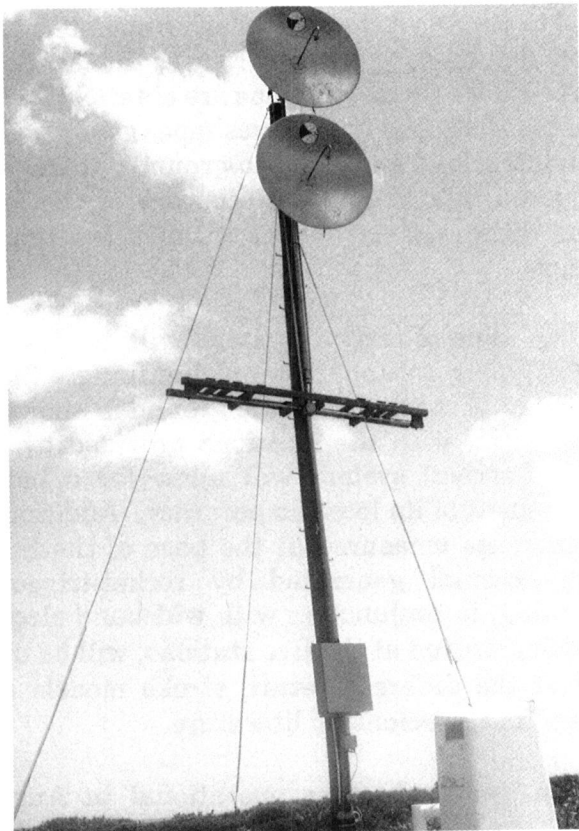


Wideband Electric-Field-Measuring Network

discharges have been collected, and operations are scheduled to continue throughout the year. The figure "Return Stroke Electric Fields Simultaneously Recorded at Five Stations" illustrates an example of electric fields generated by a return stroke and recorded at all five stations. The x-axis represents 204.8 microseconds full-scale. The top trace (SLF) shown in the graph was

inverted with respect to the bottom four traces during the data acquisition process. The correct polarity of the top trace is, therefore, the same as all other traces.

The wideband electric-field-based time-of-arrival system can be used to locate the regions of lightning activity and can be a useful operational tool for determining the compliance with the launch and landing criteria. Further research could lead to the use of the time-of-arrival system as a valuable forecasting instrument.



Microwave Antenna at UC9



Receiving Flat-Plate Antennas

The area of coverage of the system will be increased in 1992 with the addition of one, and maybe two, receiving stations. Simultaneously, the bandwidth of the receivers will be extended from 3.5 to 10 megahertz in order to increase the accuracy of the determination of the time of arrival of the electric-field signals at each station, and consequently the accuracy of the locations. A new computer system is currently being implemented and will allow real-time three-dimensional locations of the sources of the

electric field.

Contact:

W. Jafferis, 867-3404, DL-ESS-22

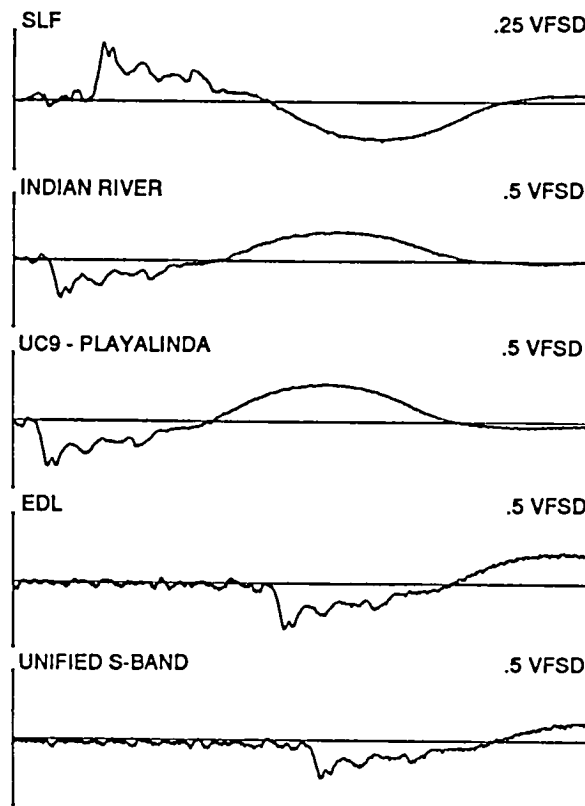
Participating Organization:

Boeing Aerospace Operations, Engineering Support Contract (P. J. Medelius)

NASA Headquarters Sponsor:

Office of Space Flight

FILE 26802111.p91 TIME 21:57:53.586854
 # POINTS: 4096 204.80 lsecs



NOTE:

FROM TOP TO BOTTOM: SLF, IR, UC9, EDL, AND USB.
 THE TOP TRACE (SLF) WAS INVERTED WITH
 RESPECT TO THE BOTTOM FOUR TRACES DURING
 THE DATA ACQUISITION PROCESS.

*Return Stroke Electric Fields
 Simultaneously Recorded at
 Five Stations*

Technology Utilization

Congress has charged NASA with the task of stimulating the widest possible use of technology resulting from the space program. Thousands of these applications, known as spinoffs, have been transferred to the public and private sectors of the U. S. economy. This transfer of technology includes spinoffs in medicine, electronics, computer systems, design, and management.

This section of the R&T report describes five

such developments of technology at Kennedy Space Center: (1) a thermal storage module, (2) an automated citrus assessment, (3) a heat pipe application for residential thermal energy storage, (4) magnetic resonance imaging, and (5) development of an oxygen concentrator. The technology from these projects has come from the space program and the application has been transferred to industry.

Automatic Tree Counting System

For the past nine years, aerial color infrared (ACIR) photographs of citrus groves (initially 10,000 acres) in Charlotte County, Florida, have been taken. These are used to identify citrus plantings and to determine the stage of growth and production when trees mature in order to assign property values to each parcel (see the figure "Aerial View of Citrus Groves"). Assess-

ments are made on the basis of tree stands, grove conditions, and productivity of the trees. A simple dual video analysis system sufficed for interpretation of the ACIR photographs and inventory of the citrus acreage. Citrus plantings have nearly doubled within the last six years, making it necessary to search for a faster system of interpretation. Otherwise, additional citrus appraisers will be needed to keep up with the future workload.



*Aerial View Citrus Groves
(scale: 1 inch equals 330 feet)*

A cooperative project between NASA Kennedy Space Center, a consortium of Florida Property Appraisers, and the Citrus Research Center at Lake Alfred was activated to use recent advances in image analysis to find a standalone system that would rapidly count objects (trees) digitized from a photograph. The system needs to be adapted to counting citrus trees in properties delineated on aerial photographs. The ACIR film has the advantage of identifying the stage of growth and health of each tree so that an estimate of production can be made. Analysis with the Automatic Tree Counting System (ATCS) will make it possible to eliminate visual interpretation by erecting a profile of each tree class (healthy, sick, missing, small, medium, full size, and damaged) by assigning spectral and intensity values to each class of tree. The computer program will read the cluster of values from each class and automatically identify each tree, tabulate the total number of tree classes, and store the data in an ASCII file. Field tree information will be acquired to determine the accuracy of the ATCS, to improve field verifications by the use in the grove of a laptop computer, and to accelerate verification time. Resulting ASCII files from ATCS can then be entered into the various spreadsheets used by the appraisers participating in the project to rapidly inventory the groves of each county.

Upon completion of the ATCS project, consideration will be made for the development of a county storage and retrieval method employing the NASA technology used to archive Shuttle maintenance photographs, whereby all digitized images are compressed and stored on laser disks, large capacity tape drives, or CD-ROM disks.

Contact:

D. L. Roberts, 867-4387, DL-ESS-41

Participating Organization:

University of Florida, Institute of Food and Agricultural Sciences (C. H. Blazquez)

NASA Headquarters Sponsor:

Office of Commercial Programs

Heat Pipes and Phase Change Materials for Residential Thermal Energy Storage

Objective

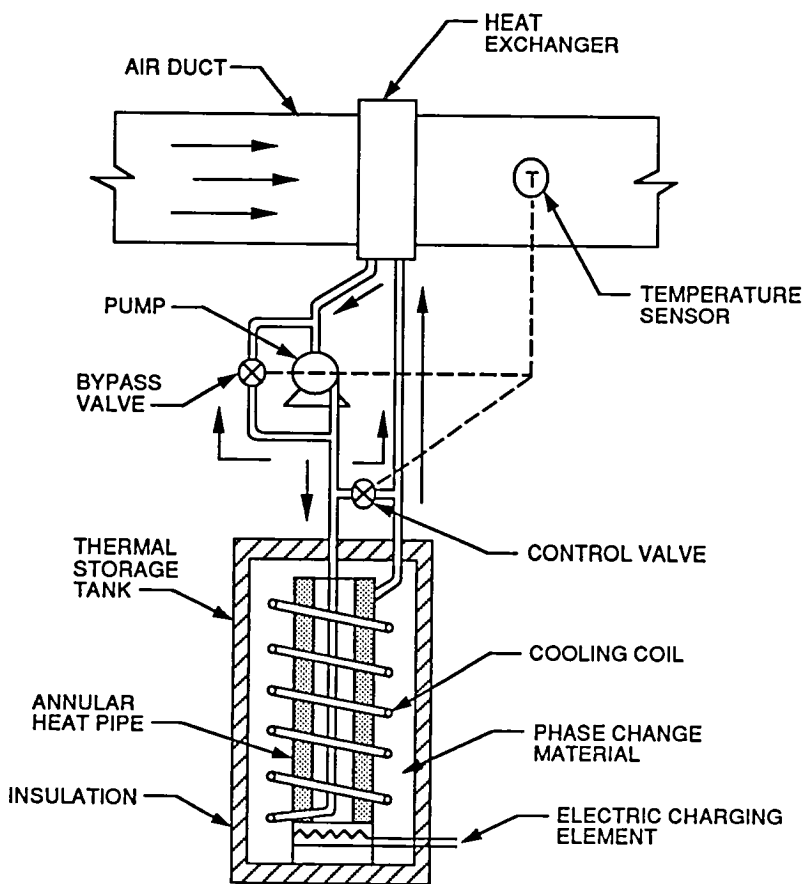
To develop a low-cost, compact Thermal Energy Storage (TES) module to augment residential space heating for utility load management. A prototype TES module that incorporates an annular heat pipe and a solid-to-solid transition material is being designed and tested at the University of Central Florida Heat Transfer Laboratory (see the figure "Thermal Energy Storage System").

Background

The regional demand for electric power fluctuates with the local time of day. Typically, utility companies provide for peak power demands by either activating smaller power plants or by purchasing surplus power from neighboring utilities. Both options, however, result in additional costs to the customers and utility. If the peak electrical demands cannot be met, such as occurred in Florida during the 1989 Christmas holidays, rolling brownouts or blackouts result. In Central Florida, maximum electric power demands occur briefly during the winter months when significant space heating is required.

Traditionally, power utilities focused only on managing the supply of electric power; however, the industry has also been developing ways to manage the demand for electricity. One way is through a concept called load management. Load management, or load leveling, involves shifting part of the regional power load from periods of peak demand to periods of relatively low demand. As a result, the need for additional power plants and the risk of brownouts is reduced.

TES is one technique for utility companies to shift the peak demand for electric power. In this concept, the energy required to heat a home or



Thermal Energy Storage System

office is stored during periods of low power demand. During times of peak power use, the stored heat is released, temporarily replacing electric space heating. Currently, hydronic, underground, and a variety of passive TES systems are being successfully employed but often necessitate significant architectural considerations, occupy valuable living space, and are expensive. An inexpensive, compact TES module that could be readily adapted into new construction or retro-fitted into existing structures is the focus of this research and development program.

Results

An electrically charged TES module has been designed to store 100,000 British thermal units (Btu) of heat at 450 degrees Fahrenheit with an energy density of approximately 18,000 Btu per cubic foot. The heat is stored within penta-

erythritol (PE), an inexpensive, nontoxic, solid-to-solid phase transition material. The heat is distributed from electric heating elements to the PE by a novel, wickless annular heat pipe (thermosyphon). The annular geometry of the heat pipe provides a large surface area for heat transfer and, consequently, promotes rapid charging. A radio-frequency signal, issued by the local utility during periods of low power demand, initiates the charging sequence of the TES module.

Upon demand, the stored heat is transferred to a residential air duct system, thereby providing a temporary replacement for direct electric resistance heating. The TES system is designed to transfer up to 15,000 Btu per hour of heat from the TES module to the residential heating system. A pumped liquid is heated within the TES module and passed into a simple air-to-liquid heat exchanger within the duct system. The rate of liquid flow and, subsequently, the rate of TES discharge is controlled by temperature sensors within the air duct system.

Conclusions

Full-scale prototype testing of the TES system will be conducted during the 1991/1992 winter season. Published results from the tests will be available in the spring of 1992.

Two projects related to the development of the TES module have been published in the Proceedings of the 26th Annual IECEC (August 1991). The articles are: (1) Visualizing the Thermal Performance of Heat Pipes with Thermochromic Liquid Crystals and (2) Performance Evaluation of a Solid-State Phase Change Material for Thermal Storage Applications.

Contact:

R. A. Turner, 867-3688, DF-FED-33

Participating Organizations:

*University of Central Florida (Dr. F. S. Gunner-
son)*

Florida Power Corporation

NASA Headquarters Sponsor:

Office of Commercial Programs

Thermal Storage Module

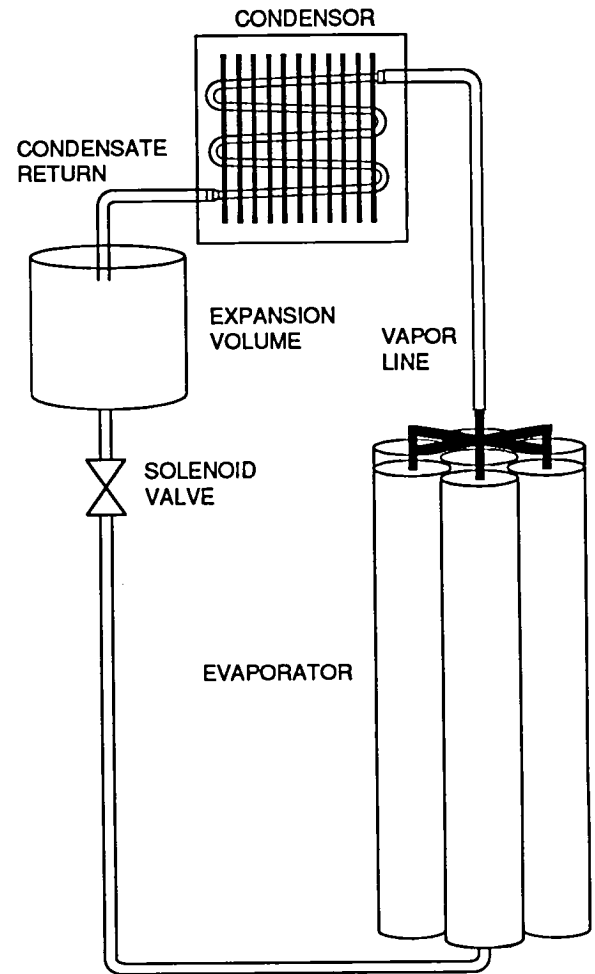
Problem Description

A problem common to many electric utilities is the fluctuation in customer demand. In most regions of the United States, these demand fluctuations reach their peak levels during the daylight or early evening hours of the winter season. In order to handle this short-term demand, most utilities purchase a type of low-cost, low-efficiency electrical generator. Since these generators are expensive and may be operated only a few hours a year, the electricity they produce can be quite expensive.

An alternative to using low-efficiency plants for peak loads would be to continue to operate higher efficiency units during off-peak periods, storing the energy until needed. Storage units being developed at the University of South Florida would provide utilities a means to save both money and energy. These savings would be passed along to the consumer in terms of lower utility bills.

System Description

The storage unit being developed is shown in the figure "Thermal Storage System for Utility Load Management" and is intended for residential installation. The system includes a total of seven cylinders for thermal storage, shown at the lower right of the figure. Each is electrically heated and contains a material with high thermal storage properties. A central tube contains a fluid that is evaporated to carry energy from the canisters, through a manifold, and to a



Thermal Storage System for Utility Load Management

condenser inside a home's normal heat ducts. Circulating room air passes over the outside surface of the condenser, condensing the vapor inside as it is heated. Condensate returns to the cylinders through a solenoid valve. The system is turned off by closing the valve and restarted when the valve is opened. An expansion tank is included in the system to handle the vapor expansion during heating.

Components

The assembly is constructed from a 6-inch outside diameter pipe with a 1-inch outside diameter tube located centrally inside. The storage material fills the space between the

canister shell and the central cooling tube. Because of the low thermal conductivity of the storage material, six aluminum fins are used to enhance overall heat transfer. Also included within the cylinder is a single helically wound cable heater, which distributes heat within the canister. The coolant used in the design is R134a. The NASA Panel for Scientific Assessment noted a zero ozone depletion potential for this material. Since it replaces the common R12 currently used in residential applications, including refrigerators, it will be readily available.

The vapor expansion tank provides enough volume for all the coolant in the system to be completely evaporated at a temperature below 150 degrees Fahrenheit. It is the largest diameter component exposed to the coolant pressure that requires relatively thick walls. Other components include a solenoid valve and a remote controller for the valve and heater. A major advantage of the design is the operational simplicity. This results in the absence of an elaborate control system and extraneous pumps and throttling valves.

System Operation

The coolant loop is first evacuated and filled with enough refrigerant so, when the solenoid valve is opened, the liquid level is a few inches above the storage canisters. In a typical installation, this requires about 3.5 pounds of R134a.

At startup, the solenoid valve is closed and the heating cables are powered. As the system temperature rises, coolant is evaporated. The vapor flows to the coil, condenses, and is trapped upstream of the solenoid valve. Once all liquid is removed from the canisters, the heat loss is stopped so nearly all energy flows into the storage material. This material is heated to a temperature of about 450 degrees Fahrenheit before the power switches are reopened. The system is left in this state until the energy is required.

When the valve is reopened, liquid coolant

again floods the coolant channel within the canister. Because of the high wall temperature, coolant is rapidly evaporated. The vapor rises to the condenser coil and recondenses, heating the circulating air in the process. The resulting condensate returns to the containment, continuing the process. The system continues to operate until the coolant vapor in the condenser coils reaches the same temperature as the circulating air stream or until the solenoid valve is again closed. At that time it is ready to be recycled.

Contact:

R. A. Turner, 867-3688, DF-FED-33

Participating Organization:

University of South Florida (R. A. Crane)

NASA Headquarters Sponsor:

Office of Commercial Programs

Magnetic Resonance Imaging Technology

Background

In November 1989, the American Cancer Society, Florida Division, Inc., and NASA Kennedy Space Center signed a Memorandum of Understanding establishing a means by which space technology could be formally transferred to the medical profession. The agreement broke new ground in the transfer of technology developed for the space program to lifesaving cancer-control applications on earth.

The Magnetic Resonance Imaging (MRI) project at the University of South Florida is one of the projects undertaken by the partnership. Currently in its second year, the project involves the development of computer software that can analyze MRI data sets, mathematically identifying different tissue types in the body and generating color-coded images. The new technology will allow for the generation of a single composite magnetic resonance image in which each tissue type is represented by a different color.

The color intensity of the tissue reflects the probability of correct tissue classification as well as the boundary definition between tissues.

Approach

MRI uses magnetic fields and radio waves to form images of soft tissues in the body, allowing for the detection of certain soft tissue tumors with greater sensitivity than any other imaging modality, including x-ray.

When a patient enters the magnetic field created by the MRI, a radio signal is beamed through the body. When the beam is turned off, the body tissue releases energy that is picked up by a scanner and converted to computer data. The data can then be used to create three-dimensional images of body tissues.

MRI has the unique capability to generate a number of image data sets with varying levels of soft-tissue contrast. Mathematical analysis of several images allows for subtle differences in image contrast or features to be enhanced providing better boundary definition of a tumor site. The MRI project is concerned with monitoring tumor response for patients who have head and neck tumors and are undergoing radiation therapy treatments.

Application

The MRI technology gained from the project will make tumor diagnosis more specific and sensitive. In addition, improvements in the ability to identify tumor location and boundaries will make the planning and treatment of patients undergoing externally directed radiation more accurate and precise.

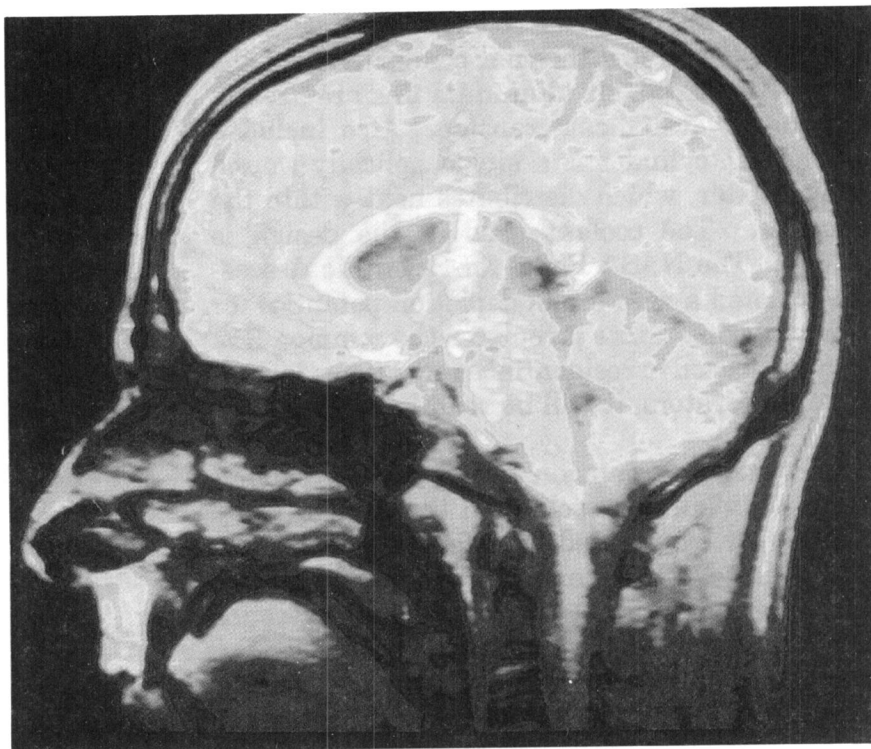


Image Enhancement of the Brain

Contact:

R. L. Butterfield, 867-3017, PT-PMO-A

Participating Organizations:

American Cancer Society

Sun Microsystems, Inc.

University of South Florida

NASA Headquarters Sponsor:

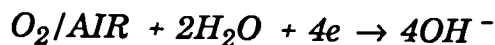
Office of Commercial Programs

Development of a Solid Polymer Electrolyte (SPE) Oxygen Concentrator

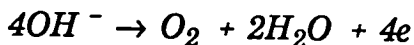
The developmental research of a solid polymer electrolyte (SPE) oxygen concentrator is based on previous work at the Kennedy Space Center on the production of high-purity oxygen for the Space Shuttle fuel cells. The objective is to conduct research toward the development and commercialization of an electrolytic device for the production of medical-grade oxygen from air.

Current methods for supplying medical-grade oxygen to patients include high-pressure gas cylinders, liquid oxygen tanks, and pressure swing adsorption (molecular sieve) oxygen concentrators. While each offers some advantages, all methods require periodic replenishment and intensive maintenance. The proposed SPE oxygen concentrator will electrochemically extract oxygen from air at near-ambient pressures and temperatures. The use of the surrounding air eliminates replenishment problems, and operating at near ambient pressures and temperatures simplifies the system, thus easing maintenance requirements.

The SPE oxygen concentrator uses a solid-polymer anion exchange membrane for the cathodic reduction of air to oxygen. The reaction is based on a four-electron process



at the cathode, and



at the oxygen electrode (anode).

A small experimental cell has been developed consisting of the SPE membrane sandwiched between two platinum screen electrodes. The

membrane is saturated with water and a direct-current voltage is placed across the electrodes. Air is brought into contact with the cathode, at which point the oxygen in the air is reduced. The resulting ions migrate across the membrane to the anode where oxygen is evolved.

The experimental cell was used to observe the electrochemical pumping of oxygen under a variety of conditions. Two important considerations examined were: (1) the effect of moisture content on cell performance and (2) the degree of contact between the membrane surface and the electrode screen. The best results were obtained when the inlet air was in a saturated state. The current densities achieved with the present electrode configuration are too low to construct a practical device. Efforts are now directed toward chemically bonding high-surface area catalyst particles directly to the membrane surface, improving the effectiveness of the electrodes.

Contact:

M. J. Lonergan, 867-7048, DM-MSL-21

Participating Organization:

Florida Solar Energy Center (A. T-Raissi, Ph.D.)

NASA Headquarters Sponsor:

Office of Commercial Programs

Materials Science

Materials science investigations are conducted in two well-equipped and well-staffed laboratories at Kennedy Space Center.

Microchemical Analysis Laboratory

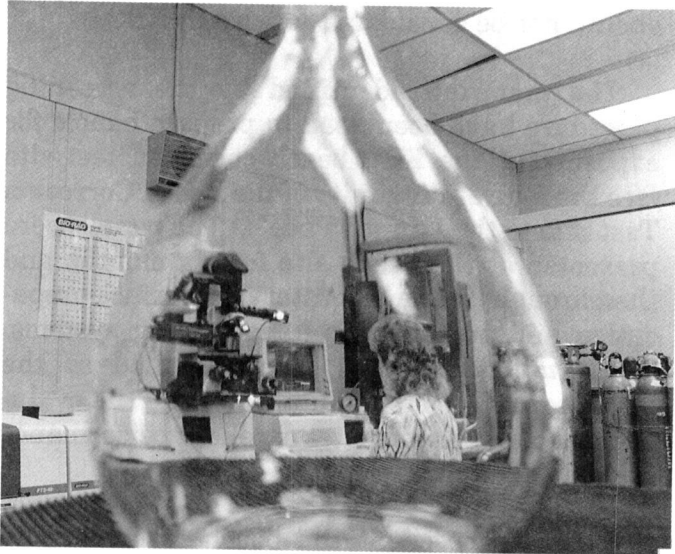
The Microchemical Analysis Laboratory employs high technology instruments (such as the electron microprobe, scanning electron microscope, infrared spectrophotometer, x-ray photoelectron spectrometer (ESCA), and mass spectrometer/gas chromatograph, as well as classical analytical methods) to identify a variety of materials. One basic function of the laboratory is to chemically identify any fluid or solid material down to the parts-per-billion range. A second basic function is to provide the investigative effort necessary to understand and solve chemical problems associated with the selection and application of materials in aerospace systems. Typical subjects for analysis are the Shuttle thermal protection system, aerospace materials (such as alloys and soft goods), and any contamination found on or in flight hardware or facilities.

Failure Analysis and Materials Evaluation Laboratory

The failure analysis section of the Failure

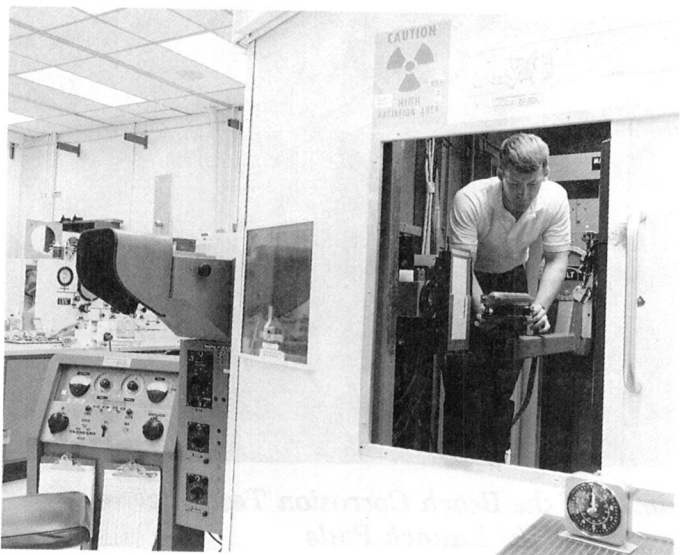
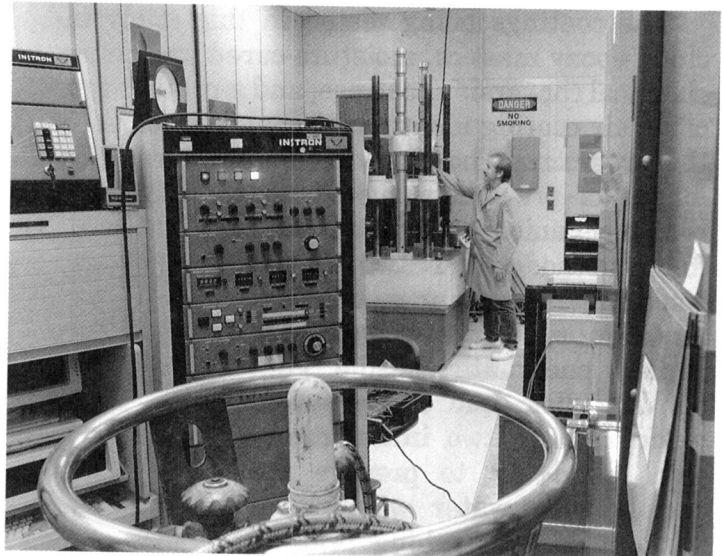
Analysis and Materials Evaluation Laboratory provides the investigative capability for determining, on a rapid turnaround basis, the causes of failures related to ground support equipment and flight hardware. The failure analysis process is conducted in the electrical/electronics, mechanical/fluid, metallurgical, and metrological laboratories, with supporting expert services within each of these areas. After the completion of an investigation, the engineer or physicist makes recommendations for preventing similar occurrences and, if necessary, devises a research program with the goal of preventing future failures.

The materials evaluation section of this laboratory includes materials and environmental testing facilities, a liquid oxygen impact testing facility, and an environmental exposure test site along the Atlantic Ocean. This section provides the investigative effort necessary to understand and solve technical problems associated with the selection and application of materials (such as plastics, elastomers, metals, and lubricants) used in flight hardware, ground support equipment, and facility systems.



Microchemical Analysis Laboratory

Materials Evaluation Laboratory



Failure Analysis Laboratory

Protective Coating Systems for Repaired Carbon Steel Surfaces

In the past, maintenance repair of corroded carbon steel surfaces required the use of abrasive blasting to adequately clean and prepare the metal surface for application of protective coatings. Recent advances in coating technology promise acceptable protective coating performance when surface preparations are less than perfect. The present study focuses on new products and techniques that may reduce the level of surface cleanliness required for corrosion protection in many areas at Kennedy Space Center (KSC).

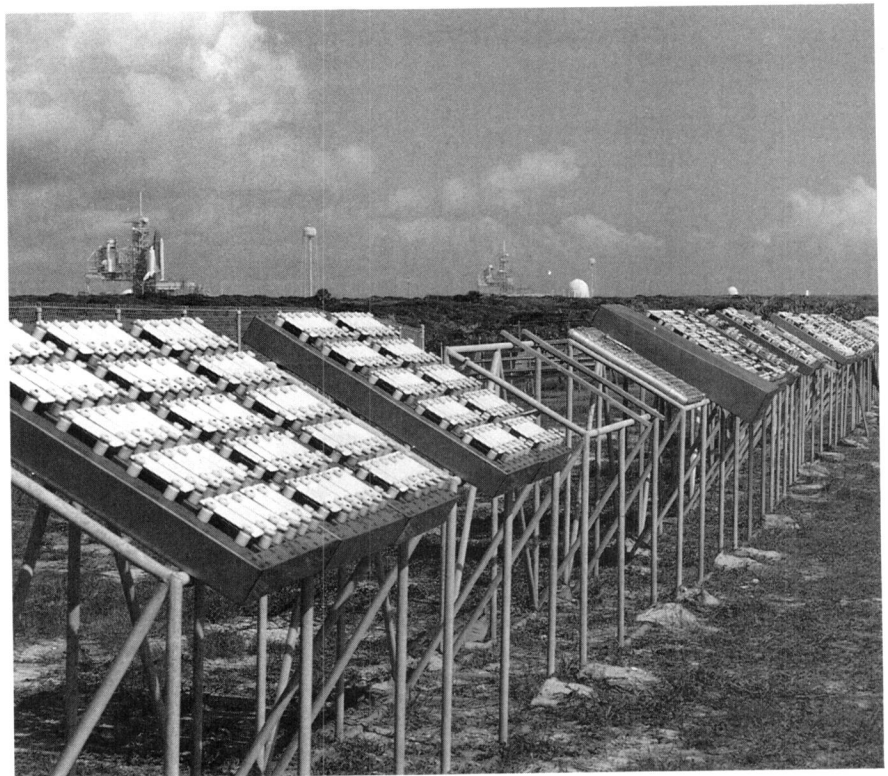
The coatings being tested in this study include epoxy mastics, moisture-cured urethanes, chemical conversion coatings, and any other type of repair coating identified during the course of the program. The study compares the performance of previously rusted panels that have been mechanically prepared using four methods and two initial conditions. The four mechanical methods used are power wire brush, pneumatic needle gun, sanding disk, and coarse wheel grinder. The two initial conditions used are to prepare the panels with water washing or without water washing prior to mechanical cleaning.

The initial screening of the many products was accomplished by exposing the prepared panels to 2,000 hours in the salt-fog chamber. The results of this screening procedure indicate varying performances of the coatings of the same generic type. This result has considerably reduced the final list of products to be tested. Further results show that the "rust converter" type coatings provide little protection in an aggressive atmosphere and

should not be considered for use at KSC.

The materials identified by the screening procedure have been used to prepare panels for exposure at the KSC beach corrosion test site (see the figure "Proximity of the Beach Corrosion Test Site to the Launch Pads"). The panels were prerusted at the beach site for six months and then brought to the laboratory for surface preparation and application of the coating systems. The completed panels were installed at the beach corrosion site in July 1990, and the evaluation at one year indicates excellent performance of many of the materials.

Panels exposed at the beach corrosion site will undergo solid rocket booster (SRB) effluent testing to simulate the conditions at the launch site. The SRB effluent tests will be accomplished by spraying simulated effluent onto two-thirds of the panels every two or three weeks. Panels at the beach will be inspected after 1, 3,



Proximity of the Beach Corrosion Test Site to the Launch Pads

6, 12, 18, 36, and 60 months and rated for rusting on a scale from 1 to 10 in accordance with ASTM D610. An expanded test plan is available under document number MTB-144-88.

Contact:

L. G. MacDowell, 867-3400, DM-MSL-22

NASA Headquarters Sponsor:

Office of Space Flight

Environmentally Compliant Coating Systems for the Shuttle Launch Sites

In 1986, a test program was started to evaluate protective coating systems on carbon steel surfaces exposed to simulated solid rocket booster (SRB) effluent. Test panels were coated with materials then available, exposed to the environment at a beach-side corrosion test site, periodically sprayed with a simulated SRB acid effluent, and evaluated after 18, 36, and 60

months. The coating systems were based on solvent-thinned, inorganic, zinc-rich primers and various solvent-thinned topcoat systems.

The findings of this study were that, in general, the thick-film topcoat products provided better chemical and corrosion resistance than the thin-film counterparts when exposed to the simulated SRB acid effluent. However, in recent years, environmental regulations have sought to restrict the use of paints and coatings with a high concentration of solvent, which could include many of the coating systems tested in this study.

The use of the solvent-based, inorganic, zinc-rich primers tested and approved in the 1986 study could be prohibited at Kennedy Space Center (KSC) in the near future due to their volatile organic content (VOC) levels. These materials all have VOC levels above 450 grams per liter (3.75 pounds per gallon), whereas the maximum levels allowed in some areas (such as California, some counties of Florida, and many



KSC Corrosion Test Site

other urban areas of the United States) are 420 grams per liter (3.5 pounds per gallon). Furthermore, legislation has dictated that this level be reduced to 350 grams per liter (2.8 pounds per gallon) by 1993. Therefore, the possibility that the inorganic, zinc-rich primers and topcoat systems presently approved at KSC will be prohibited and unavailable for use is very real.

In response to this circumstance, the current study has been expanded to search for inorganic, zinc-rich coating systems that provide superior protection to KSC launch structures and ground support equipment and fully comply with environmental regulations. Currently, the protective coating manufacturing industry is producing environmentally compliant, inorganic, zinc coatings such as high-volume solids and water-based systems. New systems are also being developed to conform to the anticipated strengthening of environmental air quality standards.

The application of these environmentally compliant coating systems was completed in April 1991 and the test panels were exposed in May 1991 to atmospheric contaminants at the KSC beach corrosion site with concurrent applications of an acid slurry made of hydrochloric acid (HCl) and alumina (Al_2O_3). To simulate the worst-case scenario experienced at the launch sites, the slurry will be applied to the test panels with no subsequent washdown. Concurrently, laboratory studies will be conducted on the primers to determine heat resistance and level of adhesion to the carbon-steel substrate.

The exposure test will be conducted for five years to determine the suitability of the coating systems. The test panels will be inspected for performance at 1, 3, 6, 12, 18, 36, and 60 months and will be formally rated in accordance with ASTM D610 at 18, 36, and 60 months. During this five-year period, there will be approximately 130 applications of the acid slurry.

Contact:

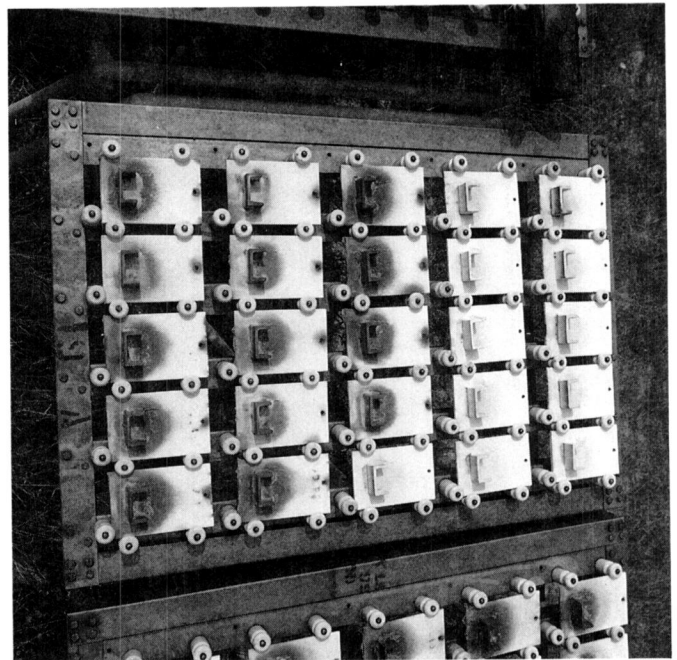
L. G. MacDowell, 867-3400, DM-MSL-22

*NASA Headquarters Sponsor:
Office of Space Flight*

Protective Top Coating Systems for the Space Transportation System Launch Environment

Zinc-rich coating systems exposed to the Space Transportation System (STS) launch environment at Kennedy Space Center (KSC) have been suffering premature failure due to the highly acidic residue produced by the solid rocket boosters. Early attempts at topcoating these zinc-rich coatings with a thin film to increase their chemical resistance have produced only marginal results.

Topcoat systems are being tested to improve coating performance for exposure to KSC's harsh environment (see the figure "Coating Evaluation of Test Panels at the Beach Corrosion Test Site"). The present study focuses on using thicker film topcoats over the zinc-rich primers to improve the chemical resistance to a marine atmosphere and to highly acidic residues.



Coating Evaluation of Test Panels at the Beach Corrosion Test Site

In 1986, 119 materials producing 67 coating systems were exposed to atmospheric contaminants at the KSC beach corrosion site with concurrent applications of an acid slurry made of hydrochloric acid (HCl) and alumina (Al_2O_3). To simulate the worst-case scenario experienced at the launch sites, the slurry was applied to the test panels with no subsequent washdown.

The current test will be conducted for five years to determine the suitability of the topcoat systems. The panels have been judged for performance at 6, 12, 18, and 36 months. The last evaluation will occur at 60 months, which will be followed by a final report. During this five-year period, there will have been approximately 130 applications of the acid slurry.

The panels have completed the 60-month exposure and the results of the evaluation will be published in the near future. Several manufacturer's topcoat products are, however, performing very well. This result has prompted consideration to prepare a list, for incorporation into KSC-STD-C-0001, that includes approved topcoat products for use when topcoats are required and specified for launch structures and ground support equipment at KSC

Contact:

L. G. MacDowell, 867-3400, DM-MSL-22

NASA Headquarters Sponsor:

Office of Space Flight

Corrosion-Protective Coatings From Electrically Conducting Polymers

In a joint research effort involving Kennedy Space Center (KSC) and the Los Alamos National Laboratory, electrically conductive polymer coatings have been developed as corrosion-protective coatings for metal surfaces. At KSC, the launch environment consists of marine, severe solar, and intermittent high-acid/elevated temperature conditions. The current zinc-rich

coatings used on launch structures have the drawback of attack of the zinc moiety by the high concentrations of hydrochloric acid (HCl) released during a Space Shuttle launch. Electrically conductive polymer coatings have been developed that impart corrosion resistance to mild steel when exposed to saline and acidic environments. Such coatings also seem to promote corrosion resistance in areas of mild steel where scratches exist in the protective coating. The objective of the research effort is to formulate coatings that provide easy application, repair, and long-term resistance to the KSC launch environment.

The research team has synthesized several conducting polymers and prepared solutions of suitable viscosity for casting films. Solvents, casting techniques, and drying conditions have been developed for coating steel coupons with pinhole-free films. For a material to qualify as a candidate for a corrosion-protective coating, the selection criteria must include ease of preparation and processing, dopability (i.e., increasing conductivity by electron donors or acceptors), electrical conductivity, environmental stability, mechanical integrity of film, adhesion to steel, and low cost.

Several conducting polymers were synthesized during the course of the research effort. In some cases, specialized monomers were synthesized before subsequent polymerization; in other cases, monomers were obtained commercially. Many of the polymers initially considered were eliminated from the study based upon the qualification criteria listed previously. For example, some of the polymers requiring specialized monomer synthesis were eliminated due to the high cost of producing such materials. Recent work has encompassed development of methods for coating steel coupons with pinhole-free films of the following pi-conjugated polymers: polyaniline, poly(3-hexyl thiophene), poly(3-octyl thiophene), poly(3-thienylmethylacetate), and poly(3-thienylethylacetate).

Adhesion to steel was the main obstacle in

the study. Adhesion problems were solved for many of the polymers through special techniques such as blends of epoxy with the polymer. The greatest success involves applying undoped, chemically prepared polymer to the surface of the steel and subsequently doping the coated surface to the conducting state.

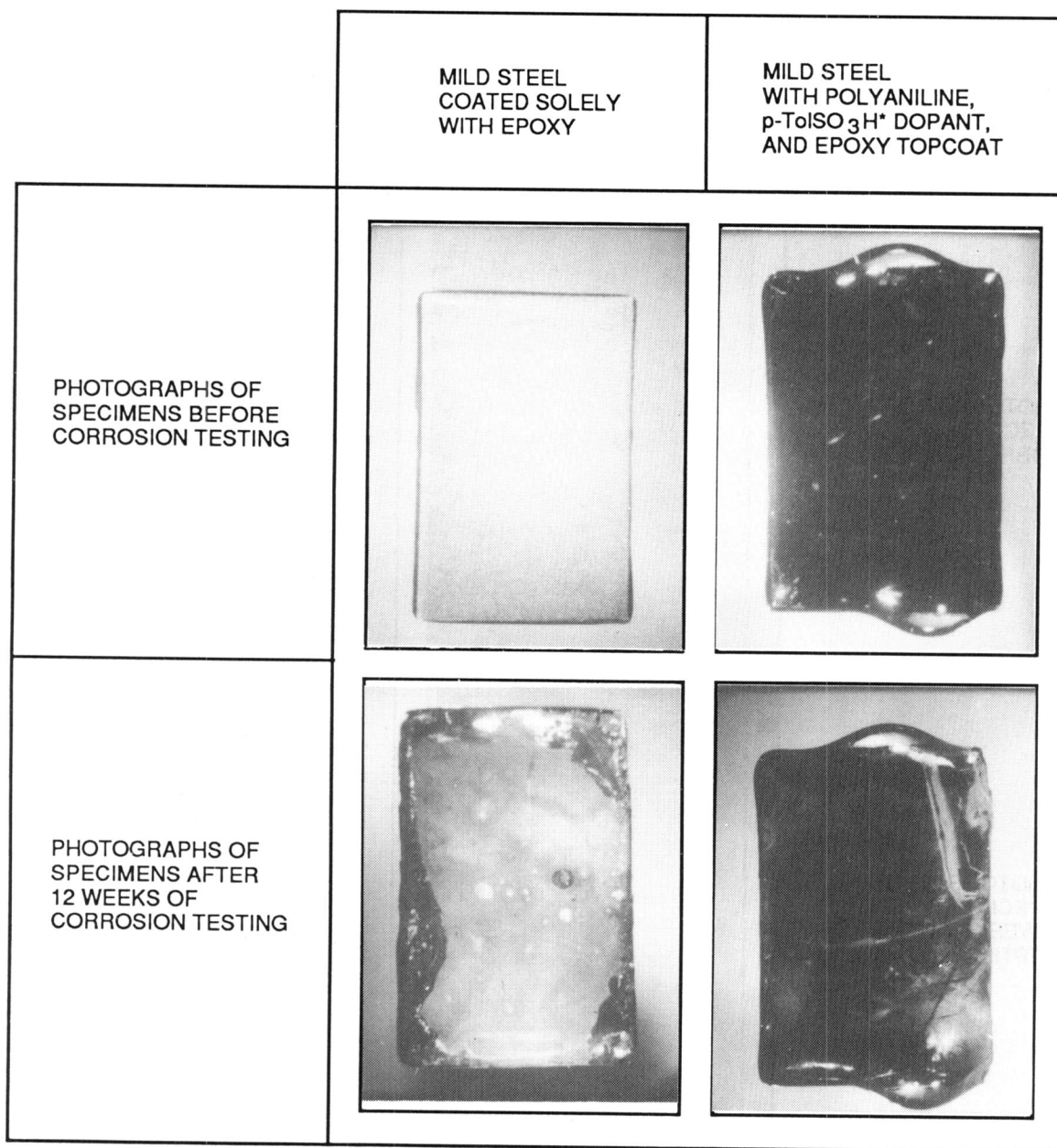
Adhesion and corrosion-resistance studies were performed with mild steel samples coated with candidate materials. The samples were exposed to salt water and to 0.1-molar (M) HCl. Although many of the polymer films adhered well to steel in salt water, the presence of acid caused some films to lift from the substrate. Results of such adhesion studies concentrated the work effort on polyaniline coatings, which were clearly superior to others tested in ease of use as well as adhesion to steel in both acid and saline environments.

The surface of the mild steel samples was initially coated with the undoped, chemically prepared polyaniline. This coating of the mild steel coupons was accomplished using solutions of polyaniline in 1-methyl-2-pyrrolidinone (NMP). A spray method was developed for applying the polyaniline/NMP solutions to the steel, which provided good coverage and good adhesion of the polyaniline to the substrate. Upon drying, the coatings of 1- to 2-mil thickness (0.001 to 0.002 inch or 0.03 to 0.05 millimeter) were doped to the conducting state. Over 25 different dopants were used during the study. The dopants that gave the best results were tetracyanoethylene (TCNE), zinc nitrate, and p-toluene sulfonic acid. Once the coating was doped to a conducting state, a topcoat of cross-linked epoxy was applied to the samples in order to impart improved abrasion resistance to the coating. The epoxy topcoat used was Ciba-Geigy Bisphenol A GY 2600 resin cured with a cycloaliphatic/aliphatic amine hardener XU265. This epoxy material is used in power plants for coating interior surfaces of stacks emitting sulfur dioxide and is known for acid resistance. The resultant coating was designed to provide the proper electronic environment as well as

coating toughness and resistance to harsh environmental conditions.

The polymer-coated steel coupons were tested for corrosion resistance in two different environments via gas/liquid cells. One environment consisted of placing each coupon in an individual vial containing enough 3.5 percent salt (NaCl) solution to cover the coated portion of the coupon. Each vial was capped with a rubber septum into which air was bubbled to ensure oxygenation of the solution. In the second environment, the only difference from the first environment was that a 0.1-M HCl solution was used rather than a saline solution. To establish a baseline for the corrosion resistance of the conductive polymer-coated samples, control samples of mild steel coated solely with the epoxy were also tested. Photographs were taken of the samples before exposure to the above environments as well as throughout the testing. In some cases, the tests were carried out for 12 weeks.

The figure "Corrosion Testing of Coated Steel Specimens in Aerated 3.5-Percent NaCl" shows photographs of samples before and after 12 weeks of exposure to an aerated 3.5-percent NaCl solution. The photograph on the top left shows mild steel coated only with epoxy before exposure. The photograph on the top right shows mild steel that was spray coated with undoped polyaniline in NMP, then doped with p-toluenesulfonic acid, and then topcoated with epoxy. The photograph on the bottom left shows the epoxy control sample after 12 weeks of exposure to the saline solution. Corrosion was evident with the control sample. Pitting was seen, and mass loss from the edges of the steel sample occurred. The photograph on the bottom right shows the polyaniline/epoxy-coated sample. No evidence of corrosion was seen, with the edges of the sample still intact and showing no mass loss. Electrically conductive polymers are typically intensely colored. Since the polyaniline is dark in color, the coating was scraped off to verify no corrosion was present. In fact, the polyaniline coating adhered to the substrate so



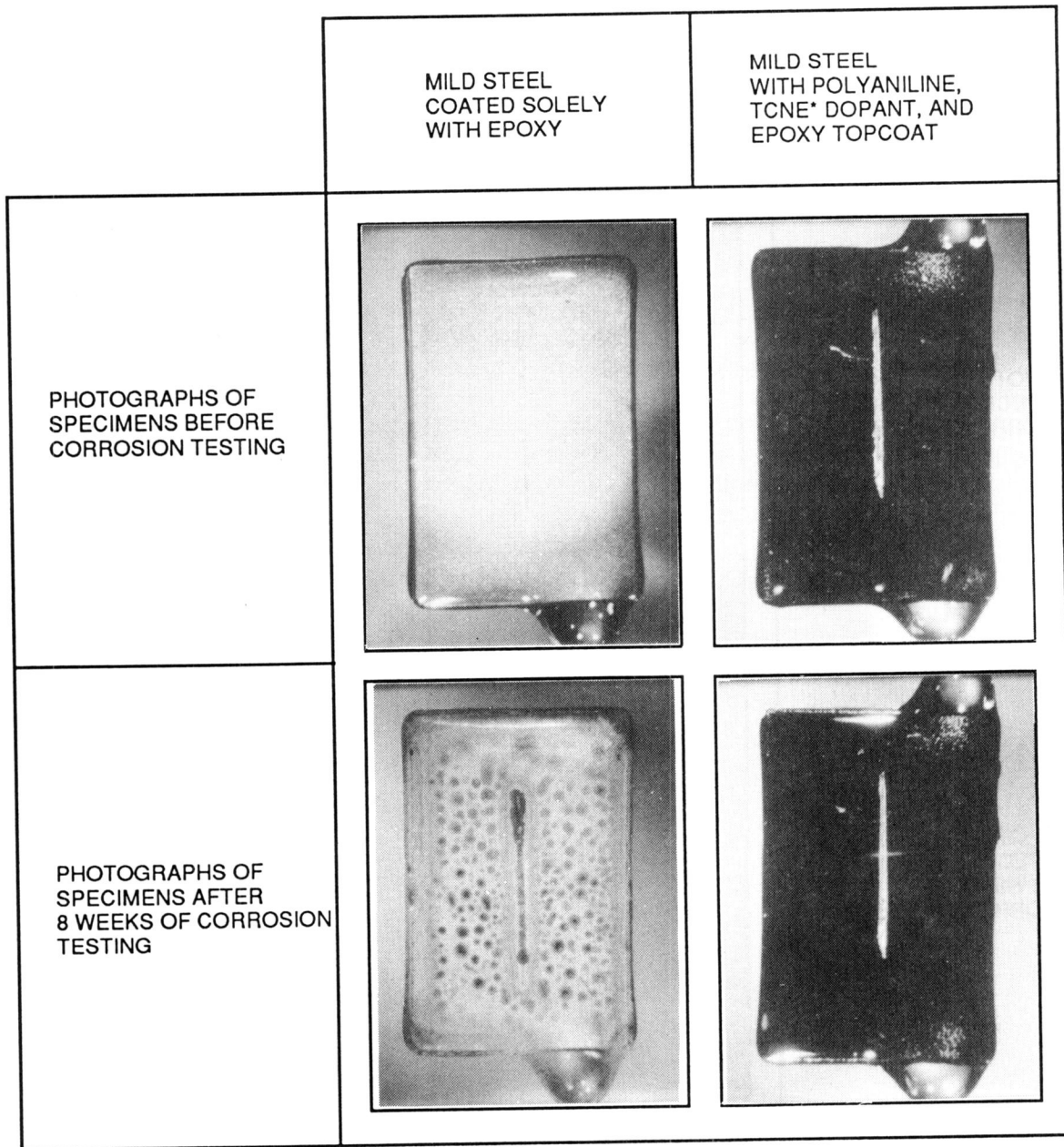
* p-TolSO₃H = p-TOLUENESULFONIC ACID

*Corrosion Testing of Coated Steel Specimens in Aerated 3.5-Percent NaCl
(magnification: 3X)*

tenaciously it was difficult to scrape the coating from the steel.

The figure "Corrosion Testing of Scribed Specimens in Aerated 0.1-M HCl" shows photographs of samples before and after 12 weeks of exposure to aerated 0.1-M HCl solution. The

photograph on the top left shows mild steel coated only with epoxy before exposure. The photograph on the top right shows mild steel that was spray coated with undoped polyaniline in NMP, then doped with TCNE, and then topcoated with epoxy. Both samples were scribed before exposure to acid. The photograph



* TCNE = TETRACYANOETHYLENE

*Corrosion Testing of Scribed Specimens in Aerated 0.1-M HCl
(magnification: 3X)*

on the bottom left shows extensive corrosion on the epoxy control sample after 8 weeks in acid. The photograph on the bottom right shows the polyaniline/epoxy-coated sample. No evidence of corrosion was seen, with the scratched surface still shiny.

Many environmental tests have been carried out in saline and acidic oxidizing environments. A marked improvement in the corrosion resistance of mild steel has been observed when using the electrically conductive polymer coatings developed in this research program as

compared to mild steel coated solely with epoxy.

Candidate coatings were initially screened by the corrosion tests previously described using aerated saline and hydrochloric acid solutions. The best candidate materials are undergoing further testing for determining their effective corrosion resistance for mild steel. Testing methods include ultraviolet radiation testing, electrochemical corrosion testing, accelerated corrosion testing in a salt-fog chamber, long-term exposure at the KSC beach corrosion testing site, pitting corrosion tests in a ferric chloride solution, and electrochemical impedance spectroscopy. Results thus far look promising, although much more testing is planned.

Contact:

K. G. Thompson, 867-3400, DM-MSL-22

Participating Organization:

Los Alamos National Laboratory (B. C. Benicewicz and D. A. Wroblewski)

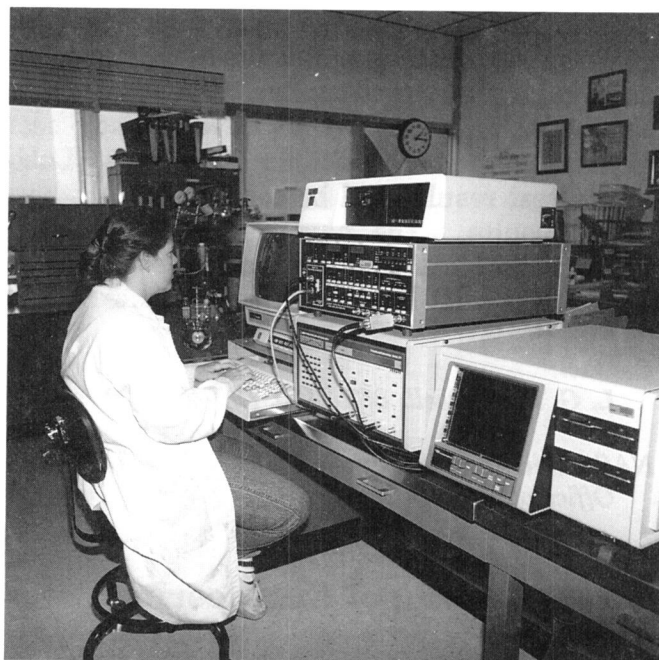
NASA Headquarters Sponsor:

Office of Space Flight

Accelerated Testing of Inorganic, Zinc-Rich Primers

Inorganic, zinc-rich coatings are used for corrosion protection of carbon steel structures at Kennedy Space Center (KSC). To be considered for use at KSC, a primer must successfully withstand exposure at the beach corrosion test site. Primers are periodically rated for rusting on a scale of 1 to 10 in accordance with ASTM D610, with a rating of 10 being the best. For preliminary approval, primers must continue to maintain a rating of 9 or better after 18 months of exposure. For final approval, primers must continue to maintain a rating of 9 or better after 60 months. Unfortunately, this process requires a considerable amount of time to place new products on the approved list.

Alternating current impedance measurement



Electrochemical Corrosion Testing System

techniques, also known as electrochemical impedance spectroscopy (EIS), are being studied as a possible method for determining the corrosion resistance of inorganic, zinc-rich primers for use at KSC. The goal of this test program is to develop an accelerated method for screening zinc-rich primers before exposing them to long-term testing at the beach corrosion test site. A reliable accelerated laboratory test method such as EIS could save time for preliminary approval of primers (see the figure "Electrochemical Corrosion Testing System").

For this method, primers are sprayed on test coupons for use in the laboratory experiments. These coupons are immersed in seawater, which is obtained from the Atlantic Ocean close to the beach corrosion site. The seawater is aerated during the test to provide the oxygen necessary for corrosion reactions. Test results should yield information on polarization resistance (R_p), which is a measure of a material's resistance to corrosion in a particular electrolyte. It is hoped that a correlation can be found between these laboratory results and the long-term field results.

This test program was started in November 1989 and is continuing. Results at this point are encouraging but preliminary. Tests are being conducted on primers that have already been exposed at the beach site for 60 months. Laboratory test results will be compared with these field results. The new-generation, zinc-rich primers now starting evaluation will also be tested to predict their field performance.

Contact:

L. G. MacDowell, 867-3400, DM-MSL-22

NASA Headquarters Sponsor:

Office of Space Flight

Stress Testing of Engineering Materials

Stress corrosion cracking (SCC) of metallic alloy materials can have a devastating impact on the safety and reliability of all types of structures, mechanisms, and high-pressure gaseous systems. Many times, this type of failure is unexpected and occurs at the worst possible moment in a schedule or critical operation of a system. Obviously, when dealing in high technology areas such as Shuttle launch and space travel, exotic metallic materials are used because of their high strength and lower weight. Typically, these types of materials are the most susceptible to the SCC phenomenon.

In response to this potential problem, work is underway to determine the SCC behavior of some of the most commonly used alloys at Kennedy Space Center (KSC). These materials range from many stainless steels to the more exotic nickel-based and aluminum alloys. As a result of this work, materials with lower susceptibility to stress corrosion will be identified for use on facilities and systems at KSC.

The work is currently being conducted under contract to Florida Atlantic University by the Department of Ocean Engineering. The materials are being tested using the slow strain rate

technique (SSRT) or constant extension rate technique (CERT) in a corrosive solution that simulates the Space Transportation System (STS) launch environment. The SSRT test has been accepted as a reliable method to judge a materials's SCC resistance in a short time. The alloys are stressed to failure at various strain rates (10^{-8} , 10^{-6} , and 10^{-4} inch per inch per second) in air and then compared to identical specimens that have been tested in the corrosive solution. Differences in fracture surfaces, stress levels, and times to failure of the specimens between the two environments are interpreted as variations in susceptibility to SCC. In addition, experiments are being conducted to determine crevice corrosion behavior and atmospheric corrosion resistance.

The initial study is complete, and the findings will be available in the near future. The failed specimens are being analyzed using scanning electron microscopy (SEM) and the results will be sent to KSC for publication. These results will help to prepare a list of engineering materials that have specific resistance to SCC in the STS launch environment.

Contact:

L. G. MacDowell, 867-3400, DM-MSL-22

Participating Organization:

Florida Atlantic University, Department of Ocean Engineering

NASA Headquarters Sponsor:

Office of Space Flight

Development of New Flooring Materials for Clean Rooms and Launch Site Facilities

NASA utilizes one of two different static-dissipating floor coverings in Shuttle assembly areas: flexible polyvinyl chloride (PVC) tiling or poured epoxy flooring material. Both have disadvantages associated with their use. PVC fails NASA's outgassing test due to the plasticiz-

er component in the formulation. The plasticizer can volatilize at room temperature and then recondense on sensitive optical surfaces. Although there are static-dissipating PVC tiles commercially available, none have qualified that have been subjected to the outgassing test. The poured epoxy flooring also performs poorly and is difficult to maintain, repair, and clean.

A Small Business Innovation Research (SBIR) project, conducted by Springborn Laboratories, identified chemically resistant polymers and has successfully developed two materials that meet NASA's requirements. Floor tiles based on high-density polyethylene and PVC have been installed in a 500-square-foot test bed in the Vehicle Assembly Building (see the figure "Floors at the Vehicle Assembly Building in the Low Bay") at Kennedy Space Center to evaluate the durability of the tiles and special conductive adhesive under actual use conditions.

Contact:

C. J. Bryan, 867-3400, DM-MSL-22

Participating Organization:

Springborn Laboratories



*Floors at the Vehicle Assembly Building
in the Low Bay*

*NASA Headquarters Sponsor:
Office of Space Flight*

Development of a New Chemical-Resistant Fabric for Protective Clothing

A program was initiated to identify a fabric for the next generation of clothing to protect workers using hazardous chemicals at Kennedy Space Center. The hazardous chemicals of interest include hydrazine, monomethylhydrazine, nitrogen tetroxide, hexane, toluene, sodium hydroxide, citric acid, 1,1,1-trichloroethane, methyl ethyl ketone, 2-propanol, and two hydraulic fluids (MIL-H-5605 and MIL-H-83282).

Tuskegee University is the prime contractor for this program. TRI/Environmental, Inc., has been subcontracted to contact various manufacturers for information concerning new barrier materials that may be suitable for use in protective clothing. Samples of promising materials have been submitted, and the physical properties and gross chemical resistance evaluation is underway. TRI/Environmental, Inc., will further evaluate the candidate materials for ease of fabrication into garments. Tuskegee University will perform permeability and degradation tests with the hazardous chemicals to determine the best material for the new chemically protective suit.

Contact:

*K. G. Thompson, 867-3400,
DM-MSL-22*

Participating Organizations:

*TRI/Environmental, Inc., (J. Stull
and D. White)*

*Tuskegee University (N. Vahdat,
Ph.D.)*

*NASA Headquarters Sponsor:
Office of Space Flight/Office of
Equal Opportunity Programs*

Compatibility of Corrosion-Resistant Alloys With Aerospace Fluids

Nineteen corrosion-resistant alloys were evaluated several years ago for corrosion resistance in the Kennedy Space Center launch environment. Five of these alloys that exhibited outstanding corrosion resistance were identified in this evaluation. These alloys, Inco G-3, Inconel 625, and Hastelloy C-4, C-22, and C-276, were selected for evaluation of their compatibility with oxygen, hydrogen, hydrazine, monomethylhydrazine, and nitrogen tetroxide. Promoted combustion tests in oxygen showed these alloys to be resistant to ignition at pressures twice as high as those required for consumption of the 300-series stainless steel alloys evaluated. Rubbing friction tests also ranked these alloys

more resistant to ignition than the 300-series stainless steel in oxygen. Particle impact tests in oxygen resulted in no ignitions at velocities as high as 30 meters per second at 69 MPa (10,000 psi).

A test chamber has been designed to perform slow-strain-rate, stress-corrosion cracking tests on the five alloys in hydrazine, nitrogen tetroxide, and monomethylhydrazine. Hydrogen embrittlement susceptibility will be evaluated by a slow-strain-rate method and by static pressurization of a thin disk after the establishment of steady-state hydrogen permeation through the disk.

Contact:

C. J. Bryan, 867-3400, DM-MSL-22

NASA Headquarters Sponsor:

Office of Space Flight

REPORT DOCUMENTATION PAGE			Form Approved OMB No. 0704-0188	
Public reporting burden for this collection of information is estimated to average 1 hour per response, including the time for reviewing instructions, searching existing data sources, gathering and maintaining the data needed, and completing and reviewing the collection of information. Send comments regarding this burden estimate or any other aspect of this collection of information, including suggestions for reducing this burden, to Washington Headquarters Services, Directorate for Information Operations and Reports, 1215 Jefferson Davis Highway, Suite 1204, Arlington, VA 22202-4302, and to the Office of Management and Budget, Paperwork Reduction Project (0704-0188), Washington, DC 20503.				
1. AGENCY USE ONLY (Leave blank)	2. REPORT DATE December 1991	3. REPORT TYPE AND DATES COVERED Technical Memorandum - 1991		
4. TITLE AND SUBTITLE Research and Technology 1991 Annual Report of the Kennedy Space Center			5. FUNDING NUMBERS	
6. AUTHOR(S)				
7. PERFORMING ORGANIZATION NAME(S) AND ADDRESS(ES) NASA John F. Kennedy Space Center Kennedy Space Center, Florida 32899			8. PERFORMING ORGANIZATION REPORT NUMBER NASA TM-103825	
9. SPONSORING / MONITORING AGENCY NAME(S) AND ADDRESS(ES) National Aeronautics and Space Administration Washington, D.C. 20546			10. SPONSORING / MONITORING AGENCY REPORT NUMBER	
11. SUPPLEMENTARY NOTES				
12a. DISTRIBUTION / AVAILABILITY STATEMENT Unclassified - Unlimited Subject Category 99			12b. DISTRIBUTION CODE	
13. ABSTRACT (Maximum 200 words) As the NASA Center responsible for assembly, checkout, servicing, launch, recovery, and operational support of Space Transportation System elements and payloads, Kennedy Space Center is placing increasing emphasis on the Center's research and technology program. In addition to strengthening those areas of engineering and operations technology that contribute to safer, more efficient, and more economical execution of our current mission, we are developing the technological tools needed to execute the Center's mission relative to future programs. The Engineering Development Directorate encompasses most of the laboratories and other Center resources that are key elements of research and technology program implementation and is responsible for implementation of the majority of the projects in this Kennedy Space Center 1991 Annual Report. For further technical information about the projects, contact David A. Springer, Projects Management Office, DE-PMO-5, (407)867-3035. Thomas M. Hammond, Technology Utilization Officer, PT-PMO-A, (407)867-3017, is responsible for publication of this report and should be contacted for any desired information regarding the Centerwide research and technology program.				
14. SUBJECT TERMS Research and Technology			15. NUMBER OF PAGES	
			16. PRICE CODE	
17. SECURITY CLASSIFICATION OF REPORT Unclassified	18. SECURITY CLASSIFICATION OF THIS PAGE Unclassified	19. SECURITY CLASSIFICATION OF ABSTRACT Unclassified	20. LIMITATION OF ABSTRACT	



NASA

National Aeronautics and
Space Administration

John F. Kennedy Space Center

Kennedy Space Center, Florida 32899
AC 407 867-2468